

WISCONSIN DEPARTMENT OF NATURAL RESOURCES, BUREAU OF WATER QUALITY

Estimations of Sources of Water Quality Impairments at Ungaged Sites in the Upper Wisconsin River Basin

A SWAT Model in Support of the Wisconsin River
TMDL

Appendix D: Estimations of Sources of Water Quality Impairments at Ungaged Sites in the Upper Wisconsin River Basin

Authors:

Ruesch, Aaron S.^{1*}
Beneke, Thomas^{1,2}
Diebel, Matthew¹
Evans, David M¹
Freihoefer, Adam¹
Hirekatur, Ann¹
Nelson, Theresa¹
Oldenburg, Patrick¹
Radecki, Andrew¹

With contributions from:

Robertson, Dale^{3†}

¹Wisconsin Department of Natural Resources, Bureau of Water Quality, Madison, WI 53707

²The Cadmus Group, Madison, WI 53703

³U. S. Geological Survey, Wisconsin Water Science Center, Middleton, WI 53562

09/15/2016

*Corresponding author: Aaron.Ruesch@wisconsin.gov

†These authors provided site-specific sediment and nutrient load estimates (Section 5.2.3 and Appendix D.5).

1 Abstract

Many streams and lakes within the Upper Wisconsin River are impaired due to excessive sediment and nutrient loading. To address water quality impairments in the Wisconsin River Basin, Total Maximum Daily Load (TMDL) allocations will be developed for sediment and phosphorus. A computer simulation model using the Soil and Water Assessment Tool (SWAT) was developed to identify the significant sources of sediment and phosphorus loads in the basin. This document describes all facets of model development. Model development for this project was an extensive effort that included: 1) configuring the model to simulate hydrology and water chemistry based on landcover, soils, topography, weather, and wastewater discharge among other drivers 2) compiling observed streamflow and estimating pollutant loads at various sites for the purposes of calibration 3) calibrating and validating the model by adjusting model parameters and 4) developing independent sub-models to simulate processes that are not represented well in SWAT.

Table of Contents

1	Abstract	2
	Abbreviations	8
2	Introduction	10
2.1	Background	10
2.2	SWAT	10
2.3	Study Area.....	11
3	Basic Model Configuration	12
3.1	Subbasin Delineation	12
3.2	Land Cover and Land Management	13
3.2.1	Land Cover (step 1).....	13
3.2.2	Crop Rotations (step 2)	14
3.2.3	Interviews with Local Experts (step 3)	15
3.2.4	Land Cover and Management Integration (step 4).....	16
3.2.5	Validation	17
3.3	Soil Data Aggregation	18
3.3.1	Component-Level Aggregation (step 1)	19
3.3.2	Map-unit-level aggregation (step 2)	20
3.4	Slope Classification	21
3.5	HRU Definition	22
3.6	Weather Data.....	22
3.7	Point Sources	23
4	Additional Model Configuration	24
4.1	Specific Agricultural Operations	24
4.1.1	Tillage.....	24
4.1.2	Inorganic Fertilizers.....	24
4.1.3	Tile drains	24
4.1.4	Irrigation	24
4.2	Canopy Storage.....	24
4.3	Soil Phosphorus.....	25
4.4	Urban Area Model	25
4.4.1	Urban Subbasin Delineation	26
4.4.2	WinSLAMM methods.....	26
4.5	Ponds and Wetlands.....	26

4.5.1	Ponds.....	27
4.6	Wetlands.....	28
4.7	Evapotranspiration Equation	29
4.8	Groundwater.....	29
4.8.1	Groundwater Inflow (Baseflow)	29
4.8.2	Baseflow Phosphorus.....	30
4.9	Manning's <i>n</i>	31
4.10	Surface Runoff Lag.....	32
5	Model Calibration and Validation	32
5.1	Software and Hardware	32
5.2	Monitoring and Load Estimation	33
5.2.1	Streamflow Monitoring	33
5.2.2	Pollutant Monitoring	33
5.2.3	Load Estimation	34
5.3	Sensitivity Analysis.....	34
5.4	Calibration and Validation Strategy	35
5.5	Assessment of Model Fit	37
5.6	Crop Yields.....	37
5.7	Streamflow.....	38
5.8	Sediment.....	39
5.9	Phosphorus.....	40
5.10	Routing sub-model and bias-correction	41
5.11	Application of Bias Correction to Ungaged Basins.....	43
5.12	Comparing SWAT Loads with Grab Sample Data	43
5.13	Mainstem TP Transport.....	44
6	Model results.....	45
6.1	Pollutant Yields.....	45
6.2	Spatial Distribution.....	45
6.3	Temporal Distribution	46
6.4	Categorical Distribution	46
6.5	Loads.....	47
6.5.1	Relative Contributions by Source Category.....	47
7	Summary	47
8	Acknowledgements.....	48

9	References.....	50
10	Tables	55
11	Figures.....	79
12	Appendices.....	119
	Appendix D.1.....	119
	Appendix D.2.....	121
	Appendix D.3.....	137
	Appendix D.4.....	153
	Appendix D.5.....	160
	D.5.1 TSS.....	161
	D.5.2 TP.....	162
	Appendix D.6.....	163
	D.6.1 Streamflow.....	164
	D.6.2 Total Suspended Solids.....	177
	D.6.3 Total Phosphorus.....	183

List of Tables

Table 1 Generalization of Cropland Data Layer crop types	55
Table 2 Decision rules used to classify crop sequences into generalized agricultural rotation types	56
Table 3 Comparison of distribution of crop rotations with transects.....	58
Table 4 Final generalized land cover and land management types used in SWAT	59
Table 5 Soil attributes used in SWAT	60
Table 6 Statewide and municipality-specific datasets used to define urban model area extent	61
Table 7 Manning’s n values used for overland flow based on specific landcovers	62
Table 8 Summary statistics of Fluxmaster load estimation models of total suspended solids.....	63
Table 9 Summary statistics of Fluxmaster load estimation models of total phosphorus.....	65
Table 10 List of parameters used in sensitivity analysis.....	67
Table 11 Adjusted plant growth parameters for modeled crops.....	68
Table 12 Validation of SWAT crop yields.....	69
Table 13 Gage sites chosen for calibration of streamflow, total suspended solids, and total phosphorus	70
Table 14 Basin-wide parameter adjustments.....	71
Table 15 Parameter adjustments by Ecological Landscape.....	72
Table 16 General performance ratings for a monthly time step	73
Table 17 Monthly summary statistics for streamflow, total suspended solids, and total phosphorus.....	74
Table 18 Bias correction coefficients.....	75
Table 19 Final fit statistics of streamflow, total suspended solids, and total phosphorus.....	76
Table 20 Annual discharge, total phosphorus, and estimated TP delivery fractions for mainstem	77
Table 21 Relative contributions of total suspended solids and total phosphorus by source type	78

List of Figures

Figure 1 Upper Wisconsin River SWAT model area.....	79
Figure 2 Map of all 337 SWAT subbasin delineations.....	80
Figure 3 Method for defining crop rotations and land management.....	81
Figure 4 Approach for generalizing land management.....	82
Figure 5 Process of merging local knowledge with Cropland Data Layer (CDL) defined rotations.....	83
Figure 6 Final landcover map.....	84
Figure 7 Validating crop rotations with transect data.....	85
Figure 8 Years of corn in crop rotation by county	86
Figure 9 Comparison of generalized crop rotation to raw Cropland Data Layer (CDL).....	87
Figure 10 Validating generalized crop rotations definition with density of dairy facilities	88
Figure 11 Validating manure application rate of generalized land management with county-level statistics..	89
Figure 12 Schematic diagram of SSURGO data structure	90
Figure 13 Flow diagram of the soil aggregation process	91
Figure 14 Schematic diagram of SSURGO map unit.....	92
Figure 15 Map of Hydrologic Soil Groups	93
Figure 16 Map of landscape slope classes.....	94
Figure 17 Locations of municipal and industrial wastewater outfalls	95
Figure 18 Scatterplots of observed versus predicted lake volumes	96
Figure 19 Example illustrating methods for calculating geometries of internally draining areas	97
Figure 20 Map showing the areas draining to ponds and wetlands	98
Figure 21 Observed versus predicted ALPHA_BF SWAT parameter	99
Figure 22 Map showing the predicted ALPHA_BF for each SWAT subbasin	100
Figure 23 Map showing the estimated concentration of phosphorus in groundwater	101
Figure 24 Location of gage sites used in the calibration process.....	102
Figure 25 Map of Wisconsin Ecological Landscapes	103
Figure 26 SWAT model calibration workflow for streamflow, sediment, and nutrients.....	104
Figure 27 Bias correction gage association.....	105
Figure 28 Map of annual average total suspended solids yields	106
Figure 29 Map of annual average total phosphorus yields	107
Figure 30 Maps of annual average total suspended solids yields by land use.....	108
Figure 31 Maps of annual average total phosphorus yields by land use.....	109
Figure 32 Boxplot showing the seasonal variability of total suspended solids yields.....	110
Figure 33 Boxplot showing the seasonal variability of total phosphorus yields	111
Figure 34 Boxplot showing the variability of total suspended solids yields by landuse	112
Figure 35 Boxplot showing the variability of total phosphorus yields by landuse.....	113
Figure 36 Boxplot showing the variability of total phosphorus yields by fertilizer type	114
Figure 37 Maps of annual average percent of in-stream total suspended solids loads by source category.....	115
Figure 38 Maps of annual average percent of in-stream total phosphorus loads by source category.....	116
Figure 39 Plot of mean discharge on the mainstem Wisconsin River between Merrill and Prairie du Sac	117
Figure 40 Annual total phosphorus vs: drainage area on the mainstem between Merrill and Prairie du Sac.....	118

Abbreviations

ArcSWAT	ArcGIS plug-in software for SWAT configuration
CDL	Cropland Data Layer
CLU	Common Land Unit
CSP EL	Central Sand Plains Ecological Landscape
DATCP	Department of Agriculture, Trade, and Consumer Protection
DAYMET	Daily surface weather and climatological summaries
DEM	Digital Elevation Model
EL	Ecological Landscape
EPA	Environmental Protection Agency
FT EL	Forest Transition Ecological Landscape
FWMC	Flow-Weighted Mean Concentration
HUC	Hydrologic Unit Code
HRU	Hydrologic Response Unit
HSG	Hydrologic Soil Group
MS4	Municipal Separate Storm Sewer System
NASS	National Agricultural Statistics Service
NED	National Elevation Dataset
NH EL	Northern Highland Ecological Landscape
NHDPlus	National Hydrography Dataset Plus
NLCD	National Land Cover Dataset
NRCS	Natural Resources Conservation Service
NSE	Nash-Sutcliffe Efficiency
NWIS	National Water Information System
OSD	Official Series Description
PBIAS	Percent Bias
PLSS	Public Land Survey System
(g)SSURGO	(gridded) Soil Survey Geographic Database
SUFI2	Sequential Uncertainty Fitting
SWAMP	System for Wastewater Applications, Monitoring, and Permits
SWAT	Soil Water Assessment Tool
SWAT-CUP	SWAT Calibration and Uncertainty Procedure
TMDL	Total Maximum Daily Load
TSS	Total Suspended Solids
TP	Total Phosphorus
USDA	United States Department of Agriculture
USGS	United States Geological Survey
USLE	Universal Soil Loss Equation
WCR EL	Western Coulees and Ridges Ecological Landscape
WDNR	Wisconsin Department of Natural Resources

WHDPlus	Wisconsin Hydrography Dataset Plus
WinSLAMM	Source Loading and Management Model for Windows
WPDES	Wisconsin Pollutant Discharge Elimination System
WRB	Upper Wisconsin River Basin
WVIC	Wisconsin Valley Improvement Company
WWI	Wisconsin Wetland Inventory

2 Introduction

2.1 Background

The Wisconsin River Basin (WRB) Total Maximum Daily Load (TMDL) project requires the calculation of a TMDL scenario that results in all streams and lakes within the project area meeting water quality standards for total suspended solids (TSS) and total phosphorus (TP). The TMDL scenario will be used to calculate allocations that result in achieving these standards. This report describes the development of the model used to locate and quantify sources of these pollutants in the basin. The process of translating model output into TMDL allocations is not described in this report.

There are two distinctly different types of pollutant sources that contribute pollutants to WRB project area: wastewater continuously discharged from set points throughout the stream system (point sources), and diffuse sources of pollutants intermittently delivered from the landscape to waterways via runoff (non-point sources).

For the purpose of simulating pollution loads under existing conditions, point-source loads are estimated using TSS and TP concentration monitoring data, sampled according to Wisconsin Pollutant Discharge Elimination System (WPDES) permit requirements, together with flow data. Together this information allows us to accurately estimation the daily load associated with each permit.

Non-point source loads are estimated using a simulation model that predicts the daily load delivered to each stream, based on factors associated with runoff, such as weather, landcover and land-management practices, landscape topography, and soil characteristics, among others. Estimates of non-point-source loads are generally less accurate than their point-source counterparts because monitoring diffuse sources similarly to how permitted dischargers are monitored is infeasible over large extents. Rather, the simulation model makes assumptions about non-point source runoff based on transferrable scientific understanding, routes the runoff and pollutants through the stream system, and compares the resulting simulated loads to monitoring data collected at downstream sites.

The simulated point and non-point source loads are used to determine the magnitude, source and location of existing pollutant loads. In order to be able to use this information to develop TMDL allocations, the simulation model must be able to segregate point and non-point sources, and for non-point sources specifically, segregate uncontrollable (i.e. natural or background) daily loads from controllable ones (i.e., anthropogenic). The Soil and Water Assessment Tool (SWAT) model contains equations that fulfill these requirements. The SWAT model was chosen to simulate the majority of both point and non-point source daily load delivery, with the exception of urban areas, which were simulated using the Source Loading and Management Model for Windows (WinSLAMM).

2.2 SWAT

The SWAT model is the product of over 30 years of efforts to accurately simulate large-scale watershed hydrology using field-scale scientific findings. It has been used to simulate

watersheds all across the globe due to its ability to simulate diverse landscapes, its openly published source code, and the ability of users to control a large degree of detail within the default model. The primary outputs of a SWAT model are quantities (streamflow or water yield) and qualities (masses of physical and chemical components concentrated in water) of water at selected sites at a daily time step.

At its core, SWAT relies on field-level units that deliver water, sediment, and chemicals to streams. The unit in SWAT is referred to as the Hydrologic Response Unit (HRU). Each SWAT HRU is defined by a discrete combination of landcover, soil, and slope characteristics. Within each HRU, the user defines what crop is growing, if and how crops are managed (e.g., fertilizer applied to an agricultural crop), how the crop responds to its direct environment and management (weather, soil, and slope), and how water responds (both surface and groundwater) to the combination of plant growth processes and the direct physical environment (with some exceptional equations such as those used to simulate hydrologic response within urban areas).

SWAT HRUs are aggregated into subbasins. Subbasins collect water and other pollutants generated by each of its HRUs, and either routes it through small surface flow paths (“tributaries”), or through sub-surface flow, which SWAT separates into interflow, shallow aquifer, and deep aquifer components.

The combination of tributary and groundwater flow is then delivered to SWAT “reaches”. SWAT reaches represent streams and rivers. The primary properties of reaches in SWAT are geometric (e.g., length, width, depth, and gradient), however recent advances in SWAT allow users to simulate other water-quality processes within reaches, such as the deposition, re-suspension, and transformation of physical and chemical constituents though the alteration of water chemistry within reaches was limited within the WRB SWAT model. Although SWAT has rudimentary tools for simulating limnological processes, due to the scale and scope of this project, these tools were not used in favor of exporting SWAT output to more flexible lake models.

2.3 Study Area

The WRB covers 23,000 km², mostly within the northcentral region of Wisconsin, with a small area in Michigan, where the watershed boundary extends into the Upper Peninsula (Figure 1). The watershed associated with this study ends at outlet of Lake Wisconsin. Below Lake Wisconsin, there are currently no TP or TSS impairments on its main stem, the Wisconsin River runs the last third of its course to join the Mississippi River in southwestern Wisconsin.

The wide range of geologic formations in the WRB means there is a correspondingly wide range of hydrologic conditions. Much of this variation is attributable to the most recent glaciation. The northern region of the project area was covered by the Wisconsin Valley and Langlade lobes of the Laurentide Ice Sheet, and is therefore not well drained. Much of this region consists of wetlands and internally drained lakes or chains of lakes. The eastern edge of the watershed exhibits highly porous aggregate material, and internally drained landforms that are reminiscent of the terminus of the Green Bay glacial lobe. The central region is characterized by highly porous sands and a very flat landscape that is reminiscent

of weathering from Glacial Lake Wisconsin (not to be confused with the present-day Lake Wisconsin). Finally, the southwestern corner of the study area, commonly referred to as the “driftless area”—due to the absence of glacial “drift”—is the only region not impacted by recent glaciation; here the landscape is well drained with steep slopes and constrained valleys.

The main stem of the Wisconsin River supports a number of large industrial facilities that discharge wastewater directly to the river. Although there is some variety in the type industry that discharges to the Wisconsin River, the largest sectors are pulp and paper, and cheese processing. The majority of land in the project area is natural—forest, wetlands, and grasslands constitute 75%—or managed for agriculture (19%). The largest cities are Wausau, Stevens Point, and Marshfield with populations of 39,000, 26,600, and 18,600 respectively.

3 Basic Model Configuration

This section details the basic configuration and data processing steps taken during the development of this SWAT project.

3.1 Subbasin Delineation

The first step of configuring a SWAT model is delineating subbasins (Figure 2). Hydrologic and regulatory transitions were used to guide the placement of TMDL subbasin transitions. TMDL subbasin transitions were identified:

1. to address specific water quality impairments where local water quality does not meet codified standards. Consideration was given to streams that are likely to be impaired, but where sufficient monitoring data do not currently exist.
2. near point source outfalls. Delineations were not required to be at precisely the location of the outfall; if we could assume that streamflow does not significantly increase between the discharge location and the next downstream subbasin division, it was not necessary to further subdivide the subbasin at the discharge location.
3. at locations where water quantity and quality were measured during the model period for use in model calibration.
4. at major transitions of water quality standards, for instance at river impoundments that receive lake criteria.
5. at major hydrologic transitions such as the confluence of two large streams or where there are significant changes in landuse/landcover.

Beyond the above criteria, we made an effort to subdivide the remaining subbasins so that the resulting subbasins are of relatively homogenous area—having similarly sized subbasins results in more accurate timing of peak flows during runoff events.

After the location of subbasin outfalls were identified, we delineated the contributing area upstream of each outfall. Although ArcSWAT can automatically delineate model subbasins,

because of our specific reasons for creating subbasins outlined above, we manually created SWAT subbasins by aggregating the Wisconsin Hydrography Dataset Plus (WHDPlus) dataset (Diebel, Menuz, & Ruesch, 2013), which contains sub-watershed delineations within the Hydrologic Unit Code (HUC) 12 basins. HUC12 basins are standard watersheds created and maintained by the United States Geologic Survey [USGS]). We delineated 337 subbasins with an average size of 69 km² (standard deviation = 80 km²); larger subbasins were located in areas with fewer water quality impairments and point sources. This size is smaller than the average HUC12 watershed (84 km²), which is the scale at which TMDL projects are often implemented.

The Wisconsin River is an unusually large TMDL project area. Consequently, much of the point and non-point load reduction efforts will occur as nested HUC12 scale projects within the overall TMDL framework.

3.2 Land Cover and Land Management

The accuracy of landcover and land management is perhaps one of the most critical components of a SWAT model. An accurate representation of agriculture is particularly important in the WRB, where agriculture covers nearly 20% of the watershed and agricultural runoff contributes the majority of the phosphorus and sediment load in many of its tributary watersheds (Section 5.2). The SWAT model provides the opportunity to distinguish between land cover and land management. One of SWAT's strengths, and one of the primary reasons it was selected for the WRB TMDL modeling effort, is its ability to model variability in land management on a daily time step.

The objective of this effort was to develop and implement a methodology to define agricultural management by integrating geospatial data and analysis, local knowledge from county land and water conservation staff, private agronomists, and field data. The methodology was applied to agricultural landcover within the WRB. The result is a raster spatial layer that defines spatiotemporal variability of agricultural land management, such as crop rotation, tillage, and nutrient application.

3.2.1 Land Cover (step 1)

The basis of the composite land cover developed for the SWAT model is the United States Department of Agriculture (USDA) National Agricultural Statistics Service (NASS) 2011 Cropland Data Layer (CDL) for Wisconsin (NASS 2011). The layer, originally created to provide agricultural information for the major crops to the USDA Agricultural Statistics Boards, provides a gridded data layer that defines growing-season land cover at a cell resolution of 900 m² for Wisconsin using satellite imagery from a variety of satellites (NASS 2011). The 2011 CDL was selected because that year had improved accuracy statistics when compared to other years, and there were no significant flooding or drought events within the growing season. To improve the CDL wetland definition, mainly related to the misclassification of forested wetlands, information from the Wisconsin Wetlands Inventory (WWI) was integrated into the 2011 CDL. The WWI coverage provides the geographic extent of wetlands that have been digitized from aerial photography, verified through photo interpretation, and compared against soil surveys, topographic maps, and previous wetland inventories (WDNR 1991).

To improve the landcover definition other basin-wide information was integrated into the 2011 CDL in the following order: Wisconsin Wetlands Inventory (WWI), hand-digitized cranberry bogs, and conservation reserve program land (CRP). The WWI coverage provides the geographic extent of wetlands that have been digitized from aerial photography, verified through photo interpretation, and compared against soil surveys, topographic maps, and previous wetland inventories (WDNR 1991). The 2011 CDL was unable to properly capture the extent of cranberries due to the timing of the satellite imagery. As a result, the cranberry bog extent was digitized from Bing aerial photo basemaps (2011). Cranberries were not represented explicitly in the SWAT model, but rather set to wetland landcover so that they could be incorporated into later versions of the SWAT model if better information on Wisconsin cranberry management becomes available. The CRP land extent was captured from a 2008 USDA Common Land Unit (CLU) attribute defining land designated as CRP. While the CRP extent can change from year to year, the use of the 2008 extent provided a midpoint condition for the simulation period.

3.2.2 Crop Rotations (step 2)

To inform the SWAT model with spatial agricultural information, we aggregated 5 years of CDL layers (2008–2012) into thematic cropping rotations. The class resolution of the CDL was originally too fine, so crops were first aggregated together into groups of similar crops or crops that are often confused in the classification process (Table 1). Crop sequences were originally defined by Public Land Service System (PLSS) $\frac{1}{4}$ -sections (approximately 160 acres¹) by choosing the majority crop within each $\frac{1}{4}$ section for each year. The dominant crop per $\frac{1}{4}$ -section for each of the five years was concatenated together to create a crop sequence for each $\frac{1}{4}$ -section for the time period (Figure 3). This analysis resulted in a five-year sequence of crops for each $\frac{1}{4}$ -section which was then classified into an agricultural rotation type based on a set of rules. After refinements associated with local knowledge (Section 3.2.3), the rotations were divided into the following general types: 1) Dairy Rotation, 2) Cash Grain, 3) Continuous Corn, 4) Pasture/Hay, and 5) Potato/Vegetable. We identified the rotation type for each $\frac{1}{4}$ -section's five-year sequence by creating a hierarchical algorithm that binned crop rotation types based on the presence or absence of certain crops that were indicative of general rotation types (Table 2). Dairy rotations, for instance, required at least one year of corn in 5 years and at least one year of alfalfa/hay. The spatially identified crop rotation types provided distinct parcels to link with more detailed, regionally specific agricultural management data.

Although the general crop rotation types provide more information than using a single year of the CDL to define agriculture in the WRB, no unified dataset exists with information regarding land management such as tillage, fertilization, and the timing of specific operations. The satellite imagery was trusted to spatially identify crops and rotation types better than a local expert, but local experts were trusted to inform the satellite-identified rotations with land management information. Local knowledge became essential as county

¹ For ease of reporting, agricultural measurements in this section of the report are described in United States customary units, however because the model operates using metric units, all other quantities are described in metric.

and regional experts were brought together to create regionally-specific information at the quarter section level.

3.2.3 Interviews with Local Experts (step 3)

The crop rotation dataset described in Section 3.2.2 provides an initial assessment of agriculture that distinguishes crop rotational themes. However, there were still uncertainties in the development of the initial crop rotation rules, which were refined in the process of interviewing local experts (Figure 4). More importantly, the analysis fails to provide a complete assessment of agricultural management, as it does not ascertain differences in similar rotations based on variability in tillage and nutrient applications. These practices differ for all crop rotations types by region based on factors such as soil condition, slope, and regional conservation directives. Management information could only be found through local knowledge.

The methodology for defining agricultural management through localized knowledge originated from an effort conducted in the Mead Lake Watershed in Central Wisconsin (Freihoefer & McGinley, 2007). In that study, they used a combination of farm surveys, transect surveys, land evaluations, and interviews completed by county staff. The study found that this process was an effective and efficient method for informing land-management operations for a SWAT model.

Upon completion of the initial definition of crop sequences using the CDL, meetings were set up with regional staff to: 1) correct the spatial definition of the sequences, and 2) develop underlying management schemes involving the timing of agricultural activities, tillage types, and rate and type of nutrient application (chemical fertilizer or manure). A set of interview questions was created for the regional staff along with a brief webinar outlining the project and the goals of the WRB TMDL team (Appendix D.1).

The meetings were targeted towards county land and water conservationists and their staff, however additional expertise from individuals such as University of Wisconsin–Extension Agricultural Agents and Natural Resources Conservation Service (NRCS) staff were welcome and recommended if county conservationists needed confirmation regarding any component of the agricultural definition. Each meeting lasted between two and four hours and was accompanied by a large map (approximately 3'x4') of the dominant crop rotations per ¼-section (160 acres) that was identified using the CDL rules (Section 3.2.2) set for 2008-2012.

Some counties provided their information on a ¼-section by ¼-section grid; staff would reference plat books, Nutrient Management Plans (NMPs), county GIS data, and other information sources to get the most accurate ¼-section level management data. However, some counties opted to take a more generalized approach by providing percentages by region or conditions under which certain management types exist. For example, Marathon County reported that approximately 60% of dairy farmers have a “daily haul” type dairy rotation and the other 40% applied liquid manure—in these cases, management activities were applied to crop rotations randomly and proportionally across the region based on the given rule. Additionally, using long-term land management inventories in the Pleasant Valley watershed in south-central Wisconsin, we found that when corn was being grown

continuously over a 5-year period according to the CDL, it was equally likely to be a cash grain operation or a dairy rotation, so these two rotations were split equally and distributed randomly across generalized rotations from the CDL that were defined as “continuous corn”.

After all interviews were complete, the land management data was digitized and refined. Many of the interviewees responded exactly the same (e.g., 10,000 gallons per acre of liquid manure was a common application rate)—these redundancies were eliminated by aggregating information together. In other cases, land management operations were thematically similar, and could therefore be aggregated together justifiably using best professional judgment. These aggregations were then reviewed by a panel of other WDNR staff, faculty from the University of Wisconsin, and private agronomists, manure haulers, and crop consultants during a 3-hour open-forum discussion. The agricultural management process was well received by the group and only minor adjustments were made to a few of the rotations. For example, the starter fertilizer applications were changed from 200 pounds per acre per year to 150 pounds per acre per year.

3.2.4 Land Cover and Management Integration (step 4)

County staff members served as local experts on agricultural land management identification and refinement of the rotation rules described in Section 3.2.3, but the spatial extent of the crop rotations defined by the USDA CDL were assumed to provide a better spatial definition. The result was two separate datasets created by steps 2 and 3 requiring the integration of the management information provided by each county and applying it to the WDNR approach developed from the USDA CDL.

The final layer integrated the interview-based land management dataset (by $\frac{1}{4}$ -section) into the CDL-based crop rotation dataset (by 900 m² pixel). The land management dataset was first converted from vector-based $\frac{1}{4}$ -sections to raster files. We then generalized the county-specific rotations into 15 unique crop rotations (Appendix D.2).

Due to misclassification of the CDL, the raster product resulting from the above integration still had issues with speckle noise. We reduced this speckle noise to avoid over-representing agriculture. To accomplish this reduction, we excluded agricultural cells that fell outside of parcels defined by the CLU layer. These exclusions were replaced by values of neighboring cells using the ArcGIS (ESRI, 2012) expand function. We also refined pixel-based crop rotation classifications within CLU boundaries by homogenizing pixels to the majority crop rotation within a CLU boundary.

To ensure the alignment of the spatial definition of crop rotations with $\frac{1}{4}$ -section land management information, we used a nearest neighbor approach. For example, if the CDL rotation analysis defined a small area of dairy rotation within an area defined by the county staff as a cash grain rotation, the closest dairy rotation management information would be applied to the CDL defined dairy rotation rather than it being overwritten as cash grain. A schematic of this process is provided in Figure 5.

Finally, to ensure that no single year was weighted too heavily with a specific crop, we duplicated each rotation three times. However, each of the three versions was staggered by

two years. For example, a dairy rotation with corn (C) and alfalfa (A) represented as CCAAAA, became three management operations: 1) CCAAAA, 2) AACCAA, and 3) AAAACC. These duplications were then randomly distributed among the locations where the original land management operation occurred. A map of the final landcover layer is provided in Figure 6.

3.2.5 Validation

3.2.5.1 Transects

WinTransect (WI DATCP, 2010) is a soil conservation assessment tool that was developed by DATCP and Purdue University. A transect survey is a road-side assessment of crop type, tillage, and residue cover. Transects were intended to be conducted on an annual basis to provide more accountability for soil conservation efforts, as well as be an option for “providing statistically reliable county and state data.” Five of the counties in the WRB had relevant transect data; Sauk County provided data from 2008-2013, Vernon County provided data from 2009-2013, Marathon County provided data from 2006-2013, Juneau County provided data from 2005-2010, and Wood County provided data from 2005-2012 for a total of 2,617 observations.

The crop types from the transect data were concatenated for each point using the same rules set as the CDL rotation identification described in Section 3.2.2. This provided a qualitative baseline assessment of the accuracy of the rotation types defined by the CDL. However, the two differed spatially since the transect points are not generalized for dominance within their respective $\frac{1}{4}$ -sections, but rather, are specific to a field. As a result, only a qualitative comparison was made between the countywide rotation distribution from the CDL rotation to the countywide rotation distribution from the transect data (Figure 7). Generally, we saw the same distribution of crop rotations, which helped validate the WDNR Approach for crop rotation identification (Table 3).

More importantly, the transect surveys were also used as a guideline for areas where gaps existed in the data. For example, most of the counties had reported two years of corn (either for grain or silage) in a six year dairy rotation. However, there were several exceptions where three or four years of corn in a six year dairy rotation was reported as the most common. To assess the validity of this the number of corn years observed in a 6 year period from transect data at dairy field points was examined (Figure 8), and the data showed that the majority of dairy operations planted 1 or 2 years of corn with some regional differences in frequency.

3.2.5.2 Crop Acreage

A simple check to see if the crop acreage was still accurate after our generalization process (Sections 3.2.1 through 3.2.4) was to compare a given crop’s areal extent from the CDL with the given crop’s extent post-CDL rotation generalizations. Corn is the crop with the highest user and producer accuracies that the CDL identifies, is the most prevalent crop in harvested acreage, and is included in the widest variety of rotation types. For these reasons, it was the best crop to use for comparison with the generalized rotations that were developed. The average annual corn acreage from the CDL is very similar to average annual corn acreage in the WDNR approach (Figure 9).

3.2.5.3 Dairy Producer Locations

The DATCP licensed dairy producer locations were used to develop a density map of dairy farmers. This density map is based on location of licensed dairy farm facilities, not the location and subsequent density of dairy farm fields. However, when the producer location densities were compared to the density of dairy rotation fields from the CDL analysis there are very similar trends (Figure 10). The initial concern was that the dairy rotation density would just follow the general density of agricultural production. However, it can be seen in Figure 10 that the non-dairy rotations defined by the CDL follow a distinctly different pattern. This validation helped to corroborate the other analyses, as it provided more certainty in the WDNR approach's ability to identify fields that are managed by dairy farms.

3.2.5.4 Total Mass of Applied Manure

Similar to past SWAT applications, cattle inventories were used to validate the amount of manure application reported by the counties, as well as the extent of our dairy rotation identification (Baumgart, 2005; Freihoefer & McGinley, 2007; Timm & McGinley, 2011).

This was done by calculating an average manure output per cow per year, multiplying that value by the total number of cows per county, and then comparing that value with the total average amount of manure applied per year to dairy fields. Of course, not all cow manure is captured and applied to dairy fields. There are other management schemes such as managed grazed lands and seasonally pastured animals that must be accounted for. Additionally, there are circumstances where manure is applied to non-dairy rotations, for example, when sold to other non-dairy farmers or used for non-fertilizer needs. These are difficult situations to account for, thus the estimates only needed to align within a reasonable range of the cattle inventory values (Figure 11). See Appendix D.4 for a table of manure comparison calculations for these counties and a summary of this appendix can be found in Table 4.

3.3 Soil Data Aggregation

Soils are a critical part of the SWAT modeling framework; properties such as texture, hydraulic conductivity, and available water capacity play a critical role in determining system hydrology. To inform the SWAT model with soil-related data, we used the county-scale Soil Survey Geographical Database (SSURGO) (NRCS 2014). The SSURGO database is structured based on three levels of information: map units, components, and horizons (Figure 12). Horizons are the fundamental unit of soil in SSURGO, and are therefore where the majority of soil information is stored in the database. Components are aggregations of horizons that represent a full soil profile, typically conforming to the Official Series Description (OSD). Map units are discrete polygons drawn on a map (originally mapped at scales from 1:12,000 to 1:63,360) that contain one or more components that are stored non-spatially in the database—that is, only a list of components and their percent composition of the map unit is given.

We chose to use the gSSURGO data distribution of SSURGO because gSSURGO is a form of the SSURGO database that is packaged in a more convenient form for large extent projects such as the WRB TMDL. The tabular data representing the components and horizons were joined together so that each component had the data required for the SWAT model (Table

5). For all these properties, the representative value (as opposed to the critical value) given by SSURGO was used.

Defining SWAT model HRUs requires balancing the need to incorporate the most important information, without overloading the model with redundant or insignificant information. To reduce the number of HRUs in the model and generally create a simpler and more efficient model, we aggregated soils together based on similarity of several key properties that impact the hydrologic cycle. This was a two-step process: first, components within map units were aggregated together, and second, map units were aggregated together based on similarity (Figure 13).

Several changes were made to the dataset before aggregation, in order to facilitate processing. Soil organic carbon content is required by SWAT, but is given by SSURGO as soil organic matter. The percent organic matter value given in SSURGO was converted to percent organic carbon by multiplying by 50%, which is the generally accepted average carbon content of soil organic matter (Brady & Weil, 2010). The hydrologic soil group (HSG) is denoted as a letter in SSURGO, either A through D, or if the soil has different characteristics when drained, as two letters, A/D, B/D or C/D, the former is if the soil is drained (e.g., through tiling or ditching), while the latter is the drainage class of soil in its natural state. In order to average the different components it was necessary to convert these letters into numbers; groups A through D were converted to integers 1 through 4 to correspond with increasingly wetter drainage conditions. Once a number was obtained for the HSG, it was treated as any other soil property in the aggregation process, then rounded to the nearest integer, and converted in the same manner to a letter once the aggregation was finished.

For those components with dual HSGs, we assumed that if greater than 10% of the area in the map unit was agriculture, the SSURGO map unit would be split into two separate polygons, one where land was assumed to be drained and the other not drained. Conversely, if the land use was not majority agriculture then the land was assumed to not be drained, and the “D” designation was chosen. Where map unit polygons were greater than 10% agriculture, raster pixels from the land cover dataset (Section 0) that represent agricultural land cover types were used to define the boundaries of drained land. For these map units, the agricultural portion of the polygon was assigned the first letter of the dual hydrologic soil group (e.g., “A” for “A/D”), and the non-agricultural portion was assigned a “D” soil type.

3.3.1 Component-Level Aggregation (step 1)

The first aggregation step was to aggregate components by map unit to conform to the SWAT soils data structure. The data structure for soils in SWAT does not directly conform to SSURGO data structure; the main difference being that there is no analogue to the SSURGO *component* level in SWAT—in other words, soils in SWAT cannot be subdivided (Figure 14). We aggregated components by computing component-weighted averages of each soil property for any given depth of soil from the soil surface to the average depth (Gatzke et al., 2011). These averages were computed using the `s1ab` function in the `aqp` package (Beaudette, Roudier, & O’Geen, 2013) in R statistical software (R Core Team,

2013). We used this algorithm to apply a depth-weighted average to each horizon, while also weighting the percent composition of each component. The depth and number of horizons of the aggregated soil profile produced by this algorithm must be specified before processing. The depth was calculated as a weighted mean of the full depths of soil profile in each of the components, with the weights equal to the percent composition of each component. Since the number of horizons was assumed not to matter as much as the maximum depth, an arbitrary number of five horizons was chosen for the aggregation algorithm.

Using the above aggregation method 48,585 individual soil components were aggregated to 1,603 map units. Because the HRUs used in SWAT were derived using unique combinations of land use, slope and soil types, this number of soil map units was still too many for efficient computation and so a second step of soils data aggregation was necessary to further reduce the number of soil types.

3.3.2 Map-unit-level aggregation (step 2)

Other researchers have aggregated soil types by their taxonomic class (Gatzke et al., 2011). However, Soil Taxonomy, the soil classification system of the US primarily classifies based on soil morphology and not necessarily on properties relevant to SWAT. We decided that the most relevant soils information to SWAT is hydrological data, specifically the HSG (Figure 15), which is one of the two components used to designate soil curve number (NRCS, 1986). Groups of the same HSG were split into clusters of homogeneous soil properties. The map units within each of these clusters were then averaged together to create an average profile for that homogeneous set of soils. These averages were then used as the soil types for the HRU definitions and the SWAT modeling.

To begin, each map unit (each of which is an aggregation of components, as described above) was placed into one of four groups according to its hydrologic soil group, A, B, C or D. To subdivide these groups further, a clustering algorithm was used to objectively create clusters of map units with homogeneous soil properties. For this purpose, we used Gaussian mixture models to assign map units to clusters. The mixture model approach we used was implemented within the `McLust` function in the `mcLust` package in R (Fraley, Raftery, Murphy, & Srucca, 2012). A mixture model is a probabilistic model for representing the presence of subpopulations within an overall population. In our case, the overall population would be the group of map units of similar hydrologic soil groups (i.e., all map units with an HSG of A), while the unknown subpopulations are the clusters of map units with similar distributions of soil properties (such as a clusters of sandier soils, shallow soils, or slow saturated conductivity). We allowed the clustering algorithm to choose any number of clusters from 1 to 100 allowing the algorithm to converge on an optimal number of clusters. The resulting numbers of clusters within each HSG were 41 for A, 41 for B, 66 for C, and 15 for D. We also reserved a separate HSG designation for drained classes that we clustered together regardless of their drained HSG type; we assumed that drained soil types are more similar to other drained soils than those without drainage. In the case of drained soil clusters, the HSG was estimated by converting the drained HSG designations to integers ($\{A,B,C,D\} = \{1,2,3,4\}$) and computing the average. A total of 11 clusters were created for drained HSG map units.

In order to use the clustering function we had to put our data in a format in which it could be used by the `Mc1ust` function. We calculated horizon depth-weighted averages of each soil property for each map unit, essentially collapsing the soil profile down to one aggregate horizon with average properties. Profile depth was still considered in the clustering algorithm using the total depth of the profile.

After each map unit had been assigned to a cluster, the map units within each cluster were aggregated together to form a composite or average soil profile. The same soil profile aggregation algorithm (Beaudette et al., 2013) used to aggregate several components together in the first step was used to combine the soil profiles of a cluster into one composite soil profile. In this implementation, each map unit was given equal weight in the aggregation algorithm.

Not every map unit was included in the clustering procedure. Several of the soil property fields of the SSURGO dataset were not populated or commonly had “no data” values; these properties were not used in the clustering process so the spurious zeros would not influence the algorithm. These properties were coarse fragments, calcium carbonate, and electrical conductivity. Albedo and pH were also excluded from the clustering algorithm. Map units that had no HSG designation were not included, nor were map units that did not have information on the soil properties of the horizons. Examining these excluded map units revealed that they were generally disturbed landscapes or those without a significant soil layer such as pits, landfills, urban or made land, rock outcrops, and water. These miscellaneous map units were all grouped together as one cluster with the exception of water. All water map units were collapsed into one using properties described in the default ArcSWAT SSURGO database².

3.4 Slope Classification

Topographic features are characterized at the subbasin level in SWAT. Using ArcSWAT software, we created a slope grid within the same grid domain as our basin-wide DEM (900 m² resolution) using the National Elevation Dataset (NED; data available from the U.S. Geological Survey). The slopes for each subbasin were grouped into five quantile classes (Figure 16) for the purpose of defining HRUs (Section 3.5). Each class contained approximately equal numbers of grid cells whose value fell within the range of values of each bin. These bins in percent were 0.0–0.5, 0.5–1.5, 1.5–3.0, 3.0–5.8, and > 5.8 (or in degrees, 0–0.87, 0.87–2.62, 2.62–5.24, 5.24–10.2 and > 10.2). After HRU definition (Section 3.5), slopes were set to back to the average slope of the HRU rather than a uniform value associated with one of the above bins. The ArcSWAT software also attempts to estimate slope lengths, however these estimates have been found to be high, and so the following alternative method was used (Baumgart, 2005):

²http://swat.tamu.edu/media/63316/SWAT_US_SSURGO_Soils.zip

Equation 1

$$LS = \frac{91.4}{(S + 1)^{0.4}}$$

where LS is the slope length in meters, and S is the average slope of the HRU expressed as a percent.

3.5 HRU Definition

The hydrologic response units in SWAT are defined by unique combinations of land use, soils, and slope class and are unique for every subbasin. If every combination were honored, there would be tens of thousands of HRUs and the model would take an impractical amount of time to run while having a number of functional redundancies within it. To reduce the number of HRUs, ArcSWAT allows for the removal of small HRUs; therefore, by setting a minimum threshold for each landcover, soils, and slope class, we reduced the number of overall HRUs, according to the following process. First, if a given landcover covered less than 1% of a subbasin, we excluded it and proportionally reallocated the remaining landcover classes so that they would add to 100%. Second, within the remaining landcover classes, if a given soil type covered less than 20% of a landcover class, it was excluded and reallocated in the same way as landcover. Finally, within the remaining landcover/soil combinations, if a given slope class covered less than 50% of a landcover/soil combination, it was excluded and reallocated. This means that only the dominant slope class is used for a given landcover/soil combination. This iterative method of exclusion resulted in 5,351 HRUs - a manageable number for performing calibrations, but yet detailed enough where there is little data resolution lost.

3.6 Weather Data

Weather data was extracted from the DAYMET 1-km gridded climate dataset (Thornton et al., 2014) for each day during the 12-year period spanning January 1, 2002 to December 31, 2013. The weather data used for each subbasin was the data associated with the gridcell in the DAYMET dataset nearest to the geometric centroid of the subbasin. The weather variables extracted from DAYMET were precipitation, minimum and maximum temperature, day length, solar radiation, and vapor pressure. Precipitation, temperature, and solar radiation were used directly as input to the SWAT model. Relative humidity was derived by dividing DAYMET vapor pressure by saturated vapor pressure that was estimated by solving the Antoine equation:

Equation 2

$$\log_{10}p = A - \frac{B}{C + T}$$

where p is saturated vapor pressure, T is average daily temperature from DAYMET, and A , B , and C are constants associated with water: 8.1, 1731, and 233 respectively. Wind speed is not a variable packaged with DAYMET. We compiled wind speed data using an online tool provided by SWAT developers at Texas A&M University (<http://globalweather.tamu.edu/>). The wind speed data is ultimately derived from the

Climate Forecast System Reanalysis (CFSR) at the National Centers for Environmental Prediction (NCEP).

Deterministic models such as SWAT usually perform better with a spin-up period of several years to allow the water budget and other physical and chemical processes of the system to equilibrate. We chose a spin-up period equal in length to the model period of 24 years. This is an unusually long spin-up period for a SWAT model. However, we found that a longer simulation was required for the unique groundwater dynamics of certain regions in the basin to equilibrate. For these 24 years, weather was stochastically simulated by SWAT using patterns of historic weather between the years of 1961 and 2010.

3.7 Point Sources

A complete inventory was conducted that compiled all permitted wastewater surface outfalls within the WRB (Figure 17). This inventory is required for simulating conditions for the SWAT modeling period of 2002–2013. The inventory process involved querying existing WDNR databases, verifying with Regional WDNR staff, and developing methods to consistently account for gaps in data.

A list of facilities with WPDES permits and their surface water outfalls within WRB was generated from WDNR's SWAMP (System for Wastewater Applications, Monitoring, and Permits) database. This list was verified by regional WDNR basin engineers to ensure no outfalls were missing from the list. In addition, their location and receiving water were also verified.

To properly calibrate the SWAT model, wastewater flows, as well as TP and TSS loads were required. Data related to discharge flows, TP concentrations, and TSS concentrations were queried from the SWAMP database. Sample values were averaged for each month from 2002 to 2013. These values were reviewed by the basin engineers for each outfall to check for anomalous values and identify data gaps.

For wastewater facilities without reporting requirements for one or more of the desired variables, the complete dataset was not available through SWAMP. Since a complete record of flow, TP, and TSS was required for each facility outfall, data gaps were filled in using other available information. Those other sources of available information included sample results submitted as part of permit applications, averages of other data available for a particular outfall, influent values for flows where influent flow equals effluent flow, the value of the closest available month, or requesting data from the facility. Also, some flow values were adjusted if it appeared that the facility discharged for only part of a particular month. To calculate TP and TSS loads for input to the SWAT model, the monthly average flows are multiplied by the TP or TSS concentrations, respectively.

For facilities with outfalls that intake river water, WDNR determined whether or not there was additional TP or TSS (above what was in the river water) added before being discharged. If not, the outfall was considered to have no net discharge and the TP and TSS concentrations were set to zero. If there was addition, we used the closest available river sample data to subtract out the river concentration from what was being discharged, giving a net discharge less than what was measured at the outfall.

4 Additional Model Configuration

4.1 Specific Agricultural Operations

4.1.1 Tillage

The types of tillage practiced on farms were reported to the WDNR by county conservation staff and local experts. County staff mapped the dominant tillage practices within each PLSS quarter section in agricultural land use. Specifically, for each PLSS ¼-section, tillage timing (e.g., spring or fall) and type (e.g., chisel disk or moldboard plow) was reported across a 6-year crop rotation. We used transect survey data collected by county staff to confirm the reported tillage types and timing using the methods described in Section 3.2.5.1. For example, fall tillage is predominant in the north central WRB and spring tillage is predominant in the southern WRB—a deviation from this pattern would flag it for further confirmation, which was mainly from professional agronomists working within the region.

4.1.2 Inorganic Fertilizers

The starter fertilizer application was changed from 0.22 to 0.17 metric tons per hectare per year with an NPK composition of 20-10-18, as per the recommendations of a panel of WDNR staff, faculty from the University of Wisconsin, private agronomists, manure haulers, and crop consultants.

A nitrogen auto-fertilization routine was added to SWAT's management operations. This operation applies nitrogen as needed to minimize plant stress due to nitrogen limitation, and therefore maintain proper plant growth. This assumption may not be realistic; as a result, the model should not be used to assess nitrogen loads in surface waters.

4.1.3 Tile drains

Tile drains were assumed to exist where agriculture rotations (Section 3.2.2) spatially intersected soil types with dual hydrologic soil group designation (Section 3.3) on slopes less than 1.5% (Section 3.4). In locations we assumed to be tile drained, we assumed that the drains were 900 mm below the surface, to drain to field capacity 48 hours after exceeding it, and with a 20 hour lag period between water reaching the drain and reaching the stream [recommended parameters, (Arnold, Kiniry, et al., 2012)].

4.1.4 Irrigation

Irrigation was assumed to exist on every potato/vegetable rotation (Section 3.2.2). In irrigated locations where tile drains were assumed to exist, irrigation wells were assumed to draw from the shallow aquifer (i.e., an adjacent, underground well), to operate only when plants were exhibiting water stress, to lose 10% to evaporation and 1% to surface runoff, and to apply 90 mm each day it operates.

4.2 Canopy Storage

The storage and evaporation capacity of the forest canopy differs substantially across forest types. We used three different values of maximum canopy storage (in mm) for evergreen, deciduous, and mixed (average of evergreen and deciduous) forests (Wu &

Johnston, 2008). These values were 2.0, 6.6, and 4.3 mm, respectively. A value of 1.25 mm was used for all other landcover types (Zinke, 1967).

4.3 Soil Phosphorus

Soil phosphorus concentrations aggregated by county, for each year spanning 1974 to the present, were obtained from the University of Wisconsin Soil Testing Laboratory (University of Wisconsin–Madison Soil Science Department, n.d.). We used the annual average soil concentration nearest the beginning of the model spin-up period, 1995, to establish the starting concentrations. Starting soil phosphorus concentrations for each subbasin were estimated by calculating an area-weighted average of each county within a subbasin. The soil testing laboratory receives almost exclusively agricultural soils. To reflect this bias in the soil phosphorus data, only agricultural HRUs were assigned the subbasin average concentration, whereas non-agricultural HRUs were assigned SWAT’s default concentration (5 mg P/Kg). This default concentration is assumed to equilibrate over the 12-year model spin-up period. Soluble phosphorus concentrations were estimated as half of the reported phosphorus using the Bray-1 method measured with a spectrophotometer (Vadas & White, 2010). Organic phosphorus concentrations were estimated by assuming that phosphorus constitutes 0.85% of organic material measured by loss of weight upon ignition (Havlin, Beaton, Tisdale, & Nelson, 2005). SWAT allows soil phosphorus values to be set at every soil horizon, in our case we changed the soil phosphorus values only for the first horizon, the rest were left at the default values.

4.4 Urban Area Model

Runoff volume and pollutant loads generated by urban areas within the WRB were simulated using the Source Loading and Management Model for Windows (WinSLAMM v10.0). Urban runoff volumes, TSS and TP loads generated by WinSLAMM were then incorporated into the SWAT model as point-source discharges. Areas modeled in WinSLAMM were removed from the SWAT subbasin extents to avoid double counting. Urban area boundaries were derived from a combination of U.S. Census TIGER files, Wisconsin 1:24k hydrography, and for permitted MS4s, maps provided by municipalities (Table 6). The extent of urban areas modeled in WinSLAMM was defined as areas within the municipal limits of cities and villages; urbanized areas within townships that have an MS4 permit; and State Department of Transportation right-of-way located within an urbanized area, and county transportation right-of-way located within an urbanized area of a county that has a permitted MS excluding the following areas:

1. Large, contiguous non-urbanized³, undeveloped areas located within the municipal limits of a city or village
2. Areas mapped as open water (according to the USGS National Hydrography Dataset) within the municipal limits of a city or village

³“Urbanized areas” is defined as an area classified as such by the 2010 Decennial Census. For the purpose of this document “urbanized area” is a specific term that relates the census and should not be confused with the overall “urban model area”.

3. Undeveloped (based on visual inspection of 2010 aerial orthophotography) floodplain islands within the municipal limits of a city or village
4. Pixels within non-permitted urbanized areas that are not classified as developed according to the landcover dataset described in Section 3.2.1

4.4.1 Urban Subbasin Delineation

For urban model areas located within permitted MS4s that provided the WDNR with GIS storm sewer, sewershed, and outfall mapping, the urban model area draining to each TMDL reach was delineated according to the mapping provided, rather than SWAT subbasin boundaries. For unpermitted MS4s, and permitted MS4s that did not provide the aforementioned GIS mapping, SWAT subbasin boundaries were used to delineate urban model subbasins.

4.4.2 WinSLAMM methods

The major environmental factors in a WinSLAMM model are weather, land use, and soils. The same weather data used in the SWAT model was used for WinSLAMM (Thornton et al., 2014)—the DAYMET pixel nearest to the centroid of each municipality. Soils information also came from the same SSURGO dataset used in the SWAT model (NRCS 2014). The SSURGO dataset was binned into soil texture classes according to recommendations described in the WinSLAMM documentation: A = sand, B = silt, and {C,D} = clay. For each combination of municipality, municipality type (MS4 or non-permitted urban), subbasin, and soil texture class, WinSLAMM was run using the nearest DAYMET precipitation data. Daily simulated particulate and filterable forms of phosphorus were translated to organic and mineral forms, respectively, when input as point sources in the SWAT model.

For landuse, we used the standard “medium density residential, no alleys” land use file. This approach was used because the average annual TSS yield predicted by WinSLAMM for permitted MS4s in Wisconsin overall using mixed landuse files has been found to be similar to the average annual TSS yield generated by the “medium density residential no-alleys” file with the drainage system defined as curb and gutter (The Cadmus Group, 2011). This approach assumes no pollutant load reduction by control measures.

The monthly TSS and TP loads generated by urban model areas was calculated using a load per unit area (or yield) approach. The monthly TSS and TP yield for sand, silt, and clay soil textures were predicted in WinSLAMM for each municipality using rainfall specific to the municipality. We calculated the total load for each watershed within a municipality by multiplying constituent yields by the area of its associated soil type mapping unit, and summing the soil-specific loads within each urban subbasin (Section 4.4.1).

4.5 Ponds and Wetlands

The SWAT model simulates rainfall storage using the *ponds*, *wetlands*, and *potholes* functions, where ponds and wetlands are defined at the subbasin level and potholes are defined at the HRU level. Due to the large geographic area covered by the WRB SWAT model, we chose to model rainfall storage using only ponds, conceding that HRU-level storage was too detailed and did not match the scale of analysis, and aggregating both

ponds and wetlands together resulted in a more parsimonious model that simplified calibration.

The ponds function in SWAT requires at a minimum, input of geometric properties and hydraulic conductivity; a number of additional parameters to control sediment and chemical processes are optional. We calculated geometric properties using a combination of WHDPlus (Diebel et al., 2013), the Wisconsin 1:24k Hydrography Geodatabase (WDNR, 2015), the Wisconsin Lake Book (WDNR 2009), and terrain analysis. We set hydraulic conductivity to zero, reserving it as a calibration parameter.

4.5.1 Ponds

The geometric properties of ponds required as input by SWAT includes all of the following: the fraction of the subbasin that drains to a pond; the storage volume at the principal and emergency overflow elevations; and the surface area at the principal and emergency overflow elevations. The principal/emergency lexicon is adopted from reservoir management, but in SWAT they refer to normal conditions and flood conditions, respectively. We considered a waterbody to be a pond if it was designated as internally drained in the Wisconsin Hydrography Geodatabase (WDNR, 2015). We used the volume of the lake stored in the database to represent the principal volume in SWAT. The Wisconsin Hydrography Geodatabase was digitized from USGS topographic maps, so we assume that the interpretation of the aerial photography associated with the USGS topography maps was representative of normal conditions. We also assume that normal surface area matches normal volumes that were taken directly from Wisconsin Lakes (WDNR 2009).

In locations where the normal volume was not listed in Wisconsin Lakes (WDNR 2009), the maximum depth of the lake typically was. For those lakes where volume was not listed, we predicted their volume based on a fitted regression using maximum depth ($p < 0.001$) and surface area ($p < 0.001$) as predictors (Figure 18).

Equation 3

$$V = e^{-0.1+1.1*\ln(A)+0.6*\ln(D)}$$

Where maximum depth was not available, we fitted a separate regression using only surface area (Figure 18).

Equation 4

$$V = e^{0.7+1.3*\ln(A)}$$

In the above equations, **V** is the volume of any given lake in acre-feet, **A** is surface area in acres, and **D** is maximum depth in feet. The volumes were then converted to hectare-meters as they are used in SWAT.

The contributing area of each pond was estimated using the WHDPlus database (Diebel et al., 2013). WHDPlus includes a polygon feature class of watersheds of each hydrographic unit in the Wisconsin Hydrography Geodatabase. The watersheds of all lake-type hydrographic units defined as “landlocked” were selected, and the sums of the areas of these watersheds were used to define the percent of each subbasin that flows to a pond.

Emergency volume and surface area were estimated using terrain analysis. We simulated overtopping of ponds by "filling" the DEM—filling the DEM raises the elevation of grid cells within internally draining areas until the landscape simulates overtopping of internally draining areas. Once the DEM was filled, we calculated the elevation difference of each filled grid cell that intersected the internally draining area associated with the landlocked lake (Figure 19). To calculate emergency volume, we summed the elevation differences and multiplied by the grid cell area. This was done for each landlocked hydrographic unit in WHDPlus, and summarized for each of the 338 subbasins in the WRB.

Equation 5

$$V_{max,s} = \sum_{l=1}^m \sum_{c=1}^n (\Delta e_c \cdot 900)_l$$

Emergency volumes of all ponds within a given subbasin $V_{max,s}$ were calculated using the above equation where l represents a landlocked lake within a subbasin, c is a grid cell associated with the internally drained area of a landlocked lake, Δe_c is the elevation difference between the original DEM and the filled DEM for any grid cell c , and 900 is equal to the area in meters of all grid cells in the DEM.

4.6 Wetlands

Wetland parameters (the same as those calculated for ponds) were calculated for each subbasin using a terrain-based approach. A digital elevation model (DEM) was filled using the Fill function in ArcGIS, filling all of the sink areas and causing all simulated water to run off of the landscape. The original DEM was subtracted from the filled DEM to derive a surface of the depth of internally drained areas or sinks. This sinks layer shows the internally drained areas for the basin.

The areas classified by the CDL as herbaceous wetlands, woody wetlands, and cranberries were considered to be areas where wetland vegetation is likely to be found. If wetland vegetation exists it can be assumed that the landscape has a consistent wetland hydrology, enough that it is expressed in the vegetation. The intersection or overlap of the sinks layer and the wetland vegetation, as identified by the CDL, was considered to be the principal wetland surface area. To calculate principal storage volume, we assumed an average water depth for any given wetland to be 0.5 m, and then multiplied this by the principal surface area. For emergency surface area, we calculated the area of the spatial union of CDL wetlands and sink areas. To calculate the emergency storage volume, the volume of sinks were summed and then added to the principal storage volume. To determine the fraction of the subbasin that contributes to wetlands, the maximum surface area of the wetlands was divided by the subbasin area. Once all ponds and wetlands geometric properties were estimated, the two were combined (Figure 20) and modeled as a single entity.

There are precedents to using a terrain-based approach to defining wetland areas in SWAT. Almendinger and Murphy (2007) considered internally drained areas as wetlands (as

identified by remote sensing⁴) if they were not connected to the main channel and lakes were considered ponds in their SWAT model. Wetlands, identified through remote sensing, were considered SWAT wetlands only if they occur on the main channel. Similarly, Kirsch, Kirsch, and Arnold (2002) considered internally drained areas as wetlands in SWAT if they overlapped with remotely-sensed-defined wetlands; if they did not, they were considered ponds. Almendinger and Murphy (2007) modeled closed internal depressions as wetlands and open (those draining to the main channel) as ponds.

4.7 Evapotranspiration Equation

We selected the Penman-Monteith equation to model potential evapotranspiration across all subbasins, because it outperformed the other two options in SWAT (the Hargreaves and Priestley-Taylor equations) in both Nash-Sutcliffe coefficient and percent bias, when comparing modeled water yield to observed water yield. at 29 sites across the basin. The Penman-Monteith equation is an energy balance and aerodynamic formula that computes water evaporation from vegetated surfaces. The equation estimates evapotranspiration rates based on solar radiation, temperature, wind speed, and relative humidity.

4.8 Groundwater

4.8.1 Groundwater Inflow (Baseflow)

In SWAT, the relative contribution and timing of streamflow as baseflow is determined by the ALPHA_BF parameter and can be adjusted for each subbasin. An effort was made to regionalize this variable to account for the wide variations in baseflow conditions across the WRB. A regression model was fitted that relates baseflow to upstream watershed characteristics. Then this model was used to predict ALPHA_BF at ungauged sites in the WRB. In order to construct a model relating baseflow contribution to watershed characteristics it was necessary to obtain observed values of baseflow. The Baseflow Program (Arnold, Allen, Muttiah, & Bernhardt, 1995) was used to estimate baseflow from daily streamflow data. All monitoring stations in Wisconsin (USGS 2014) that met the requirements of the Baseflow Program were used, excluding sites with upstream watersheds less than 50 km² or greater than 1,000 km² (Arnold, Muttiah, Srinivasan, & Allen, 2000).

The baseflow algorithm requires continuous daily observations of streamflow for at least one year, from which it determines the baseflow contribution from the hydrograph. After the observed data were downloaded, they were processed to ensure that only contiguous periods of streamflow of at least one year were used in the routine. For this analysis gaps of up to nine days were allowed in the record and still considered contiguous. If a monitoring site had one or more gaps of longer than nine days, it was split at the gaps into separate records and each part assessed independently. Therefore, it was possible for a monitoring site to have several periods of contiguous streamflow records.

⁴ Specifically, the remotely sensed imagery was from the WISCLAND data set; a dataset of landcover determined from LANDSAT imagery.

The Baseflow Program was run at each USGS gage site and the program output and ALPHA_BF was estimated (Arnold et al., 1995). This smoothing algorithm produces several outputs, one for each successive pass of the smoothing filter. The final pass (third and smoothest) was used in the regression model. For sites with multiple records, the Baseflow program values were averaged, weighting the values by the length of the record.

The resulting ALPHA_BF estimates from the Baseflow Program were site-specific, and thus were only valid for upstream subbasins. To parameterize ALPHA_BF for ungauged subbasins, we fit a multiple linear regression model to predict baseflow using upstream watershed characteristics. Data regarding the landscape characteristics of the watershed for each monitoring station were retrieved from WHDPlus (Diebel et al., 2013). Additionally, the Environmental Protection Agency’s (EPA) Ecoregion boundaries level III was used as a categorical variable. We tested a suite of geologic, soil, and topographic watershed characteristics that could potentially affect baseflow by calculating Pearson’s correlation coefficients and visually analyzing scatterplots. The final model was selected based on R^2 . We used residual plots to examine evidence of model bias. The best model (Equation 6 and Figure 21) used average slope of watershed, average permeability, and the EPA ecoregion boundaries. The ecoregion boundaries were used as a factor on the watershed slope term. The ecoregion term with slope was meant to allow for the expression of the effect of slope on the baseflow contribution in different regions in the WRB (e.g., different slope terms for the Driftless Area and the Central Sands ecoregions).

Equation 6

$$A = \beta_0 + \beta_1 E_1 S + \beta_2 E_2 S + \beta_3 E_3 S + \beta_4 E_4 S + \beta_4 P$$

Where **A** represents the SWAT ALPHA_BF parameter controlling baseflow, **P** is average surface permeability of the watershed, **S** is the average slope of the watershed, while **E₁₋₄** are dummy variables denoting one of four ecoregion within the WRB (i.e., the slope term of **S** varies by ecoregion).

This model was used to predict the ALPHA_BF for every small watershed in the WHDPlus dataset. An area-weighted average of these small watersheds was taken for each SWAT subbasin to aggregate the ALPHA_BF predictions. These values were used to update ALPHA_BF in the groundwater files for each subbasin. The resulting distribution of the ALPHA_BF parameter in the WRB can be found in Figure 22.

4.8.2 Baseflow Phosphorus

Time-variable TP concentrations in groundwater are not modeled by SWAT, but are rather set manually based on an estimate of naturally occurring TP (GW_SOLP parameter in SWAT). Rather than estimating a single value of baseflow phosphorus concentration for the entire WRB, we attempted to regionalize this parameter. In the Wisconsin River Basin SWAT model, we used values of reference baseflow phosphorus from a USGS study of nutrient concentrations in wadeable streams in Wisconsin (Robertson, Graczyk, et al., 2006) where the authors used a multiple linear regression equation to predict reference phosphorus in nutrient boundaries known as “environmental phosphorus zones”, which

they use as a way of dividing the state into smaller homogeneous regions. These zones were derived in an earlier study by Robertson, Saad, and Heisey (2006).

For each of the phosphorus zones, the percent land area in agricultural use and percent land in urban use was calculated along with the number of point sources. Using these variables, a multiple linear regression model predicting the concentration of phosphorus was fitted (Equation 7). To represent the scenario where human impact is negligible, the values of the predictors of this model (all of which represent human impact) are set to zero. With the predictors set to zero (i.e., model intercept), the predicted value of the model is the median phosphorus concentration when human impact is zero (Equation 8). The SWAT subbasins were overlaid with the phosphorus zones, and the predicted reference phosphorus was calculated for each subbasin using an area-weighted average. These reference phosphorus levels were input into SWAT using the groundwater soluble phosphorus parameter.

Equation 7

$$P = e^{\beta_0 + \beta_1 A + \beta_2 U + \beta_3 \log_{10}(O)}$$

Here, **A**, **U**, and **O** are the percent of the watershed in agricultural and urban land use and the number of point source outfalls, respectively. When these are set to zero, the equation reduces to simply:

Equation 8

$$P = e^{\beta_0}$$

The resulting distribution of the groundwater phosphorus in the WRB can be found in Figure 23.

Robertson et al. (2006) intended their background phosphorus values to estimate median phosphorus concentration in streams when there is no human impact in the watershed. They do not specifically estimate the groundwater or baseflow contribution to reference phosphorus concentration. We assume that the median reference phosphorus estimate is an accurate estimate of baseflow phosphorus concentration because a landscape under natural conditions (one without human impact) will experience much less runoff, and that the median estimate represents low-runoff conditions (NRCS 1986).

4.9 Manning's n

Manning's n is an empirically derived coefficient that represents the roughness of a flow path. In SWAT, Manning's n can be set for HRUs (representing the roughness for overland flow), tributary channels, and reach channels, which tend to be ordered in value from high in upland areas to low in lowland tailwater channels. Overland flow Manning's N values (Table 7) were defined based on lookup tables in scientific literature (Engman, 1986; McCuen, 1989). Tributary channel Manning's n values were set to 0.065 based on Baumgart (2005) and reach Manning's n values were set to 0.043 based on the average of the Eau Claire and Little Rib Rivers values from a flood insurance study conducted in 2010 (FEMA, 2010).

4.10 Surface Runoff Lag

Subbasin areas range from 0.5 to 440 km² in the WRB SWAT model. Because of the wide range of subbasin size, we used the surface runoff lag coefficient (SURLAG) to adjust runoff timing to match time of concentration at gage sites. We initially set SURLAG to values between 1 and 2 with each value linearly scaled to the size of each subbasin. After calibration (Section 5.4), SURLAG values ranged between 0.01 and 0.8.

5 Model Calibration and Validation

5.1 Software and Hardware

To run SWAT itself, we used a customized version of revision 637. The customization incorporates new routines that improve the prediction of soil phosphorus concentrations (Vadas & White, 2010). The customization was coded into Revision 637 and recompiled by Mike White (SWAT Developer) and colleagues at the Agricultural Research Service (ARS).

The primary software used for calibrating streamflows and in-stream pollutants was SWAT-CUP 2012 v.5.1.6.2 (SWAT Calibration and Uncertainty Programs). SWAT-CUP allows users to adjust parameters in various ways:

- Adjustment type
 - Relative adjustment by a scalar
 - Absolute adjustment by addition or subtraction
 - Uniformly replacing values
- Adjustment filters
 - Hydrologic Soil Group
 - Soil Texture Class
 - Land-use
 - Subbasin
 - Slope
 - Other manual or configuration-file-specific conditions

SWAT-CUP software was chosen because it is relatively easy to set up and understand, it is flexible enough for most users with typical SWAT projects, and it offers a parallel processing module for users that are calibrating large projects with many HRUs. We chose to use the parallel processing module because of a substantial reliance on auto-calibration. Auto-calibration was required due to the large number of HRUs in the WRB and the number of calibration sites for streamflow, sediment, and phosphorus that span a wide range of land-use, soil, and topographic geographies. Because we chose to run SWAT scenarios in parallel using SWAT-CUP, we were committed to using the SWAT-CUP-specific SUFI-2 algorithm (Sequential Uncertainty Fitting), which is non-iterative or convergent within a set of simulations (i.e. the parameter adjustments of each subsequent model run do not rely on objective function values of any prior model run) and is thus amendable to parallel computing.

Because we relied heavily on auto-calibration using parallel processing, we required computing resources with many processors, enough random access memory (RAM) to support numerous runs across processors, and disk storage with short access times and minimized latency. We chose to rent cloud computing from Amazon Web Services Elastic Cloud Computing (EC2) service. All calibration computing for the WRB SWAT model was executed on an EC2 instance with 16 dual-core Intel Xeon E5-2680 processors, 60 gigabytes of RAM, and a solid-state drive with 750 general purpose Input/Output Operations per Second (IOPS) and 3000 burst IOPS.

5.2 Monitoring and Load Estimation

5.2.1 Streamflow Monitoring

Daily streamflow observations (Figure 24) were collected from two sources (See Table 13 in Section 5.7 for site information), the USGS NWIS (2014), and data collected at reservoir spillways obtained through personal communication with the Wisconsin Valley Improvement Company (WVIC). Daily streamflow were used during an initial manual calibration phase to ensure that the peak and timing of large events (particularly snowmelt) were captured by the SWAT model. However the final calibrated model was assessed using the average daily streamflow within each month.

5.2.2 Pollutant Monitoring

To estimate loads accurately, concentration samples must be paired with continuous daily streamflow. Therefore, sampling was limited to sites where a USGS NWIS gage site was located (Figure 24). Although USGS supplied large volumes of streamflow data, in a few cases the network of USGS gage sites was deemed insufficient in spatial coverage, and therefore several new USGS gages were installed (Big Rib River, Pine River, Fenwood Creek, Freeman Creek, Little Eau Pleine River, Plover River, Mill Creek, Big Roche-A-Cri Creek, Yellow River at Necedah, Lemonweir River) where large areal gaps existed.

Within this network, several sites had loads already estimated (Muskellunge Creek and Link Creek) through previous studies conducted by USGS (Garn, Robertson, Rose, & Saad, 2010; Robertson, Rose, & Saad, 2005). Some sites had enough concentration samples to estimate loads between 2002 and 2013, however the majority of USGS gage sites did not. Therefore, the WDNR collected instantaneous concentration samples where loads had not already been calculated or sample sizes of concentration samples were insufficient.

The WDNR collected water chemistry samples to fill data spatial data gaps between 2009 and 2013. At each site, concentration samples were taken at bi-weekly intervals throughout the whole year within the sampling period, which results in less biased and more precise load estimates than other sampling strategies such as “storm chasing” (Robertson & Roerish, 1999). Prior concentration sampling and the additional 2009–2013 WDNR data collection effort were then compiled, paired with streamflow, and used in an empirical model to estimate daily TSS and TP loads.

5.2.3 Load Estimation

Computation of loads for each monitored site was based on the regression methods [also referred to as the rating-curve methods (Cohn, 2005)] and implemented in the U.S. Geological Survey program Fluxmaster (Schwarz, Hoos, Alexander, & Smith, 2006). This method commonly is used for load estimation when infrequent water-quality data are available over long periods of time (Cohn, 2005). Daily loads, L , were computed on the basis of relations between constituent load and three explanatory variables—daily streamflow, Q , day of the year, T (in radians), and decimal year, DT . The regression models use the log-transform of load and streamflow to improve the linear relation and account for multiplicative errors. Two different pre-defined regression models were examined for each site (Equation 9 and Equation 10):

Equation 9

$$L = \beta_0 + \beta_1 Q + \beta_2 \sin(2\pi T) + \beta_3 \cos(2\pi T) + \beta_4 DT$$

Equation 10

$$L = \beta_0 + \beta_1 Q + \beta_2 Q^2 + \beta_3 \sin(2\pi T) + \beta_4 \cos(2\pi T) + \beta_5 DT + \beta_6 DT^2$$

The sine and cosine terms provide seasonality in the load–discharge relation, while the decimal year term enables data from various years to be included in developing a relation, even if there is a trend in the relation.

Water quality and streamflow data, used in calibrating Equation 9 and Equation 10 for each site, were collected from January 1, 1995 to December 31, 2014. Water-quality data were obtained from two databases: the USGS National Water Information System (USGS, 2014) and the EPA Storage and Retrieval (STORET) database (U. S. EPA, 2014). Flow data were also obtained from the USGS NWIS database (USGS, 2014). For each site, the specific stations for which water quality and associated streamflow data were obtained are given in Table 8 and Table 9.

The regression model with the lowest standard error, SE, and ratio of the total estimated load to the total observed load for days with water quality measurements, O/E, was chosen to compute daily loads for each site. Because a log transformation was used in the models, final computed daily loads were adjusted to account for a retransformation bias by use of the minimum variance unbiased estimate procedure (Cohn, Delong, Gilroy, Hirsch, & Wells, 1989) or the adjusted maximum likelihood method (Cohn, 2005). If a site did not meet a general standard of performance based on O/E and SE, the site was not used. Load estimates were only used for calibration and validation for periods within which samples were being actively collected. Summary statistics of models for each site are given in Table 8 and Table 9 and detailed model information is provided in Appendix D.5.

5.3 Sensitivity Analysis

A literature review of 21 highly cited journal articles was conducted to assess which and how SWAT parameters have been adjusted in other projects (Table 10). Some parameters

were adjusted uniformly based on a set value and others were adjusted relatively, depending on how much was known about their response or if the parameters varied geographically. For example, soil available water capacity (SOL_AWC) varied for each soil type in the basin, so we varied its value between 50 and 150% of its original value. However, we had no spatial information about the soil evaporation compensation factor (ESCO), so we varied its value uniformly across all HRUs. Because the sensitivity is strongly related to the width of the range over which the value was varied, we only conducted a qualitative analysis.

The qualitative analysis was carried out one-at-a-time for each of the parameters found in the Table 10. One-at-a-time sensitivity analyses were conducted by running the model 25 times for each parameter holding all others constant, collecting streamflow, sediment, and TP loads from the model output, and plotting the change in each output parameter given a unit change in parameter value. In this way the effect of one parameter could be isolated and its impact on the model assessed.

5.4 Calibration and Validation Strategy

For the purpose of debugging, exploratory analysis, and general calibration, the full model with 5,351 HRUs was reduced to 1,651 by increasing percent thresholds for preserving land-use, soil, and slope classes to at least 5, 50, and 50% respectively (discussed in more detail in Section 3.5). The 1,651-HRU model was only used for narrowing the ranges of parameter adjustments, whereas the full model was used to calibrate the final parameter values and the model uncertainty associated with those parameter ranges.

Because hydrologic properties vary widely across the WRB, we chose to split parameter sets using geographical filters that were known *a priori* to bound similar hydrologic properties. First, we divided up USGS gage sites, and the SWAT subbasins associated with them, using an edited version of Ecological Landscapes of Wisconsin (WDNR, 2012). In this edited version of Ecological Landscapes (EL), some ELs were lumped together to improve the parsimony of the overall model and simplify calibration (Figure 25). Lumping was guided based on the similarity of hydrographs of nearby USGS gage sites. For example, the North Central Forest and Forest Transition (FT) landscape boundaries, and the Central Sand Plains and Central Sand Hills (CSP) regions were grouped together resulting in a total of 4 zones. Within each of these zones, all parameter adjustments were equal with the exception of two additional splits - on A/B and C/D hydrologic soil groups. The Western half of the region is dominated by C/D type soils and the Eastern half of the region is dominated by A/B type soils (see Figure 15 in Section 3.3.2), which provided an effective method for explaining differences in the hydrographs of USGS gage sites on either side of the East/West HSG divide. In some cases, we divided HSG groups when adjusting parameters at the subbasin level. In these cases, we assigned HSGs to subbasins based on the areal majority HSG within a subbasin.

SWAT model calibration is rarely executed using all model data simultaneously, with all calibration data sets, nor is it done linearly from start to finish. Rather, SWAT model calibration is typically done iteratively and piecemeal, as new information is gained about the model's response to individual or multiple simultaneous parameter adjustment.

However, a general workflow was followed for calibrating the WRB SWAT model that follows guidance in SWAT literature (Figure 26), with an additional first step added following guidance in Baumgart, 2005. First, annual average crop yields from SWAT were compared to basin-wide average yields (aggregated from county-level data) compiled from NASS. Second, daily streamflow was calibrated within each EL independently. Once daily streamflow was calibrated satisfactorily at all sites, we then calibrated monthly sediment, and then monthly TP, each independently for each ecoregion. Because sediment and TP are strongly linked in the model, they were often calibrated simultaneously or iteratively.

Separate data sets were used for calibration and validation of the model; specifically 75% of observations were used for calibration and the remaining 25% were set aside for validation. However, the calibration dataset needed to have had at least 4 years of data, and each year must not have had more than 50% missing data; if these two criteria were not met, then all data were used for calibration. If the calibration dataset was split, 25% of years were randomly chosen for validation.

Some monitoring stations were eliminated from calibration and validation datasets. The criteria for filtering were as follows:

- If monitoring stations were redundant (on the same stream/river with similar hydrologic properties), the site with the most data was used and the remaining were not used at all.
- If the hydrograph clearly showed that streamflow was strongly affected by upstream reservoir management, the site was not used.
- If the load estimate (Section 5.2) model at a site did not perform well (i.e., it was overly biased, or the standard error was unsatisfactory), the site was not used.

Reservoirs were excluded from direct integration into the SWAT model calibration process. Ideally, reservoirs would be integrated to provide a seamless, unified model for the purposes of the TMDL calculation, however there are critical tradeoffs to this benefit. First, when this study was conducted, the current version of SWAT did not have routines complex enough to simulate the types of reservoir dynamics needed for the large impaired reservoirs on the system, mainly Big Eau Pleine Reservoir, Lake Petenwell, and Castle Rock Lake. Second, it is difficult to calibrate the water balance of reservoirs in SWAT that have little additional storage, without having them “dry up” during low-flow periods. Finally, there was no option to simulate flow-through (i.e., “run-of-the-river”) reservoirs in SWAT comparable compared to the accuracy of simply simulating them as a large, wide, low-gradient rivers, and therefore each reservoir was treated as such. Because of the above limitations, the SWAT model was calibrated for streamflow at reservoirs when treated as a river. However, SWAT was not calibrated for sediment and TP below mainstem reservoirs. Instead, TP was adjusted along the mainstem below reservoirs by developing a sub-model that scales the cumulative load estimated by SWAT according to the measured load retention at specific sites (Section 5.13). TSS retention on the mainstem was ignored because the TSS allocations will only be assigned to reaches located the Baraboo River basin where the likelihood of a sediment impairment is much higher than elsewhere in the WRB.

5.5 Assessment of Model Fit

We followed well established guidelines in the scientific literature for assessing model fit. Moriasi et al. (2007) has been cited nearly 2,775 times (August, 2016, www.scholar.google.com) because it establishes numeric benchmarks for model performance that are adaptable to most SWAT (and other hydrologic models, empirical and mechanistic) applications. The numeric criteria are calculated using three objective functions: 1) percent bias (PBIAS), 2) Nash-Sutcliffe efficiency (NSE), and 3) root mean square error standard deviation ratio (RSR). However, RSR was not used as a performance standard in this study. The equations for PBIAS and NSE are as follows:

Equation 11

$$PBIAS = \left[\frac{\sum_{i=1}^n (Y_i^{sim} - Y_i^{obs}) * 100}{\sum_{i=1}^n Y_i^{obs}} \right]$$

Equation 12

$$NSE = 1 - \left[\frac{\sum_{i=1}^n (Y_i^{sim} - Y_i^{obs})^2}{\sum_{i=1}^n (Y_i^{obs} - Y_i^{mean})^2} \right]$$

“where Y_i^{obs} is the i th observation of the constituent being evaluated, Y_i^{sim} is the i th simulated value for the constituent being evaluated, Y_i^{mean} is the mean of observed data for the constituent being evaluated, and n is the total number of observations” (Moriasi et al., 2007). Moriasi et al. (2007) also provide general benchmarks that represent categorical, qualitative interpretations (very good, good, satisfactory, and unsatisfactory) of numeric criteria (See Table 16 in Section 5.8 for pollutant-specific benchmarks).

We used these numeric criteria, in combination with visualizations (e.g., hydrographs, observed versus predicted scatterplots) during calibration. During the phases when we calibrated manually, we mainly used visualizations as a guide for inspecting model fit. During the phases when we were auto-calibrating (using the SUFI-2 algorithm within SWAT-CUP software, Section 5.1), we used either (not simultaneously) PBIAS or NSE as calibration targets. Generally, NSE was used more often for calibrating to runoff events, and PBIAS was used for baseflow and overall water budget.

5.6 Crop Yields

Crop yields were calibrated for alfalfa, corn grain, corn silage, soybeans, potatoes, green beans, and sweet corn. County-level crop yield data were acquired from the National Agriculture Statistics Service (NASS 2013) to compare to SWAT crop yield output. Crop yields were calibrated first because accurate simulation of runoff is strongly dependent on the accurate simulation of plant growth.

The default plant growth parameters in SWAT are often out of date and therefore do not consider advancements in crop genetics, changes in planting densities, or other alterations in management that have led to major yield increases in the last two decades. Crop growth parameters were adjusted to represent more recent literature values to more accurately

simulate the reality in the field (Table 11). By adjusting several parameters in this process we were able to keep all parameters closer to literature values than by adjusting BIO_E alone (a common crop yield calibration strategy). The SWAT documentation suggests that because BIO_E (radiation use efficiency parameter) is so sensitive that it should be adjusted last (Arnold, 1994), and the above calibration process honors that recommendation.

The estimated crop yields outputs from SWAT (Table 12) are represented as metric tons per hectare of dry matter (0% moisture), however county yields from NASS are crop-dependent (e.g., short tons per acre for green beans, bushels per acre for corn grain, or hundredweight per acre for potatoes). Data from NASS consist of surveys from farms, which means that yield moisture weights are not necessarily standard, although a standard range of moisture values exists for most of these crops. For instance, NASS assumes the typical moisture values for alfalfa, corn grain, and soybeans to be around 14%, 15%, and 13%, respectively. Literature reviews were conducted to determine typical moisture contents of corn silage, potato, green beans, and sweet corn of approximately 70%, 80%, 90%, and 75%, respectively (Akhavan et al., 2010; Delahaut & Newenhouse, 1997; University of Georgia Vegetable Team, 2013; Williams & Lindquist, 2007).

5.7 Streamflow

After exploring model sensitivity to typically adjusted parameters, we began calibrating streamflow. Streamflow estimates from SWAT were calibrated by comparing model estimates to observed flow at 29 USGS gage stations and 2 reservoir spillways (See Figure 24 in Section 5.2) operated by WVIC (Table 13). Only approved (A) and approved/estimated (A:e) measurements from NWIS were used. The objective functions used to assess model fit were NSE and PBIAS. Objective functions serve different purposes in calibrating hydrologic models and as such, we optimized different objective functions depending on the goal. For example, we aimed to maximize NSE when adjusting parameters associated with high flow or runoff events because an optimized NSE tends to favor the calibration of larger values, and we aimed to minimize PBIAS when adjusting parameters associated with low flow or baseflow because it better represents an overall water budget and ensures there are no systemic over or under-estimations.

For all ecoregions, USGS gage sites were used for calculating the objective function value of model estimates with the exception of the Northern Highland (NH) EL. The NH EL contains only two gages that are not significantly impacted by anthropogenic water regulation. The two remaining gage sites drain relatively small watersheds, both of which contain a significant fraction of land that does not contribute to surface runoff. To supplement these data, we included observed data from 2 reservoir outfalls, Lake Alice (Kings Dam) and Lake Mohawkson (Herb Mitchell Landing). Because these two reservoirs are managed for storage, they did not calibrate well at a monthly time step, however they provided a means for assuring that the calibration at the other 2 USGS gage sites were representative of the general water budget of the whole NH EL.

It is often useful to separate surface runoff from baseflow when calibrating certain parameters. For example, the curve number and surface runoff lag coefficient (CN2/CNOP and SURLAG in SWAT, respectively) can be useful for calibrating the amount and timing of

surface runoff, and the baseflow alpha factor and groundwater delay (ALPHA_BF and GW_DELAY in SWAT, respectively) can be useful for calibrating the amount and timing of baseflow. Initially, baseflow and surface runoff were separated by choosing the lowest 50% and highest 25% of daily streamflow observations, respectively. In some cases, we chose only certain months of the year as calibration targets. For example, for surface runoff we calibrated CN2/CNOP and ESCO only during summer months, but snowmelt parameters we only calibrated to daily observations from February through June (See Table 10 from Section 5.3 for parameter descriptions). Daily streamflow were calibrated with a mixture of manual and auto-calibration. The final parameter adjustments are listed in Table 14 and Table 15. Daily calibration of streamflow was mainly done within the generalized model with fewer HRUs (See Section 5.4). When daily streamflow fit well within the generalized version of the model, we ensured that it also translated to a good fit with the full model and at a monthly time step.

The final monthly streamflow calibration with the full model performed well with respect to standard benchmarks of accuracy (Table 16 and Table 17). The streamflow calibration at all sites were satisfactory (PBIAS < 25% and NSE > 0.5) except for two sites in the NH EL (Link Creek and Muskellunge Creek) both of which have small watersheds, much of which is internally drained or wetland, which makes watershed delineation difficult. As an additional verification that the water budget in the NH EL was calibrated well, we used 3 other sites within the NH EL (Wisconsin River at Kings Dam, Wisconsin River at Herb Mitchell Landing, and Wisconsin River at Rhinelander)—these sites have heavily modified streamflow, so they were only used as a rough indicator of the calibration of the water budget by visualizing how the simulated hydrographs compared to observed. Of the 29 sites, 17 had very good PBIAS (less than 10%), and 19 out of 29 sites had very good NSE (greater than 0.75). However, some sites did not meet satisfactory measures of accuracy during validation—3 out of 29 sites had greater than 25% PBIAS and 5 out of 29 sites had NSE less than 0.5. However, 2 of the 5 sites that did not validate satisfactory based on NSE are directly below dams (Petenwell and Castle Rock dams), but there was very little validation bias at these sites (11% and 6%, respectively), so the lack of fit is likely due to disparities in timing from unnatural releases at the reservoir spillways.

5.8 Sediment

Following a widely accepted workflow for SWAT model calibration, once streamflow was calibrated to a desired level of accuracy (i.e., meeting standard benchmarks of accuracy for monthly data, listed in Table 16), we began calibrating monthly sediment loads (Figure 26). We used monthly sediment loads estimated using Fluxmaster software (Section 5.2.3) at 13 sites (See Table 13 in Section 5.2) across the basin for calibration and validation.

There are very few parameters in SWAT that control sediment delivery independent of streamflow, and the most sensitive of these parameters are only adjustable at the scale of the entire basin (e.g., SPCON and SPEXP, See Table 10 in Section 5.3 for parameter descriptions). Although, with detailed information about agricultural best-management practices or channel erosion, there are a few parameters that can be adjusted for sediment independent of streamflow, these details were not available for the entire WRB. This presented a challenge for calibration given that the basin varies widely in sediment

transport due to the variation of topography from steep slopes in the Western Coulees and Ridges (WCR) EL to nearly zero percent slopes in the CSP EL, trapping features such as wetlands and internally draining lakes, soil types from dense clays to loose soils along a West/East divide, and highly permeable aggregates along the terminus of the Green Bay glacial lobe of the most recent ice age.

Without adjusting parameters beyond what has been described in the model configuration (Sections 3 and 4), sediment was significantly over-estimated at all sites. To address this over estimation, we began by assuming that a fraction of agricultural producers are implementing best-management practices, and that this should be reflected in the model, so we set the USLE practice factor (USLE_P) to 0.4 and increased the effect of leaf cover on agricultural crops (USLE_C = 0.1), which resulted in sediment yield estimates similar to those reported by county land management staff (roughly 2 pounds per acre, or 2.2 kilograms per hectare). Next, we used the SPCON and SPEXP parameters to estimate sediment delivery in the most erosive ELs (WCR and western FT). When a reasonable calibration was achieved at gage sites by using only these two parameters, finer level control was achieved by using Manning's N [CH_N(1,2)] for each EL. Where the fit was not sufficient at the level of an EL, we adjusted parameters independently for subbasins with majority A/B or C/D HSG (See Table 15 in Section 5.7 for a complete list of parameter adjustment) as described in Section 5.4.

Using SPCON, SPEXP, and Manning's n , a reasonable calibration was achieved for months experiencing large storm events, however there was still a lack of fit during low flow periods, particularly in areas with less erosive soils. In these cases, channel erosion parameters [CH_COV(1,2)] were used to increase low-flow sediment loads, with minimal adjustment to the overall sediment budget.

The final calibrated model fit well according to the standard benchmark of accuracy based on PBIAS (NSE is typically not used as an assessment criterion for TSS, however it is reported along with PBIAS in Table 17). All sites were calibrated satisfactorily (PBIAS < 55%) except for 2 of the 13, and 3 of the 13 fit at the level of "very good" (PBIAS < 15%). Of the validation set, all 8 validated sites were satisfactory except for 2. However, none were in the "very good" category. The only site that did not calibrate satisfactorily for both the calibration and validation sets was the Eau Claire River at Kelly, WI, which under-predicted 65% for both. The Eau Claire River watershed has a mixture of internally drained and well-drained topographies, and porous sandy soils and dense clays. There are no other major drainages in the basin with these mixtures of characteristics, which presented a challenge for calibration while keeping the model as parsimonious as possible. In the end, because the Eau Claire site was well calibrated for TP, we chose to keep the model parsimonious rather than adjusting parameters specific to the Eau Claire River watershed to force the model to fit.

5.9 Phosphorus

Following the same widely accepted workflow for calibration (See Figure 26 in Section 5.4), we began calibrating TP after a reasonable fit was achieved for TSS, although because TP and TSS are closely linked within the SWAT model, the two constituents were often

calibrated simultaneously or iteratively. As with TSS, we used monthly TP loads estimated using Fluxmaster software (Section 5.2.3) at 25 sites (See Table 13 in Section 5.2) across the basin for calibration and validation.

The main control that we used for adjusting TP in the SWAT model is the width of grassed waterways (FILTERW). Instead of using this parameter according to the literal specifications in the SWAT model documentation, we chose to use this parameter as a way of simulating TP deposition between the edge of a field (HRU load) and the stream channel. The SWAT model is written in such a way that, aside from using the wetlands functions directly (which are meant to simulate depressional storage), there is no buffer between HRUs and stream channels. In reality, there are often significant buffers between agricultural fields and stream channels, especially within the WRB. For example, in the western FT EL, where the majority of dairy agriculture is located, most perennial streams are guarded by a wide riparian buffer that captures water during storm events, but is not necessarily a depressional landscape. Conversely, in the WCR EL, valleys tend to be more constrained and the landscape very well drained, therefore a narrower FILTERW was used for HRUs in that region (See Table 15 in Section 5.7 for a complete list of parameter adjustments).

After setting FILTERW to appropriately buffer streams from TP delivery, our estimates of TP were still too high during low flow periods in some regions, indicating that our initial estimate of baseflow phosphorus was likely set too high. This phenomenon was most prevalent in the CSP EL, and the sandier and glacially affected part of the FT EL (the Eau Claire and Plover Rivers). For these watersheds, we decreased the groundwater soluble phosphorus parameter (GWSOLP).

The final calibrated model fit well according to the standard benchmark of accuracy based on PBIAS (as with TSS, NSE is typically not used as an assessment criterion for TSS; however, it is reported along with PBIAS in Table 17). All sites were calibrated satisfactorily (PBIAS < 70%), and 19 of the 25 sites fell within the “very good” category for calibration. Only one site (Fenwood Creek) of the 16 was not validated satisfactorily. This is due to poor fit in streamflow during the validation period where there was a 108% overestimation. This can be explained by the fact that the data used for validation for Fenwood Creek fell within a relatively low-flow period, which is typically the most difficult to model in SWAT (see Section 5.10 ahead for more details). However, as the overestimation does not result in a significant difference in overall load, as compared to the rest of the simulated years, given the strong validation everywhere else (11 out of the 16 validation sites fell within the “very good” category), this deviation was not considered important to the overall TMDL.

5.10 Routing sub-model and bias-correction

Preliminary investigations of bias in the WRB SWAT model revealed that phosphorus is not stored in stream channels but rather flushes through each reach at the time of concentration, and that phosphorus release is not temperature dependent. Rather, only rudimentary tools are available in SWAT for addressing this issue (White et al., 2014). In reality, some fraction of the upland load is stored in channel sediments, and released at a

lagged time period, often in a way that relates to seasonal temperature fluctuations. To address the above issue, we developed a methodology for correcting these biases outside of the SWAT model. The bias correction was only implemented on SWAT HRU loads and non-permitted urban loads, but not point-source or MS4 loads. The methodology uses two functions to correct SWAT model results. The first function was a decay function that allowed loads to persist for a maximum of 8 months within a stream channel:

Equation 13

$$TP_{a1,m} = \sum_{l=1}^8 TP_{0,m} * e^{(a+b*l)}$$

where $TP_{a1,m}$ is the first adjusted total phosphorus load for any given month, $TP_{0,m}$ is the original total phosphorus load for any given month, l is the number of months prior to m , and a and b are calibration coefficients. The second function was a sinusoidal function that adjusted loads to a seasonal trend:

Equation 14

$$TP_{a2,m} = TP_{a1,m} * \left(c + d * \sin \left(\left(\frac{2\pi}{e} \right) * m + f \right) \right)$$

where $TP_{a2,m}$ is the second adjusted total phosphorus load for any given month, $TP_{a1,m}$ is the solution to Equation 13, m is the month number (e.g., January = 1), and c , d , e , and f are calibration coefficients that relate to the vertical shift, amplitude, frequency, and phase shift of a sinusoidal function, respectively.

Coefficients a through f were optimized for each calibration site in the basin using the Nelder and Mead (1965) optimization algorithm that minimized the value of a custom objective function. The custom objective function was designed to simultaneously address seasonal bias as well as overall bias:

Equation 15

$$F = (1 + PBIAS) * RMSE$$

Equation 16

$$PBIAS = \frac{\left| \sum_{i=1}^n (TP_{a2,m} - TP_{0,m})_i \right|}{\sum_{i=1}^n TP_{0,m,i}}$$

Equation 17

$$RMSE = \sqrt{\frac{\sum_{i=1}^n (TP_{a2,m} - TP_{0,m})^2}{n}}$$

Each gauge site was fitted with its own set of coefficients (Table 18). At all sites the model was fit, the optimization minimized PBIAS to nearly zero (Table 19). For simplicity and parsimony, the bias correction model was only fitted at sites without an upstream nested gage.

5.11 Application of Bias Correction to Ungaged Basins

Fitting coefficients to adjust TP loads at a given site only corrects loads at that given site. The adjustments need to be applied to ungaged basins. We applied adjustments to all ungaged basins by adjusting HRU flows and loads. Adjusting HRU loads directly will be useful for splitting anthropogenic from background loads when calculating load reductions for the TMDL.

For the purpose of adjusting HRU outputs, ungaged basins (and their associated HRUs) were linked with their downstream gage location. In cases where a downstream gage site was not present, we linked ungaged basins with nearby gages of similar landcover, soil type, and slope characteristics using best professional judgment (Figure 27).

The same methods used to correct bias for TP were also used to correct bias in streamflow and TSS. However, streamflow was corrected only using the decay function given that there is little evidence from comparisons of Fluxmaster versus SWAT streamflow of an intra-annual, harmonic pattern of residual error. Summary statistics of streamflow and TSS are also shown in Table 19.

5.12 Comparing SWAT Loads with Grab Sample Data

The final stage in tributary model calibration and validation was to qualitatively compare modeled TP loads to concentrations from grab samples taken from sites around the basin. Monthly load calibration sites require large sample sizes for fitting a load model (Section 5.2.3). However, there are many more sites within the WRB where samples have been taken with less frequency and/or consistency. Although the sampling at these sites is inadequate for fitting a load model, the data can be used to compare SWAT output to aggregate statistics of concentration at a grab sample site. To draw this comparison, at each site where grab samples were taken, we first translated SWAT loads into a simulation-wide, flow-weighted mean concentration:

Equation 18

$$FWMC = \frac{\sum_m^{144} TP_m}{\sum_m^{144} V_m}$$

where in month m , TP_m is the mass of TP and V_m is the volume of water to flow past that site within that month, summed across all 144 months in the 12-year simulation. Next, we calculated growing season medians (May through October) from grab sample data at each site, and corrected for variability in temperature and precipitation during the period when grab samples were taken. Finally, at each site, we compared the SWAT $FWMC$ to the corrected growing season median to ensure there were no sites where the deviation was qualitatively unreasonable.

We found a grouping of sites where this comparison was indeed qualitatively unreasonable (See SE Till Plains Omernik Ecoregion in Figure 25). The SE Till Plains ecoregion of the WRB was ungauged for TP loads, and the ecological landscape in this region is different than its neighbors (i.e. it does not classify neatly as either WCR or CSP ELs). Initially this region was lumped with the CSP EL for parsimony, but our FWMC comparison with growing season medians showed that we were likely overestimating in this region. After grouping this region with the FT EL for parameter adjustment, the *FWMC* estimates from SWAT compared much more favorably to growing season median observations.

5.13 Mainstem TP Transport

Because the SWAT model was not calibrated to mainstem Wisconsin River stations downstream of Merrill, a separate method was needed to estimate transport on the mainstem. This section addresses the question: what fraction of tributary TP loads are delivered to points downstream? The time scale of the analysis is the average annual load over the 2010–13 period when the highest frequency monitoring occurred.

Because TP load estimates are tightly tied to flow records, we first evaluated the quality of the flow records at mainstem stations. There are twelve stations with daily streamflow on the mainstem between Merrill and Muscoda. Muscoda is downstream of Lake Wisconsin and therefore outside of the study area, but its long term record was useful for validating the quality of streamflow data at other gaging stations. Four of the twelve stations are operated by the United States Geological Survey (USGS), and are considered to be the most accurate. The other stations are operated by hydroelectric companies, most of which report data to the Wisconsin Valley Improvement Corporation (WVIC). The data from most of these stations is of unknown quality. We first fit a linear regression between mean discharge and drainage area for the four USGS gages (Figure 39). We then created a “sum of tributaries” flow for each station by summing measured flows where available, and SWAT modeled flows on ungauged tributaries. Of the WVIC stations, three (Stevens Point, Wisconsin Rapids, and Nekoosa) are closely aligned to the USGS gage regression and slightly below the sum of tributaries estimates. Mean flows at the other four WVIC stations (Wausau, Dubai, Petenwell, and Castle Rock) are significantly lower than predicted by the USGS gage regression and sum of tributaries estimates. Flow at the Prairie du Sac dam, which is operated by Alliant Energy, is significantly higher than predicted by the USGS gage regression and sum of tributaries estimate. Based on this evaluation, TP load estimates at the USGS gages and the three WVIC stations where flows align with the USGS regression should be considered most accurate.

Next, we compared the measured average annual TP load at the Wisconsin Dells station (454 mt) to the sum of gauged tributary loads where available, SWAT-estimated loads for ungauged areas, and direct discharges to the mainstem (623 mt) (Table 20), giving a net TP retention of 27% (73% delivery). To distribute this TP retention through the mainstem, we calculated delivery fractions (maximum=1, i.e. no net increase) for reservoir reaches to match the pattern in measured TP load, particularly at stations with apparently unbiased flow estimates. For example, all of the retention observed between Merrill and Rothschild was assumed to happen between Wausau and Rothschild because that reach contains Lake Wausau and the TP load estimate at Rothschild is assumed to be more accurate than at

Wausau. TP delivery through Lake Dubay was estimated at Stevens Point rather than at the Lake Dubay dam because flow at Dubay appears to be underestimated. TP delivery through Petenwell and Castle Rock was estimated by matching the observed TP load at Wisconsin Dells while assuming 100% delivery between Castle Rock and Wisconsin Dells and balancing the differences between measured and predicted loads at the Petenwell and Castle Rock dams. Even with 100% delivery, the sum of TP loads between Wisconsin Dells and Prairie du Sac (Lake Wisconsin) is underestimated, though this discrepancy is probably due to the overestimate of flow at Prairie du Sac. Overall, this process of distributing TP retention through the mainstem Wisconsin River produces a pattern that closely matches the observed pattern and is consistent with expectations that retention should be generally proportional to water residence time (Figure 40).

6 Model results

The SWAT model provides model results in various formats. The most commonly used spatial scales for output are HRUs, subbasins, and reaches. HRU-level output can be thought of as “edge-of-field”, subbasin-level output are the aggregate of all HRUs in a given subbasin, and reach output are simulated flows and loads at any given river reach associated with a subbasin. SWAT provides the option of creating output at daily, monthly, and annual time-steps. There is no one single best way to analyze the results. However, it can be useful to aggregate across different axes of space, time, and type of pollutant source to assess the model. It can also be useful to analyze both pollutant loads (total mass) and yields (i.e. total mass normalized by area). The results described in the following subsections are after correction using the routing sub-model (Section 5.10)

6.1 Pollutant Yields

Loads were aggregated to annual average yields per subbasin to illustrate “hot spots” of TSS and TP delivery. Yields were calculated as the average annual load divided by the subbasin area.

6.2 Spatial Distribution

Both TSS and TP follow similar spatial patterns, which is typical because they are both strongly correlated with runoff. In general TSS and TP yields are greatest in agricultural areas (Figure 29 and Figure 30). However, TSS yields tend to be higher in areas with higher slopes, particularly the WCR EL, whereas TP yields are lower in this region than in the western FT EL where row cropping is more prevalent (dairy cropping in particular).

Soils and landscape morphology are also important factors governing pollutant yields. Areas with high densities of agriculture may have low pollutant load yields if crops are cultivated on highly porous soils, such as the potato/vegetable cultivation areas in the CSP EL. Similarly, areas that have more internal drainage (such as the Plover River which is located along a remnant glacial terminus) have much lower TSS and TP yields regardless of heavy agricultural use.

It can also be useful to split yield maps by pollutant source type (Figure 30 and Figure 31). When split, it illustrates that TSS and TP yields are largely driven by developed (excluding

MS4s) and agricultural uses. However, natural areas (forest, grassland, and wetland) can also be significant sources of TSS—in the WCR EL, forests and grasslands often deliver significant yields of sediment when they are located on very steep slopes. This is not as much the case with TP—regardless of slope, natural areas tend to contribute only minimal yields due to the lack of fertilizer application. In developed areas, even though there is less fertilizer applied, TP yields are still high due to elevated TSS yields and higher runoff in general.

6.3 Temporal Distribution

Non-point source pollution loads are not evenly distributed over time. There are certain times of the year when TSS and TP yields can be 1–2 orders of magnitude greater than others (Figure 32 and Figure 33). Agricultural non-point loads tend to be the lowest in winter months when the model is simulating snow cover. Runoff tends to be highest in early spring (usually beginning in March) when snow begins melting, and with runoff, simulated TSS and TP yields are greater. This pattern is particularly evident in March and April—for many dairy operations, the model is simulating solid manure applications once monthly between January and April, and simulated TP yields tend to be the greatest when snow mixed with frozen manure begins to melt (Section 6.4). Summer months also yield higher TSS and TP than winter months due to more frequent rain events and greater precipitation overall, however plant cover and reduced fertilization result in less pollutant yield than in spring months. Simulated TP yields in October are slightly higher due to some agricultural operations in the model programmed to fertilize at that time.

6.4 Categorical Distribution

To prioritize non-point pollutant reduction, it can be useful to analyze pollutant yields by land use and land management (Figure 34, Figure 35, and Figure 36). The model simulates the lowest TSS and TP yields from forests, grasslands, and wetlands, with wetlands yielding the smallest contribution of TSS, and grasslands yielding the smallest contribution of TP. Of the three agriculture types (dairy, cash grain, and potato/vegetable), dairy yields the highest TSS and TP, and potato/vegetable yields the lowest TSS and TP. Some of this difference is associated with land management (e.g., dairy operations use corn stover for silage, which leaves less residue resulting in more erosion). However, some of the difference is also associated with location (e.g., potato/vegetable rotations tend to be grown on more porous soils). Developed land use yields less TSS than agriculture, but higher TSS than all natural landcover types, and yields the second highest TP of all landuse types.

The type of fertilizer used on agricultural fields is also an important determinant of TP yield (Figure 36). Solid manure application yields by far the greatest TP due to the timing of application being before and during snowmelt in the spring months. Liquid manure application occurs in May after most of the snow has melted and soil saturation begins to decline, and therefore has TP yields much lower than solid application types. Synthetic fertilization has yields nearly an order of magnitude less than solid. This is due in part to the timing of application, but also that nutrient ratios in synthetic fertilizers are optimized for crop growth, which reduces or stabilizes soil phosphorus concentrations over time.

6.5 Loads

The SWAT model outputs pollutant loads (mass) directly in the default output. The loads described in this section are the loads output by SWAT corrected with the routing sub-model (Section 5.10).

6.5.1 Relative Contributions by Source Category

Yields can be informative for identifying “hot spots”. However, the hottest spots may not be the problem if they are small and isolated. Instead, it can be useful to look at overall loads by source (Table 21). By only analyzing the model using yields, it would lead you to the conclusion that natural landuse contribute insignificant pollutant loads, however because 75% of the basin has a natural landcover, its contribution becomes significant (20% of overall TSS load and 18% of overall TP load). The second-most prevalent landcover is agriculture, which also has high TSS and TP yields, and therefore agriculture is the dominant pollutant source overall (55% of the overall TSS load, and 53% of the overall TP load). Within agriculture types, dairy agriculture is the most prevalent (11% of overall landuse, compared to 9% other agriculture) and the highest yielding for both TSS and TP, and therefore contributes the greatest TSS and TP loads of all agriculture types and all other landuses (40% of overall TSS and 44% of overall TP). Urban landuse (MS4 and non-permitted urban areas) contribute a substantial fraction of the overall TSS loads (19%), with a somewhat lesser contribution of the overall TP load (12%). Point sources contribute a relatively small fraction of the overall TSS load (5%), but a significant fraction of the overall TP load (18%).

These relative contributions are not spatially uniform, however. Figure 37 and Figure 38 show the relative contribution of TSS and TP for each landuse category for each reach in the SWAT model. For both TSS and TP, the maps of the relative contributions of agriculture look much like the maps of yield because in agricultural areas, these sources tend to dominate all others. The maps of naturally occurring TSS and TP show that the natural sources dominate the NH EL. Point sources generally do not contribute a significant fraction of TSS, but for TP they are dominant only when discharging into headwater streams. Also, point sources are a significant contributor of TP when accumulated in the mainstem of the Wisconsin River. Urban Areas are generally a minority source of TP except for a few headwater streams the lie directly below an urbanized area. However, urban areas can in many cases be the majority of TSS contribution.

7 Summary

Output from the SWAT model described in this report inform the development of TSS and TP allocations for achieving water quality standards for all waterbodies in the WRB. The SWAT model was chosen for this purpose, because it allows the integration of point and non-point sources, and produces output that segregates controllable and uncontrollable pollutant loading sources, which are critical pieces of information for developing TMDL allocations.

The WRB SWAT model was configured to estimate pollutant loading from 337 spatially explicit subbasins throughout the basin (Section 3.1). Within each subbasin, the model

produced specific results for HRUs, which are discrete combinations of landcover/land-management (Section 0), soil type (Section 3.3), and topographic slope class (Section 3.4). Within an HRU, a hydrologic response is simulated given environmental determinants such as weather (Section 3.6) and landscape position (Section 4.5), as well as how the land-management determinants such as crop rotations (Section 3.2.2), fertilization (Sections 3.2.5.4 and 4.1.2), and tillage (Section 4.1.1). The resulting simulated surface runoff and groundwater (Section 4.8) are then routed through each reach in the Wisconsin River network.

To quantify the performance of the model, we compared SWAT output to monitoring data (Section 5). First, we used crop yield estimates from county-level agricultural censuses to ensure that plants in the SWAT model were growing appropriately (Section 5.6). We then compared simulated streamflow to monitored streamflow at 29 sites (Section 5.7). The accuracy of pollutant loads were quantified (Sections 5.9 and 5.10) by comparing SWAT loads to a more accurate and precise, site-specific, empirical model that predicts a continuous time series of loads using pairs of bi-weekly, instantaneous samples of pollutant concentration and streamflow (Section 5.2.3). Using the above comparisons, we calibrated the model (Section 5.4) until a satisfactory fit was achieved based on quantitative assessments of fit (Section 5.5). Finally, an additional empirical model was created to simulate the effects of hydrologic and pollutant routing and reduce model bias (Section 5.11).

The final model predictions are exceptionally accurate (See Table 19 in Section 5.10), and it is therefore appropriate to use model output for estimating monthly pollutant loads between the years of 2002 and 2013, the relative contribution of pollutant loading by source, and the prediction of loads for ungaged basins. Due to the exceptional accuracy and model detail, the model could also be used for exploring sources of TSS and TP in finer detail for watershed and best-management-practice planning. For example, the model could be used to prioritize the allocation of resources toward subbasins, soil types, crop rotations, fertilization strategies, or specific times of the year (e.g., cover cropping) In summary, the model provides the best current comprehensive understanding of sources of TSS and TP pollution throughout the WRB, and will therefore be a critical aid in implementing the TMDL plan to progress toward water quality improvement.

8 Acknowledgements

The authors have many partners to thank that contributed to this project. Peter Vadas provided new insight into soil phosphorus dynamics, ultimately leading to new routines in SWAT that better capture phosphorus transformations and improve soil phosphorus concentrations. Mike White and Georgie Mitchell retro-fitted the new soil phosphorus routines from Peter Vadas into an archived version of SWAT working with Nancy Sammons to ensure that the code was being implemented in the latest working version of SWAT. Paul Baumgart and Jim Almendinger generously provided their insight and quality improvement through conversations and review of the model. Terry Kafka contributed greatly to the collection of specific agricultural management information. Countless county staff and regional agronomist contributed invaluable information for improving the

representation of agriculture in the SWAT model. Tom Gallagher, Cristhian Mancilla, Yuki Tanimoto, and Jim Palumbo provided insight and additional model comparison, which ultimately illustrated errors in the model that could be fixed prior to the release. Laura Ward-Good provided time running independent models to improve the curve number values for different tillage types. Andy Somor and Tom Beneke provided their time comparing the Wisconsin River model to other SWAT models they had built, resulting in faster debugging and improved calibration. Bob Smail provided specific information and maps regarding irrigation, tiling, and ditching in the Central Sands region. Laura Rozumalski conducted the literature review that informed the sensitivity analysis of the SWAT model. Finally, we thank Guy Hydrick for providing GIS support and data processing for the WinSLAMM modeling effort. This project would not have been possible without these generous contributions.

9 References

- Akhavan, S., Abedi-Koupai, J., Mousavi, S. F., Afyuni, M., Eslamian, S. S., & Abbaspour, K. C. (2010). Application of SWAT model to investigate nitrate leaching in Hamadan-Bahar Watershed, Iran. *Agriculture, Ecosystems and Environment*, 139(4), 675–688. <http://doi.org/10.1016/j.agee.2010.10.015>
- Almendinger, J. E., & Murphy, M. S. (2007). *Constructing a SWAT model of the Willow River watershed, western Wisconsin*. Retrieved from http://www.smm.org/static/scwrs/tapwaters_willowriver2.pdf
- Arnold, J. G. (1994). SWAT (Soil and Water Assessment Tool). Grassland, Soil and Water Research Laboratory, USDA, Agricultural Research Service.
- Arnold, J. G., Allen, P. M., Muttiah, R., & Bernhardt, G. (1995). Automated base flow separation and recession analysis techniques. *Groundwater*, 33(6), 1010–1018.
- Arnold, J. G., Kiniry, J. R., Srinivasan, R., Williams, J. R., Haney, E. B., & Neitsch, S. L. (2012). Soil & Water Assessment Tool input/output documentation version 2012. Texas Water Resources Institute. Retrieved from <http://swat.tamu.edu/media/69296/SWAT-IO-Documentation-2012.pdf>
- Arnold, J. G., Moriasi, D. N., Gassman, P. W., Abbaspour, K. C., White, M. J., Srinivasan, R., ... Jha, M. K. (2012). SWAT: model use, calibration, and validation. *Transactions of the ASABE*, 55(4), 1491–1508.
- Arnold, J. G., Muttiah, R. S., Srinivasan, R., & Allen, P. M. (2000). Regional estimation of base flow and groundwater recharge in the Upper Mississippi River basin. *Journal of Hydrology*, 227(1), 21–40.
- Baumgart, P. (2005). *Source allocation of suspended sediment and phosphorus loads to Green Bay from the Lower Fox River subbasin using the Soil and Water Assessment Tool (SWAT)*. Retrieved from http://www.uwgb.edu/watershed/reports/related_reports/load-allocation/lowerfox_tss-p_load-allocation.pdf
- Beaudette, D. E., Roudier, P., & O'Geen, A. T. (2013). Algorithms for quantitative pedology: A toolkit for soil scientists. *Computers and Geosciences*, 52, 258–268. <http://doi.org/10.1016/j.cageo.2012.10.020>
- Brady, N. C., & Weil, R. R. (2010). *Elements of the nature and property of soils*. Upper Saddle River, NJ: Pearson Prentice Hall.
- Cohn, T. A. (2005). Estimating contaminant loads in rivers: An application of adjusted maximum likelihood to type 1 censored data. *Water Resources Research*, 41(7).
- Cohn, T. A., Delong, L. L., Gilroy, E. J., Hirsch, R. M., & Wells, D. K. (1989). Estimating

- constituent loads. *Water Resources Research*, 25(5), 937–942.
- Cole, T. M., & Wells, S. A. (2016). CE-QUAL-W2: A two-dimensional, laterally averaged, hydrodynamic and water quality model, version 3.71. Portland, OR: Department of Civil and Environmental Engineering, Portland State University.
- Delahaut, K. A., & Newenhouse, A. C. (1997). *Growing beans and peas in Wisconsin: a guide for fresh market growers* (No. A3685).
- Diebel, M., Menuz, D., & Ruesch, A. S. (2013). *1:24K hydrography attribution data*. Madison, WI. Retrieved from ftp://dnrftp01.wi.gov/geodata/hydro_va_24k
- Engel, B., Storm, D., White, M., Arnold, J., & Arabi, M. (2007). A hydrologic/water quality model application protocol. *Journal of the American Water Resources Association*, 43(5), 1223–1236. <http://doi.org/10.1111/j.1752-1688.2007.00105.x>
- Engman, E. T. (1986). Roughness coefficients for routing surface runoff. *Journal of Irrigation and Drainage Engineering*, 112(1), 39–53.
- Environmental Systems Research Institute. (2012). ArcGIS Desktop. Redlands, CA.
- Federal Emergency Management Agency. (2010). *Flood insurance study: Marathon County, Wisconsin and incorporated areas* (No. 55073CV000A). Retrieved from http://www.ci.wausau.wi.us/Portals/0/Departments/Inspections/Documents/FloodplainStudy/FloodInsuranceStudyReport_MarathonCounty.pdf
- Fraley, C., Raftery, A. E., Murphy, T. B., & Srucca, L. (2012). *mclust Version 4 for R: Normal Mixture Modeling for Model-Based Clustering, Classification, and Density Estimation*. Retrieved from <https://www.stat.washington.edu/research/reports/2012/tr597.pdf>
- Freihoefer, A., & McGinley, P. (2007). *Mead Lake watershed sediment and nutrient export modeling*. Stevens Point, WI.
- Garn, H. S., Robertson, D. M., Rose, W. J., & Saad, D. A. (2010). *Hydrology, water quality, and response to changes in phosphorus loading of Minocqua and Kawaguesaga Lakes, Oneida County, Wisconsin, with special emphasis on effects of urbanization* (No. 2010–5196). Retrieved from <http://pubs.usgs.gov/sir/2010/5196/pdf/sir20105196.pdf>
- Gatzke, S. E., Beaudette, D. E., Ficklin, D. L., Luo, Y., O'Geen, A. T., & Zhang, M. (2011). Aggregation strategies for SSURGO data: effects on SWAT soil inputs and hydrologic outputs. *Soil Science Society of America Journal*, 75(5), 1908–1921.
- Havlin, J., Beaton, J. D., Tisdale, S. L., & Nelson, W. L. (2005). *Soil fertility and fertilizers: An introduction to nutrient management* (7th ed.). Upper Saddle River, NJ: Pearson Prentice Hall.
- Jokela, B., & Peters, J. (2009). Dairy manure nutrients: variable but valuable. Marshfield, WI: University of. Retrieved from <http://www.soils.wisc.edu/extension/wfapmc/dbsearch.php?yr=2009&auth=jokela&submit=Go>
- Kirsch, K., Kirsch, A., & Arnold, J. G. (2002). Predicting sediment and phosphorus loads in the Rock River Basin using SWAT. *Transactions of the ASAE*, 45(6), 1757–1769.

- Laboski, C., & Peters, J. (2012). *Nutrient application guidelines for field, vegetable, and fruit crops in Wisconsin* (No. A2809). Retrieved from <http://corn.agronomy.wisc.edu/Management/pdfs/A2809.pdf>
- McCuen, R. H. (1989). *Hydrologic analysis and design*. Englewood Cliffs, NJ: Prentice-Hall.
- Moriyasi, D. N., Arnold, J. G., Van Liew, M. W., Bingner, R. L., Harmel, R. D., & Veith, T. L. (2007). Model evaluation guidelines for systematic quantification of accuracy in watershed simulations. *Transactions of the ASABE*, 50(3), 885–900.
- National Agricultural Statistics Service. (2011). Cropland Data Layer. Retrieved from <http://nassgeodata.gmu.edu/CropScape/>
- National Agricultural Statistics Service Wisconsin Field Office. (2013). 2013 Wisconsin agricultural statistics. Retrieved from <http://quickstats.nass.usda.gov/results/CD8890FD-566F-3F66-8C8A-CB932E358991>
- Natural Resources Conservation Service. (1986). *Urban Hydrology for Small Watersheds* (No. TR-55). Retrieved from http://www.nrcs.usda.gov/Internet/FSE_DOCUMENTS/stelprdb1044171.pdf
- Natural Resources Conservation Service. (2006). *Wisconsin conservation planning technical note 1: nutrient management*. Retrieved from <http://datcp.wi.gov/uploads/Farms/pdf/TechNoteNutrientMgmt.pdf>
- Natural Resources Conservation Service. (2014). The Gridded Soil Survey Geographic (gSSURGO) database for Wisconsin. Retrieved from <http://datagateway.nrcs.usda.gov>
- Nelder, J. A., & Mead, R. (1965). A simplex method for function minimization. *The Computer Journal*, 7(4), 308–313.
- Omernik, J. M. (1987). Ecoregions of the conterminous United States. *Annals of the Association of American Geographers*, 77(1), 118–125.
- Robertson, D. M., Graczyk, D. J., Garrison, P. J., Lizhu, W., LaLiberte, G., & Bannerman, R. (2006). *Nutrient concentrations and their relations to the biotic integrity of wadeable streams in Wisconsin* (No. Professional Paper 1722). Retrieved from http://pubs.usgs.gov/pp/pp1722/pdf/PP_1722.pdf
- Robertson, D. M., & Roerish, E. D. (1999). Influence of various water quality sampling strategies on load estimates for small streams. *Water Resources Research*, 35(12), 3747–3759.
- Robertson, D. M., Rose, W. J., & Saad, D. A. (2005). *Water quality, hydrology, and phosphorus loading to Little St. Germain Lake, Wisconsin, with special emphasis on the effects of winter aeration and ground-water inputs* (No. 2005-5071). Retrieved from <http://pubs.usgs.gov/sir/2005/5071/>
- Robertson, D. M., Saad, D. A., & Heisey, D. M. (2006). A regional classification scheme for estimating reference water quality in streams using land-use-adjusted spatial regression-tree analysis. *Environmental Management*, 37(2), 209–229.
- Santhi, C., Arnold, J. G., Williams, J. R., Dugas, W. A., Srinivasan, R., & Hauck, L. M. (2001).

- Validation of the SWAT model on a large river basin with point and nonpoint sources. *Journal of the American Water Resources Association*, 37(5), 1169–1188.
<http://doi.org/10.1111/j.1752-1688.2001.tb03630.x>
- Schwarz, G. E., Hoos, A. B., Alexander, R. B., & Smith, R. A. (2006). The SPARROW surface water-quality model: theory, application and user documentation. In *U. S. Geological Survey techniques and methods report, book* (Vol. 6). Reston, VA.
- Team, R. C. (2013). R: A language and environment for statistical computing. Vienna, Austria: R Foundation for Statistical Computing. Retrieved from <http://www.r-project.org>
- The Cadmus Group. (2011). *Total Maximum Daily Loads for Total Phosphorus and Total Suspended Solids in the Rock River Basin*.
- Thornton, P. E., Thornton, M. M., Mayer, B. W., Wilhelmi, N., Wei, Y., Devarakonda, R., & Cook, R. B. (2014). Daymet: Daily Surface Weather Data on a 1-km Grid for North America, Version 2. Retrieved from <https://daymet.ornl.gov/>
- Timm, A., & McGinley, P. (2011). *SWAT Model for Mill Creek, Portage and Wood Counties–Wisconsin*. Stevens Point, WI.
- United States Environmental Protection Agency. (2014). Storage and Retrieval (STORET) database. Retrieved from <http://www.epa.gov/storet/index.html>
- United States Geological Survey. (2014). National Water Information System. Retrieved from <http://waterdata.usgs.gov/nwis/>
- University of Georgia Vegetable Team. (2013). *Commercial Snap Bean Production in Georgia* (No. Bulletin 1369). Athens, GA. Retrieved from http://extension.uga.edu/publications/files/pdf/B_1369_4.PDF
- University of Wisconsin–Madison Soil Science Department. (n.d.). UW Soil and Forage Lab. Retrieved November 3, 2013, from <http://uwlab.soils.wisc.edu/>
- Vadas, P. A., & White, M. J. (2010). Validating soil phosphorus routines in the SWAT model. *Transactions of the ASABE*, 53(5), 1469–1476.
- Walker, W. W. (1996). *Simplified procedures for eutrophication assessment and prediction: User manual* (No. W-96-2). Vicksburg, MS.
- White, M. J., Storm, D. E., Mittelstet, A., Busteed, P. R., Haggard, B. E., & Rossi, C. (2014). Development and testing of an in-stream phosphorus cycling model for the Soil and Water Assessment Tool. *Journal of Environmental Quality*, 43(1), 215–223.
- Williams, M. M., & Lindquist, J. L. (2007). Influence of planting date and weed interference on sweet corn growth and development. *Agronomy Journal*, 99, 1066–1072.
<http://doi.org/10.2134/agronj2007.0009>
- Wisconsin Department of Agriculture Trade and Consumer Protection. (2010). WinTransect. Madison, WI.
- Wisconsin Department of Natural Resources. (1991). *Wisconsin Wetlands Inventory*.

Retrieved from <http://dnr.wi.gov/topic/wetlands/inventory.html>

Wisconsin Department of Natural Resources. (2009). *Wisconsin Lakes*.

Wisconsin Department of Natural Resources. (2012). *Ecological landscapes of Wisconsin* (No. Handbook 1805.1). Madison, WI. Retrieved from <http://dnr.wi.gov/topic/landscapes/Book.html>

Wisconsin Department of Natural Resources. (2015). *Getting started with WDNR 24K hydro geodatabase*. Madison, WI. Retrieved from http://dnr.wi.gov/maps/gis/documents/GETTING_STARTED_WITH_WDNR_24K_HYDRO_GEODATABASE.pdf

Wu, K., & Johnston, C. A. (2008). Hydrologic comparison between a forested and a wetland/lake dominated watershed using SWAT. *Hydrological Processes*, 22(10), 1431–1442.

Zinke, P. J. (1967). *Forest interception studies in the United States*. Oxford, U. K.: Pergamon Press.

10 Tables

Table 1 Crop classifications from the Cropland Data Layer (CDL) were aggregated into groups of similar crops or crops that are often confused in the classification process.

<i>Aggregated class</i>	<i>CDL code</i>	<i>CDL class description</i>
Corn	1	Corn
	28	Oats
Alfalfa	36	Alfalfa
	37	Other Hay/Non Alfalfa
	58	Clover/Wildflowers
	176	Grass/Pasture
Soybeans and grains	4	Sorghum
	5	Soybeans
	21	Barley
	22	Durum Wheat
	23	Spring Wheat
	24	Winter Wheat
	25	Other Small Grains
	27	Rye
	29	Millet
	30	Speltz
	39	Buckwheat
	205	Triticale
	Potatoes	43
Vegetables	12	Sweet Corn
	42	Dry Beans
	47	Misc. Veggies & Fruits
	49	Onions
	50	Cucumbers
	53	Peas
	206	Carrots
	216	Peppers

Table 2 Decision rules used to classify crop sequences into generalized agricultural rotation types. The conditions were tested hierarchically in the order they are listed in the table. That is, the test for pasture (the last in the table) could only be met if all tests above returned false. Each symbol represents a set of crop types: C = corn (including sweet corn pre-local knowledge); S = soybeans; P = potatoes; DB = dry beans; V = onions, cucumbers, peas, carrots, peppers, sweet corn (not including sweet corn post-local knowledge); A = alfalfa, sorghum, barley, durum wheat, spring wheat, winter wheat, other small grains, rye, oats, millet, speltz, buckwheat, clover/wildflowers, triticale; Pas = other hay/non-alfalfa, pasture/grass, pasture/hay.

Rotation	Ordered ruleset	
	Pre-local knowledge	Post-local knowledge
Continuous Corn	C >= 4 year	C >= 3 years No S, P, V, A, Pas
Cash Grain	C >= 1 year S >= 1 year C and S >= 3 year	C and S >= 2 years No P, V, A, Pas
Corn / Dry Beans	C >= 2 year DB >= 2 year	
Dry Beans	DB >= 2 years A >= 2 years No C, S, P, V	
Dairy (Generic)		A and Pas >= 1 year C and S >= 1 year
Dairy (1 year C, 1 year S)	C = 1 year S = 1 year A >= 1 year No P, V, DB	
Dairy (2 year C)	C = 2 years A >= 1 years No P, V, DB	
Dairy (1 year C, 2 Year S)	C = 1 years S >= 2 years A >= 1 of 5 years No P, V, DB	
Dairy (2 year C, 1 Year S)	C >= 2 years S >= 1 year C and S >= 2 years A >= 1 year No P, V, DB	
Dairy (3 year C)	C = 3 years A >= 1 year No P, V, DB	
Dairy (No Corn)	S >= 1 year A >= 1 year No C, P, V, DB	
Dairy/Potato	C >= 1 year P >= 1 year A >= 1 year No S, V, DB	P >= 1 year A >= 1 year No V
Potato	P >= 2 years N C, S, DB, V	
Potato/Veg.		P and V >= 1 year
Potato/Corn	C >= 1 year P >= 1 year C + P >= 4 years	
Potato/Corn/Dry Beans	C >= 1 year P >= 1 year DB >= 1 year	

Table 2 Decision rules used to classify crop sequences into generalized agricultural rotation types. The conditions were tested hierarchically in the order they are listed in the table. That is, the test for pasture (the last in the table) could only be met if all tests above returned false. Each symbol represents a set of crop types: C = corn (including sweet corn pre-local knowledge); S = soybeans; P = potatoes; DB = dry beans; V = onions, cucumbers, peas, carrots, peppers, sweet corn (not including sweet corn post-local knowledge); A = alfalfa, sorghum, barley, durum wheat, spring wheat, winter wheat, other small grains, rye, oats, millet, speltz, buckwheat, clover/wildflowers, triticale; Pas = other hay/non-alfalfa, pasture/grass, pasture/hay.

<i>Rotation</i>	<i>Ordered ruleset</i>	
	<i>Pre-local knowledge</i>	<i>Post-local knowledge</i>
Potato/Corn/Soybean	C >= 1 year P >= 1 year S >= 1 year	
Potato/Corn/Veg.	P >= 1 year V >= 1 year C >= 1 year	A and Pas >= 1 year C and S >= 1 year
Pasture	Pas and A >= 4 years No C, S, P, V, DB	Pas and A >= 2 years No C, S, P, V

Table 3 Comparison of distribution of crop rotations between transects and our (WDNR) approach described in Sections 3.2.1 through 3.2.4.

<i>Rotation Type</i>	<i>Transect Count</i>	<i>Transect (%)</i>	<i>WDNR Approach Acreage</i>	<i>WDNR Approach (%)</i>
Cash Grain	608	23	309,000	20
Dairy	946	36	633,000	40
Pasture/Hay	414	16	447,000	28
Potato/Vegetable	68	3	188,000	12
Insufficient	581	22	-	-
Total	2,617	100	1,577,000	100

Table 4 The agricultural land cover classes represented within SWAT are shown here with the class of land use and land management. The rotation codes are Cg=corn grain, Cs=corn silage, So=soybean, Po=potato, Vg=vegetable, A=Alfalfa, O/A=oats/alfalfa. Tons are English tons. Note that the SWAT Landuse is a code used by SWAT and is a placeholder for unique agricultural practices and are not truly representative of the landcover and is only included here for reference.

<i>SWAT Landuse</i>	<i>Type</i>	<i>Definition</i>
SWHT	Dairy	Cg-Cs-O/A-A-A-A - Spring Chisel – 10,000 ga/acre/year Liquid Manure
WWHT	Dairy	O/A-A-A-A-Cg-Cs - Spring Chisel – 10,000 ga/acre/year Liquid Manure
DWHT	Dairy	A-A-Cg-Cs-O/A-A - Spring Chisel – 10,000 ga/acre/year Liquid Manure
RYE	Dairy	Cg-Cs-O/A-A-A-A - Spring Chisel - 25 tons/acre/year Solid Manure
BARL	Dairy	O/A-A-A-A-Cg-Cs - Spring Chisel - 25 tons/acre/year Solid Manure
OATS	Dairy	A-A-Cg-Cs-O/A-A - Spring Chisel - 25 tons/acre/year Solid Manure
RICE	Dairy	Cg-O/A-A-A-A-A - Spring Chisel - 25 tons/acre/year Solid Manure
PMIL	Dairy	A-A-A-A-Cg-O/A - Spring Chisel - 25 tons/acre/year Solid Manure
TIMO	Dairy	A-A-Cg-O/A-A-A - Spring Chisel - 25 tons/acre/year Solid Manure
BROS	Dairy	Cg-Cs-O/A-A-A-A - Fall Chisel – 10,000 ga/acre/year Liquid Manure
BROM	Dairy	O/A-A-A-A-Cg-Cs - Fall Chisel – 10,000 ga/acre/year Liquid Manure
FESC	Dairy	A-A-Cg-Cs-O/A-A - Fall Chisel – 10,000 ga/acre/year Liquid Manure
BLUG	Dairy	Cg-Cs-O/A-A-A-A - Fall Chisel - 25 tons/acre/year Solid Manure
BERM	Dairy	O/A-A-A-A-Cg-Cs - Fall Chisel - 25 tons/acre/year Solid Manure
CWGR	Dairy	A-A-Cg-Cs-O/A-A - Fall Chisel - 25 tons/acre/year Solid Manure
WWGR	Dairy	Cs-Cs-O/A-A-A-A - Fall Chisel – 10,000 ga/acre/year Liquid Manure
SWGR	Dairy	O/A-A-A-A-Cs-Cs - Fall Chisel – 10,000 ga/acre/year Liquid Manure
RYEG	Dairy	A-A-Cs-Cs-O/A-A - Fall Chisel – 10,000 ga/acre/year Liquid Manure
RYER	Dairy	Cs-Cs-O/A-A-A-A - Fall Chisel - 25 tons/acre/year Solid Manure
RYEA	Dairy	O/A-A-A-A-Cs-Cs - Fall Chisel - 25 tons/acre/year Solid Manure
SIDE	Dairy	A-A-Cs-Cs-O/A-A - Fall Chisel - 25 tons/acre/year Solid Manure
BBLS	Dairy	Cs-Cs-O/A-A-A-A - Fall MB Plow – 10,000 ga/acre/year Liquid Manure
LBLS	Dairy	O/A-A-A-A-Cs-Cs - Fall MB Plow – 10,000 ga/acre/year Liquid Manure
SWCH	Dairy	A-A-Cs-Cs-O/A-A - Fall MB Plow – 10,000 ga/acre/year Liquid Manure
INDN	Dairy	Cs-Cs-O/A-A-A-A - Fall MB Plow - 25 tons/acre/year Solid Manure
ALFA	Dairy	O/A-A-A-A-Cs-Cs - Fall MB Plow - 25 tons/acre/year Solid Manure
CLVS	Dairy	A-A-Cs-Cs-O/A-A - Fall MB Plow - 25 tons/acre/year Solid Manure
CLVR	Dairy	Cg-Cs-O/A-A-A-A - Fall MB Plow – 10,000 ga/acre/year Liquid Manure
CLVA	Dairy	O/A-A-A-A-Cg-Cs - Fall MB Plow – 10,000 ga/acre/year Liquid Manure
SOYB	Dairy	A-A-Cg-Cs-O/A-A - Fall MB Plow – 10,000 ga/acre/year Liquid Manure
CWPS	Dairy	Cg-Cs-O/A-A-A-A - Fall MB Plow - 25 tons/acre/year Solid Manure
MUNG	Dairy	O/A-A-A-A-Cg-Cs - Fall MB Plow - 25 tons/acre/year Solid Manure
LIMA	Dairy	A-A-Cg-Cs-O/A-A - Fall MB Plow - 25 tons/acre/year Solid Manure
LENT	Cash Grain	Cg-Cg-So-Cg-Cg-So - Fall Chisel/Spring Disk
PNUT	Cash Grain	Cg-So-Cg-Cg-So-Cg - Fall Chisel/Spring Disk
FPEA	Cash Grain	So-Cg-Cg-So-Cg-Cg - Fall Chisel/Spring Disk
PEAS	Cash Grain	Cg-So-Cg-So-Cg-So - Fall Chisel/Spring Disk
SESB	Cash Grain	So-Cg-So-Cg-So-Cg - Fall Chisel/Spring Disk
COTS	Cash Grain	Cg-So-Cg-So-Cg-So - No Till
COTP	Cash Grain	So-Cg-So-Cg-So-Cg - No Till
SGBT	Potato/Vegetable	Po-Vg-Vg-Po-Vg-Vg - Deep Till Potato Years/Cultivate Vegetable Years
POTA	Potato/Vegetable	Vg-Po-Vg-Vg-Po-Vg - Deep Till Potato Years/Cultivate Vegetable Years
SPOT	Potato/Vegetable	Vg-Vg-Po-Vg-Vg-Po - Deep Till Potato Years/Cultivate Vegetable Years
ONIO	Cranberries	Continuous cranberry bog (treated as herbaceous wetlands)
CRRT	Pasture/Hay	Continuous Grasses

Table 5 Soil attributes used in SWAT and the methods used to cluster SSURGO map units. The listed soil attributes are all soil properties used in SWAT. Not all these properties were used to cluster soil map units. The aggregation method is the aggregation function used to simplify the properties used in the clustering algorithm. Also listed are the original tables where the soil properties are located in SSURGO.

<i>Variable</i>	<i>Used in clustering?</i>	<i>Aggregation method</i>	<i>SSURGO table</i>	<i>Column name</i>
Albedo dry	No	surface horizon	component	albedodry_r
Available water capacity (cm/cm)	Yes	depth-weighted mean	chorizon	awc_r
Bulk density (g/cm ³)	No	depth-weighted mean	chorizon	dbovendry_r
Calcium carbonate (%)	No	depth-weighted mean	chorizon	caco3_r
Clay (%)	Yes	depth-weighted mean	chorizon	claytotal_r
Electric conductivity (dS/m)	No	depth-weighted mean	chorizon	ec_r
Horizon depth (mm)	No	Sum of all horizons	chorizon	hzdepb_r
Hydrologic soil group	Yes	category	component	hydgrp_r
Organic carbon (%)	No	depth-weighted mean	chorizon	cbn_r
pH	No	depth-weighted mean	chorizon	ph1to1h2o_r
Rock fragments (%)	No	depth-weighted mean	chfrags	fragvol_r
Sand (%)	Yes	depth-weighted mean	chorizon	sandtotal_r
Saturated conductivity (µm/sec)	Yes	depth-weighted mean	chorizon	ksat_r
Silt (%)	No	depth-weighted mean	chorizon	silttotal_r
USLE erodibility	Yes	depth-weighted mean	chorizon	usle_kwfact

Table 6 Statewide and municipality-specific datasets used to define urban model area extent.

<i>Model Area</i>	<i>Dataset</i>
City and Village Municipal limits	TIGER Minor Civil Divisions (“State-based”) with PL 94-171 Attributes
Urbanized Areas	TIGER 2010 Urban Areas Western Great Lakes
Open Water	Open water features (i.e. lakes, reservoirs, wide streams, and rivers) as defined by the USGS 1:24,000 National Hydrography Dataset
Marathon County City/Village/Town Limits	Marathon County Planning and Zoning
City of Baraboo Municipal Limits	City of Baraboo Public Works/Engineering
City of Marshfield Municipal Limits	City of Marshfield Engineering
City of Wisconsin Rapids Municipal Limits	City of Wisconsin Rapids Engineering

Table 7 Manning's *n* values used for overland flow based on specific landcovers.

<i>Landcover</i>	<i>Manning's n</i>
Developed, Open Space	0.054
Deciduous Forest	0.36
Evergreen Forest	0.32
Mixed Forest	0.4
Grassland/Pasture	0.35
Wetlands	0.18
Chisel	0.11
Moldboard	0.1
Spring Disk	0.4
Deep Till	0.3
No Till	0.12

Table 8 Summary statistics of Fluxmaster (Schwarz et al., 2006) load estimation models of total suspended solids (TSS). Identification numbers are associated with the National Water Information System (NWIS, USGS, 2014). The start and end dates denote the times when sampling occurred, but the sampling may not have been regular within that period (i.e., there may be two or more periods of regular sampling). The loads reported are in units of gigagrams (thousands of metric tons) per year (mean for years 2011–13). The columns O/E and SE report the average ratio of observed versus estimated loads and standard errors, respectively. The value in the par. column represents how many parameters were used in the regression. Sites with which there are no summary statistics means that either there was insufficient data to fit the model, or that the terms in the model did not explain the variability in load.

Station Name	NWIS ID	Total Suspended Solids						
		<i>n</i>	<i>start</i>	<i>end</i>	<i>load (Gg/yr)</i>	<i>O/E</i>	<i>SE</i>	<i>par.</i>
Baraboo River at Main Street, Reedsburg, WI	054041665	55	15-Sep-2011	5-Nov-2013	11,665	0.90	21.24	7
Baraboo River near Baraboo, WI	05405000	177	10-Jan-2002	18-Dec-2013	18,837	0.80	11.76	7
Big Eau Pleine River at Big Eau Pleine Dam	05399600	97	14-Oct-2009	25-Nov-2013	2,660	1.28	12.62	7
Big Eau Pleine River at Stratford, WI	05399500	138	14-Jul-2005	25-Nov-2013	5,985	0.95	29.36	5
Big Rib River at Rib Falls, WI	05396000	92	12-Apr-2010	8-Oct-2013	2,827	1.30	23.21	7
Big Roche a Cri Creek at Hwy 21	05401556	91	12-May-2010	7-Nov-2013	320	1.06	9.25	7
Eau Claire River at Kelly, WI	05397500	94	12-Apr-2010	8-Nov-2013	1,842	1.05	14.87	7
Fenwood Creek at Bradley, WI	05399550	94	14-Oct-2009	16-Dec-2013	224	1.00	32.25	5
Freeman Creek at Halder, WI	05399580	93	14-Oct-2009	25-Nov-2013	222	0.94	28.12	7
Lemonweir at New Lisbon	05403500	89	13-May-2010	5-Nov-2013	2,577	1.03	6.59	7
Little Eau Pleine River near Rozellville, WI	05400220	91	27-Apr-2010	8-Nov-2013	1,154	0.97	18.60	7
Mill Creek at County Hwy PP	05400718	93	13-Apr-2010	8-Nov-2013	501	1.02	20.35	7
Mill Creek near Hewitt, WI	05400664	28	21-Feb-2002	26-Nov-2002	629	0.99	31.28	7
Mill Creek near Junction City, WI	05400705	22	21-Feb-2002	26-Nov-2002	804	0.72	22.64	7
Pine River at Center Avenue near Merrill, WI	05395063	90	26-Apr-2010	8-Oct-2013	578	0.96	25.37	7
Plover River at Hwy 10/66	05400513	97	13-Apr-2010	8-Nov-2013	759	1.00	9.67	5
Prairie River near Merrill, WI	05394500	97	22-Oct-2009	8-Oct-2013	1,257	1.02	16.04	5
Spirit River at Spirit Falls	05393500	22	10-Mar-2005	14-Sep-2010	—	—	—	—
Spirit River at Spirit River Dam	05393600	1	4-Jun-2013	4-Jun-2013	—	—	—	—
Ten Mile Creek near Nekoosa	05401050	100	17-Nov-2009	7-Nov-2013	500	0.98	10.59	7
West Branch of Baraboo River at Hillsboro, WI	05404116	52	23-Aug-2005	25-Apr-2013	771	1.38	33.21	7
Wisconsin River at Castle Rock Dam	05403200	3	30-Nov-2009	3-Aug-2011	—	—	—	—

Table 8 Summary statistics of Fluxmaster (Schwarz et al., 2006) load estimation models of total suspended solids (TSS). Identification numbers are associated with the National Water Information System (NWIS, USGS, 2014). The start and end dates denote the times when sampling occurred, but the sampling may not have been regular within that period (i.e., there may be two or more periods of regular sampling). The loads reported are in units of gigagrams (thousands of metric tons) per year (mean for years 2011–13). The columns O/E and SE report the average ratio of observed versus estimated loads and standard errors, respectively. The value in the par. column represents how many parameters were used in the regression. Sites with which there are no summary statistics means that either there was insufficient data to fit the model, or that the terms in the model did not explain the variability in load.

Station Name	NWIS ID	Total Suspended Solids						
		<i>n</i>	<i>start</i>	<i>end</i>	<i>load (Gg/yr)</i>	<i>O/E</i>	<i>SE</i>	<i>par.</i>
Wisconsin River at Chuck's Landing	05398000	—	—	—	—	—	—	—
Wisconsin River at Herb Mitchell Landing	—	—	—	—	—	—	—	—
Wisconsin River at Lake DuBay Dam	05400295	12	11-Oct-2006	11-Sep-2007	—	—	—	—
Wisconsin River at Merrill, WI	05395000	129	8-Jan-2002	12-Dec-2013	8,792	0.96	7.78	7
Wisconsin River at Nekoosa Dam	05400975	—	—	—	—	—	—	—
Wisconsin River at Rainbow Lake	05391000	—	—	—	—	—	—	—
Wisconsin River at Rhinelander	05391090	30	6-May-1999	11-Dec-2001	1,240	0.97	3.67	7
Wisconsin River at Rothschild, WI	05398000	—	—	—	—	—	—	—
Wisconsin River at Stevens Point Dam	05400320	5	20-Jan-2009	8-Sep-2009	—	—	—	—
Wisconsin River at Wausau Dam	05395300	—	—	—	—	—	—	—
Wisconsin River at Wisconsin Dells	05404000	132	10-Jan-2002	18-Dec-2013	47,959	0.94	9.21	7
Wisconsin River at Wisconsin Rapids	05400760	111	22-Jan-2002	20-Nov-2013	49,802	0.92	9.44	7
Wisconsin River below Prairie du Sac Dam	05405990	—	—	—	—	—	—	—
Yellow River at Babcock	05402000	47	13-Oct-2010	4-Sep-2012	3,311	1.15	14.56	7
Yellow River at Hwy 21	05403000	90	12-May-2010	7-Nov-2013	2,769	0.98	12.96	7

Table 9 Summary statistics of Fluxmaster (Schwarz et al., 2006) load estimation models of total phosphorus (TP). Identification numbers are associated with the National Water Information System (NWIS, USGS, 2014). The start and end dates denote the times when sampling occurred, but the sampling may not have been regular within that period (i.e., there may actually be two or more periods of regular sampling). The loads reported are in units of megagrams (metric tons) per year (mean for years 2011–13). The columns O/E and SE report the average ratio of observed versus estimated loads and standard errors, respectively. The value in the par. column represents how many parameters were used in the regression.

Station Name	NWIS ID	Total Phosphorus						
		<i>n</i>	<i>start</i>	<i>end</i>	<i>load (Mg/yr)</i>	<i>O/E</i>	<i>SE</i>	<i>par.</i>
Baraboo River at Main Street, Reedsburg, WI	054041665	66	15-Sep-2011	5-Nov-2013	50	0.99	8.1	7
Baraboo River near Baraboo, WI	05405000	175	10-Jan-2002	18-Dec-2013	77	1.02	5.2	7
Big Eau Pleine River at Big Eau Pleine Dam	05399600	99	14-Oct-2009	25-Nov-2013	33	1.00	7.5	7
Big Eau Pleine River at Stratford, WI	05399500	147	22-May-2002	25-Nov-2013	65	1.04	14.2	7
Big Rib River at Rib Falls, WI	05396000	93	12-Apr-2010	4-Nov-2013	37	1.00	13.1	5
Big Roche a Cri Creek at Hwy 21	05401556	90	12-May-2010	7-Nov-2013	3	0.97	4.8	5
Eau Claire River at Kelly, WI	05397500	99	22-May-2002	8-Nov-2013	20	1.02	16.9	7
Fenwood Creek at Bradley, WI	05399550	96	14-Oct-2009	16-Dec-2013	4	0.89	15.9	5
Freeman Creek at Halder, WI	05399580	94	14-Oct-2009	25-Nov-2013	2	1.01	18.9	5
Lemonweir at New Lisbon	05403500	88	13-May-2010	5-Nov-2013	50	0.97	5.2	7
Little Eau Pleine River near Rozellville, WI	05400220	91	27-Apr-2010	8-Nov-2013	30	1.05	7.7	5
Mill Creek at County Hwy PP	05400718	93	13-Apr-2010	8-Nov-2013	20	1.09	9.4	7
Mill Creek near Hewitt, WI	05400664	31	21-Feb-2002	26-Nov-2002	7	1.12	10.7	7
Mill Creek near Junction City, WI	05400705	25	21-Feb-2002	26-Nov-2002	23	0.98	14.7	7
Pine River at Center Avenue near Merrill, WI	05395063	91	26-Apr-2010	4-Nov-2013	6	1.00	10.5	5
Plover River at Hwy 10/66	05400513	96	13-Apr-2010	8-Nov-2013	5	1.02	5.2	7
Prairie River near Merrill, WI	05394500	98	22-Oct-2009	4-Nov-2013	12	1.03	5.9	5
Spirit River at Spirit Falls	05393500	31	21-May-2002	14-Sep-2010	7	0.95	12.2	7
Spirit River at Spirit River Dam	05393600	92	12-Apr-2010	4-Nov-2013	7	1.07	4.7	7
Ten Mile Creek near Nekoosa	05401050	102	17-Nov-2009	7-Nov-2013	3	1.01	3.3	7
West Branch of Baraboo River at Hillsboro, WI	05404116	52	23-Aug-2005	25-Apr-2013	4	1.06	24.2	7
Wisconsin River at Castle Rock Dam	05403200	101	17-Nov-2009	7-Nov-2013	326	0.97	4.3	7
Wisconsin River at Chuck's Landing	05398000	93	13-Apr-2010	8-Nov-2013	232	1.03	3.4	7
Wisconsin River at Herb Mitchell Landing	—	93	12-Apr-2010	4-Nov-2013	82	1.01	1.8	7

Table 9 Summary statistics of Fluxmaster (Schwarz et al., 2006) load estimation models of total phosphorus (TP). Identification numbers are associated with the National Water Information System (NWIS, USGS, 2014). The start and end dates denote the times when sampling occurred, but the sampling may not have been regular within that period (i.e., there may actually be two or more periods of regular sampling). The loads reported are in units of megagrams (metric tons) per year (mean for years 2011–13). The columns O/E and SE report the average ratio of observed versus estimated loads and standard errors, respectively. The value in the par. column represents how many parameters were used in the regression.

<i>Station Name</i>	<i>NWIS ID</i>	<i>Total Phosphorus</i>						
		<i>n</i>	<i>start</i>	<i>end</i>	<i>load (Mg/yr)</i>	<i>O/E</i>	<i>SE</i>	<i>par.</i>
Wisconsin River at Lake DuBay Dam	05400295	105	11-Oct-2006	8-Nov-2013	300	1.04	7.6	7
Wisconsin River at Merrill, WI	05395000	182	8-Jan-2002	12-Dec-2013	126	1.02	3.2	7
Wisconsin River at Nekoosa Dam	05400975	114	29-Oct-2008	7-Nov-2013	415	1.03	4.1	7
Wisconsin River at Rainbow Lake	05391000	27	28-Jul-1999	29-Nov-2001	14	1.06	4.9	7
Wisconsin River at Rhinelander	05391090	32	6-May-1999	11-Dec-2001	16	0.99	2.4	7
Wisconsin River at Rothschild, WI	05398000	93	12-Apr-2010	8-Nov-2013	221	0.99	3.4	7
Wisconsin River at Stevens Point Dam	05400320	104	16-Oct-2008	8-Nov-2013	308	1.01	3.4	7
Wisconsin River at Wausau Dam	05395300	93	12-Apr-2010	4-Nov-2013	136	1.02	3.5	7
Wisconsin River at Wisconsin Dells	05404000	174	10-Jan-2002	18-Dec-2013	428	1.00	3.9	7
Wisconsin River at Wisconsin Rapids	05400760	171	22-Jan-2002	20-Nov-2013	331	0.98	3.7	7
Wisconsin River below Prairie du Sac Dam	05405990	90	14-Apr-2010	5-Nov-2013	561	0.97	5.8	7
Yellow River at Babcock	05402000	53	13-Oct-2010	26-Sep-2012	43	1.04	12.1	7
Yellow River at Hwy 21	05403000	90	12-May-2010	7-Nov-2013	47	1.00	6.8	5

Table 10 List of parameters used in sensitivity analysis, how often they were used for calibration in the 21 studies that were reviewed, the parameter range that was analyzed, and how the parameters were adjusted. The letters “r” and “u” in the Adjustment column denote whether the parameter was adjusted relative to its original value, or if the value was set uniformly, respectively. The value listed for relative adjustments is the percent added or subtracted from the original value.

SWAT Parameter	Description	Citations	Low	High	Adjustment
CN2/CNOP	Curve number	19	-50	50	r
SOL_AWC	Soil available water capacity	16	-50	50	r
ESCO	Soil evaporation compensation factor	15	0	1	u
SOL_K	Soil hydraulic conductivity	13	-50	50	r
ALPHA_BF	Baseflow alpha factor	12	0	1	u
CH_K(1,2)	Channel hydraulic conductivity	12	-0.01	150	u
CH_N(1,2)	Channel Manning's N	11	0	0.5	u
GWQMN	Threshold of shallow groundwater for return flow	11	0	5000	u
GW_DELAY	Groundwater delay time	10	0	500	u
SLSUBBSN	HRU slope length	10	-50	50	r
HRU_SLP	HRU slope	9	-50	50	r
SURLAG	Surface runoff lag coefficient	9	0	15	u
GW_REVAP	Groundwater revap coefficient	8	0.02	0.2	u
USLE_P	USLE practice factor	8	0	1	u
BIOMIX	Biological mixing efficiency	7	0	1	u
CANMX	Maximum canopy storage	7	0	100	u
CH_COV(1,2)	Channel cover factor, erodibility	7	0	1	u
EPCO	Plant uptake compensation factor	7	0.001	1	u
RCHRG_DP	Deep aquifer percolation factor	7	0	1	u
SFTMP	Snowfall temperature	7	-10	5	u
SPCON	Re-entrainment of channel sediment, linear parameter	7	0.0001	0.05	u
CH_ERODMO	Channel erodibility by month	6	0	1	u
REVAPMN	Threshold of shallow groundwater for revap	6	0	500	u
SPEXP	Re-entrainment of channel sediment, exponential parameter	6	1	2	u
OV_N	Overland Manning's N	5	0.1	0.3	u
SMTMP	Snowmelt temperature	5	-2	20	u
SOL_ALB	Soil albedo	5	-20	20	r
SOL_Z	Soil depth	5	-50	50	r
TIMP	Snow pack temperature lag factor	5	0.01	1	u
SMFMN	Melt factor for snow on June 21	4	0	10	u
SMFMX	Melt factor for snow on December 21	4	0	10	u
SOL_BD	Soil bulk density	4	-50	50	r
USLE_K	USLE soil erodibility factor	4	-50	100	r
BLAI	Maximum potential leaf area index	3	-50	50	r
USLE_C	USLE cover factor	3	-20	20	r
CH_S(1,2)	Channel slope	2	-50	100	r
FILTERW	Width of edge-of-field filter strip	2	0	10	u
PPERCO	Phosphorus percolation coefficient	2	10	17.5	u
SOL_ORGP	Soil organic phosphorus concentration	2	0	4000	u
SOL_LABP	Soil labile phosphorus concentration	2	0	100	u
ALPHA_BNK	Baseflow alpha factor for bank storage	1	0	1	u
CMN	Rate factor for humus mineralization of organic nutrients	1	0.001	0.003	u
EVRCH	Reach evaporation adjustment factor	1	0.5	1	u
ERORGP	Phosphorus enrichment ratio for loading with sediment	1	2	4	u
PHOSKD	Phosphorus soil partitioning coefficient	1	100	200	u

Table 11 Adjusted plant growth parameters for modeled crops (with plant database identification code and default values in parentheses).

<i>Crop</i> <i>(SWAT code)</i>	<i>SWAT Parameter</i>					
	BIO_E <i>((kg/ha)/(MJ/m²))</i>	BLAI <i>m²/m²</i>	CHTMX <i>(m)</i>	HVSTI <i>(yield/biomass)</i>	T_BASE <i>(°C)</i>	T_OPT <i>(°C)</i>
Alfalfa (52)	8 (20)	3 (4)				
Corn Grain (19)	37 (39)	6.5 (3)				
Corn Silage (20)	40 (39)	6.5 (4)				
Soybean (56)	39 (25)	6.5 (3)			9 (10)	27 (25)
Potato (70)	32 (20)	5.5 (4)				
Green Bean (84)	41 (25)	6.5 (1.5)	1 (0.6)	0.65 (0.1)	7 (10)	30 (19)
Sweet Corn (21)	44 (39)	6.5 (2.5)		0.65 (0.5)	8 (12)	29 (24)

Table 12 SWAT crop yields (Megagrams per hectare), converted- SWAT crop yields (common US crop metric), and National Agricultural Statistics Survey (NASS) crop yields. Estimated yields are reported as the average annual yield from 2002–2013. Estimated yields are converted to US yields based on the common metric conversion factor and moisture percentage they are commonly reported as within the US.

<i>Crop</i>	<i>Estimated Yield (Mg/ha)</i>	<i>Estimate yield (US units)</i>	<i>US Units</i>	<i>Moisture Content (%)</i>	<i>Conversion Factor</i>	<i>NASS Yields (US Units)</i>
Alfalfa, hay	5.9	2.6	short tons/acre, dry	0.0	0.45	2.6
Corn	7.7	146	bushels/acre	15.5	15.9	145
Corn silage	13.2	17	short tons/acre, moist	65.0	0.45	17
Soybeans	2.4	41	bushels/acre	13.0	14.9	41
Potatoes	9.5	423	hundredweight/acre	80.0	8.9	425
Green beans	1.0	4.6	short tons/acre, moist	90.0	0.45	4.3
Sweet corn	3.5	6.2	short tons/acre, moist	75.0	0.45	7.5

Table 13 U.S. Geological Survey (USGS) and Wisconsin Valley Improvement Company (WVIC, note that these sites do not have an identification number) gage sites chosen for calibration of streamflow, total suspended solids (TSS), and total phosphorus (TP). A “Y” indicator represents if the data was available and used in calibration, and an “N” indicator represents if the data was available, but not used in calibration. The ecoregion column contains values associated with one or more of the Ecological Landscapes that are within the watershed that drains to the station. (WCR = Western Coulees and Ridges, FT = Forest Transition, CSP = Central Sand Plains, NH = Northern Highlands). Cells marked with an asterisk are sites where flow is heavily regulated by dam operators, and therefore streamflow was visually inspected to ensure on overall water budget fit, but monthly fit was not quantitatively assessed.

<i>Station Name</i>	<i>Ecoregion</i>	<i>USGS NWIS ID</i>	<i>Streamflow</i>	<i>TSS</i>	<i>TP</i>
Baraboo River at Main Street, Reedsburg, WI	WCR	05405000	Y	Y	Y
Baraboo River near Baraboo, WI	WCR	054041665	Y	Y	Y
Big Eau Pleine River at Big Eau Pleine Dam	FT	05399600	*	N	N
Big Eau Pleine River at Stratford, WI	FT	05399500	Y	N	Y
Big Rib River at Rib Falls, WI	FT	05396000	Y	N	Y
Big Roche a Cri Creek at Hwy 21	CSP	05401556	Y	Y	Y
Eau Claire River at Kelly, WI	FT	05397500	Y	Y	Y
Fenwood Creek at Bradley, WI	FT	05399550	Y	N	Y
Freeman Creek at Halder, WI	FT	05399580	Y	N	Y
Lemonweir at New Lisbon	CSP/WCR	05403500	Y	Y	Y
Link Creek	NH	05392083	Y	–	Y
Little Eau Pleine River near Rozellville, WI	FT	05400220	Y	Y	Y
Mill Creek at County Hwy PP	FT	05400718	Y	Y	Y
Muskellunge Creek, Muskellunge Lake Outlet	NH	05390680	Y	–	Y
Pine River at Center Avenue near Merrill, WI	FT	05395063	Y	N	Y
Plover River at Hwy 10/66	FT	05400513	Y	Y	Y
Prairie River near Merrill, WI	FT	05394500	Y	Y	Y
Spirit River at Spirit Falls	FT	05393500	Y	N	Y
Spirit River at Spirit River Dam	FT	05393600	*	–	N
Ten Mile Creek near Nekoosa	CSP	05401050	Y	Y	Y
West Branch of Baraboo River at Hillsboro, WI	WCR	05404116	Y	N	N
Wisconsin River at Castle Rock Dam	NH/FT/CSP	05403200	Y	–	N
Wisconsin River at Lake DuBay Dam	NH/FT	05400295	Y	–	Y
Wisconsin River at Merrill, WI	NH/FT	05395000	Y	Y	Y
Wisconsin River at Nekoosa Dam	NH/FT/CSP	05400975	Y	–	Y
Wisconsin River at Petenwell Dam	NH/FT/CSP	05401400	Y	–	N
Wisconsin River at Rothschild, WI	NH/FT	05398000	Y	–	Y
Wisconsin River at Stevens Point Dam	NH/FT/CSP	05400320	Y	–	Y
Wisconsin River at Wisconsin Dells	NH/FT/CSP	05404000	N	N	N
Wisconsin River at Wisconsin Rapids	NH/FT/CSP	05400760	Y	N	N
Wisconsin River below Prairie du Sac Dam	NH/FT/CSP/WCR	05405990	N	–	N
Wisconsin River Kings Dam	NH/FT	WVIC	*	–	–
Wisconsin River at Herb Mitchell Landing	NH/FT	WVIC	*	–	–
Wisconsin River Rhinelander	NH/FT	05391090	*	–	–
Yellow River at Babcock	FT	05402000	Y	Y	Y
Yellow River at Hwy 21	FT/CSP	05403000	Y	Y	Y

Table 14 Basin-wide parameter adjustments. A “u” adjustment represents a uniform value parameter adjustment, and an “r” adjustment represents a relative scalar adjustment. For uniform adjustments, the parameters was set at its value basin-wide, but for relative adjustments, the value represents the proportion increase (i.e. the final value will be equal to $(1 + v)s$ where v is the original parameter value and s is the scalar listed here. The filter denotes elements that were modified—if none is listed, the parameter adjustment applied to all.

<i>Parameter</i>	<i>Adjustment</i>	<i>Filter</i>	<i>Value</i>
SMTMP	u		-0.2
SFTMP	u		-0.2
TIMP	u		0.2
SMFMN	u		0.8
SMFMX	u		3.2
SNOCVMX	u		40
SNO50COV	u		0.5
CH_W2	r		-0.6
CH_W1	r		-0.7
CH_D	r		-0.7
CH_S1	r		0.8
CH_S2	r		0.8
HRU_SLP	u	Wetlands	0.005
SLSUBBSN	u	Wetlands	90
OV_N	u	Grasslands	0.3
SPCON	u		0.001
SPEXP	u		1.7
ADJ_PKR	u		0.8
USLE_P	u	Agriculture and urban	0.4
USLE_P	u	Open water	0.001
USLE_C	u	Agriculture	0.1
HEAT_UNITS	u	Grasslands	2200
HVSTI	u	Grasslands	0.75
FILTERW	u	Forest/Wetlands	7

Table 15 Parameter adjustments by Ecological Landscape (WDNR, 2012). Parameter adjustment values are listed under each Ecological Landscape abbreviation (WCR = Western Coulees and Ridges, FT = Forest Transition, CSP = Central Sand Plains, NH = Northern Highlands). A “u” adjustment represents a uniform value parameter adjustment, and an “r” adjustment represents a relative scalar adjustment. For uniform adjustments, the parameters was set at its value basin-wide, but for relative adjustments, the value represents the proportion increase (i.e. the final value will be equal to $(1 + v)s$ where v is the original parameter value and s is the scalar listed here. The filter denotes elements that were modified—if none is listed, the parameter adjustment applied to all.

<i>Parameter</i>	<i>Adj.</i>	<i>Filter</i>	<i>WCR</i>	<i>FT</i>	<i>CSP</i>	<i>NH</i>
CN2/CNOP	r	A/B	-0.12	0.02	-0.18	-0.18
		C/D			-0.16	
ESCO	u	A/B	0.49	0.77	0.86	0.7
		C/D		0.98	0.98	
SURLAG	r	A/B	-0.6	-0.95	-0.99	-0.99
		C/D		-0.7	-0.83	
SOL_BD	r	A/B	-0.16	–	0.16	–
		C/D		0.15	–	
SOL_Z	r	A/B	0.20	–	-0.20	–
		C/D		–	–	
SOL_K	r	A/B	0.20	0.1	–	–
		C/D		0.16	–	
SOL_AWC	r	–	-0.40	–	–	–
ALPHA_BF	r	A/B	-0.96	-0.77	5.4	-0.85
		C/D		3.3	2.2	
GW_DELAY	u	A/B	270	4.5	170	450
		C/D		1	2.4	
GWQMN	u	A/B	0	0	630	0
		C/D		–	1100	
GW_REVAP	u	Deciduous forest	0.04	–	–	0.2
		All else		–	–	0.02
REVAPMN	u	–	210	–	–	0
PND_EVOL	r	–	–	0.8	–	–
PND_FR	r	–	–	0.5	–	-0.5
FILTERW	u	Agriculture, A/B	4	5	12	14
		Agriculture, C/D		14	–	
CH_N1	u	A/B	0.03	0.03	0.03	0.03
		C/D		–		
CH_N2	u	A/B	0.03	0.03	0.03	0.03
		C/D		–	0.07	
CH_COV1	u	A/B	–	0.04	0.07	0.005
		C/D		–	–	
CH_COV2	u	A/B	–	0.2	0.2	0.2
		C/D		–		

Table 16 General performance ratings for a monthly time step (from Moriasi et al., 2007)

<i>Performance Rating</i>	<i>RSR</i>	<i>NSE</i>	<i>PBIAS (%)</i>		
			Streamflow	Sediment	N, P
Very good	$0.00 \leq RSR \leq 0.50$	$0.75 < NSE \leq 1.00$	$PBIAS < \pm 10$	$PBIAS < \pm 15$	$PBIAS < \pm 25$
Good	$0.50 < RSR \leq 0.60$	$0.65 < NSE \leq 0.75$	$\pm 10 \leq PBIAS < \pm 15$	$\pm 15 \leq PBIAS < \pm 30$	$\pm 25 \leq PBIAS < \pm 40$
Satisfactory	$0.60 < RSR \leq 0.70$	$0.50 < NSE \leq 0.65$	$\pm 15 \leq PBIAS < \pm 25$	$\pm 30 \leq PBIAS < \pm 55$	$\pm 40 \leq PBIAS < \pm 70$
Unsatisfactory	$RSR > 0.70$	$NSE \leq 0.50$	$PBIAS \geq \pm 25$	$PBIAS \geq \pm 55$	$PBIAS \geq 70$

Table 17 Monthly summary statistics [*n*=sample size, PBIAS=percent bias (Equation 11), NSE=Nash-Sutcliffe efficiency (Equation 12)] of model fit for streamflow, total suspended solids (TSS) and total phosphorus (TP) shown for each of the calibration (cal) and validation (val) sets. A positive PBIAS is an indication of over-prediction and a negative PBIAS is indicative of under-prediction.

Station Name	streamflow						TSS						TP					
	n		PBIAS		NSE		n		PBIAS		NSE		n		PBIAS		NSE	
	cal	val	cal	val	cal	val	cal	val	cal	val	cal	val	cal	val	cal	val	cal	val
Baraboo River at Main Street, Reedsburg, WI	24	-	15.3	-	0.73	-	24	-	7.6	-	0.60	-	24	-	24.6	-	-0.02	-
Baraboo River near Baraboo, WI	108	36	-2.1	-6.8	0.83	0.90	108	12	-32.0	-25.8	0.81	0.83	120	12	-1.7	-8.5	0.79	0.79
Big Eau Pleine River at Stratford, WI	108	36	6.5	2.8	0.81	0.73	-	-	-	-	-	-	84	12	21.5	-1.1	0.51	0.91
Big Rib River at Rib Falls, WI	36	15	0.8	-11.7	0.87	0.83	-	-	-	-	-	-	24	12	5.6	19.0	0.78	0.87
Big Roche a Cri Creek at Hwy 21	32	12	17.3	11.8	0.63	0.71	24	12	75.8	31.5	-0.33	0.58	24	12	12.6	49.2	0.64	-0.58
Eau Claire River at Kelly, WI	108	36	17.8	32.0	0.68	0.59	24	12	-65.3	-66.7	0.04	0.10	36	12	43.7	-1.8	0.85	0.81
Fenwood Creek at Bradley, WI	36	15	21.1	105.9	0.67	0.04	-	-	-	-	-	-	36	12	24.4	420.0	0.38	-8.35
Freeman Creek at Halder, WI	36	15	12.7	8.9	0.64	0.85	-	-	-	-	-	-	36	12	-18.5	-51.3	0.74	0.35
Lemonweir at New Lisbon	32	12	-0.8	-3.9	0.88	0.85	24	12	34.9	96.6	-2.29	-3.58	24	12	-3.9	-8.3	0.57	0.62
Link Creek	22	-	19.0	-	-0.51	-	-	-	-	-	-	-	25	-	-30.2	-	-0.43	-
Little Eau Pleine River near Rozellville, WI	33	12	-9.7	29.9	0.71	0.52	36	-	-9.5	-	0.52	-	24	12	19.5	3.1	0.66	0.87
Mill Creek at County Hwy PP	33	12	1.8	8.2	0.88	0.64	36	-	30.1	-	0.58	-	36	-	39.1	-	0.74	-
Muskellunge Creek, Muskellunge Lake Outlet	23	-	47.4	-	-4.12	-	-	-	-	-	-	-	25	-	-74.0	-	-2.51	-
Pine River at Center Avenue near Merrill, WI	33	12	2.2	12.8	0.77	0.61	-	-	-	-	-	-	36	-	42.0	-	0.75	-
Plover River at Hwy 10/66	33	12	-20.1	-21.5	0.57	0.54	24	12	-33.0	-40.1	0.39	-0.04	24	12	0.1	-12.7	0.72	0.72
Prairie River near Merrill, WI	108	36	-16.3	-16.5	0.81	0.81	36	12	41.7	36.8	0.71	0.78	36	12	-30.9	-35.4	0.72	0.63
Spirit River at Spirit Falls	108	36	3.7	4.6	0.87	0.79	-	-	-	-	-	-	24	-	-33.2	-	0.66	-
Ten Mile Creek near Nekoosa	108	36	-0.9	2.8	0.80	0.56	36	12	-38.0	-18.0	0.44	0.49	36	12	9.4	2.0	0.59	-1.01
West Branch of Baraboo River at Hillsboro, WI	108	36	12.7	23.4	0.72	0.49	-	-	-	-	-	-	-	-	-	-	-	-
Wisconsin River at Castle Rock Dam	108	36	7.6	6.0	0.79	-0.29	-	-	-	-	-	-	-	-	-	-	-	-
Wisconsin River at Lake DuBay Dam	108	36	6.1	3.2	0.86	0.90	-	-	-	-	-	-	48	12	11.0	-5.6	0.65	0.89
Wisconsin River at Merrill, WI	144	-	-8.9	-	0.73	-	132	-	6.8	-	0.32	-	120	-	-13.3	-	0.66	-
Wisconsin River at Nekoosa Dam	108	36	-2.9	-4.0	0.86	0.87	-	-	-	-	-	-	48	12	10.6	-8.2	0.76	0.62
Wisconsin River at Petenwell Dam	108	36	6.3	16.5	0.81	-0.37	-	-	-	-	-	-	-	-	-	-	-	-
Wisconsin River at Rothschild, WI	108	36	-6.6	-7.4	0.88	0.82	-	-	-	-	-	-	24	12	11.6	-1.1	0.81	0.85
Wisconsin River at Stevens Point Dam	108	36	-7.7	-0.5	0.88	0.79	-	-	-	-	-	-	48	12	3.3	56.0	0.74	-0.93
Wisconsin River at Wisconsin Rapids	108	36	-3.9	1.3	0.85	0.91	-	-	-	-	-	-	-	-	-	-	-	-
Yellow River at Babcock	108	36	6.8	-3.4	0.86	0.75	24	-	-7.5	-	0.61	-	24	-	-5.7	-	0.66	-
Yellow River at Hwy 21	36	8	0.5	1.0	0.87	0.66	24	12	16.5	16.5	0.65	0.02	36	-	13.6	-	0.65	-

Table 18 Sample sizes (n), degrees of freedom (df), and fitted parameter values of optimized models (see Equation 13 and Equation 14 for the usage of parameters a–f) used to correct biases and simulate routing for streamflow, total suspended solids (TSS), and total phosphorus (TP).

<i>Station Name</i>	<i>Variable</i>	<i>n</i>	<i>df</i>	<i>a</i>	<i>b</i>	<i>c</i>	<i>d</i>	<i>e</i>	<i>f</i>
Baraboo River near Baraboo, WI	streamflow	144	142	2.6	-2.6	-	-	-	-
	TSS	120	114	0.5	-0.7	0.6	-0.4	12.1	1.6
	TP	132	126	0.1	-0.9	1.1	0.1	12.1	3.9
Big Eau Pleine River at Stratford, WI	streamflow	144	142	3.0	-3.1	-	-	-	-
	TSS	95	89	3.2	-3.4	1.5	-1.4	11.6	1.6
	TP	88	82	2.7	-3.5	1.5	0.9	12.9	0.2
Big Rib River at Rib Falls, WI	streamflow	51	49	2.6	-2.6	-	-	-	-
	TSS	36	30	1.8	-2.8	2.1	1.2	12.4	-0.7
	TP	36	30	2.4	-2.5	0.8	0.3	11.7	-0.4
Big Roche a Cri Creek at Hwy 21	streamflow	44	42	5.4	-5.6	-	-	-	-
	TSS	36	30	-0.1	-0.3	1.8	0.8	12.6	-0.1
	TP	36	30	0.7	-0.6	0.3	0.1	9.2	-1.0
Eau Claire River at Kelly, WI	streamflow	144	142	2.7	-3.0	-	-	-	-
	TSS	27	21	4.3	-2.6	0.7	-0.6	21.0	4.7
	TP	48	42	2.9	-4.6	3.5	2.0	9.1	-0.9
Fenwood Creek at Bradley, WI	streamflow	51	49	5.8	-6.1	-	-	-	-
	TSS	48	42	3.8	-3.8	0.6	-0.5	13.4	3.1
	TP	48	42	2.7	-4.2	2.8	0.6	13.9	0.1
Freeman Creek at Halder, WI	streamflow	51	49	6.5	-6.7	-	-	-	-
	TSS	48	42	1.0	-1.0	2.4	-1.3	10.3	2.2
	TP	48	42	2.1	-3.2	4.0	-1.3	9.5	-4.1
Lemonweir at New Lisbon	streamflow	44	42	10.8	-10.8	-	-	-	-
	TSS	36	30	-0.6	-0.4	0.7	0.5	12.5	0.7
	TP	36	30	-0.4	-0.9	1.9	0.8	10.4	0.3
Little Eau Pleine River near Rozellville, WI	streamflow	43	41	3.4	-3.4	-	-	-	-
	TSS	25	19	0.8	-1.5	0.8	0.7	11.2	-0.7
	TP	34	28	0.2	-1.3	1.7	0.6	12.6	0.0
Pine River at Center Avenue near Merrill, WI	streamflow	45	43	4.8	-4.9	-	-	-	-
	TSS	36	30	0.3	-1.4	2.2	1.8	11.1	0.1
	TP	36	30	4.0	-5.1	1.8	1.2	9.6	-0.7
Plover River at Hwy 10/66	streamflow	45	43	0.9	-1.1	-	-	-	-
	TSS	36	30	0.5	-0.3	2.9	-2.3	11.1	1.9
	TP	36	30	-0.5	-0.5	1.0	-0.3	10.1	2.0
Ten Mile Creek near Nekoosa	streamflow	144	142	1.2	-1.5	-	-	-	-
	TSS	48	42	0.8	-0.5	1.9	1.3	10.5	-1.0
	TP	48	42	-0.2	-0.9	1.6	0.2	10.7	1.5
Wisconsin River at Merrill, WI	streamflow	144	142	0.4	-0.9	-	-	-	-
	TSS	132	126	0.0	-0.3	1.0	0.2	13.5	-0.4
	TP	132	126	-0.2	-0.6	1.5	0.8	12.5	0.6
Yellow River at Babcock	streamflow	143	141	8.8	-8.9	-	-	-	-
	TSS	19	13	4.7	-3.5	0.7	0.6	13.1	1.1
	TP	22	16	3.7	-3.9	1.3	0.8	18.2	1.5

Table 19 Final fit statistics of streamflow, total suspended solids (TSS), and total phosphorus (TP) of SWAT model after bias-correction and adjusting for routing.

Station Name	Fit?	Streamflow			TSS			TP		
		n	NSE	PBIAS	n	NSE	PBIAS	n	NSE	PBIAS
Baraboo River at Main Street, Reedsburg, WI	N	144	0.80	0.0	24	-0.16	66.8	24	0.58	24.7
Baraboo River near Baraboo, WI	Y	144	0.86	0.0	120	0.81	0.0	132	0.89	0.0
Big Eau Pleine River at Stratford, WI	Y	144	0.77	0.0	–	–	–	96	0.45	0.2
Big Rib River at Rib Falls, WI	Y	51	0.82	0.0	–	–	–	36	0.79	0.0
Big Roche a Cri Creek at Hwy 21	Y	44	0.79	0.0	36	0.15	0.4	36	0.80	0.0
Eau Claire River at Kelly, WI	Y	144	0.70	0.0	36	0.80	9.5	48	0.85	0.0
Fenwood Creek at Bradley, WI	Y	51	0.65	0.0	–	–	–	48	0.36	0.0
Freeman Creek at Halder, WI	Y	51	0.71	0.0	–	–	–	48	0.69	0.0
Lemonweir at New Lisbon	Y	44	0.88	0.0	36	0.78	0.0	36	0.76	0.0
Little Eau Pleine River near Rozellville, WI	Y	45	0.71	0.7	36	0.47	4.8	36	0.80	0.5
Mill Creek at County Hwy PP	N	45	0.78	10.0	36	0.52	66.5	36	0.79	30.4
Pine River at Center Avenue near Merrill, WI	Y	45	0.75	0.0	–	–	–	36	0.82	0.0
Plover River at Hwy 10/66	Y	45	0.65	0.0	36	0.87	0.0	36	0.90	-0.4
Prairie River near Merrill, WI	N	144	0.63	-9.5	48	0.34	-40.4	48	0.69	-16.6
Spirit River at Spirit Falls	N	144	0.64	10.4	–	–	–	24	0.41	-25.7
Ten Mile Creek near Nekoosa	Y	144	0.85	0.0	48	0.69	0.0	48	0.92	0.0
West Branch of Baraboo River at Hillsboro, WI	N	144	0.70	17.3	–	–	–	–	–	–
Wisconsin River at Castle Rock Dam	N	144	0.69	17.2	–	–	–	–	–	–
Wisconsin River at Lake DuBay Dam	N	144	0.77	14.5	–	–	–	60	0.41	14.9*
Wisconsin River at Merrill, WI	Y	144	0.70	0.0	132	0.76	0.2	132	0.70	0.0
Wisconsin River at Nekoosa Dam	N	144	0.78	8.0	–	–	–	60	0.54	12.1*
Wisconsin River at Petenwell Dam	N	144	0.68	19.9	–	–	–	–	–	–
Wisconsin River at Rothschild, WI	N	144	0.78	-1.1	–	–	–	36	0.81	5.6
Wisconsin River at Stevens Point Dam	N	144	0.79	2.4	–	–	–	60	0.35	18.8*
Wisconsin River at Wisconsin Dells	N	144	0.78	6.6	–	–	–	–	–	–
Wisconsin River at Wisconsin Rapids	N	144	0.77	7.0	–	–	–	–	–	–
Wisconsin River below Prairie du Sac Dam	N	69	0.85	-0.2	–	–	–	–	–	–
Yellow River at Babcock	Y	144	0.81	0.9	24	0.59	5.6	24	0.64	0.4
Yellow River at Hwy 21	*	44	0.83	0.0	36	0.1	-1.3	36	0.56	-2.0

*Accuracy measures are reported here as a benchmark, but are not valid due to the exclusion of explicit reservoir settling processes, and are therefore consistently over-predicted (See Sections 5.4 and 5.13)

Table 20 Average annual (2010-13) discharge, total phosphorus (TP) load, and estimated TP delivery fractions for mainstem Wisconsin River monitoring stations.

<i>Station Name</i>	<i>Drainage Area (km²)</i>	<i>TP Delivery Fraction</i>	<i>Measured Discharge (cfs)</i>	<i>Sum of Tributary Discharge (cfs)</i>	<i>Measured TP Load (mt)</i>	<i>Sum of Tributary TP Load (mt)</i>	<i>Sum of Tributary TP Load with Delivery (kg)</i>
Merrill	7148	-	2205	-	125	125	125
Wausau	7925	1	2159	2460	129	148	148
Rothschild	10412	0.945	3281	3277	225	238	225
DuBay	12691	0.88	3758	4182	314	365	310
Stevens Point	12924	1	4122	4254	317	372	317
Wisconsin Rapids	13934	1	4416	4637	344	423	368
Nekoosa	14672	1	4661	4941	431	469	414
Petenwell	15462	0.815	4606	5215	330	481	347
Castle Rock	18285	0.913	5469	6116	352	538	369
Wisconsin Dells	20720	1	6726	6972	454	622	454
Prairie du Sac	23776	1	8512	7985	616	753	584
Muscoda	26936	-	8959	-	-	-	-

Table 21 Relative contributions of total suspended solids (TSS) and total phosphorus (TP) by source type. Loads are expressed as the average total mass exported across the whole study area. The areal footprint of point sources is irrelevant, and therefore their areas and yields are not reported.

Source	Area		TSS			TP		
	km ²	(%)	Load (Mg)	Percent (%)	Yield (Mg/ha)	Load (kg)	Percent (%)	Yield (kg/ha)
Natural	17,010	74.7	15,638	17.4	0.01	134,540	18.2	0.08
Agriculture	4,355	19.1	52,122	58.1	0.12	391,527	52.9	0.90
Cash Grain	1,230	5.4	11,339	12.6	0.09	54,553	7.4	0.44
Dairy	2,381	10.5	37,807	42.2	0.16	325,045	43.9	1.37
Potato/Vegetable	745	3.3	2,976	3.3	0.04	11,929	1.6	0.16
MS4	277	1.2	5,490	6.1	0.20	21,311	2.9	0.77
Developed	1,140	5.0	11,954	13.3	0.10	44,248	7.6	0.49
Point Source	–	–	4,492	5.0	–	137,020	18.5	–
Total	22,782	100.0	89,696	100.0	0.04	740,344	100.0	0.32

11 Figures

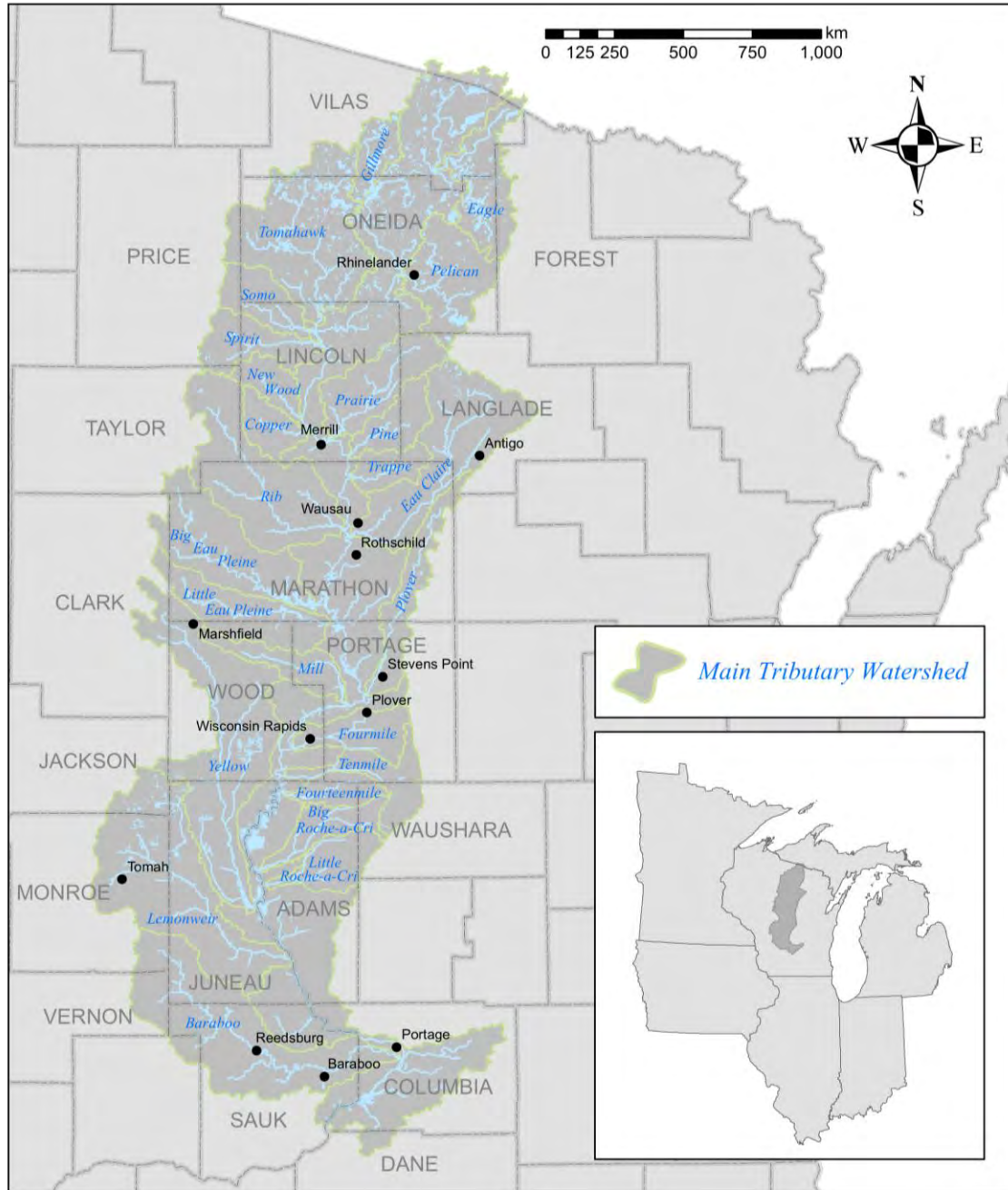


Figure 1 Upper Wisconsin River SWAT model area with large municipal separate stormwater systems (MS4s with populations greater than 5,000) and major tributary watersheds labeled.

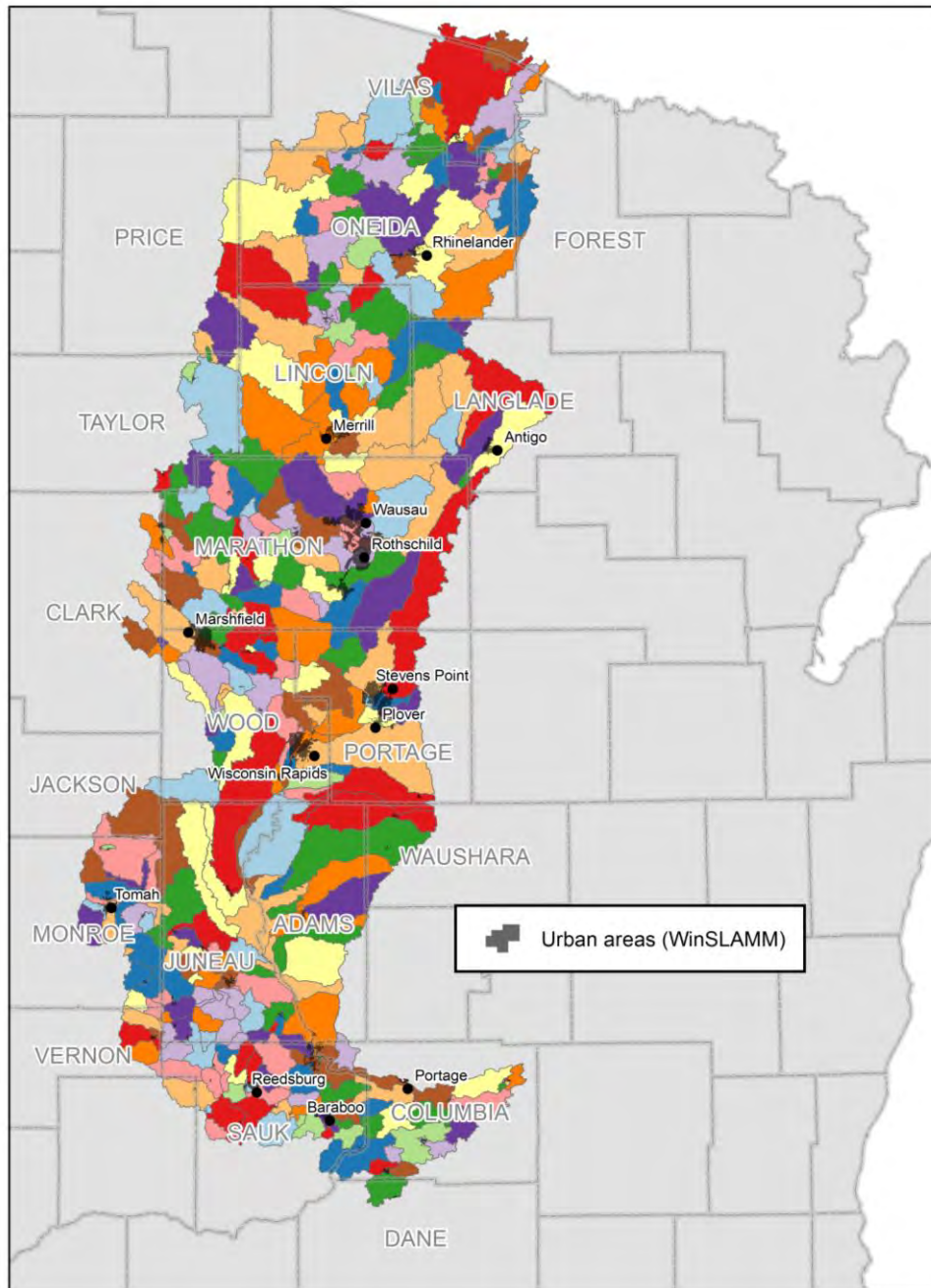


Figure 2 Map of all 337 SWAT subbasin delineations. The gray areas denoted by black polygons, were not modeled in SWAT, and therefore their areas were “cut out” of the subbasin delineation where they overlaid.

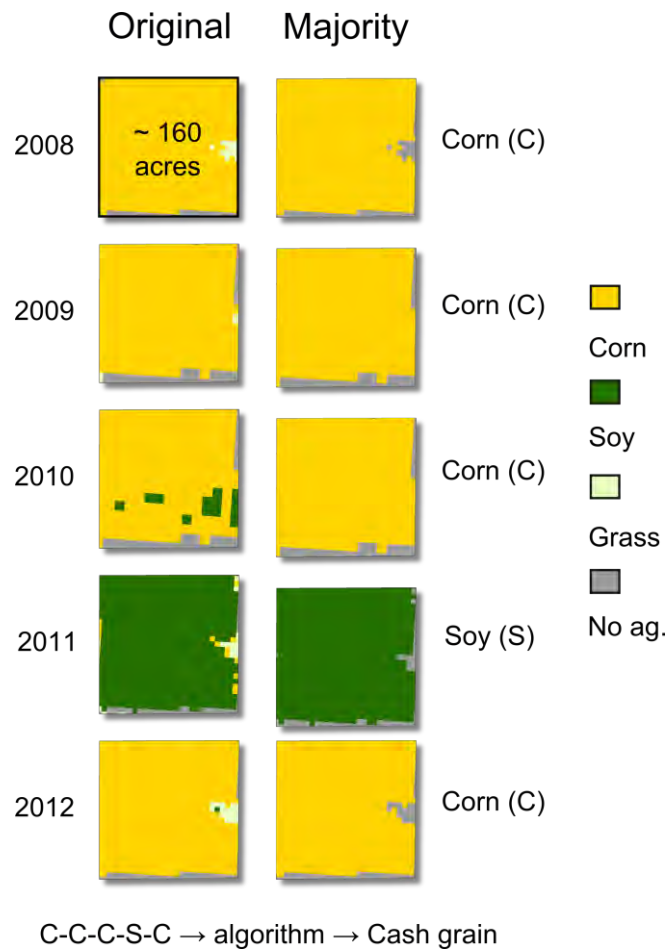


Figure 3 WDNR Approach for defining crop rotations and land management for the WRB SWAT model. Crop classifications were generalized to the majority within a Public Land Survey System (PLSS), 160-acre (65-hectare) 1/4-section. A majority crop sequence was then constructed for each 1/4 section. A custom algorithm was built to translate each crop sequence to a generalized agricultural rotation type.

**Initial Rotations – Pre-Local Knowledge
(By 1/4 Section)**

	Rotation Type	Acres	Category/Total Acres		
Cash Grain	Cash Grain	341,882	Cash Grain – 494,817		
	Continuous Corn	152,935			
	Dairy	Dairy, 1 Year Corn	22,394	Dairy – 362,973	
		Dairy, 2 Years Corn	245,973		
		Dairy, 3 Years Corn	64,207		
		Dairy, Corn/Potato	13,587		
Dairy, Soybean	16,812				
Potato/Vegetable	Potatoes	10,542	Potato/Vegetable – 141,667		
	Potatoes / Corn	17,250			
	Potatoes / Corn / Dry Beans	23,375			
	Potatoes / Corn / Soy	7,149			
	Potatoes / Corn / Vegetables	7,852			
	Potatoes / Dry Beans	8,693			
	Potatoes / Sweet Corn	27,180			
	Potatoes / Sweet Corn / Dry Beans	18,480			
	Potatoes / Sweet Corn / Soy	4,381			
	Potatoes / Sweet Corn / Vegetables	7,480			
	Sweet Corn / Dry Beans	7,367			
	Sweet Corn / Potatoes	1,918			
	Pasture/Hay	Pasture/Hay		572,439	Pasture/Hay – 620,342
		Alfalfa		47,903	
Other		Corn, Dry Beans	7,724	Other – 308,150	
	Dry Beans	678			
	Insufficient	299,594			
	No Agriculture	154			

**Rotations – Post-Local Knowledge
(By CLU)**

Land Cover	Acres
Cranberries	20,467
Dairy Rotation	487,239
Cash Grain Rotation	257,192
Potato/Vegetable Rotation	172,464
Pasture/Hay	295,325

Rotation Acreage Change

Rotation Type	Change (CLU-1/4 Section Rotations)
Cash Grain	-237,625
Dairy	124,266
Potato/Vegetable	30,797
Pasture/Hay	-325,017

Figure 4 Our initial assessment of typical crop rotations were often too explicit or simply did not exist in reality. After meeting with local experts, our rotations were generalized into 5 major classes, shown in the “Post-Local Knowledge” table.

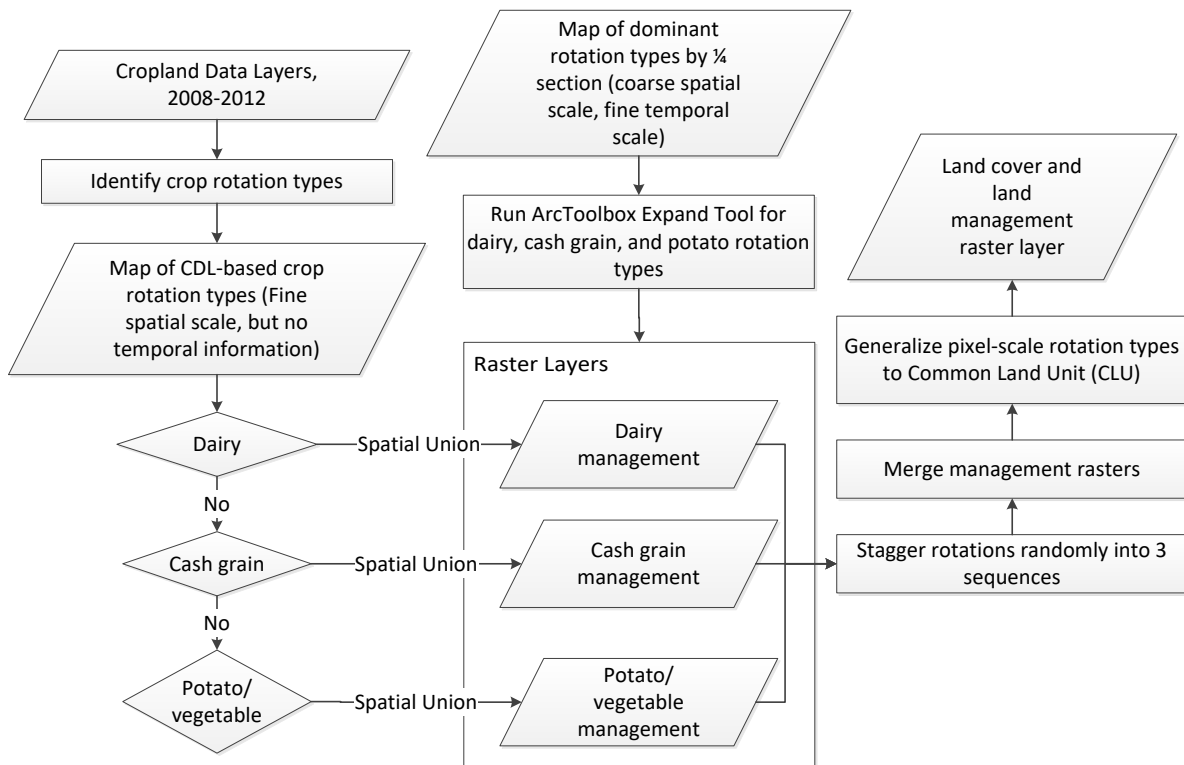


Figure 5 Process of merging local knowledge with Cropland Data Layer (CDL) defined rotations

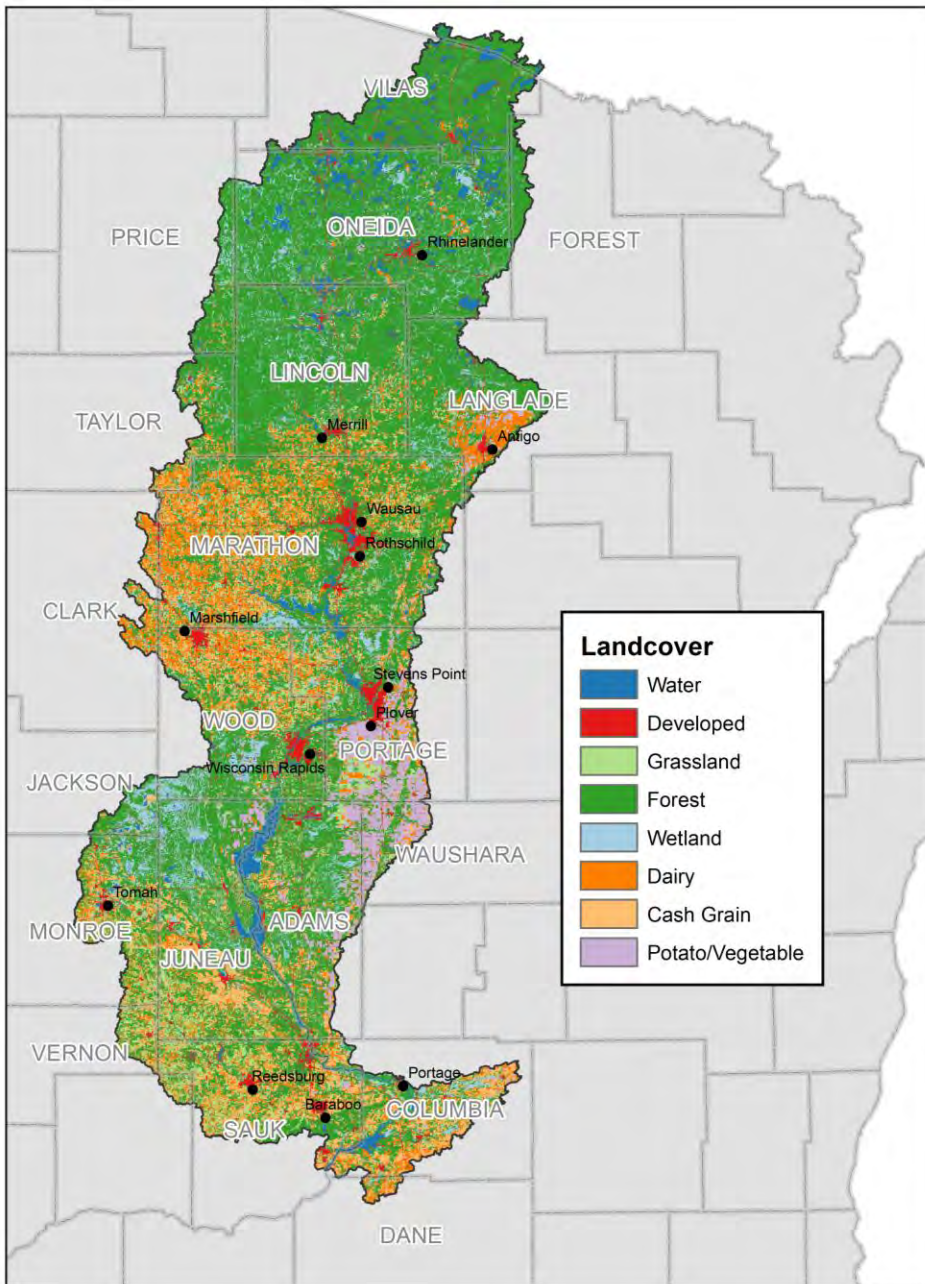
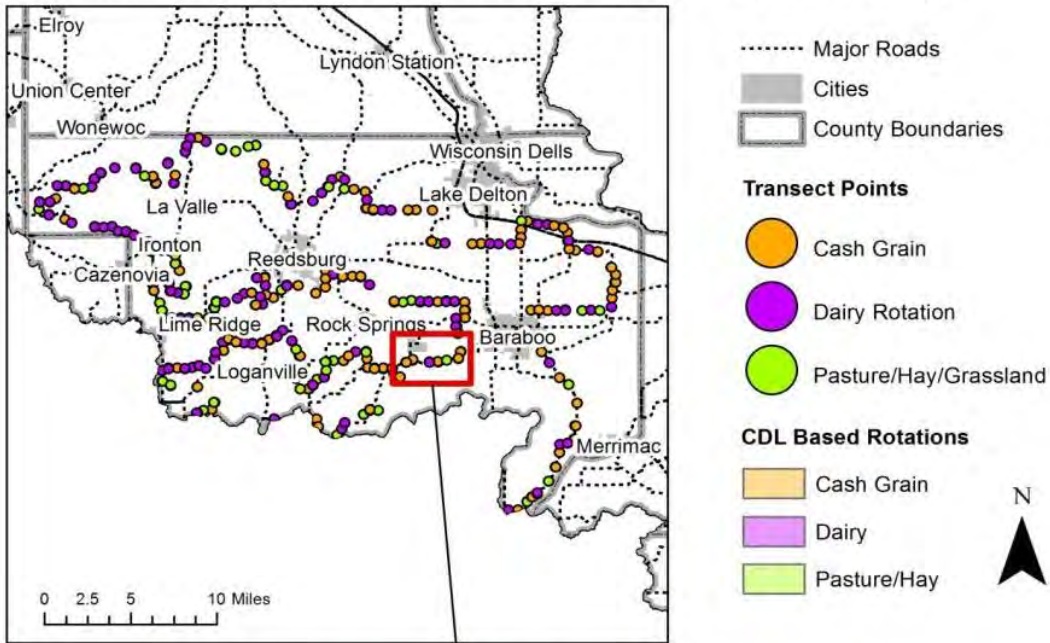


Figure 6 Final landcover map used for configuration of SWAT model. Dairy, Cash Grain, and Potato/Vegetable rotations refer to landcovers delineating in the process described in Section 3.2.2.

Crop Rotations Categorized by Transect Survey Points (Sauk County)



Comparison of CDL and Transect Based Crop Rotations (Sauk County)

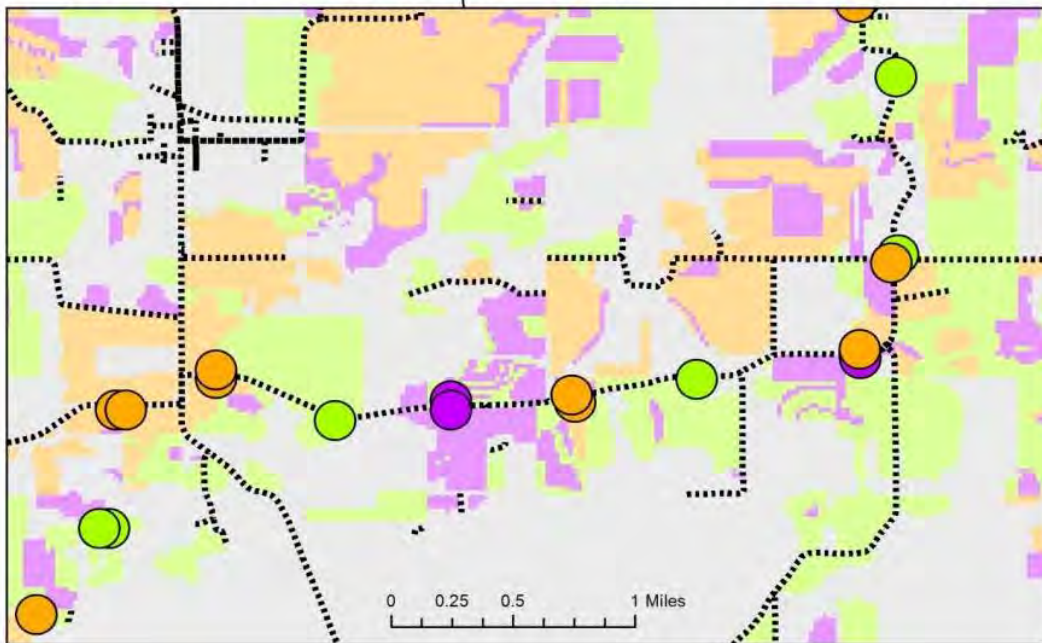


Figure 7 Maps showing an example of a qualitative comparison of pixel-based Cropland Data Layer (CDL) crop rotations to transect point crop rotations. The same algorithm was used to generalize a crop rotation from a 5-year sequence for both the CDL and transect data.

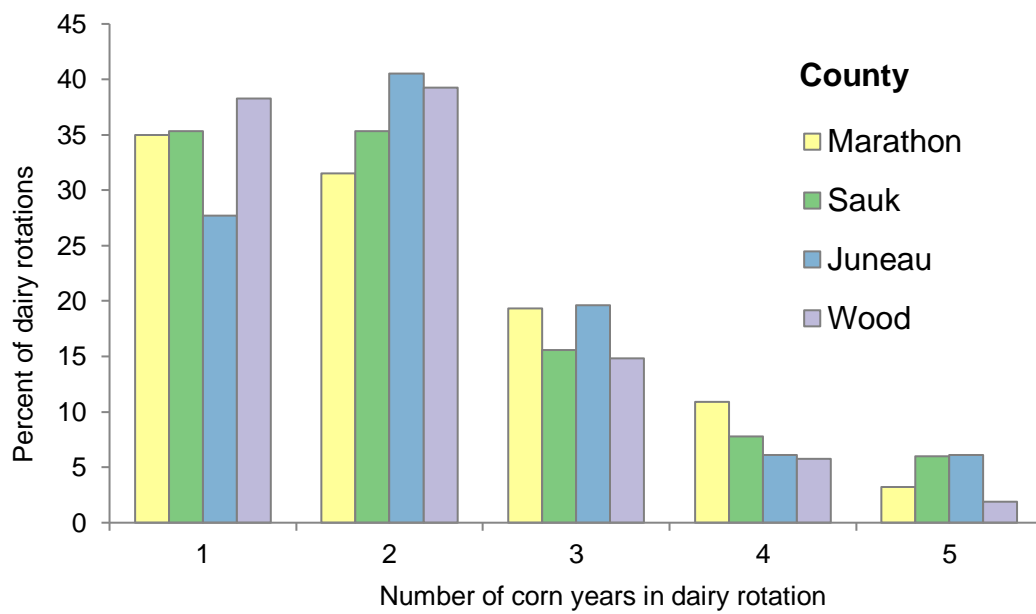


Figure 8 The number of years of corn planted in a typical 6-year dairy crop rotation varied by region.

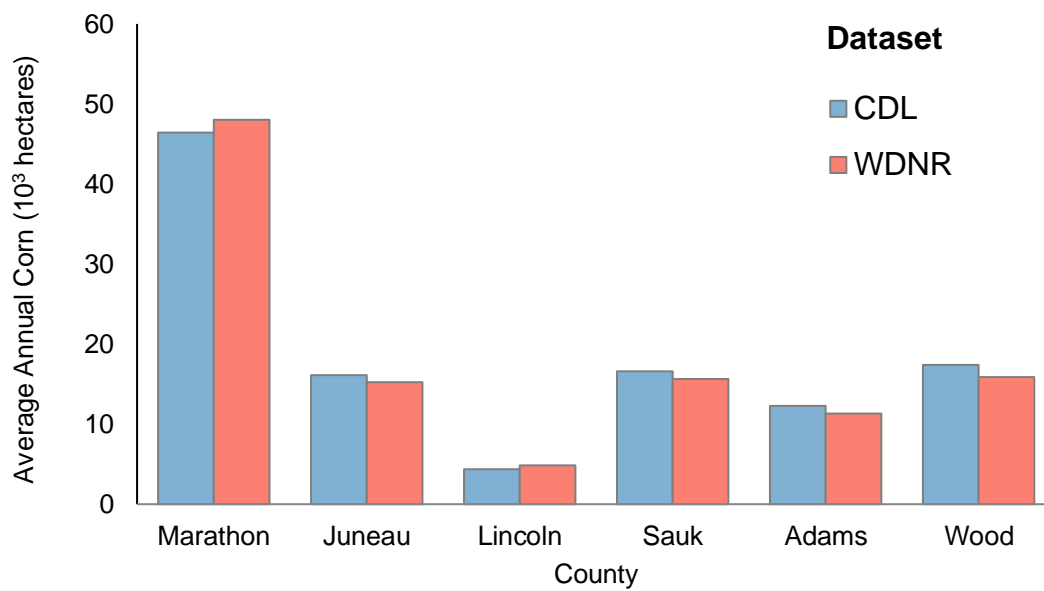


Figure 9 Comparison of corn area (thousands of hectares) of raw Cropland Data Layer (CDL) to our (WDNR) generalized version that was ultimately used in the SWAT model. Regardless of county, the WDNR generalized version matches the original product well, which validates that the rotational generalization as well as the numbers of corn years used in dairy and cash grain rotations match well with reality.

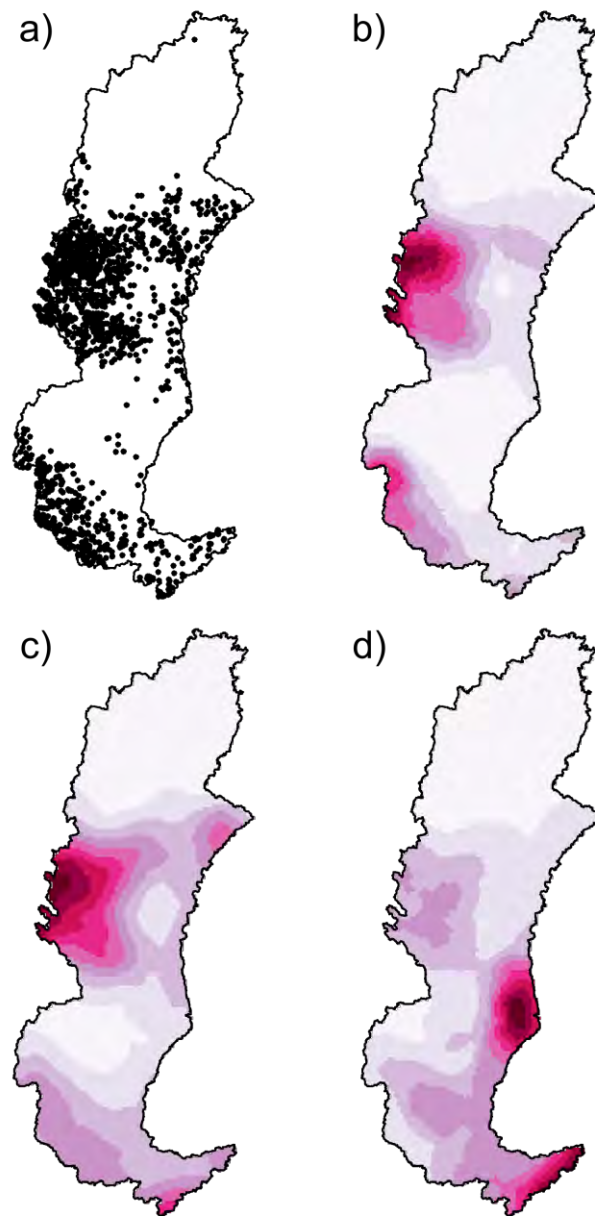


Figure 10 Comparison of the locations of dairy production facilities [provided by the Wisconsin Department of Agriculture, Trade, and Consumer Protection (DATCP)] to areas defined as dairy rotation from the generalized landcover and land management dataset described in Sections 3.2.1 through 3.2.4. The locations of dairy production facilities provided by DATCP (a) and their densities (b) align well with density of generalized dairy rotations used in this study (c). The locations of non-dairy agricultural production are also shown (d) to illustrate that the pattern of identified dairy rotations did not simply follow the pattern of overall agriculture.

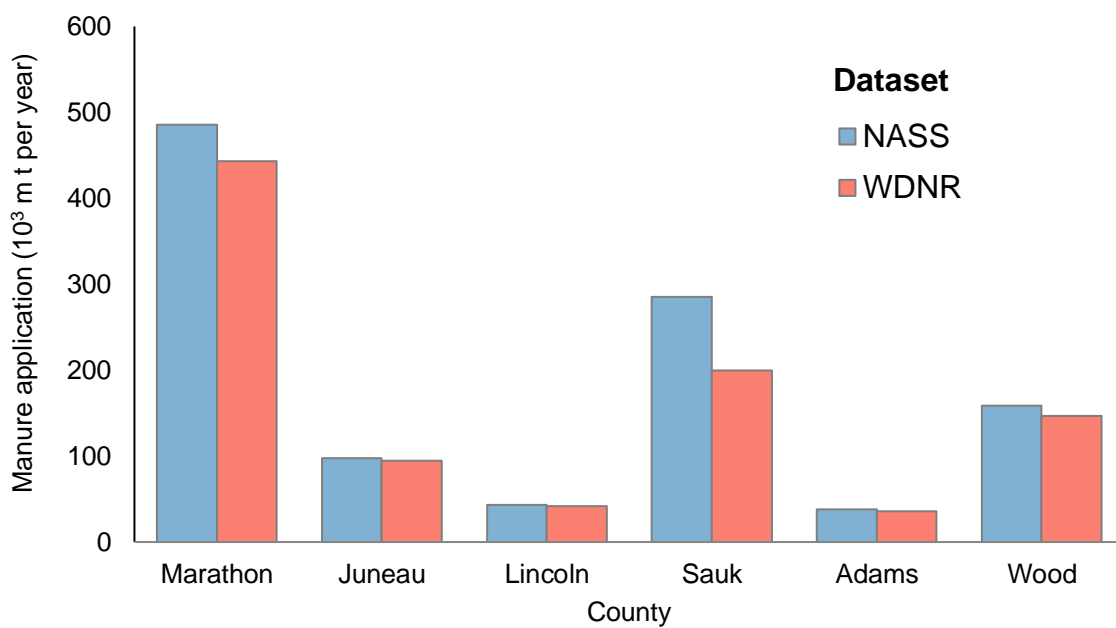


Figure 11 Comparison of masses of applied manure between the National Agricultural Statistics Service countywide estimates and ours (WDNR). Specific methods for calculating manure masses can be found in the balance sheets in Appendix D.4.

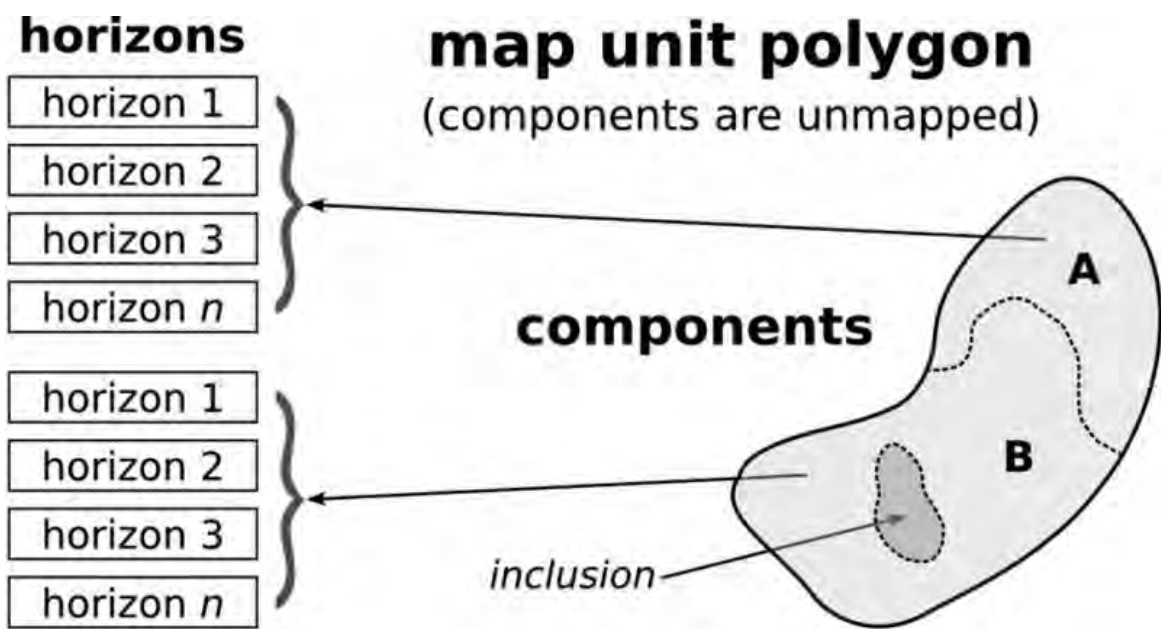


Figure 12 Schematic diagram of SSURGO data structure [taken from Gatzke et al. (2011)].

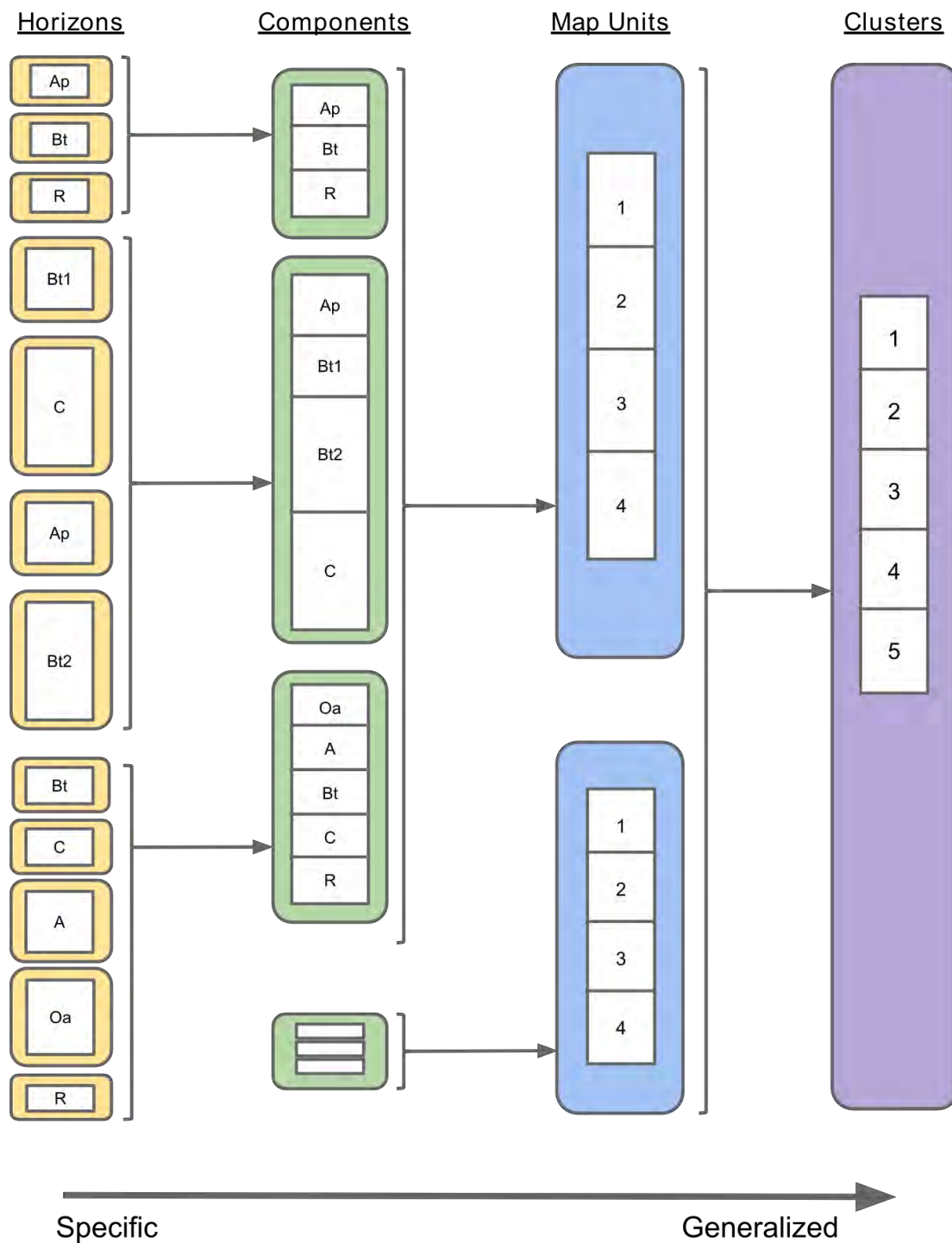


Figure 13 Flow diagram of the soil aggregation process. Horizons are grouped together according to which component they belong. Components are grouped together according to which map unit they belong to. A weighted average is calculated, based upon the component percentage. Mapunits are grouped together according to hydrologic soil group, and they are then assigned to a cluster based on a clustering algorithm. Clusters are created by aggregated map units together using a depth-weighted average of soil properties for each horizon.

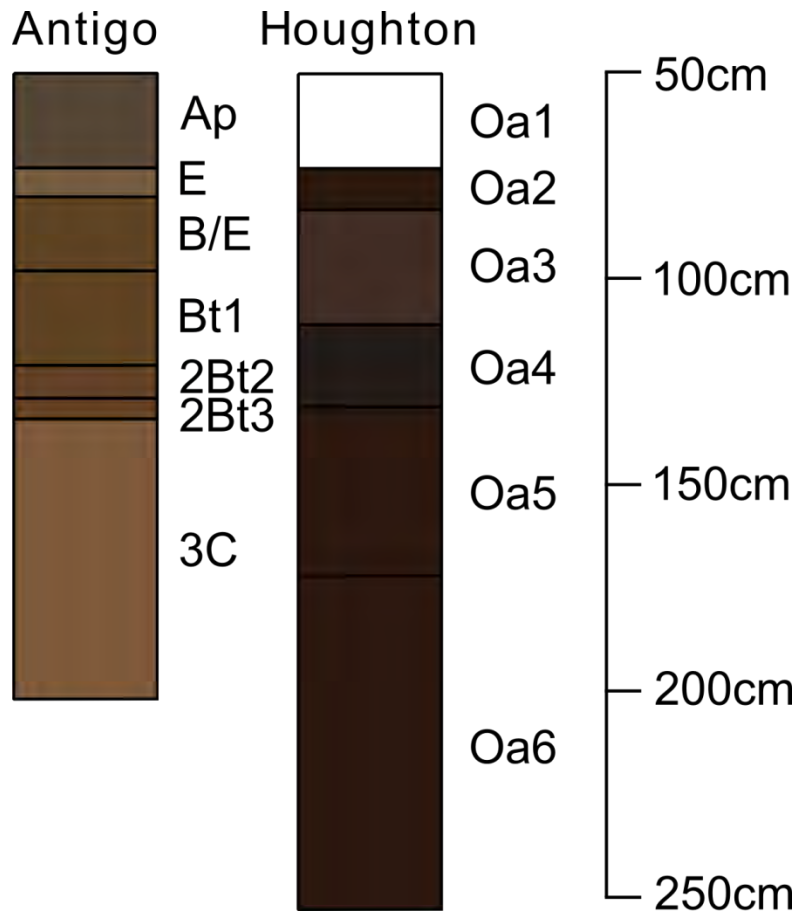


Figure 14 Schematic diagram of SSURGO map unit. Antigo and Houghton are each components within the map unit. Within each map unit are varying numbers of components with varying horizon depths (e.g., Ap and O1 are the surface horizons for Antigo and Houghton respectively). Components were aggregated to map units by averaging soil properties (e.g., percent sand) horizontally across horizons.

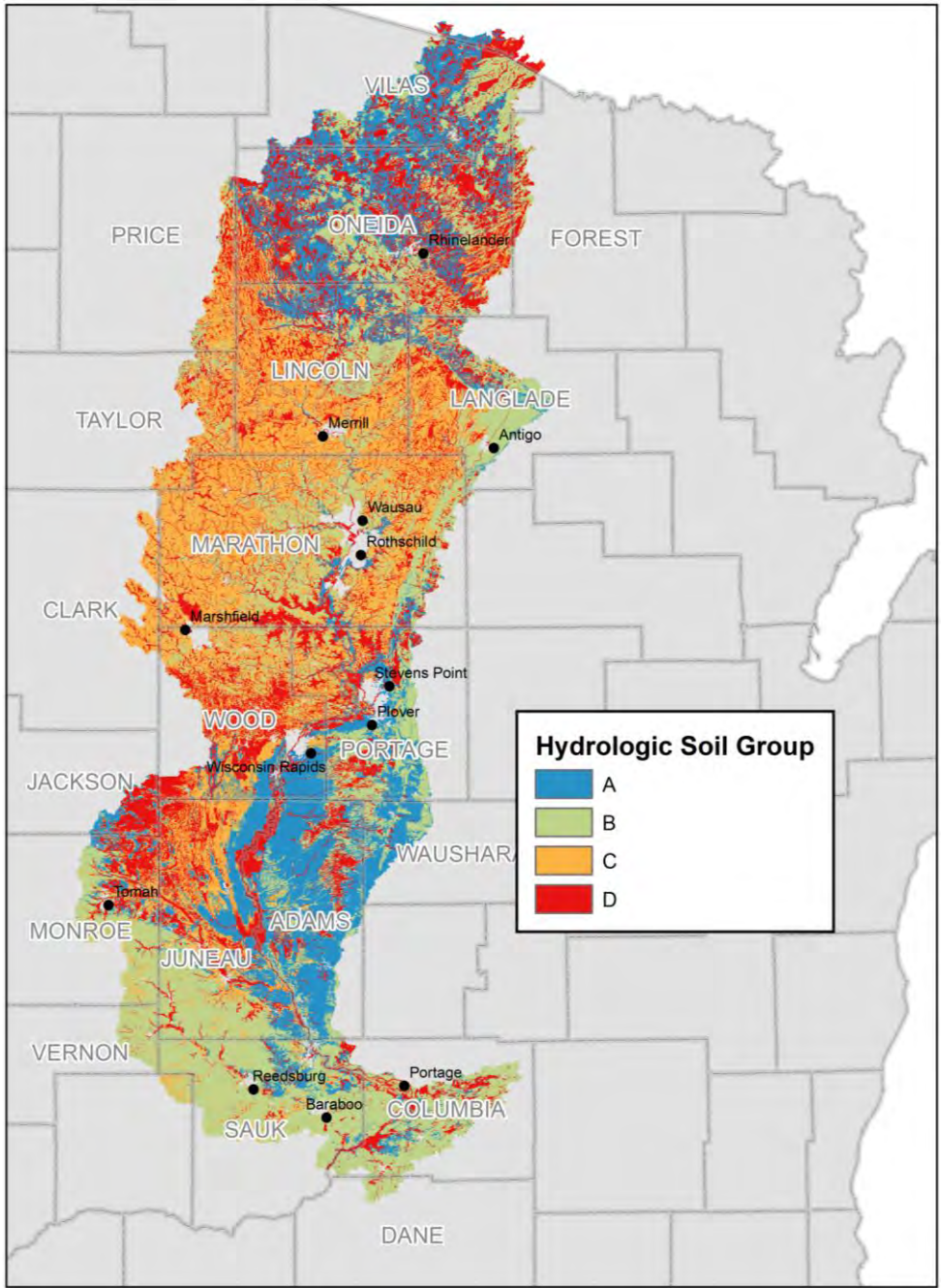


Figure 15 Hydrologic Soil Group is a good indicator of how downstream hydrology will be impacted by upstream soils. The gradient from A to D represents a gradient from well-drained to poorly-drained, respectively.

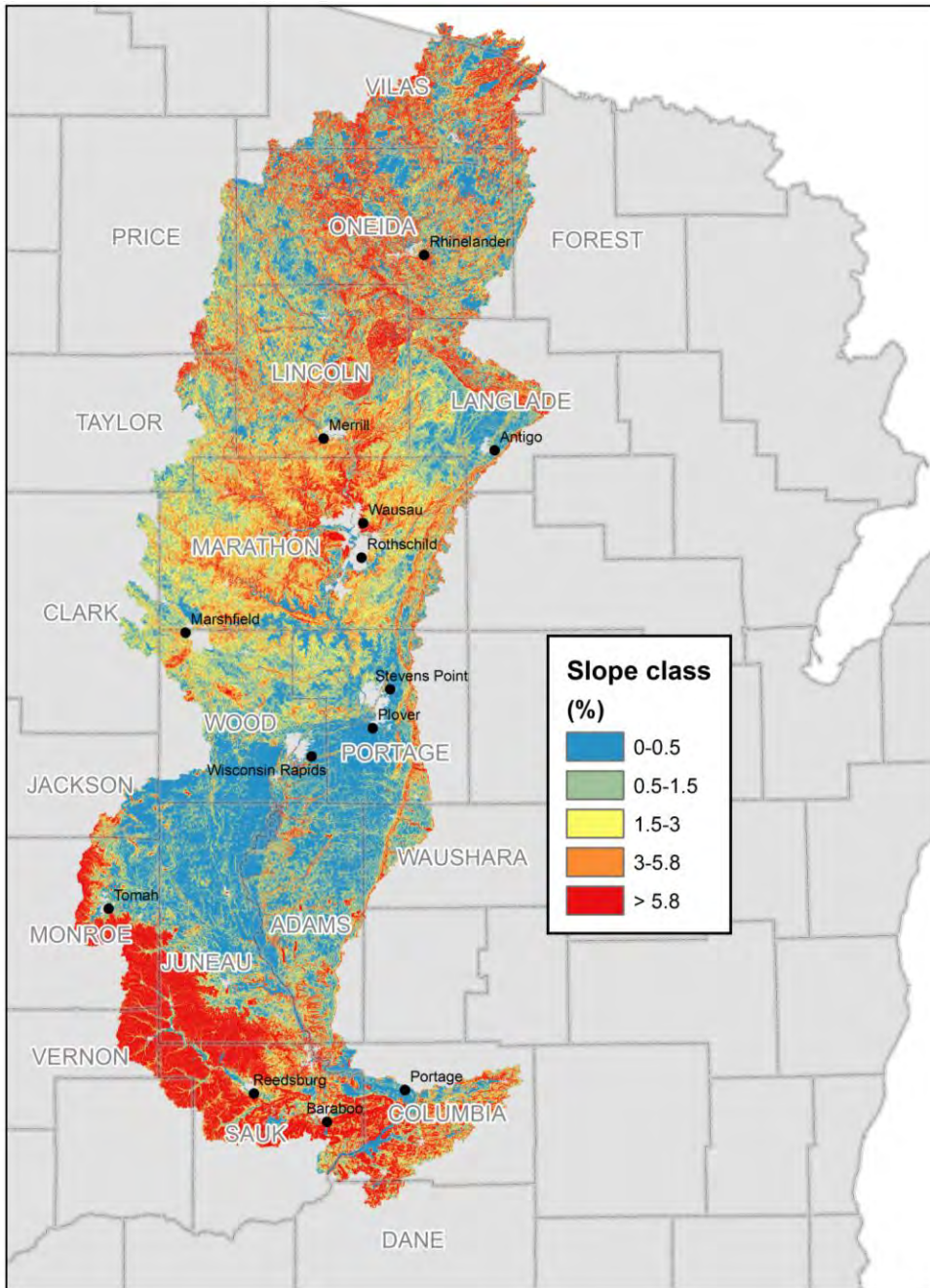


Figure 16 Map of landscape slope classes. Each slope class represents a quintile (e.g., 20% of slopes are between 0 and 0.5%). These slope classes were used for defining HRUs described in Section 3.5).

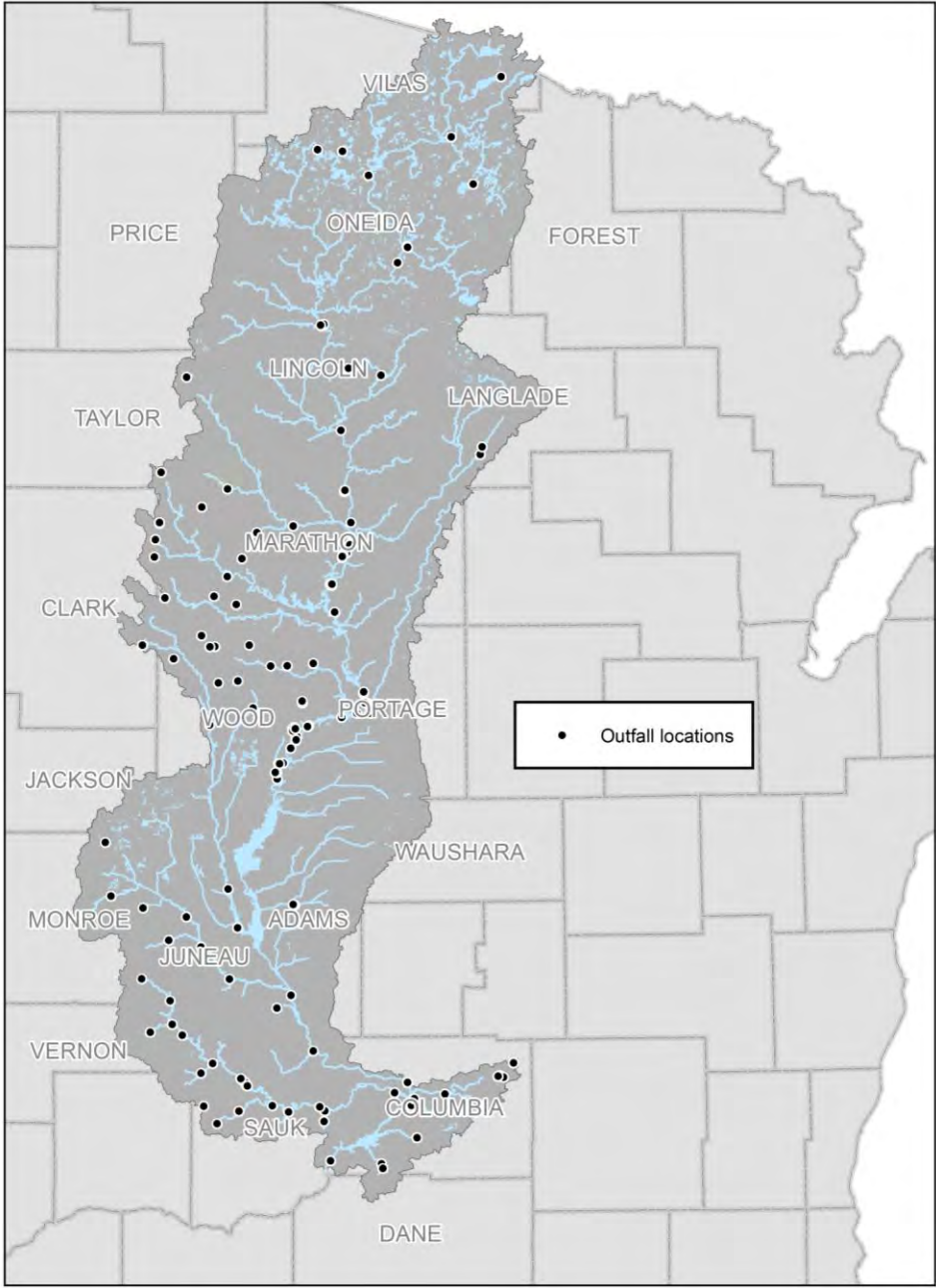


Figure 17 Locations of municipal and industrial wastewater outfalls.

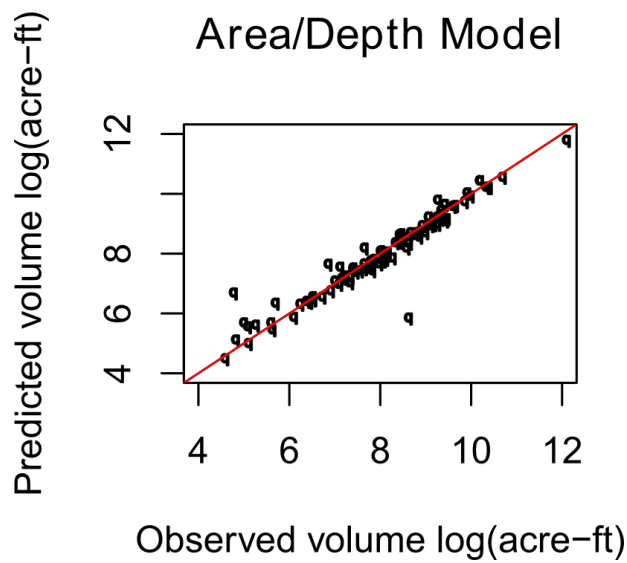
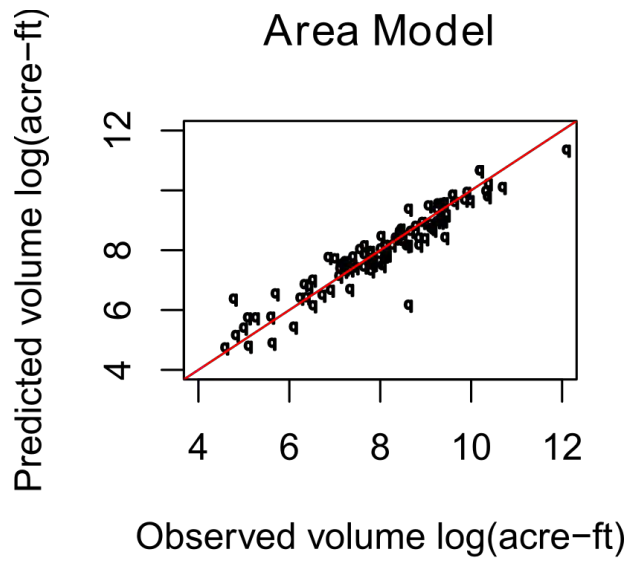


Figure 18 Scatterplots of observed versus predicted lake volumes used to parameterize geometric properties of ponds in SWAT. The area/depth model used lake surface area and maximum depth to predict lake volume and the area model used only lake surface area to predict its volume. The area/depth model explains 92% of the variability in volumes and the area model explains 89% of the variability in volumes.

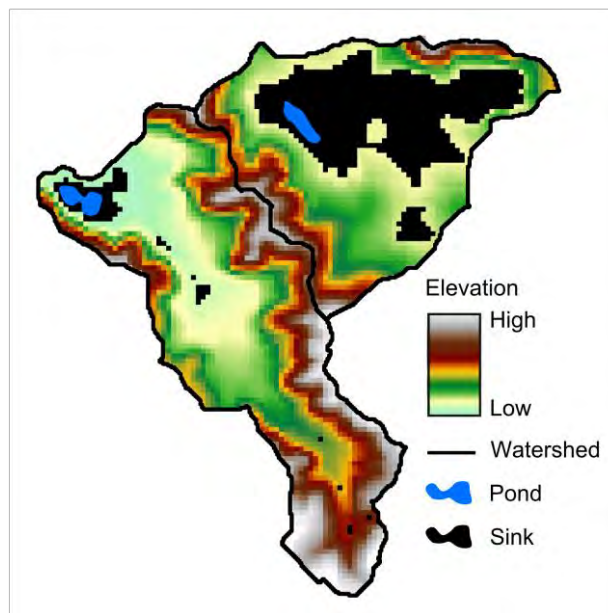


Figure 19 Example image of a filled digital elevation model (DEM) used to estimate maximum storage volume and surface area of landlocked lakes for parameterizing geometries of ponds in SWAT. The green to white gradient represents elevation from low to high. Blue polygons are landlocked lakes. Black polygons are the extent of grid cells associated with the internally draining area that flows to a landlocked lake. Black polygons not intersecting a landlocked lake were not used in surface area and volume calculations. The black watershed boundary represents the overall drainage area of each pond.

SWAT Ponds and Wetlands

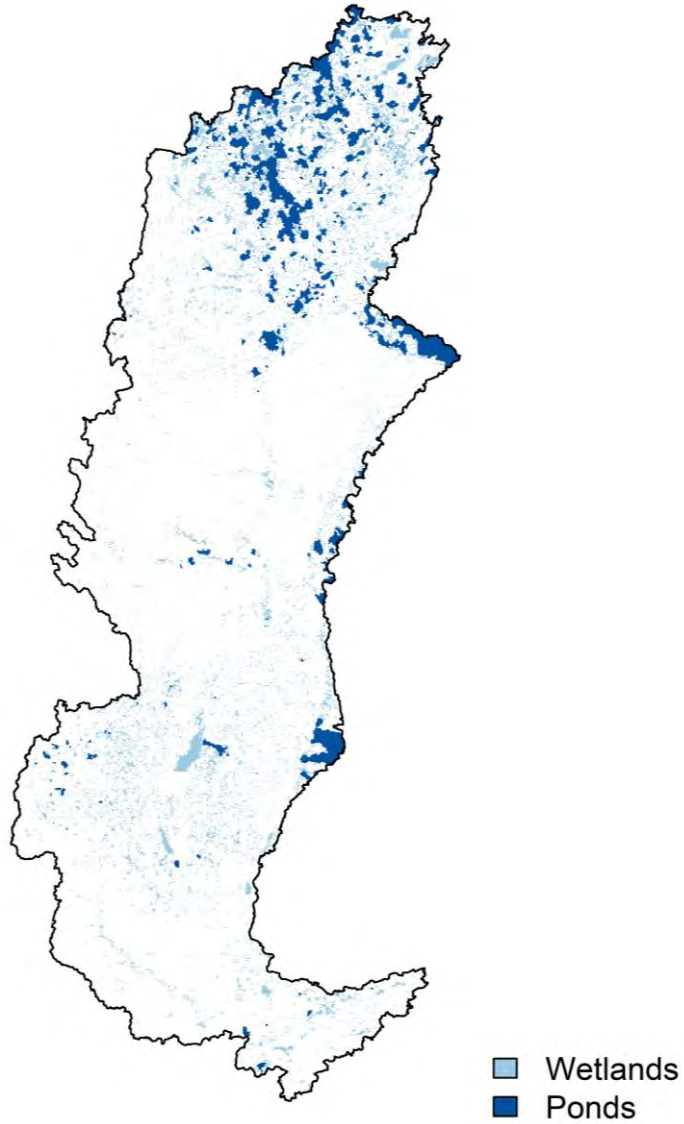


Figure 20 Map showing the areas draining to ponds and wetlands in the Wisconsin River Basin SWAT model.

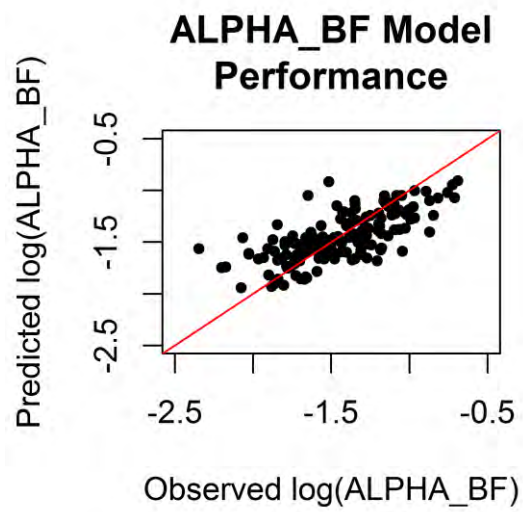


Figure 21 Observed verses predicted ALPHA_BF SWAT parameter. Observed ALPHA_BF was calculated for each USGS gage site (USGS 2014) by the Baseflow Program (Arnold et al., 1995).

ALPHA_BF Parameter

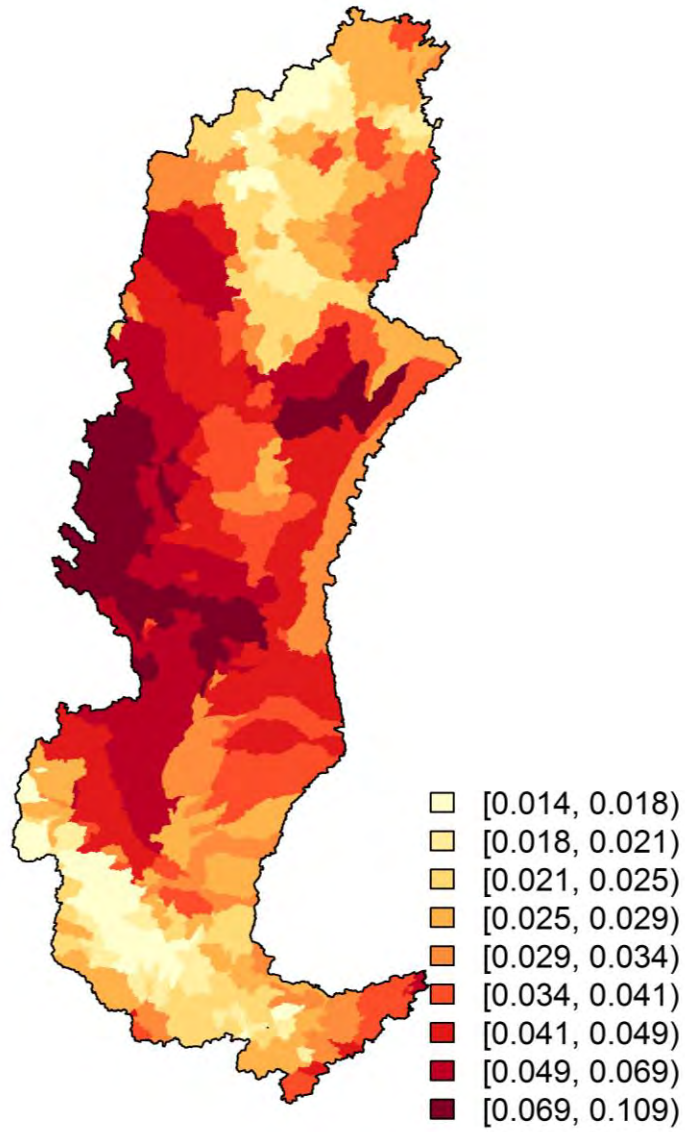


Figure 22 Map showing the predicted ALPHA_BF for each SWAT subbasin. Higher (darker) values indicate a slower response of groundwater to recharge and lighter values indicate greater baseflow.

Groundwater Phosphorus

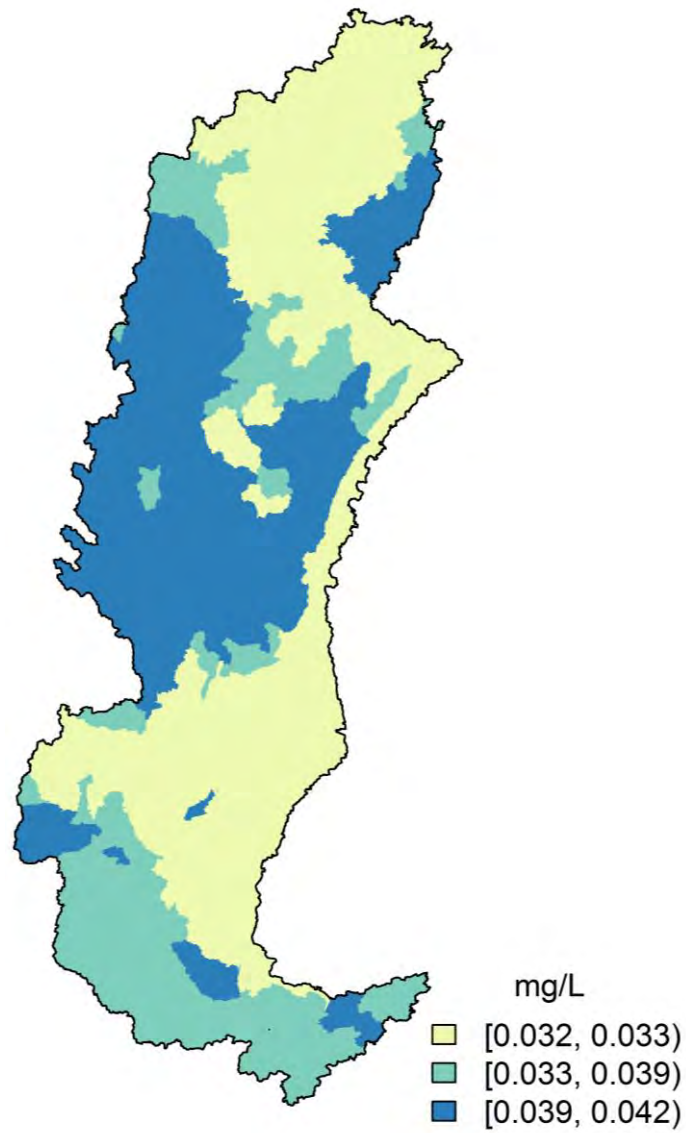


Figure 23 Map showing the estimated concentration of phosphorus in groundwater in the Wisconsin River Basin. Values were obtained from Robertson, Saad, and Heisey (2006)

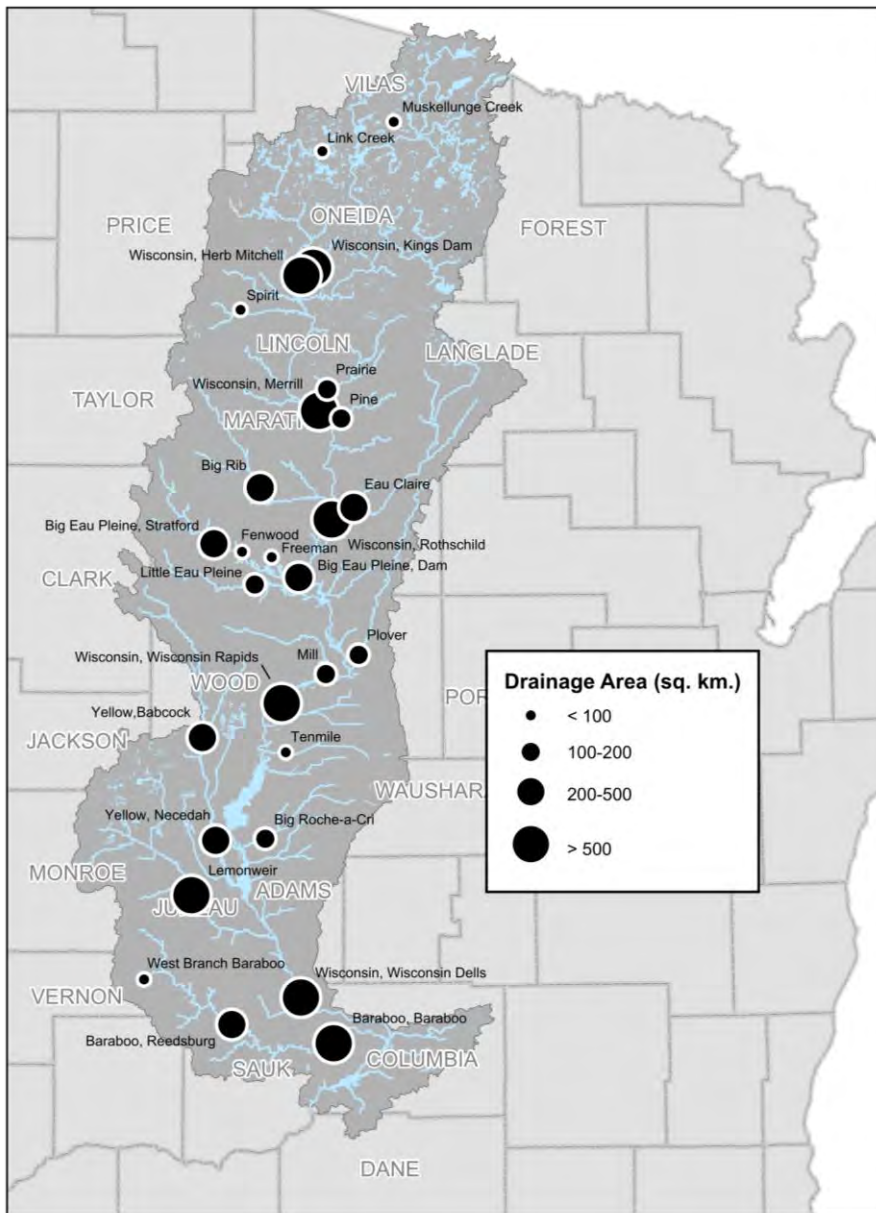


Figure 24 Location of gage sites used in the calibration process. Circle sizes are representative of drainage area size, however the sizes are not proportional.

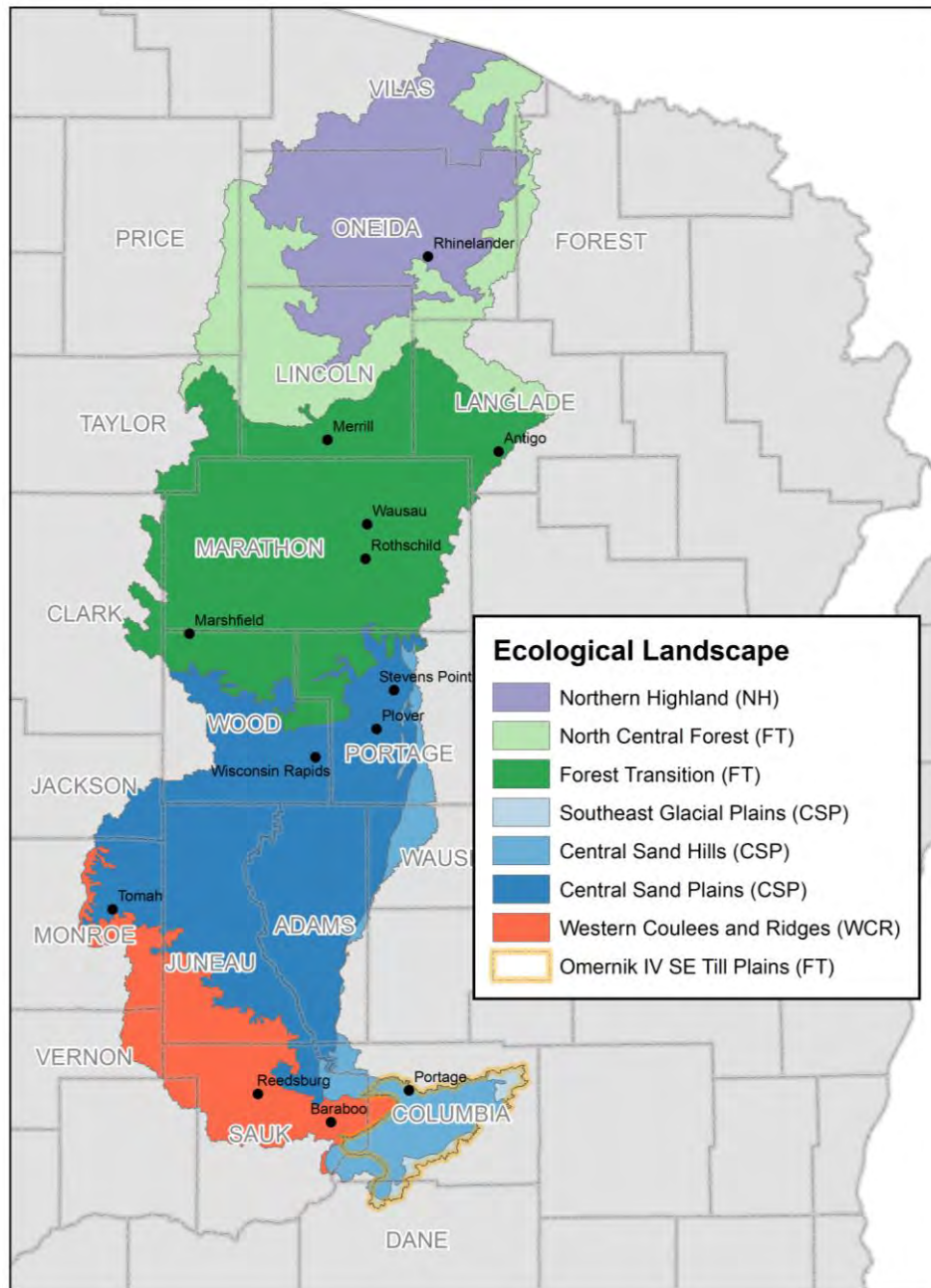
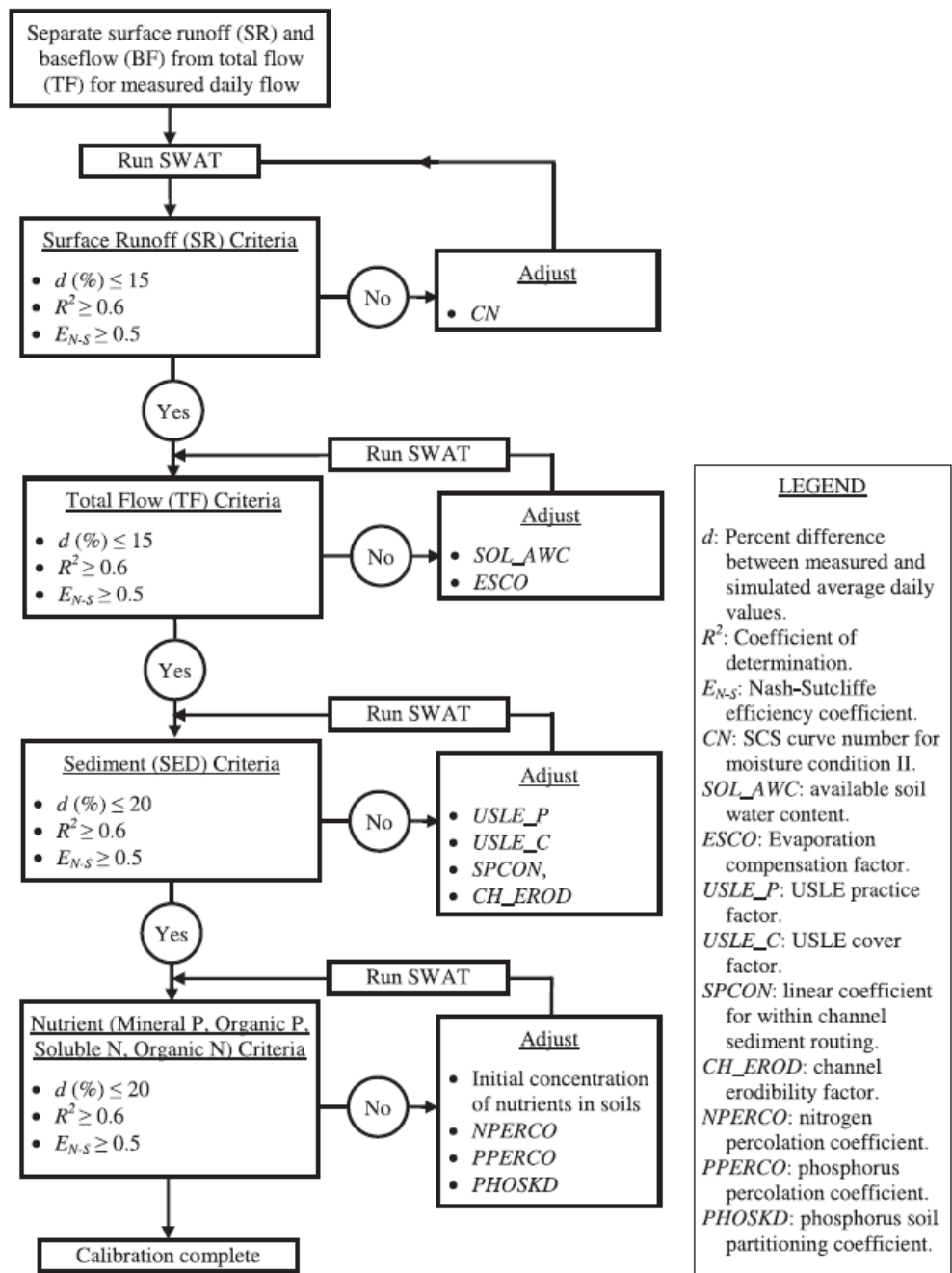


Figure 25 Map of Wisconsin Ecological Landscapes (WDNR, 2012) that were used for bounding parameter adjustments in the calibration process. Some ecological landscapes were dissolved together to minimize the complexity of the model while retaining the most important information. Each hue represents a dissolved ecoregion (e.g., the three blue hues were dissolved into the Central Sand Plains). The abbreviations in the legend also represent these dissolved ecoregions and are the abbreviations used throughout the text (NH=Northern Highland, FT=Forest Transition, CSP=Central Sand Plains, WCR=Western Coulees and Ridges). The Omernik (Omernik, 1987) delineation of the Southeastern Till Plains was used as a guide in final calibration adjustments described in Section 5.12.



LEGEND

d: Percent difference between measured and simulated average daily values.

R^2 : Coefficient of determination.

E_{N-S} : Nash-Sutcliffe efficiency coefficient.

CN: SCS curve number for moisture condition II.

SOL_AWC: available soil water content.

ESCO: Evaporation compensation factor.

USLE_P: USLE practice factor.

USLE_C: USLE cover factor.

SPCON: linear coefficient for within channel sediment routing.

CH_EROD: channel erodibility factor.

NPERCO: nitrogen percolation coefficient.

PPERCO: phosphorus percolation coefficient.

PHOSKD: phosphorus soil partitioning coefficient.

Figure 26 SWAT model calibration workflow for streamflow, sediment, and nutrients (from Engel, Storm, White, Arnold, & Arabi, 2007 and Arnold, Moriasi, et al., 2012, adapted from Santhi et al., 2001).

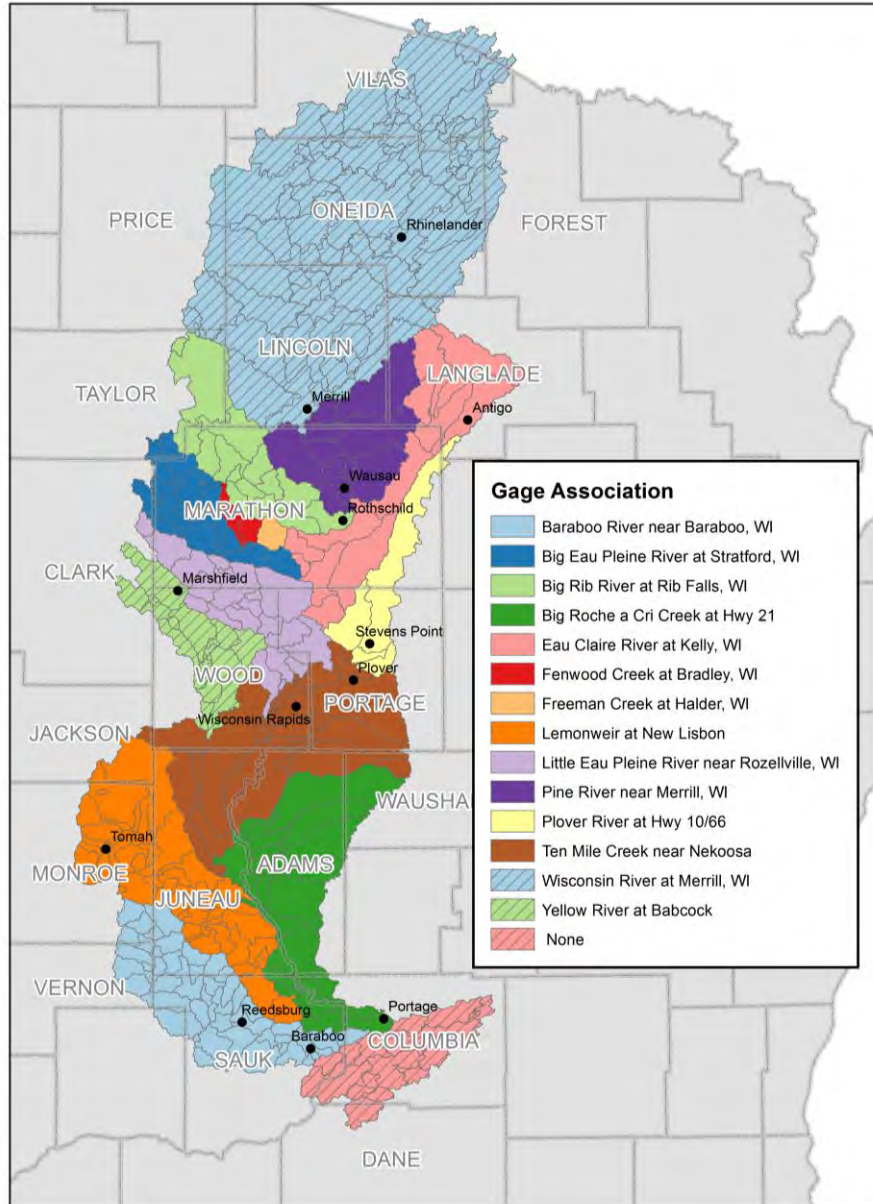


Figure 27 Each subbasin was associated with either a downstream or nearby gaging station for the routing and bias correction sub-model.

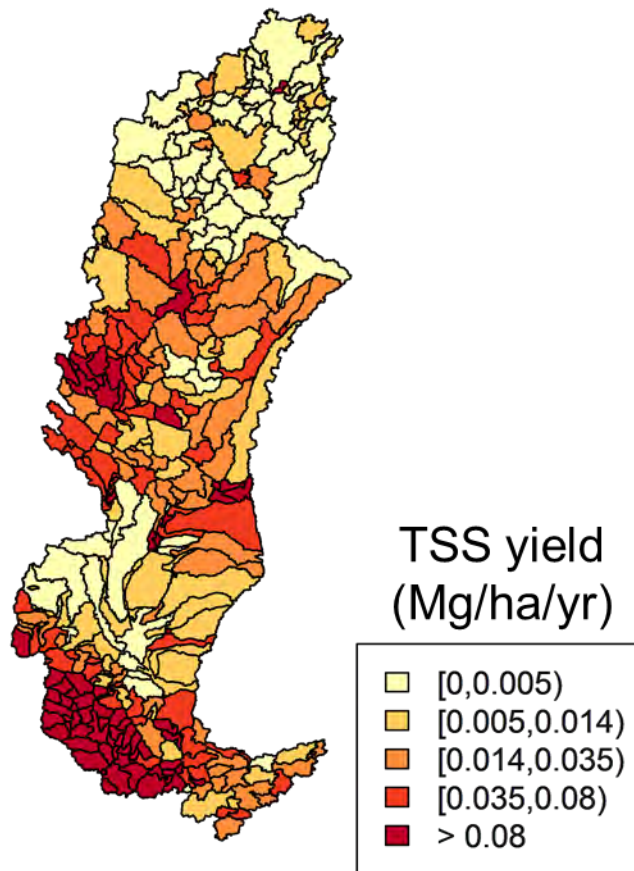


Figure 28 Map of annual average total suspended solids (TSS) yields (load normalized by area) for each subbasin in the SWAT model. Color classifications are associated with quintiles (i.e., 20% of subbasins yield between 0 and 0.005 Mg/ha/yr).

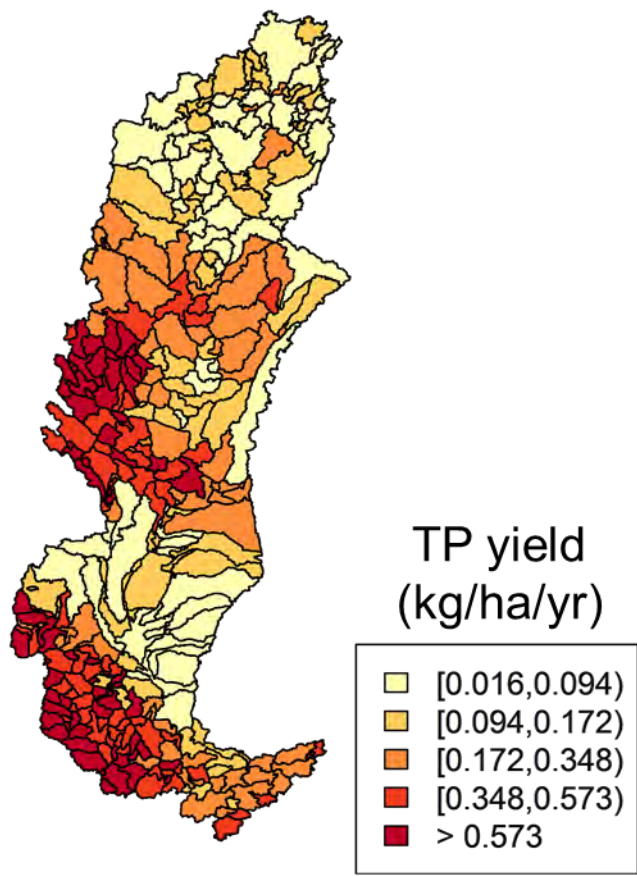


Figure 29 Map of annual average total phosphorus (TP) yields (load normalized by area) for each subbasin in the SWAT model. Color classifications are associated with quintiles (i.e., 20% of subbasins yield between 0.016 and 0.094 kg/ha/yr).

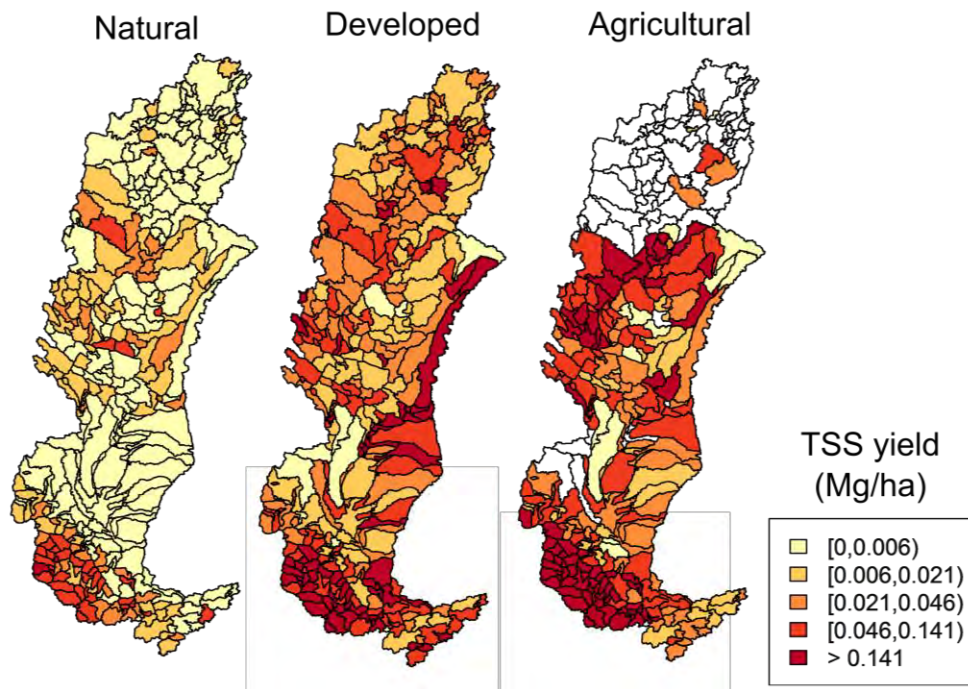


Figure 30 Maps of annual average total suspended solids (TSS) yields (load normalized by the area of each source type) for each subbasin and non-point source type in the SWAT model. Color classifications are associated with quintiles (i.e., 20% of subbasin/source combinations yield between 0 and 0.006 Mg/ha/yr).

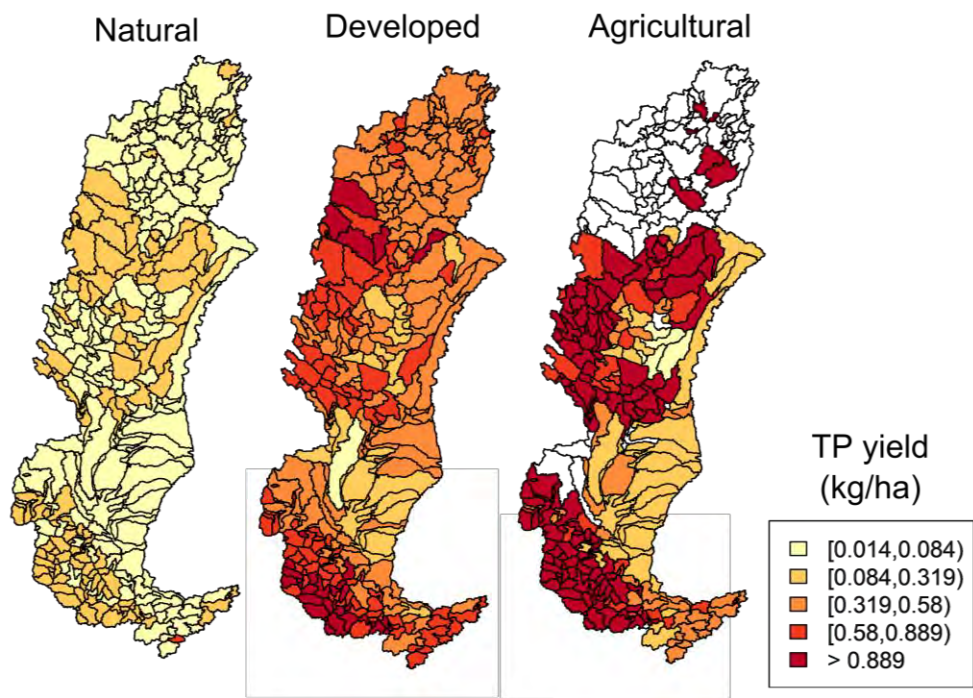


Figure 31 Maps of annual average total phosphorus (TP) yields (load normalized by the area of each source type) for each subbasin and non-point source type in the SWAT model. Color classifications are associated with quintiles (i.e., 20% of subbasin/source combinations yield between 0.014 and 0.084 kg/ha/yr).

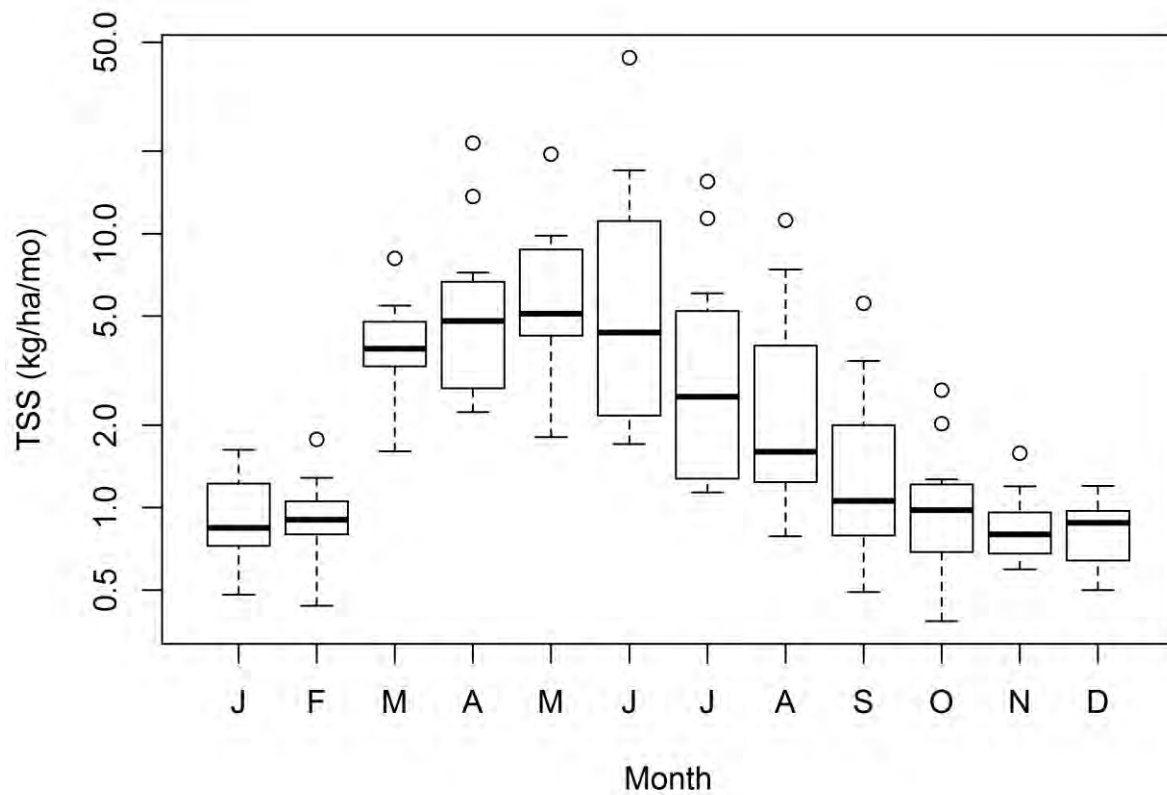


Figure 32 Boxplot showing the seasonal variability of total suspended solids yields (TSS) across the project area. Each box illustrates variability in yield across the 12 simulation years. For each month, the thick line represents the median monthly TSS yield (total load divided by the project area), the boxes represent the interquartile ranges, the whiskers represent the range, and the dots represent outliers.

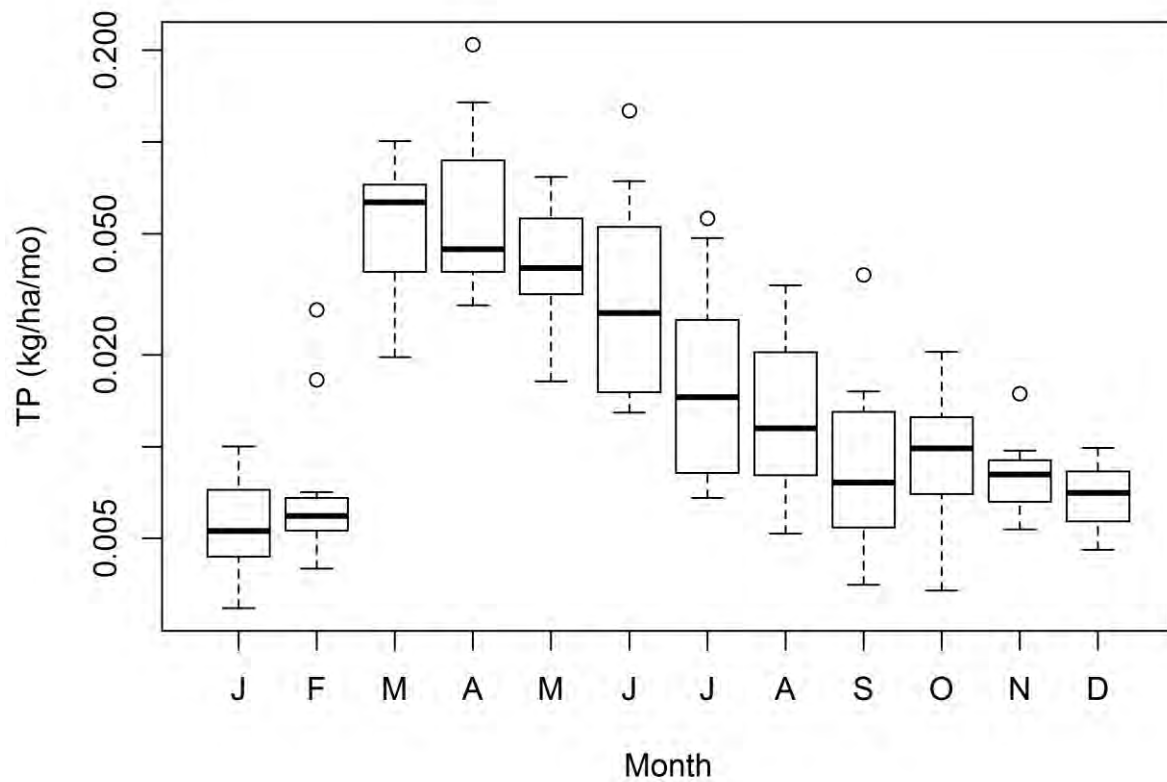


Figure 33 Boxplot showing the seasonal variability of total phosphorus (TP) across the project area. Each box illustrates variability in yield across the 12 simulation years. For each month, the thick line represents the median monthly TP yield (total load divided by the project area), the boxes represent the interquartile ranges, the whiskers represent the overall ranges, and the dots represent outliers.

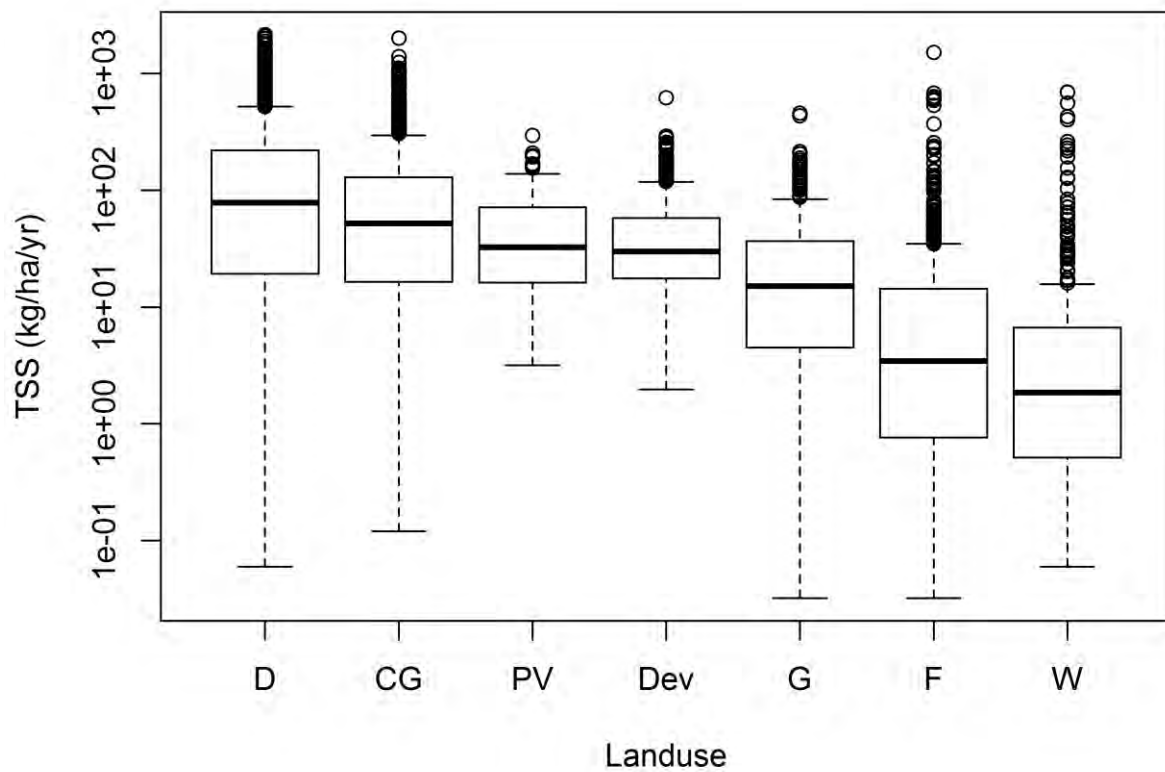


Figure 34 Boxplot showing the variability in total suspended solids (TSS) yield by each agricultural landuse-type (D=dairy, CG=corn grain, PV=potato/vegetable, Dev=developed, G=grassland, F=forest, W=wetland) across the entire project area. Each box and whisker set represents the variability of annual average TSS yield (HRU-based load divided by HRU area) across HRUs.

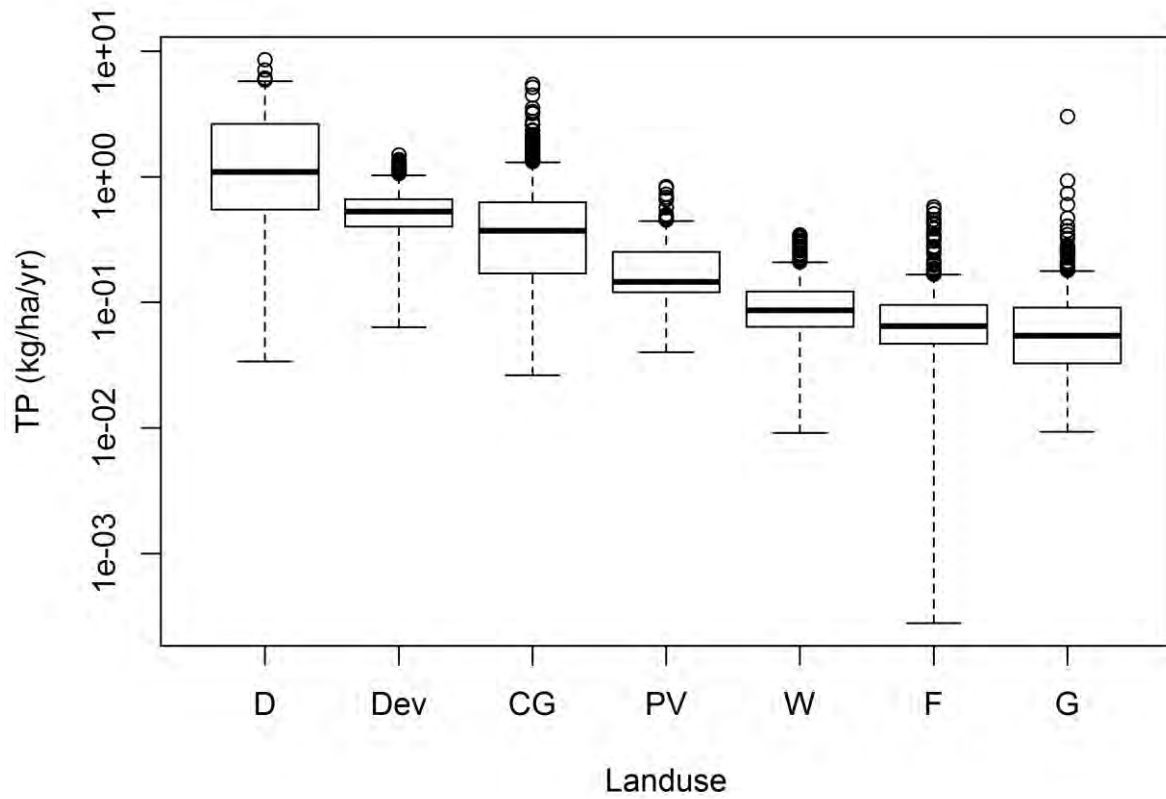


Figure 35 Boxplot showing the variability of total suspended solids (TSS) yield by landuse-type (D=dairy, CG=corn grain, PV=potato/vegetable, Dev=developed, G=grassland, F=forest, W=wetland) distributions throughout the entire project area. Each box and whisker set represents the variability of annual average TSS yield (HRU-based load divided by HRU area) across HRUs.

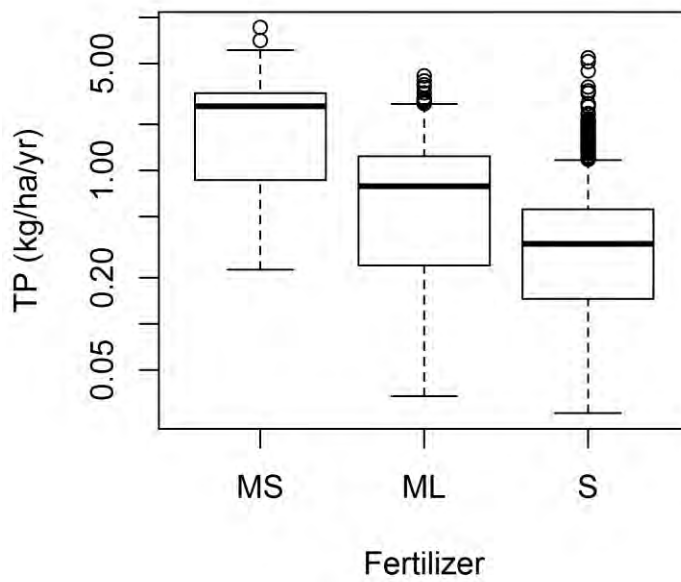


Figure 36 Boxplot showing the variability of annual average total phosphorus (TP) yield by fertilizer-type (MS=manure solid, ML=manure liquid, S=synthetic) across the whole study area. Each box and whisker set represents the variability of annual average TP yield (HRU-based load divided by HRU area) across agricultural HRUs.

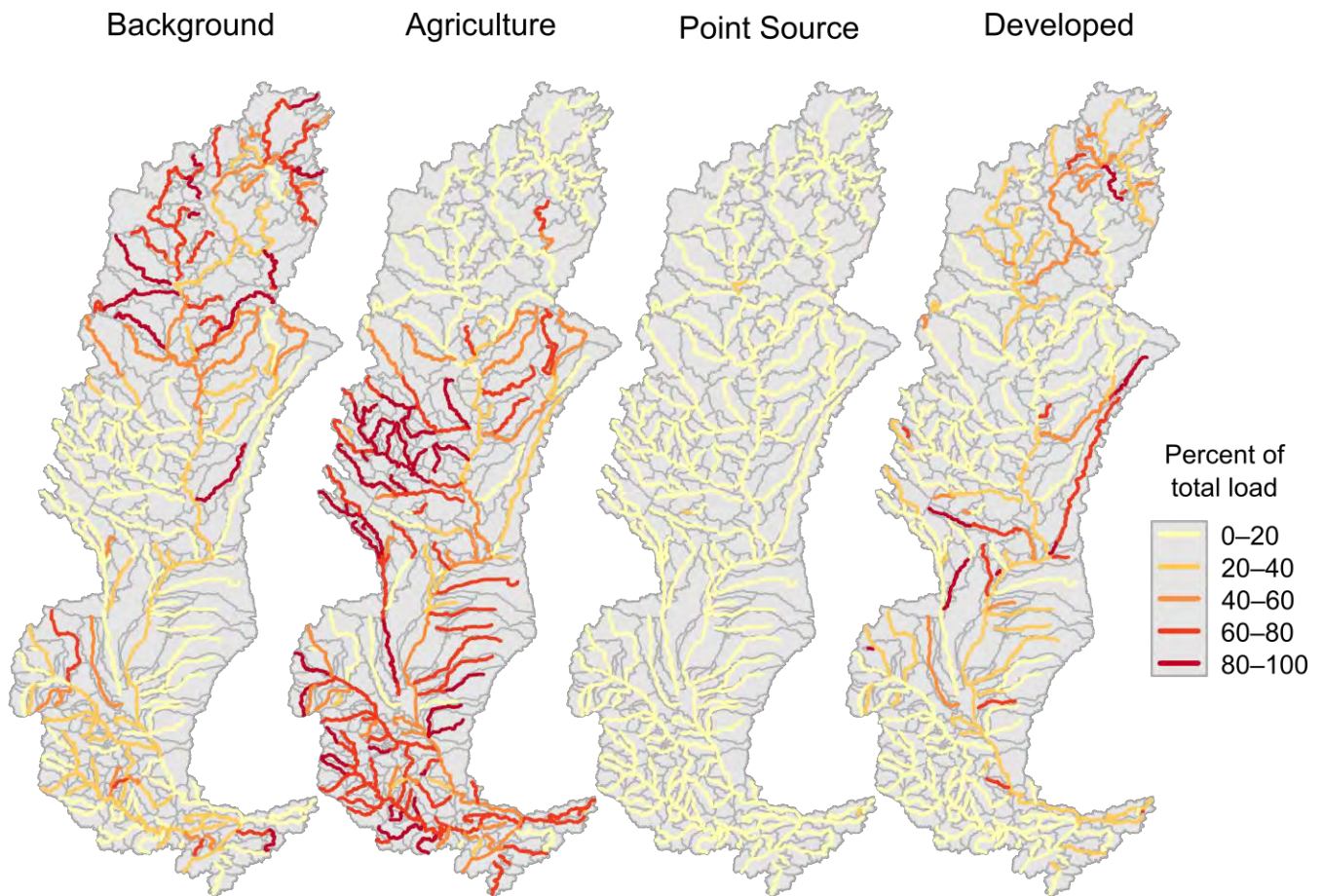


Figure 37 Maps illustrating the simulated annual average percent of in-stream total suspended solids (TSS) loads contributed by each source category. The color gradient represents the relative contribution, in percent, not the total mass. Background contributions include loads generated by forest, wetland, and grassland landcovers; developed includes developed landcover in the SWAT model, plus permitted and non-permitted developed areas simulated in WinSLAMM.

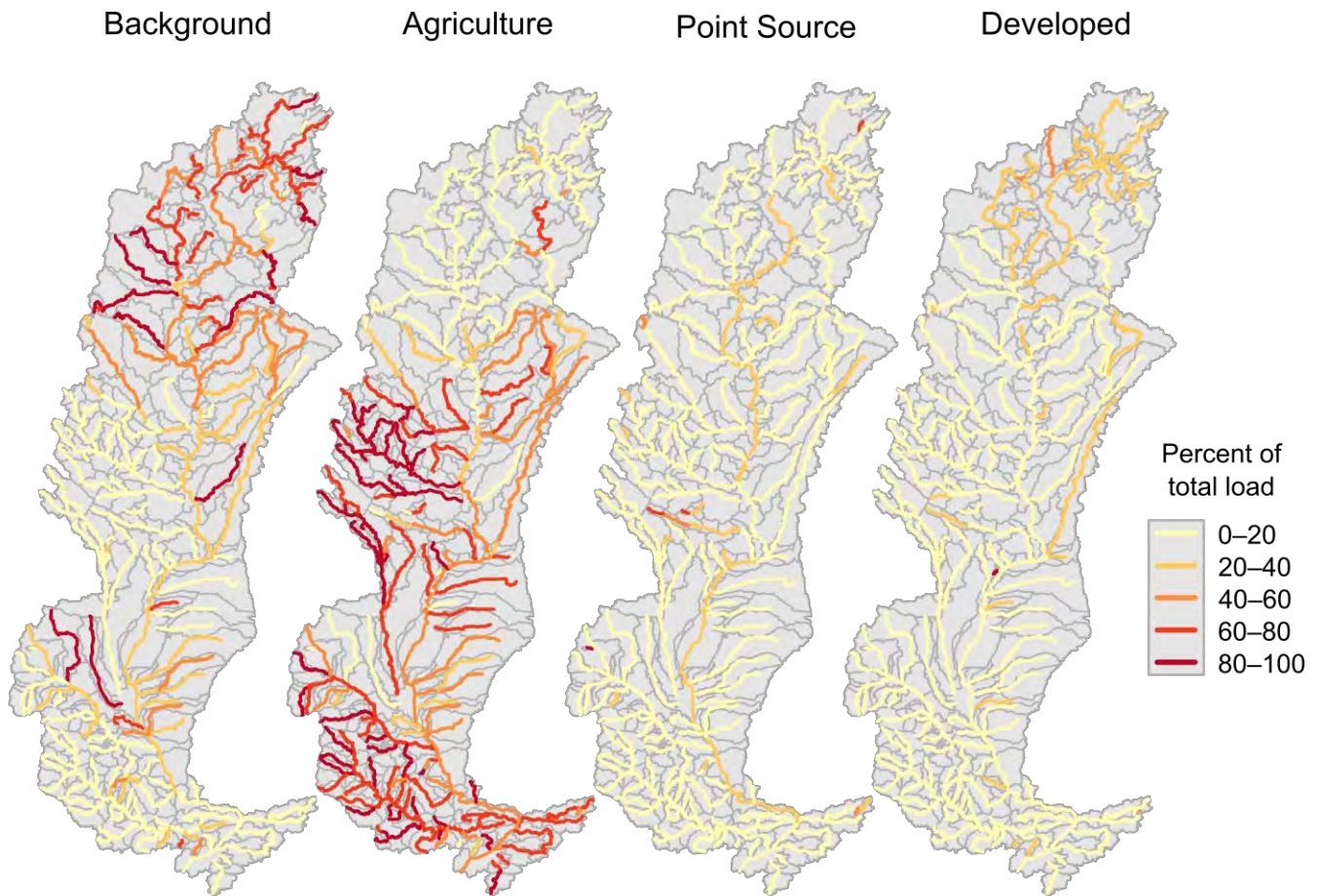


Figure 38 Maps illustrating the simulated average annual percent of in-stream total phosphorus (TP) loads contributed by each source category. The color gradient represents the relative contribution, in percent, not the total mass. Background contribution includes the portion of the load generated by forest, wetland, and grassland landcover, and developed includes the developed landcover in the SWAT model plus permitted and non-permitted urban areas simulated in WinSLAMM.

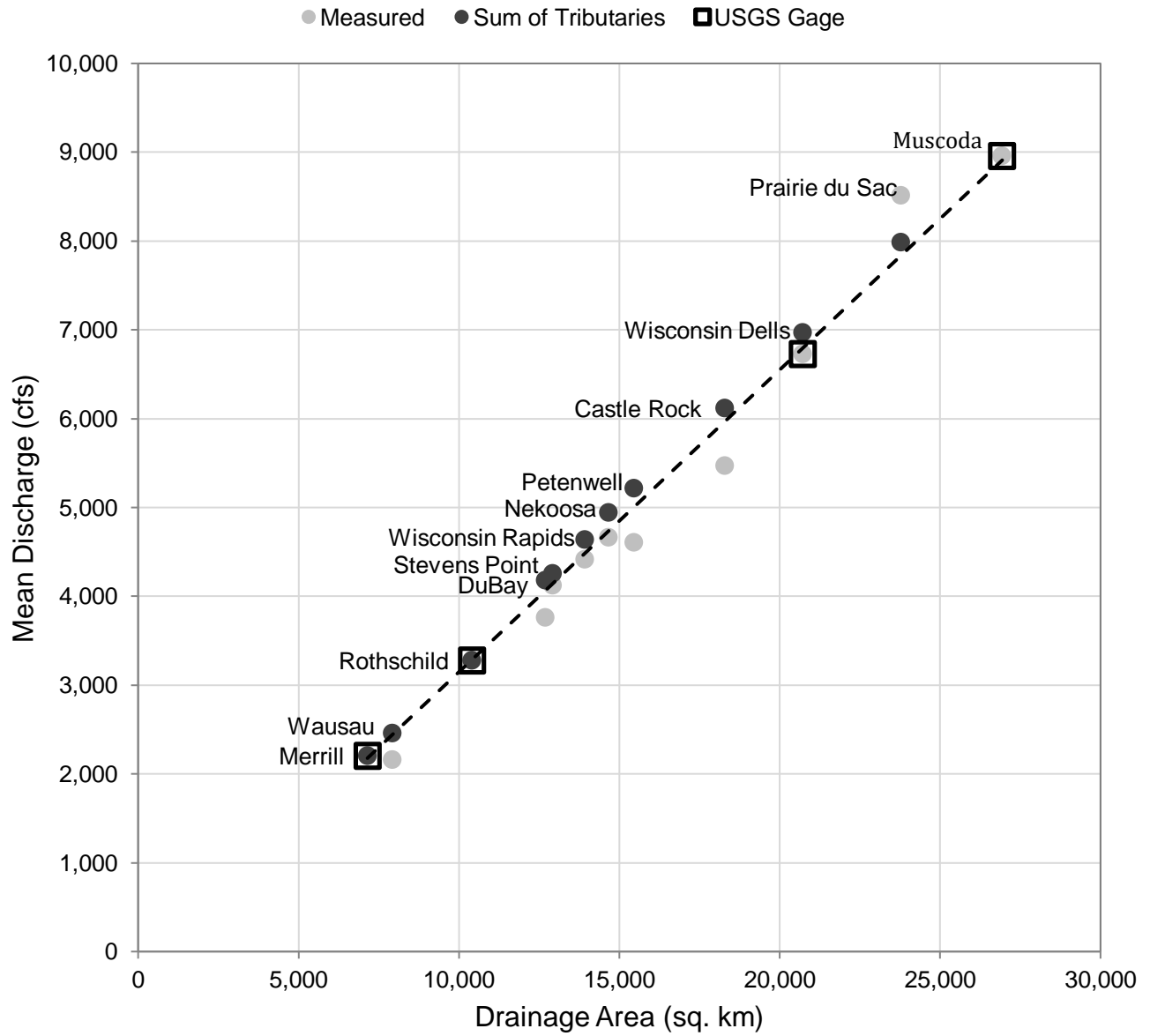


Figure 39 Plot of mean discharge (2010-13) on the mainstem Wisconsin River between Merrill and Prairie du Sac. The sum of tributary flows is based on measured flows where available, and SWAT modeled flows on ungauged tributaries. The dashed line is a linear regression of the USGS gage sites only.

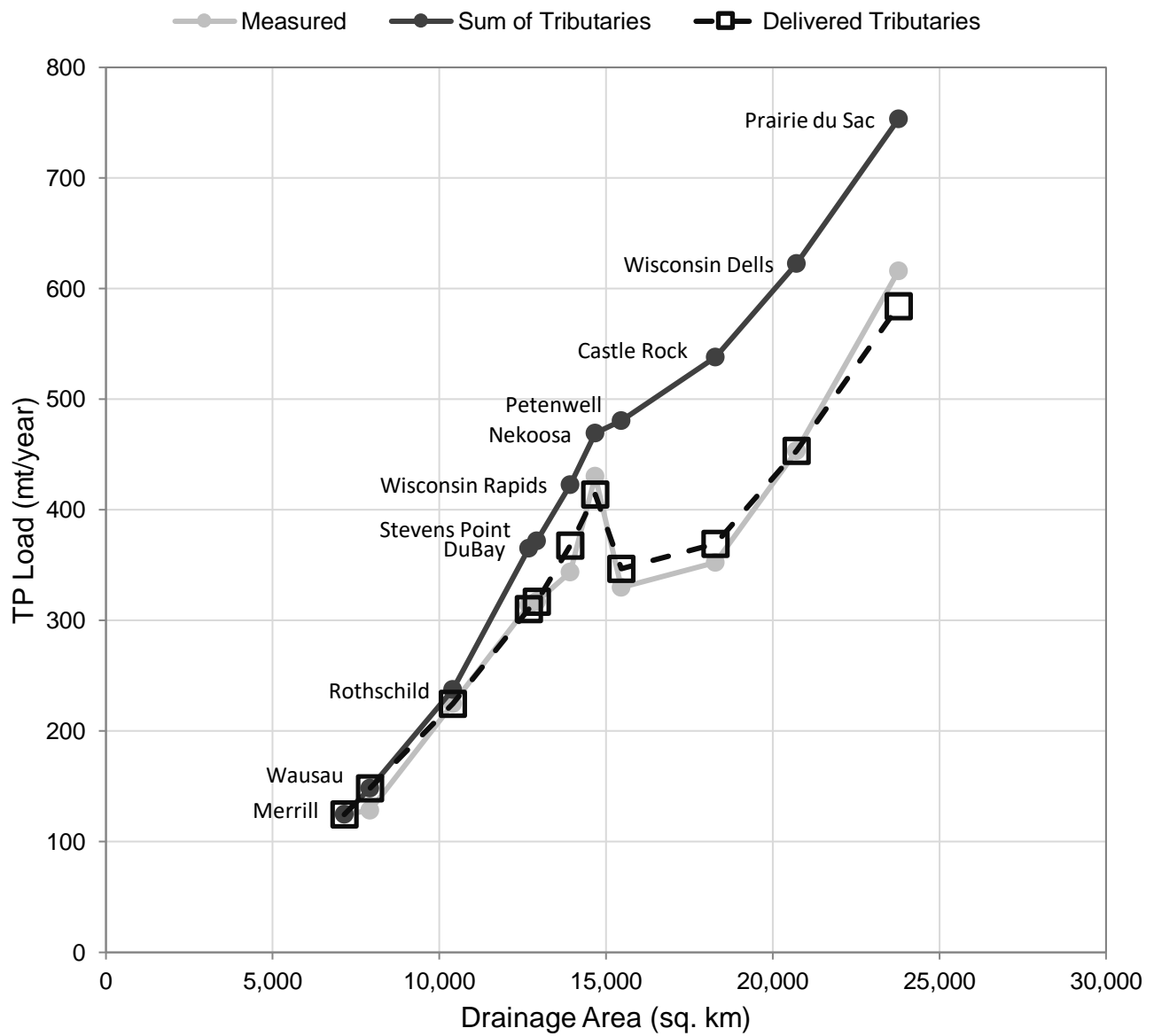


Figure 40 Mean annual total phosphorus (TP) load (2010-13) vs: drainage area on the mainstem of the Wisconsin River between Merrill and Prairie du Sac. The sum of tributary loads is a combination of measured loads where available, and SWAT modeled loads on ungauged tributaries. Delivered tributary loads were calculated by applying the delivery fractions in Table 20.

12 Appendices

Appendix D.1

Detailed information was collected from local agricultural experts to inform the SWAT model of specific land management operations. Below is a list of example questions used in these interviews:

- 1) What are the approximate planting dates and harvest dates for each crop type identified on the map?
- 2) Agricultural areas were identified as “insufficient” if we did not have enough data to define a certain crop rotation. Identifying these areas, however, is very important for our modeling efforts. Are there “insufficient” areas that you can tell us about? Do you know the general crop rotations?
- 3) Can we make any inferences about certain crop rotation schemes? (An example might be that any continuous corn crop rotation means that they certainly don’t do no-till, etc.)
- 4) One of our greatest struggles has been distinguishing between satellite imagery results for areas identified as land cover types such as pasture, hay, grassland, etc. Are you able to generally identify which areas are grazed, which are harvested, and which are left unutilized? Can you distinguish between light pasture (low animal density) and heavy pasture (high animal density)?
- 5) Are there crop rotations that you know of in your county that aren’t represented on the map?
- 6) Are there areas where farmers are growing multiple crops per season? Additionally, are cover crops a common practice in your county? If so, can cover crops be correlated with a certain crop type or crop rotation?
- 7) The satellite imagery can only distinguish between corn and sweet corn. It can’t identify seed corn vs. feed corn vs. corn for ethanol or grain products. More importantly, it can’t provide information about what corn is silage and what isn’t. Are there any general assumptions that can be made about grain rotations and their likelihood of being used for silage?
- 8) In (insert county name), are there general relationships between the crop rotation type and the tillage practices? Or, are there relationships between the general geographic location and the tillage practices (in example, the southwest portion of the county may cultivate more often than the northeast)?
- 9) Can tillage practices be correlated with things other than rotation? For instance, are there soil type limitations that create tillage differences across the county?
- 10) What are the approximate tillage dates for the different crop rotations?
- 11) What are the predominant tillage patterns, in terms of timing and type of tillage?

- 12) Are tillage practices generally predictable, or do they vary year-to-year (based on market pressures, environmental conditions, etc.)?
- 13) Is there a relationship between crop rotation type and nutrient application?
- 14) For each rotation, can you provide an estimate as to how much is applied, how often it is applied, and what type is applied?
- 15) What rotations receive chemical fertilizer?
- 16) What are the most common N:P:K ratios in your county for chemical fertilizers?
- 17) Are there any “hotspots” that require further investigation?
- 18) Are there any areas pertinent to nutrient runoff that you can identify? These might be landscape factors such as areas of major erosion, water diversion systems, soil conservation efforts, etc.
- 19) Are there areas where you can identify tile drainage?
- 20) Is tile drainage field specific or is it a function of slope, soil type, or some other land characteristic?
- 21) Are there any other concerns you think should be considered when assessing phosphorus and sediment contributions from your county as part of the Wisconsin River Basin TMDL?

Appendix D.2

Generic crop rotation operations used in SWAT model. The labeled number is simply a code that identifies each crop rotation—these codes will be useful for interpreting the maps provided in Appendix D.3. Crops are abbreviated as Cg (corn grain), Cs (corn silage), A (alfalfa), So (soybeans), Po (potatoes), and Vg (rotated sweet corn and snap beans).

300 - Cg-Cs-O/A-A-A-A (LQ) Spring Chisel -10,000 ga/acre/yr

Year	Month	Day	Operation	Type	Amount	Unit
1	4	29	Manure	Dry Weight	5,582	kg/ha
1	5	1	Tillage	Chisel Plow		
1	5	15	Plant	Corn Grain		
1	5	15	Fertilizer	20:10:18	168	kg/ha
1	11	1	Harvest	Corn Grain		
2	4	29	Manure	Dry Weight	5,582	kg/ha
2	5	1	Tillage	Chisel Plow		
2	5	15	Plant	Corn Silage		
2	5	15	Fertilizer	20:10:18	168	kg/ha
2	9	15	Harvest	Corn Silage		
3	4	14	Manure	Dry Weight	1,675	kg/ha
3	4	17	Tillage	Chisel Plow		
3	4	25	Plant	Alfalfa		
3	8	10	Harvest	Alfalfa		
4	6	1	Harvest	Alfalfa		
4	7	15	Harvest	Alfalfa		
4	8	30	Harvest	Alfalfa		
5	6	1	Harvest	Alfalfa		
5	7	15	Harvest	Alfalfa		
5	8	30	Harvest	Alfalfa		
6	6	1	Harvest	Alfalfa		
6	7	15	Harvest	Alfalfa		
6	8	30	Harvest	Alfalfa		
6	10	15	Tillage	Chisel Plow		

301 - Cg-Cs-O/A-A-A-A (DH) Spring Chisel - 25 tons/acre/year

Year	Month	Day	Operation	Type	Amount	Unit
1	1	31	Manure	Dry Manure	3362.5	kg/ha
1	2	28	Manure	Dry Manure	3362.5	kg/ha
1	3	31	Manure	Dry Manure	3362.5	kg/ha
1	4	29	Manure	Dry Manure	3362.5	kg/ha
1	5	1	Tillage	Chisel Plow		
1	5	15	Plant	Corn Grain		
1	5	15	Fertilizer	20:10:18	168.0	kg/ha
1	11	1	Harvest	Corn Grain		
2	1	31	Manure	Dry Manure	3362.5	kg/ha
2	2	28	Manure	Dry Manure	3362.5	kg/ha
2	3	31	Manure	Dry Manure	3362.5	kg/ha
2	4	29	Manure	Dry Manure	3362.5	kg/ha
2	5	1	Tillage	Chisel Plow		
2	5	15	Plant	Corn Silage		
2	5	15	Fertilizer	20:10:18	168.0	kg/ha
2	9	15	Harvest	Corn Silage		
3	1	31	Manure	Dry Manure	1120.8	kg/ha
3	2	28	Manure	Dry Manure	1120.8	kg/ha
3	3	31	Manure	Dry Manure	1120.8	kg/ha
3	4	14	Manure	Dry Manure	1120.8	kg/ha
3	4	17	Tillage	Chisel Plow		
3	4	25	Plant	Alfalfa		
3	8	10	Harvest	Alfalfa		
4	6	1	Harvest	Alfalfa		
4	7	15	Harvest	Alfalfa		
4	8	30	Harvest	Alfalfa		
5	6	1	Harvest	Alfalfa		
5	7	15	Harvest	Alfalfa		
5	8	30	Harvest	Alfalfa		
6	6	1	Harvest	Alfalfa		
6	7	15	Harvest	Alfalfa		
6	8	30	Harvest	Alfalfa		
6	10	15	Tillage	Chisel Plow		

**302 - Cg-O/A-A-A-A-A (DH) Spring Chisel - 25
tons/acre/year**

Year	Month	Day	Operation	Type	Amount	Unit
1	1	31	Manure	Dry Weight	3362.5	kg/ha
1	2	28	Manure	Dry Weight	3362.5	kg/ha
1	3	31	Manure	Dry Weight	3362.5	kg/ha
1	4	29	Manure	Dry Weight	3362.5	kg/ha
1	5	1	Tillage	Chisel Plow		
1	5	15	Plant	Corn Grain		
1	5	15	Fertilizer	20:10:18	168	kg/ha
1	11	1	Harvest	Corn Grain		
2	1	31	Manure	Dry Weight	1,121	kg/ha
2	2	28	Manure	Dry Weight	1,121	kg/ha
2	3	31	Manure	Dry Weight	1,121	kg/ha
2	4	14	Manure	Dry Weight	1,121	kg/ha
2	4	17	Tillage	Chisel Plow		
2	4	25	Plant	Alfalfa		
2	8	10	Harvest	Alfalfa		
3	6	1	Harvest	Alfalfa		
3	7	15	Harvest	Alfalfa		
3	8	30	Harvest	Alfalfa		
4	6	1	Harvest	Alfalfa		
4	7	15	Harvest	Alfalfa		
4	8	30	Harvest	Alfalfa		
5	6	1	Harvest	Alfalfa		
5	7	15	Harvest	Alfalfa		
5	8	30	Harvest	Alfalfa		
6	6	1	Harvest	Alfalfa		
6	7	15	Harvest	Alfalfa		
6	8	30	Harvest	Alfalfa		
6	10	15	Tillage	Chisel Plow		

303 - Cg-Cs-O/A-A-A-A (LQ) Fall Chisel -10,000 ga/acre/yr

Year	Month	Day	Operation	Type	Amount	Unit
1	5	1	Tillage	Cultivation		
1	5	15	Plant	Corn Grain		
1	5	15	Fertilizer	20:10:18	168	kg/ha
1	11	1	Harvest	Corn Grain		
1	11	12	Manure	Liquid	5,582	kg/ha
1	11	15	Tillage	Chisel Plow		
2	5	1	Tillage	Cultivation		
2	5	15	Plant	Corn Silage		
2	5	15	Fertilizer	20:10:18	168	kg/ha
2	9	15	Harvest	Corn Silage		
2	10	15	Manure	Liquid	5,582	kg/ha
2	10	18	Tillage	Chisel Plow		
3	4	14	Manure	Liquid	1675	kg/ha
3	4	17	Tillage	Cultivation		
3	4	25	Plant	Alfalfa		
3	8	10	Harvest	Alfalfa		
4	6	1	Harvest	Alfalfa		
4	7	15	Harvest	Alfalfa		
4	8	30	Harvest	Alfalfa		
5	6	1	Harvest	Alfalfa		
5	7	15	Harvest	Alfalfa		
5	8	30	Harvest	Alfalfa		
6	6	1	Harvest	Alfalfa		
6	7	15	Harvest	Alfalfa		
6	8	30	Harvest	Alfalfa		
6	10	15	Tillage	Chisel Plow		

304 - Cg-Cs-O/A-A-A-A (DH) Fall Chisel - 25 tons/acre/year

Year	Month	Day	Operation	Type	Amount	Unit
1	1	31	Manure	Dry Weight	3362.5	kg/ha
1	2	28	Manure	Dry Weight	3362.5	kg/ha
1	3	31	Manure	Dry Weight	3362.5	kg/ha
1	4	29	Manure	Dry Weight	3362.5	kg/ha
1	5	1	Tillage	Cultivation		
1	5	15	Plant	Corn Grain		
1	5	15	Fertilizer	20:10:18	168.0	kg/ha
1	11	1	Harvest	Corn Grain		
1	11	15	Tillage	Chisel Plow		
2	1	31	Manure	Dry Weight	3362.5	kg/ha
2	2	28	Manure	Dry Weight	3362.5	kg/ha
2	3	31	Manure	Dry Weight	3362.5	kg/ha
2	4	29	Manure	Dry Weight	3362.5	kg/ha
2	5	1	Tillage	Cultivation		
2	5	15	Plant	Corn Silage		
2	5	15	Fertilizer	20:10:18	150.0	kg/ha
2	9	15	Harvest	Corn Silage		
2	10	1	Tillage	Chisel Plow		
3	1	31	Manure	Dry Weight	1120.8	kg/ha
3	2	28	Manure	Dry Weight	1120.8	kg/ha
3	3	31	Manure	Dry Weight	1120.8	kg/ha
3	4	14	Manure	Dry Weight	1120.8	kg/ha
3	4	17	Tillage	Cultivation		
3	4	25	Plant	Alfalfa		
3	8	10	Harvest	Alfalfa		
4	6	1	Harvest	Alfalfa		
4	7	15	Harvest	Alfalfa		
4	8	30	Harvest	Alfalfa		
5	6	1	Harvest	Alfalfa		
5	7	15	Harvest	Alfalfa		
5	8	30	Harvest	Alfalfa		
6	6	1	Harvest	Alfalfa		
6	7	15	Harvest	Alfalfa		
6	8	30	Harvest	Alfalfa		
6	10	15	Tillage	Chisel Plow		

305- Cs-Cs-O/A-A-A-A (LQ) Fall Chisel -10,000 ga/acre/yr

Year	Month	Day	Operation	Type	Amount	Unit
1	5	1	Tillage	Cultivation		
1	5	15	Plant	Corn Silage		
1	5	15	Fertilizer	20:10:18	168	kg/ha
1	9	15	Harvest	Corn Silage		
1	10	15	Manure	Liquid	5,582	kg/ha
1	10	18	Tillage	Chisel Plow		
2	5	1	Tillage	Cultivation		
2	5	15	Plant	Corn Silage		
2	5	15	Fertilizer	20:10:18	168	kg/ha
2	9	15	Harvest	Corn Silage		
2	10	15	Manure	Liquid	5582	kg/ha
2	10	18	Tillage	Chisel Plow		
3	4	14	Manure	Liquid	1,675	kg/ha
3	4	17	Tillage	Cultivation		
3	4	25	Plant	Alfalfa		
3	8	10	Harvest	Alfalfa		
4	6	1	Harvest	Alfalfa		
4	7	15	Harvest	Alfalfa		
4	8	30	Harvest	Alfalfa		
5	6	1	Harvest	Alfalfa		
5	7	15	Harvest	Alfalfa		
5	8	30	Harvest	Alfalfa		
6	6	1	Harvest	Alfalfa		
6	7	15	Harvest	Alfalfa		
6	8	30	Harvest	Alfalfa		
6	10	15	Tillage	Chisel Plow		

306 - Cs-Cs-O/A-A-A-A (DH) Fall Chisel - 25 tons/acre/year

Year	Month	Day	Operation	Type	Amount	Unit
1	1	31	Manure	Dry Weight	3362.5	kg/ha
1	2	28	Manure	Dry Weight	3362.5	kg/ha
1	3	31	Manure	Dry Weight	3362.5	kg/ha
1	4	29	Manure	Dry Weight	3362.5	kg/ha
1	5	1	Tillage	Cultivation		
1	5	15	Plant	Corn Silage		
1	5	15	Fertilizer	20:10:18	168	kg/ha
1	9	15	Harvest	Corn Silage		
1	10	1	Tillage	Chisel Plow		
2	1	31	Manure	Dry Weight	3362.5	kg/ha
2	2	28	Manure	Dry Weight	3362.5	kg/ha
2	3	31	Manure	Dry Weight	3362.5	kg/ha
2	4	29	Manure	Dry Weight	3362.5	kg/ha
2	5	1	Tillage	Cultivation		
2	5	15	Plant	Corn Silage		
2	5	15	Fertilizer	20:10:18	168	kg/ha
2	9	15	Harvest	Corn Silage		
2	10	1	Tillage	Chisel Plow		
3	1	31	Manure	Dry Manure	1120.8	kg/ha
3	2	28	Manure	Dry Manure	1120.8	kg/ha
3	3	31	Manure	Dry Manure	1120.8	kg/ha
3	4	14	Manure	Dry Manure	1120.8	kg/ha
3	4	17	Tillage	Cultivation		
3	4	25	Plant	Alfalfa		
3	8	10	Harvest	Alfalfa		
4	6	1	Harvest	Alfalfa		
4	7	15	Harvest	Alfalfa		
4	8	30	Harvest	Alfalfa		
5	6	1	Harvest	Alfalfa		
5	7	15	Harvest	Alfalfa		
5	8	30	Harvest	Alfalfa		
6	6	1	Harvest	Alfalfa		
6	7	15	Harvest	Alfalfa		
6	8	30	Harvest	Alfalfa		
6	10	15	Tillage	Chisel Plow		

**307 - Cs-Cs-O/A-A-A-A (LQ) Fall MB Plow -10,000
ga/acre/yr**

Year	Month	Day	Operation	Type	Amount	Unit
1	5	1	Tillage	Cultivation		
1	5	15	Plant	Corn Silage		
1	5	15	Fertilizer	20:10:18	168	kg/ha
1	9	15	Harvest	Corn Silage		
1	10	15	Manure	Liquid	5,582	kg/ha
1	10	18	Tillage	MB Plow		
2	5	1	Tillage	Cultivation		
2	5	15	Plant	Corn Silage		
2	5	15	Fertilizer	20:10:18	168	kg/ha
2	9	15	Harvest	Corn Silage		
2	10	15	Manure	Liquid	5,582	kg/ha
2	10	18	Tillage	MB Plow		
3	4	14	Manure	Liquid	1,675	kg/ha
3	4	17	Tillage	Cultivation		
3	4	25	Plant	Alfalfa		
3	8	10	Harvest	Alfalfa		
4	6	1	Harvest	Alfalfa		
4	7	15	Harvest	Alfalfa		
4	8	30	Harvest	Alfalfa		
5	6	1	Harvest	Alfalfa		
5	7	15	Harvest	Alfalfa		
5	8	30	Harvest	Alfalfa		
6	6	1	Harvest	Alfalfa		
6	7	15	Harvest	Alfalfa		
6	8	30	Harvest	Alfalfa		
6	10	15	Tillage	MB Plow		

**308 - Cs-Cs-O/A-A-A-A (DH) Fall MB Plow - 25
tons/acre/year**

Year	Month	Day	Operation	Type	Amount	Unit
1	1	31	Manure	Dry Weight	3362.5	kg/ha
1	2	28	Manure	Dry Weight	3,363	kg/ha
1	3	31	Manure	Dry Weight	3,363	kg/ha
1	4	29	Manure	Dry Weight	3,363	kg/ha
1	5	1	Tillage	Cultivation		
1	5	15	Plant	Corn Silage		
1	5	15	Fertilizer	20:10:18	168	kg/ha
1	9	15	Harvest	Corn Silage		
1	10	1	Tillage	MB Plow		
2	1	31	Manure	Dry Weight	3,363	kg/ha
2	2	28	Manure	Dry Weight	3362.5	kg/ha
2	3	31	Manure	Dry Weight	3362.5	kg/ha
2	4	29	Manure	Dry Weight	3362.5	kg/ha
2	5	1	Tillage	Cultivation		
2	5	15	Plant	Corn Silage		
2	5	15	Fertilizer	20:10:18	150	kg/ha
2	9	15	Harvest	Corn Silage		
2	10	1	Tillage	MB Plow		
3	1	31	Manure	Dry Manure	1120.8	kg/ha
3	2	28	Manure	Dry Manure	1120.8	kg/ha
3	3	31	Manure	Dry Manure	1120.8	kg/ha
3	4	14	Manure	Dry Manure	1120.8	kg/ha
3	4	17	Tillage	Cultivation		
3	4	25	Plant	Alfalfa		
3	8	10	Harvest	Alfalfa		
4	6	1	Harvest	Alfalfa		
4	7	15	Harvest	Alfalfa		
4	8	30	Harvest	Alfalfa		
5	6	1	Harvest	Alfalfa		
5	7	15	Harvest	Alfalfa		
5	8	30	Harvest	Alfalfa		
6	6	1	Harvest	Alfalfa		
6	7	15	Harvest	Alfalfa		
6	8	30	Harvest	Alfalfa		
6	10	15	Tillage	MB Plow		

**309 - Cg-Cs-O/A-A-A-A (LQ) Fall MB Plow -10,000
ga/acre/yr**

Year	Month	Day	Operation	Type	Amount	Unit
1	5	1	Tillage	Cultivation		
1	5	15	Plant	Corn Grain		
1	5	15	Fertilizer	20:10:18	1675	kg/ha
1	11	1	Harvest	Corn Grain		
1	11	12	Manure	Liquid	5,582	kg/ha
1	11	15	Tillage	MB Plow		
2	5	1	Tillage	Cultivation		
2	5	15	Plant	Corn Silage		
2	5	15	Fertilizer	20:10:18	168	kg/ha
2	9	15	Harvest	Corn Silage		
2	10	15	Manure	Liquid	5,582	kg/ha
2	10	18	Tillage	MB Plow		
3	4	14	Manure	Liquid	1,675	kg/ha
3	4	17	Tillage	Cultivation		
3	4	25	Plant	Alfalfa		
3	8	10	Harvest	Alfalfa		
4	6	1	Harvest	Alfalfa		
4	7	15	Harvest	Alfalfa		
4	8	30	Harvest	Alfalfa		
5	6	1	Harvest	Alfalfa		
5	7	15	Harvest	Alfalfa		
5	8	30	Harvest	Alfalfa		
6	6	1	Harvest	Alfalfa		
6	7	15	Harvest	Alfalfa		
6	8	30	Harvest	Alfalfa		
6	10	15	Tillage	MB Plow		

**310 - Cg-Cs-O/A-A-A-A (DH) Fall MB Plow - 25
tons/acre/year**

Year	Month	Day	Operation	Type	Amount	Unit
1	1	31	Manure	Dry Weight	3362.5	kg/ha
1	2	28	Manure	Dry Weight	3,363	kg/ha
1	3	31	Manure	Dry Weight	3,363	kg/ha
1	4	29	Manure	Dry Weight	3,363	kg/ha
1	5	1	Tillage	Cultivation		
1	5	15	Plant	Corn Grain		
1	5	15	Fertilizer	20:10:18	168	kg/ha
1	11	1	Harvest	Corn Grain		
1	11	15	Tillage	MB Plow		
2	1	31	Manure	Dry Weight	3362.5	kg/ha
2	2	28	Manure	Dry Weight	3,363	kg/ha
2	3	31	Manure	Dry Weight	3,363	kg/ha
2	4	29	Manure	Dry Weight	3,363	kg/ha
2	5	1	Tillage	Cultivation		
2	5	15	Plant	Corn Silage		
2	5	15	Fertilizer	20:10:18	168	kg/ha
2	9	15	Harvest	Corn Silage		
2	10	1	Tillage	MB Plow		
3	1	31	Manure	Dry Manure	1120.8	kg/ha
3	2	28	Manure	Dry Manure	1120.8	kg/ha
3	3	31	Manure	Dry Manure	1120.8	kg/ha
3	4	14	Manure	Dry Manure	1120.8	kg/ha
3	4	17	Tillage	Cultivation		
3	4	25	Plant	Alfalfa		
3	8	10	Harvest	Alfalfa		
4	6	1	Harvest	Alfalfa		
4	7	15	Harvest	Alfalfa		
4	8	30	Harvest	Alfalfa		
5	6	1	Harvest	Alfalfa		
5	7	15	Harvest	Alfalfa		
5	8	30	Harvest	Alfalfa		
6	6	1	Harvest	Alfalfa		
6	7	15	Harvest	Alfalfa		
6	8	30	Harvest	Alfalfa		
6	10	15	Tillage	MB Plow		

400 - Cg-Cg-So-Cg-Cg-So (Fall Chisel/Spring Disk)

Year	Month	Day	Operation	Type	Amount	Unit
1	5	1	Tillage	Disk Plow		
1	5	15	Plant	Corn Grain		
1	5	15	Fertilizer	20:10:18	168	kg/ha
1	11	1	Harvest	Corn Grain		
1	11	20	Tillage	Chisel Plow		
2	5	1	Tillage	Disk Plow		
2	5	15	Plant	Corn Grain		
2	5	15	Fertilizer	20:10:18	168	kg/ha
2	11	1	Harvest	Corn Grain		
2	11	20	Tillage	Chisel Plow		
3	5	1	Tillage	Disk Plow		
3	5	30	Plant	Soybean		
3	10	25	Harvest	Soybean		
3	11	1	Tillage	Chisel Plow		
4	5	1	Tillage	Disk Plow		
4	5	15	Plant	Corn Grain		
4	5	15	Fertilizer	20:10:18	168	kg/ha
4	11	1	Harvest	Corn Grain		
4	11	20	Tillage	Chisel Plow		
5	5	1	Tillage	Disk Plow		
5	5	15	Plant	Corn Grain		
5	5	15	Fertilizer	20:10:18	168	kg/ha
5	11	1	Harvest	Corn Grain		
5	11	20	Tillage	Chisel Plow		
6	5	1	Tillage	Disk Plow		
6	5	30	Plant	Soybean		
6	10	25	Harvest	Soybean		
6	11	1	Tillage	Chisel Plow		

401 - Cg-So-Cg-So-Cg-So (Fall Chisel/Spring Disk)

Year	Month	Day	Operation	Type	Amount	Unit
1	5	1	Tillage	Disk Plow		
1	5	15	Plant	Corn Grain		
1	5	15	Fertilizer	20:10:18	168	kg/ha
1	11	1	Harvest	Corn Grain		
1	11	20	Tillage	Chisel Plow		
2	5	1	Tillage	Disk Plow		
2	5	30	Plant	Soybean		
2	10	25	Harvest	Soybean		
2	11	1	Tillage	Chisel Plow		
3	5	1	Tillage	Disk Plow		
3	5	15	Plant	Corn Grain		
3	5	15	Fertilizer	20:10:18	168	kg/ha
3	11	1	Harvest	Corn Grain		
3	11	20	Tillage	Chisel Plow		
4	5	1	Tillage	Disk Plow		
4	5	30	Plant	Soybean		
4	10	25	Harvest	Soybean		
4	11	1	Tillage	Chisel Plow		
5	5	1	Tillage	Disk Plow		
5	5	15	Plant	Corn Grain		
5	5	15	Fertilizer	20:10:18	168	kg/ha
5	11	1	Harvest	Corn Grain		
5	11	20	Tillage	Chisel Plow		
6	5	1	Tillage	Disk Plow		
6	5	30	Plant	Soybean		
6	10	25	Harvest	Soybean		
6	11	1	Tillage	Chisel Plow		

402 - Cg-So-Cg-So-Cg-So (No Till All Years)

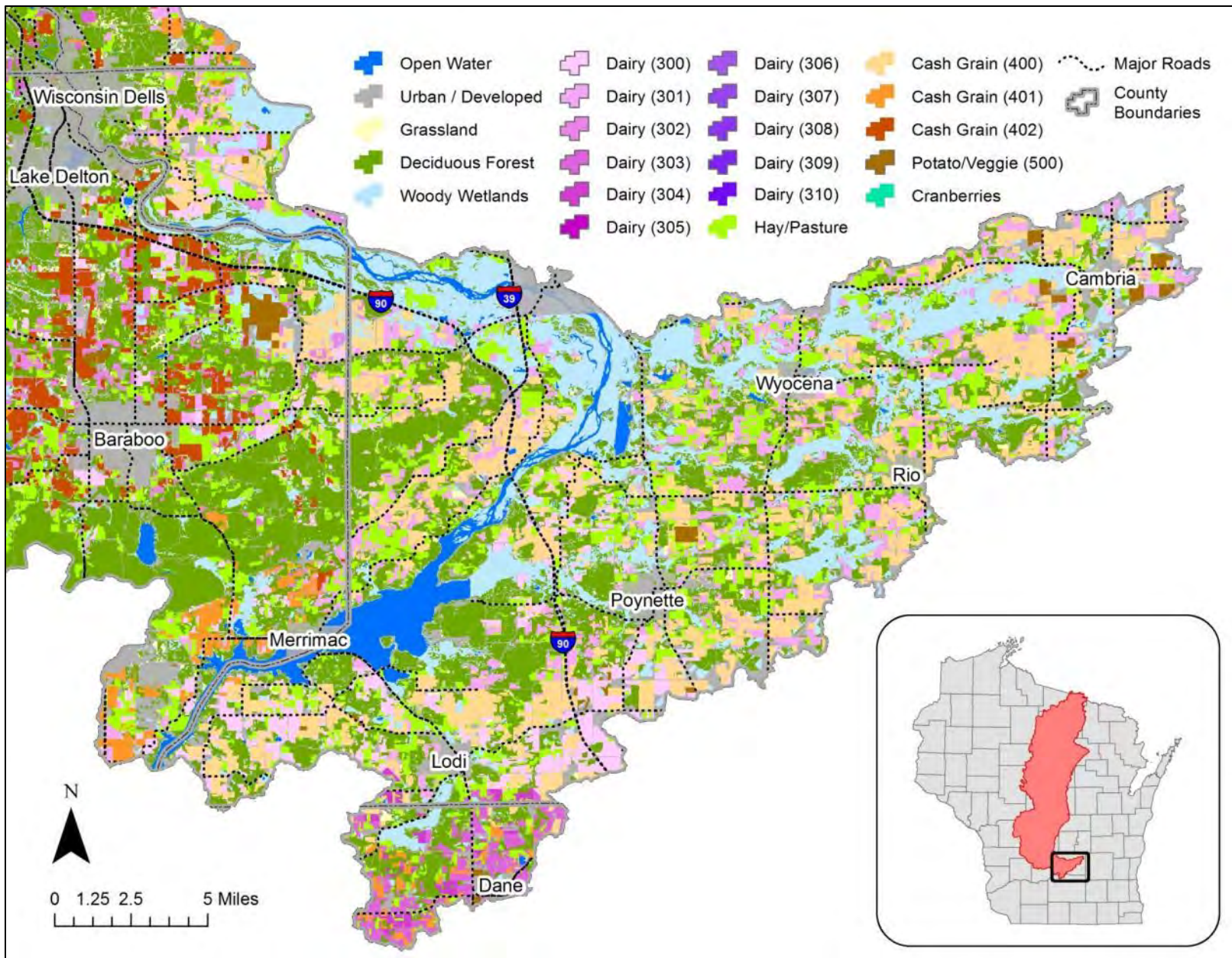
Year	Month	Day	Operation	Type	Amount	Unit
1	5	1	Tillage	Cultivation		
1	5	15	Plant	Corn Grain		
1	5	15	Fertilizer	20:10:18	168	kg/ha
1	11	1	Harvest	Corn Grain		
2	5	1	Tillage	Cultivation		
2	5	30	Plant	Soybean		
2	10	25	Harvest	Soybean		
3	5	15	Plant	Corn Grain		
3	5	15	Fertilizer	20:10:18	168	kg/ha
3	11	1	Harvest	Corn Grain		
4	5	1	Tillage	Cultivation		
4	5	30	Plant	Soybean		
4	10	25	Harvest	Soybean		
5	5	15	Plant	Corn Grain		
5	5	15	Fertilizer	20:10:18	168	kg/ha
5	11	1	Harvest	Corn Grain		
6	5	1	Tillage	Cultivation		
6	5	30	Plant	Soybean		
6	10	25	Harvest	Soybean		

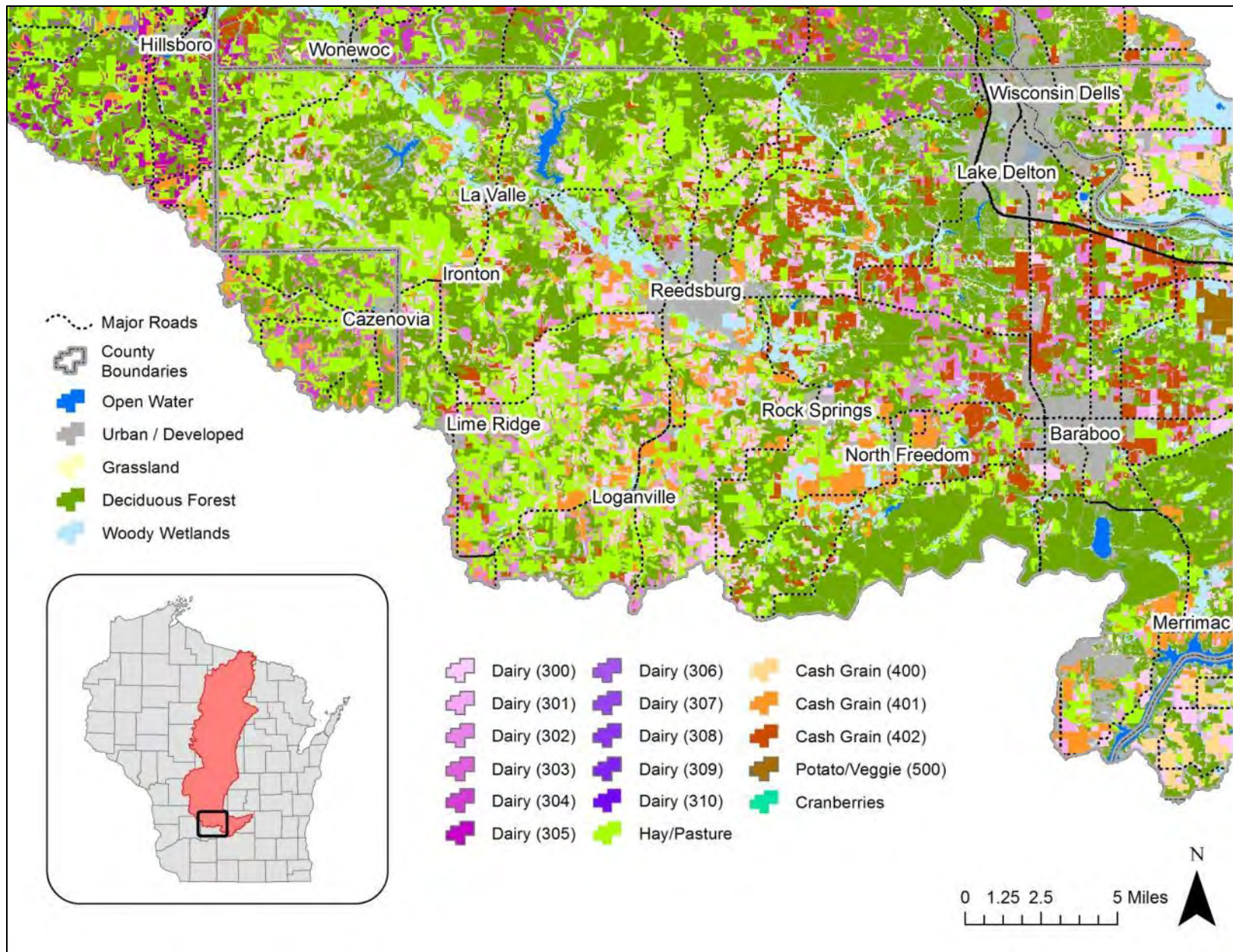
500 - Po-Vg-Vg-Po-Vg-Vg

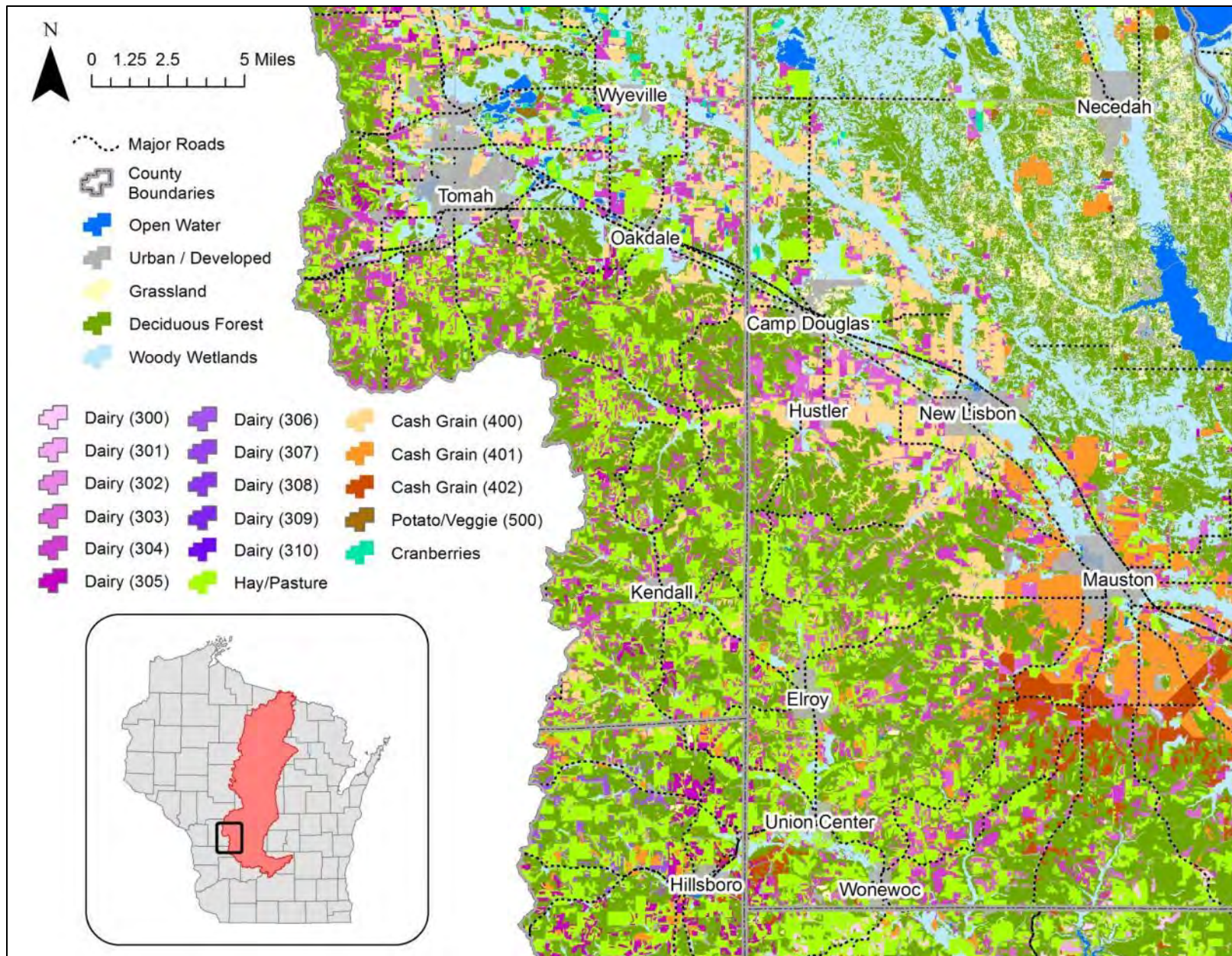
Year	Month	Day	Operation	Type	Amount	Unit
1	4	30	Tillage	MB Plow		
1	4	30	Plant	Potato		
1	4	30	Fertilizer	20:10:18	280	kg/ha
1	6	1	Tillage	Mounding		
1	6	15	Fertilizer	18:46:00	112	kg/ha
1	8	20	Harvest	Potato		
2	5	15	Tillage	Cultivator		
2	5	20	Plant	Snap Beans		
2	5	20	Fertilizer	20:10:18	168	kg/ha
2	7	15	Harvest	Snap Beans		
3	5	15	Tillage	Cultivator		
3	5	20	Plant	Sweet Corn		
3	5	20	Fertilizer	20:10:18	168	kg/ha
3	6	1	Fertilizer	18:46:00	168	kg/ha
3	8	30	Harvest	Sweet Corn		
4	4	30	Tillage	MB Plow		
4	4	30	Plant	Potato		
4	4	30	Fertilizer	20:10:18	280	kg/ha
4	6	1	Tillage	Mounding		
4	6	15	Fertilizer	18:46:00	112	kg/ha
4	8	20	Harvest	Potato		
5	5	15	Tillage	Cultivator		
5	5	20	Plant	Snap Beans		
5	5	20	Fertilizer	20:10:18	168	kg/ha
5	7	15	Harvest	Snap Beans		
6	5	15	Tillage	Cultivator		
6	5	20	Plant	Sweet Corn		
6	5	20	Fertilizer	20:10:18	168	kg/ha
6	6	15	Fertilizer	18:46:00	168	kg/ha
6	8	30	Harvest	Sweet Corn		

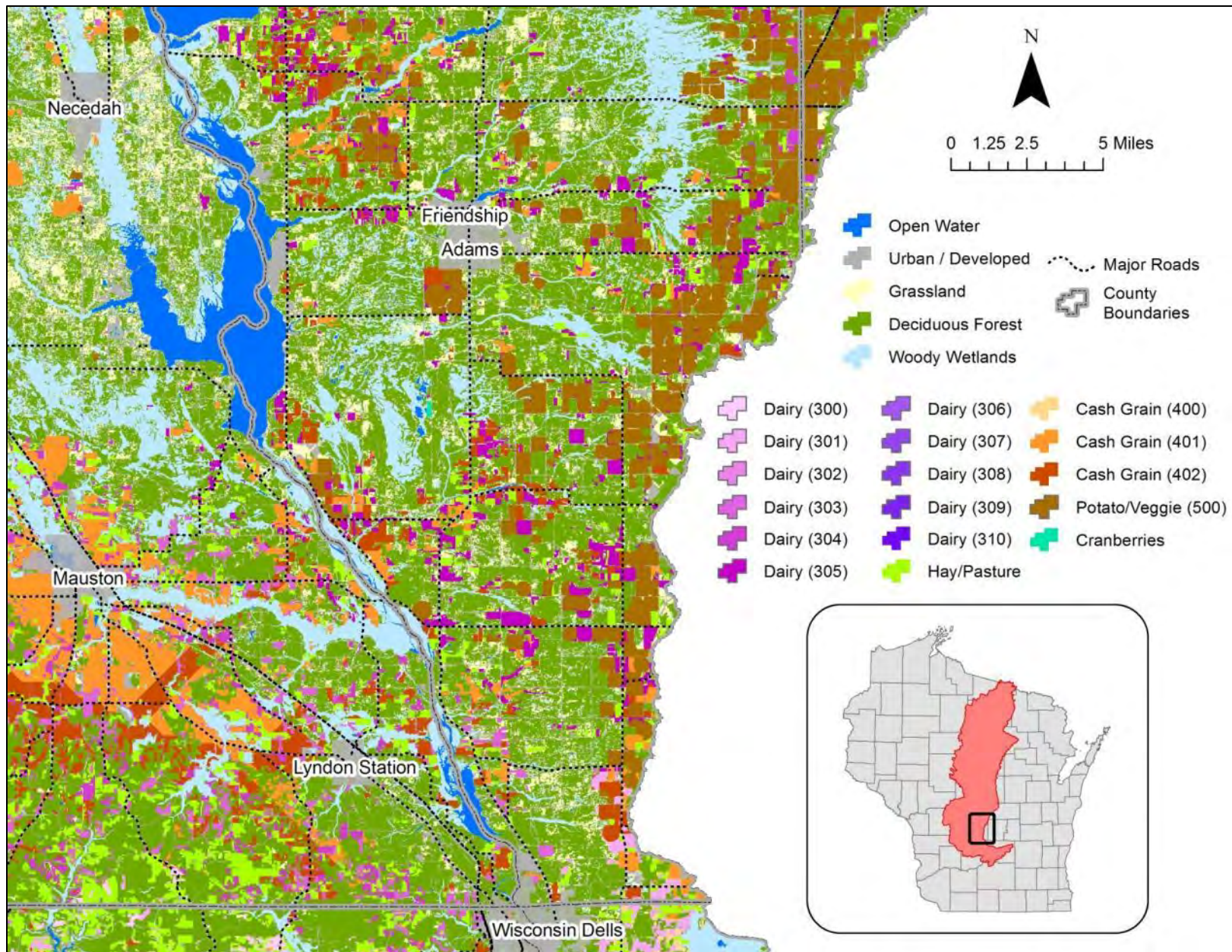
Appendix D.3

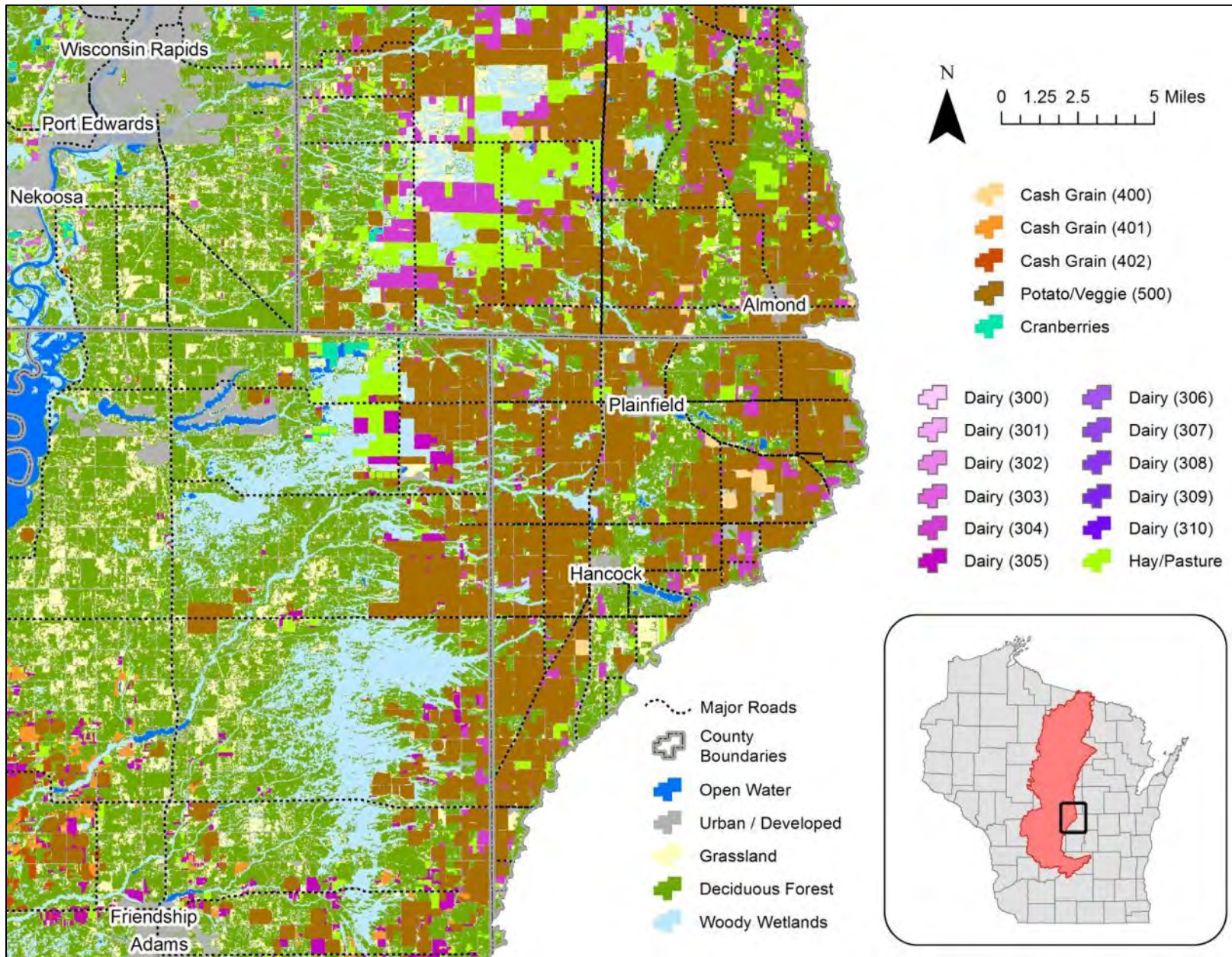
Maps of integrated crop rotations and land management operation used in SWAT. The codes listed next to agricultural legend items refer to the codes [e.g., Dairy (301)] used in Appendix D.2.

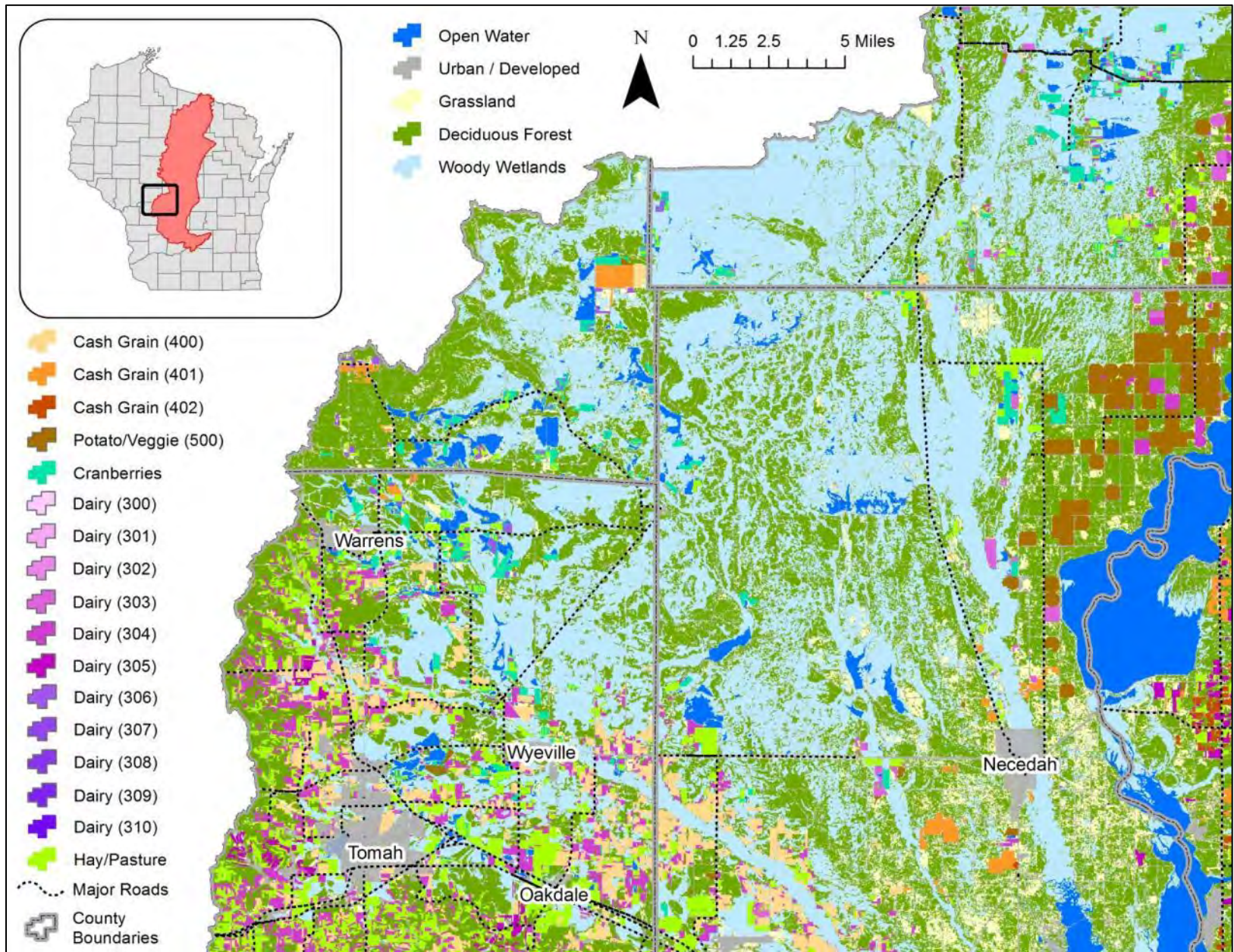


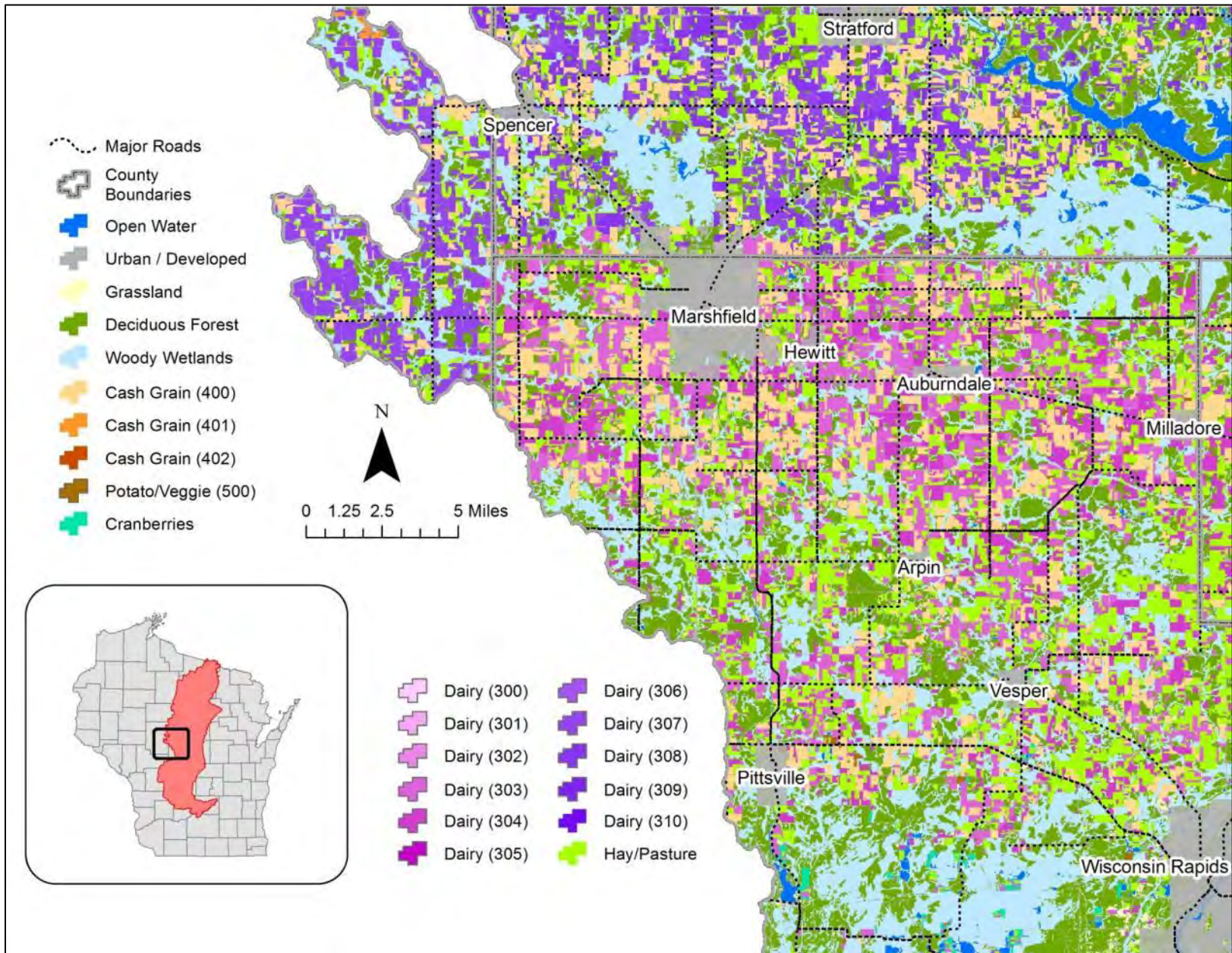


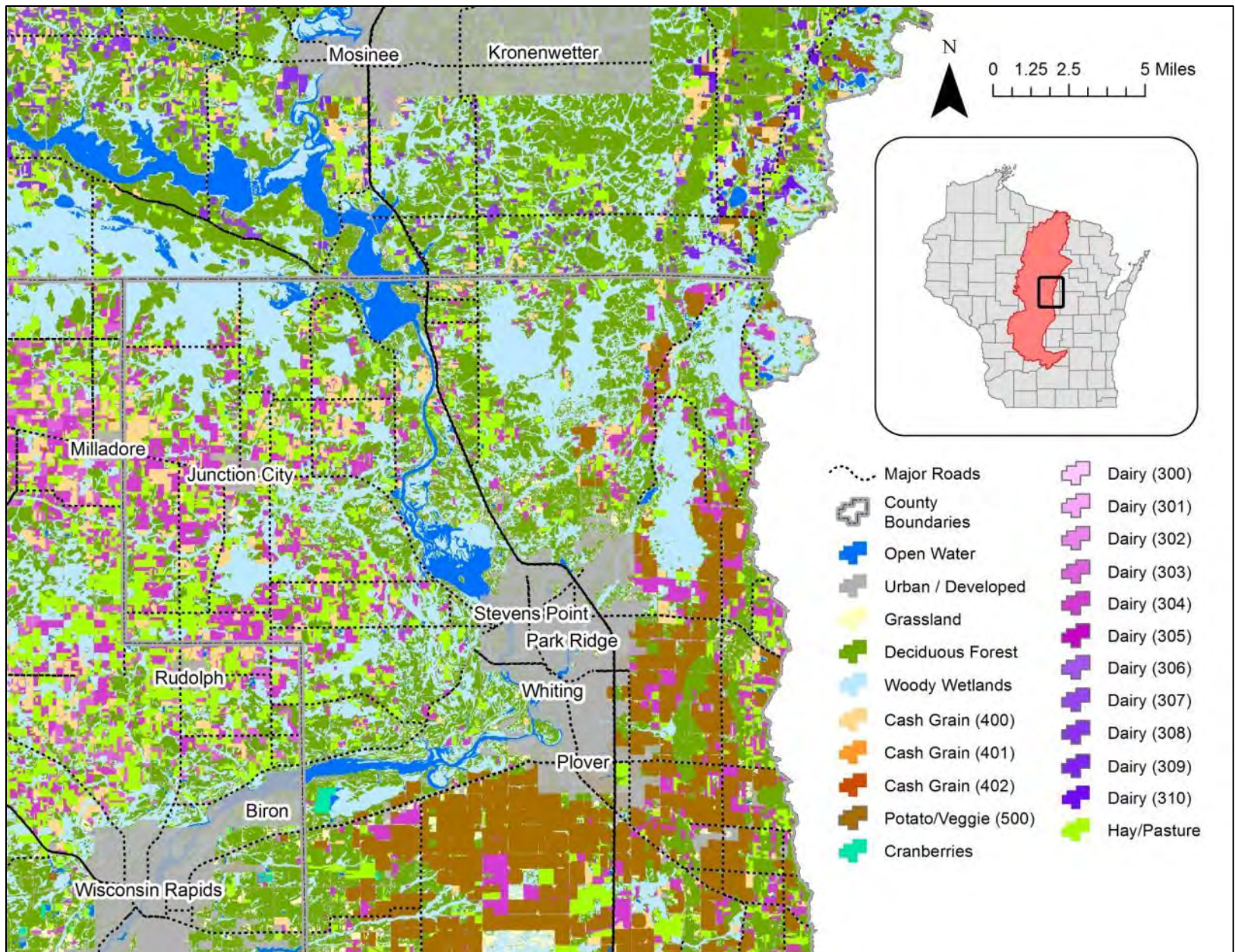


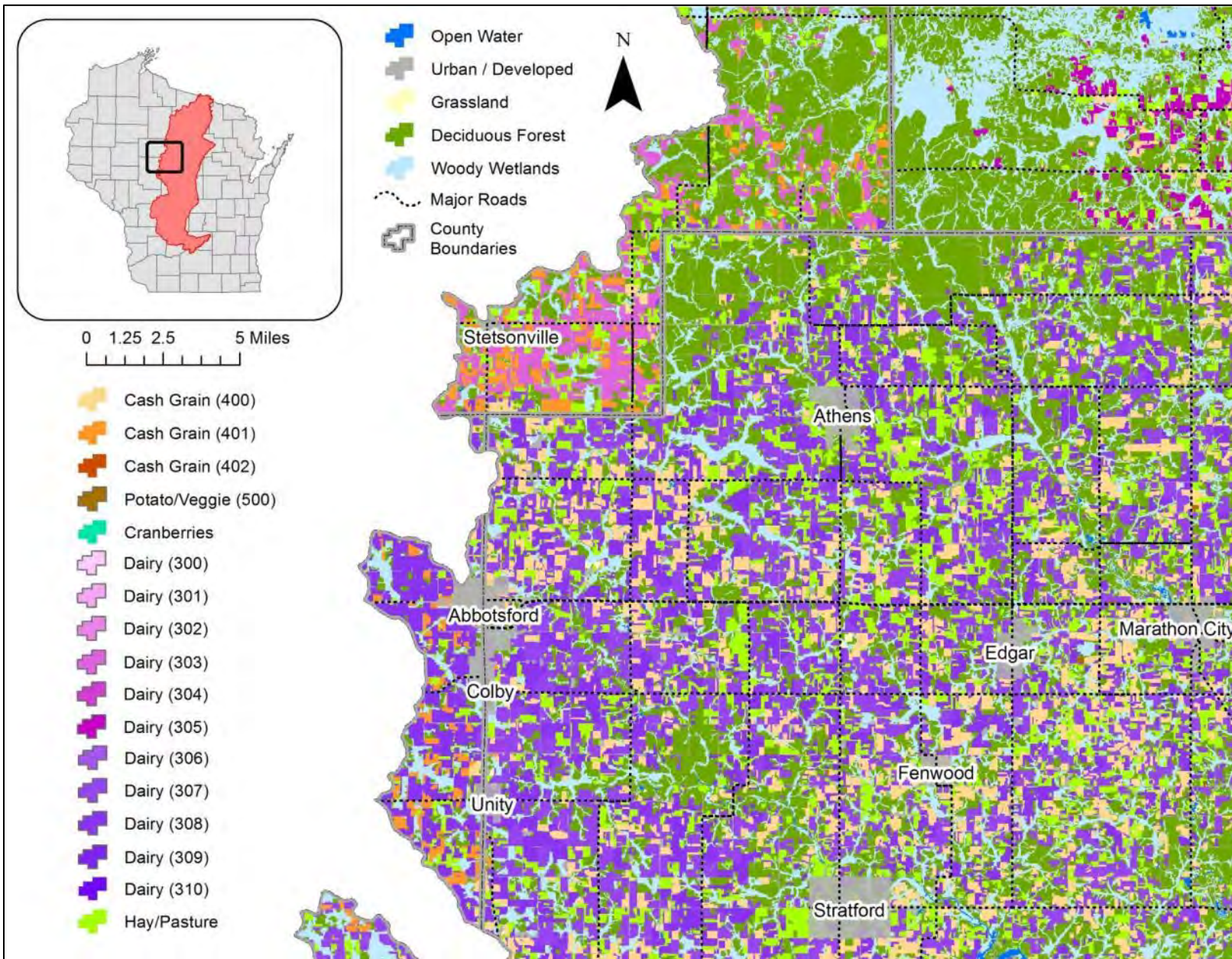


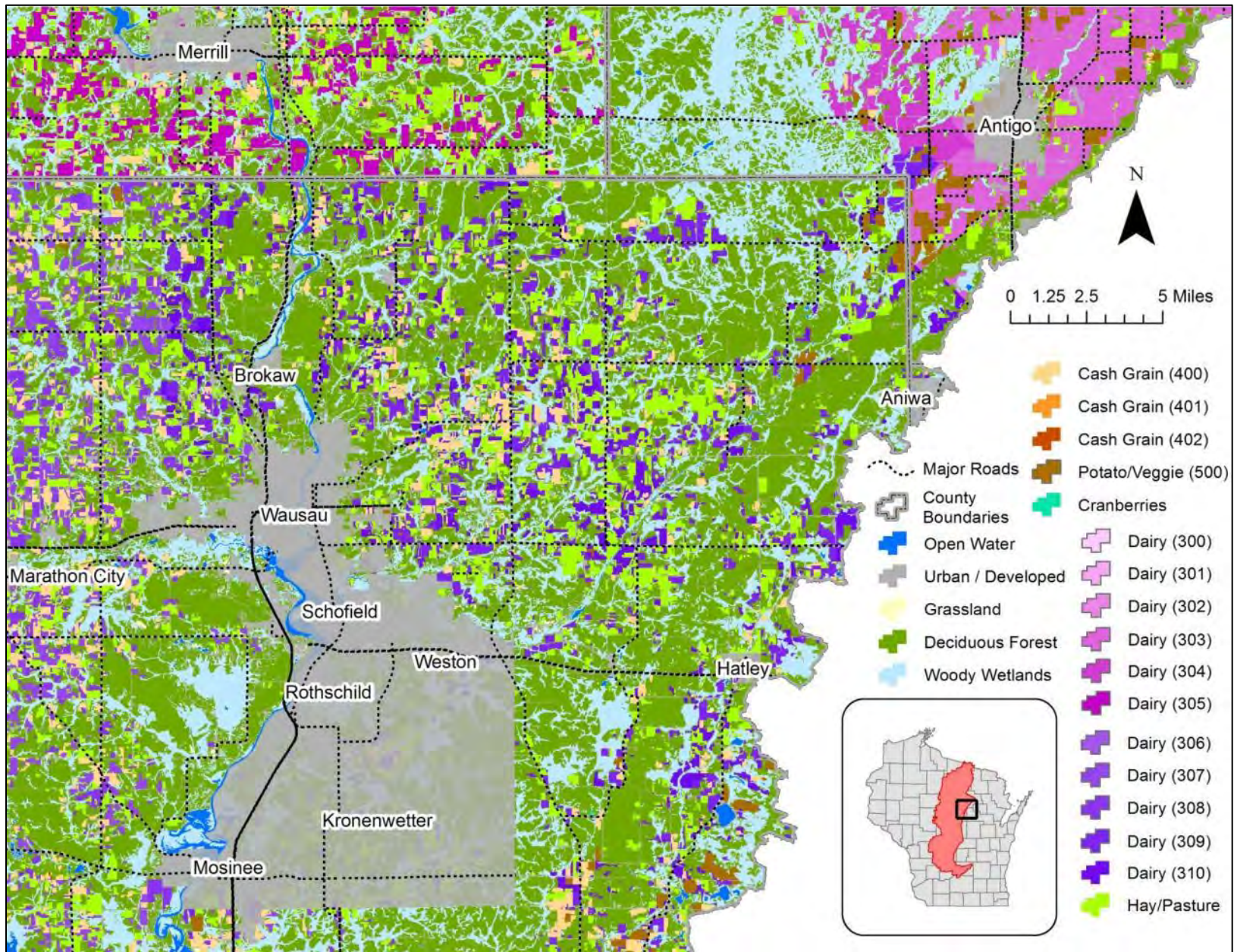


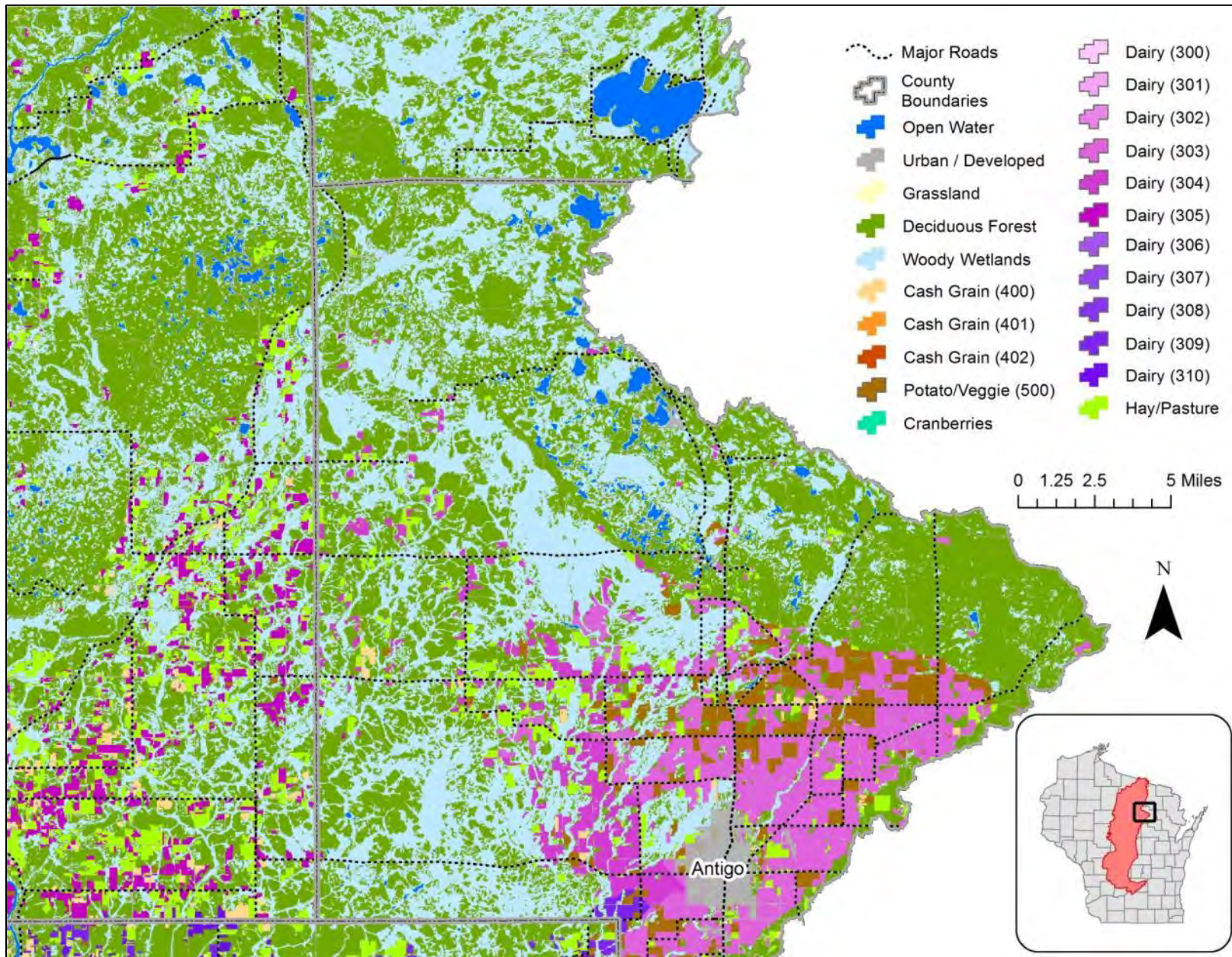


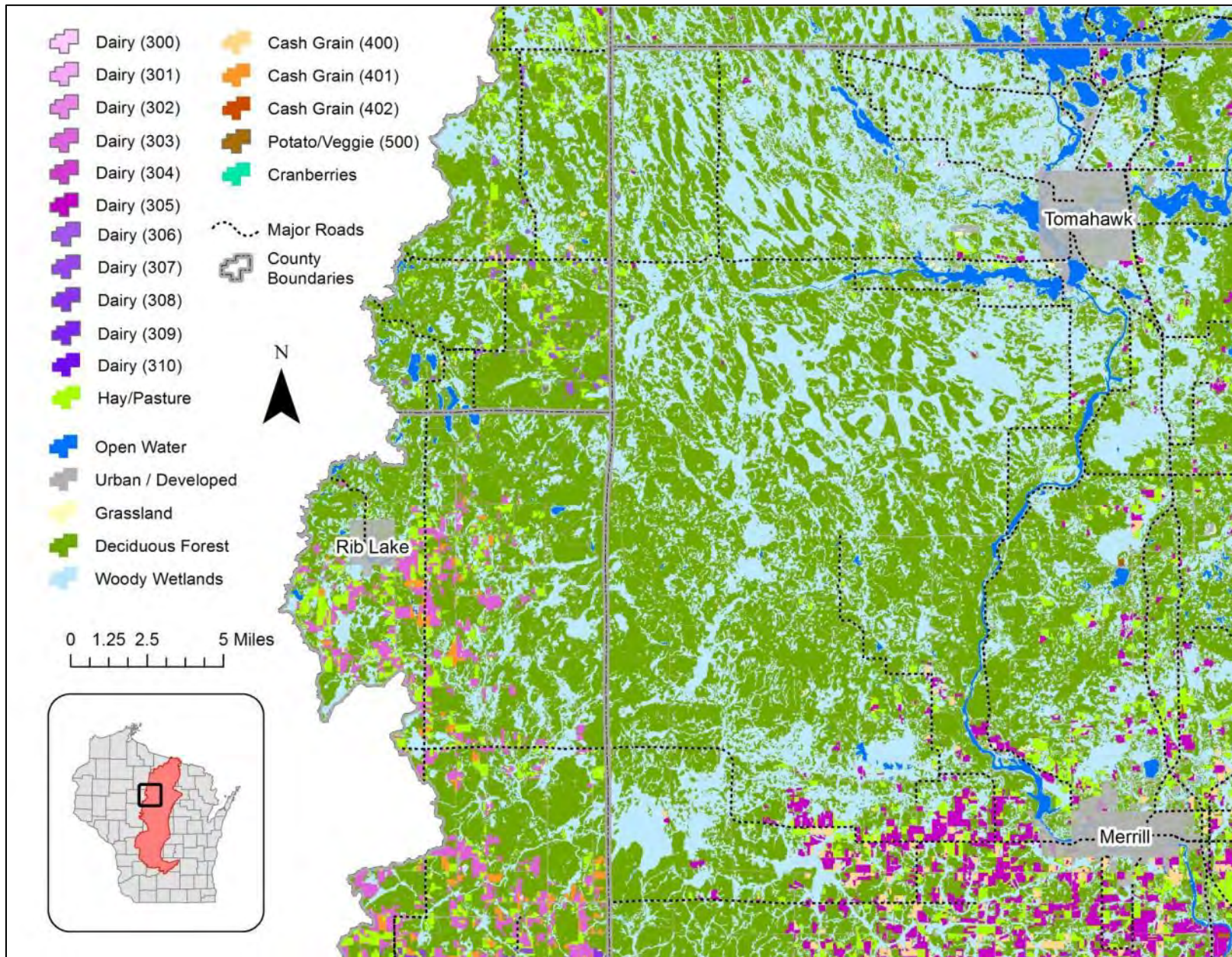


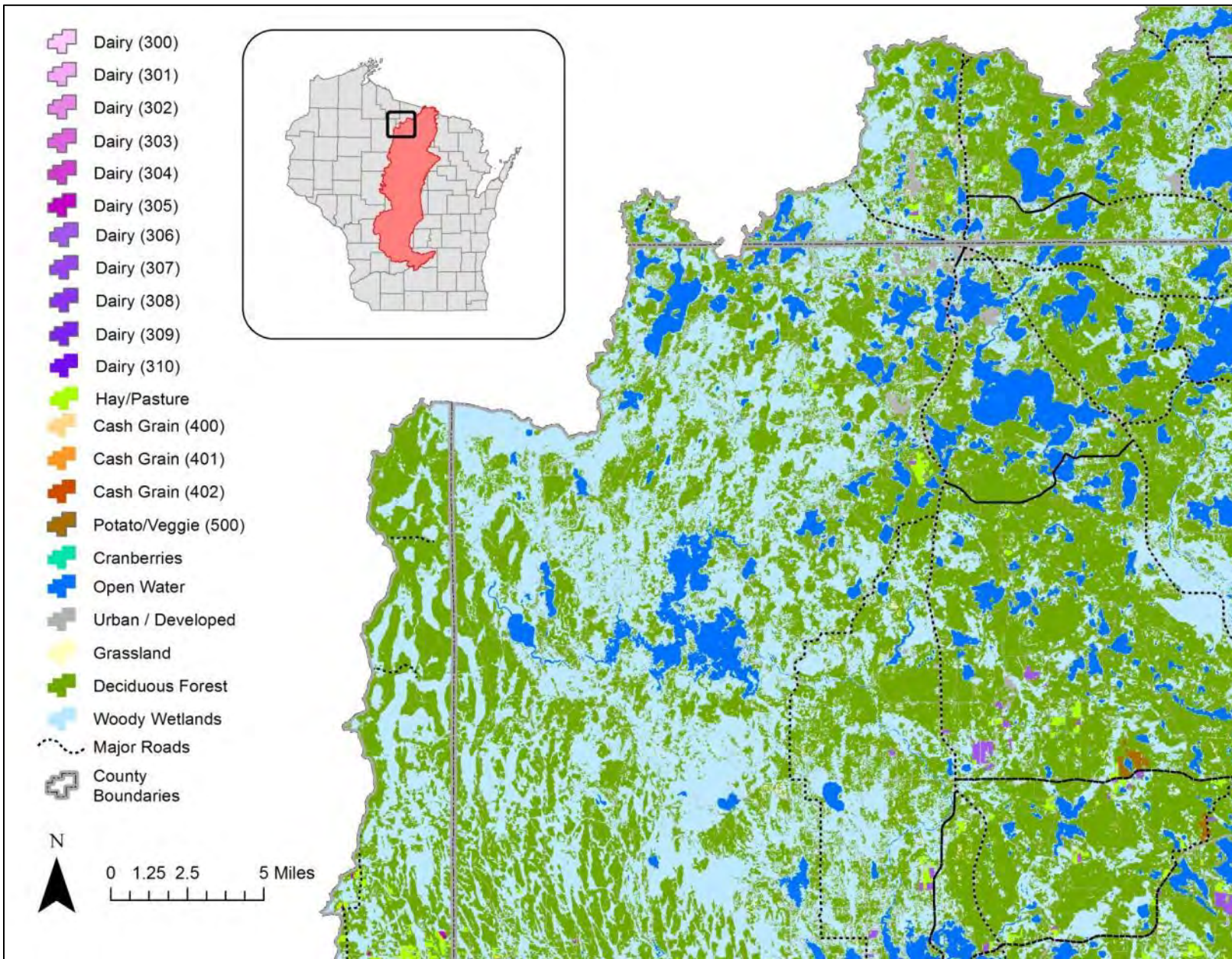


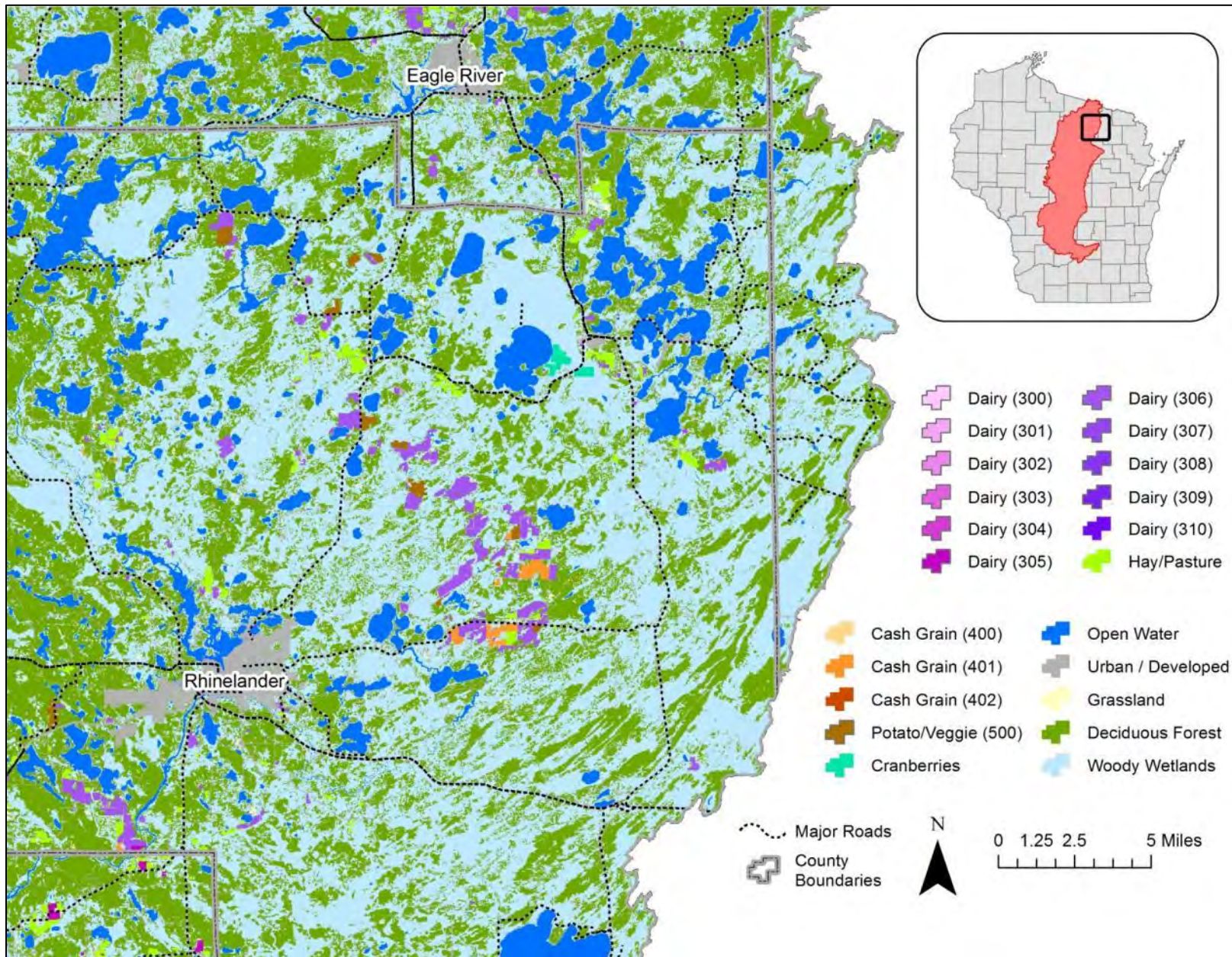


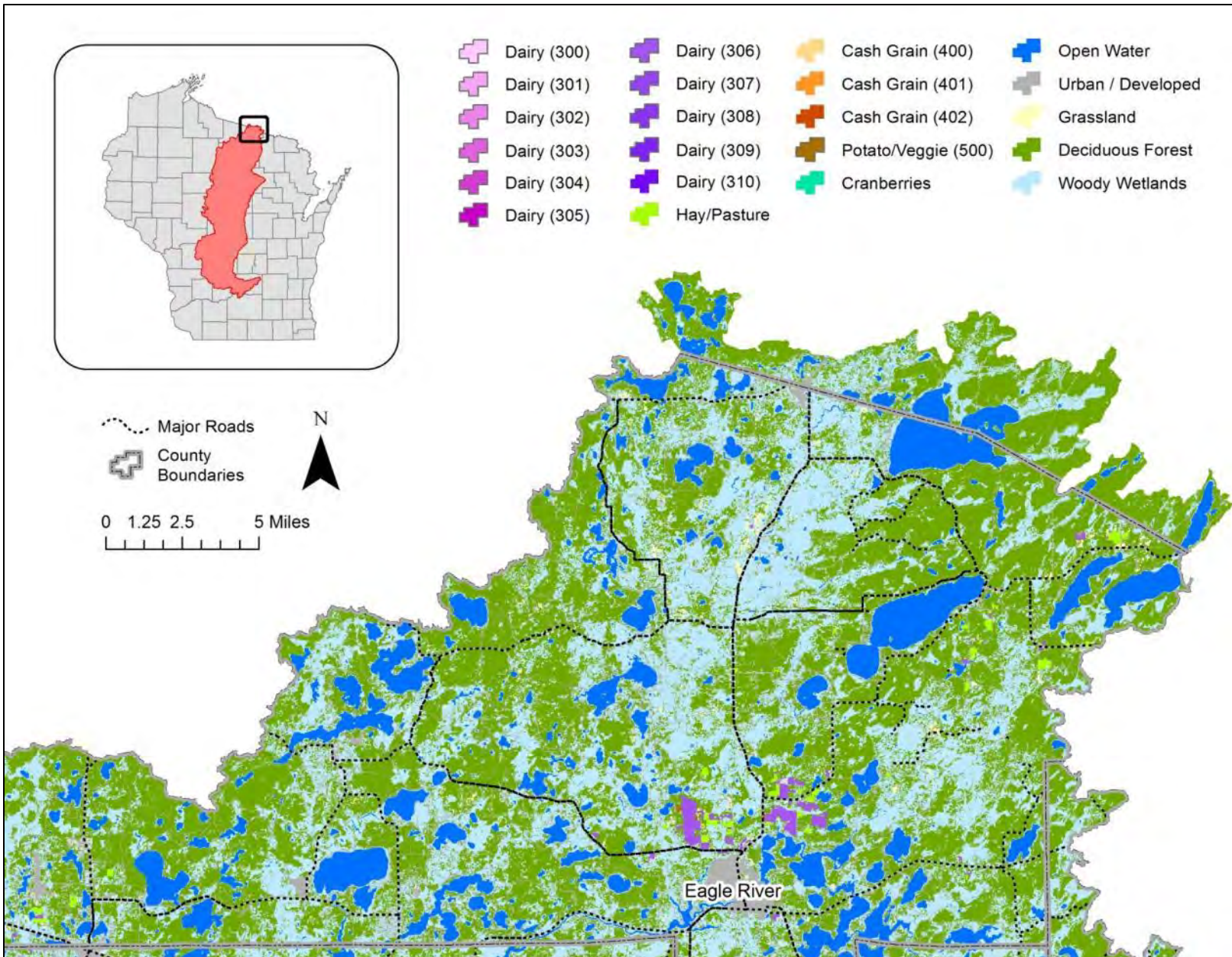












Appendix D.4

We have provided balance sheets that compare manure estimates by county to the total amount applied in the SWAT model. Balance sheets were only created for the counties that have a sizeable dairy industry within the Wisconsin River Basin (see Figure 1 for locations of counties within the basin). SWAT uses dry weight values for manure application, so reported values of liquid and solid manure were converted to dry weight values in kg/ha. The conversion process required the determination of the dry weight percentages of dry manure and liquid manure. Based on previous research 6% dry weight for liquid manure and 24% dry weight for solid manure were used (Jokela & Peters, 2009; Laboski & Peters, 2012; NRCS, 2006). For liquid manure conversions, it was also assumed that there are 8.3 pounds per every gallon of manure based on the DATCP dairy manure estimation calculator.

We learned from agricultural experts (e.g., county conservations and private agronomists) that the general distribution of cattle sizes on a dairy farm is approximately 50% calves and heifers (approximately 150–750 lbs.) and 50% lactating and dry adult cows (750–1400 lbs.). According to the DATCP dairy manure output values from the manure estimation calculator and the animal size distribution estimates, the average manure output per dairy cow is 16 short tons per acre per year (DATCP, 2000).

MARATHON COUNTY

CDL Dairy Acres	230,306
% Daily Haul Acres	0.40
% Storage Acres	0.60
% 6-Year Rotation Receiving Manure (corn years)	0.33
% Dry (Liquid)	0.06
% Dry (Solid)	0.24
Pounds manure per gallon liquid	8.34
Storage Application Rate - Corn Years (ga/acre/yr)	10,000
Storage Application Rate - 1st Year Alfalfa (ga/acre/yr)	3,000
DH Application Rate - Corn Years (tons/acre/yr)	25
DH Application Rate - 1st Year Alfalfa (tons/acre/yr)	8
Cattle Census 2010 (head cattle)	139,500
Avg. manure output per year (tons/cow)	16
Census Dry Weight Output (lbs/6-year rotation)	6,428,160,000
FROM DAIRY CDL PIXELS	
CDL Rotation Dry Weight Total from DH (lbs/6-year rotation)	2,579,422,346
CDL Rotation Dry Weight Total from Storage (lbs/6-year rotation)	1,590,379,696
CDL Rotation Dry Weight Total from DH & Storage (lbs/6-year rotation)	4,169,802,042
FROM CONTINUOUS CORN CDL PIXELS	
Total Continuous Corn (Acres)	6,600
% Cont. Corn Assumed to be Dairy (Acres)	0.50
Dairy from Cont. Corn pixels (Acres)	3,300
CDL Rotation Dry Weight Total from DH (lbs/6-year rotation)	36,962,361
CDL Rotation Dry Weight Total from Storage (lbs/6-year rotation)	31,707,370
CDL Rotation Dry Weight Total from DH & Storage (lbs/6-year rotation)	68,669,731
GRAZED LANDS ESTIMATE	
Land Area (Acres)	12,349
Dry Weight Output - Assuming 1.5 cows per acre (lbs/6-year rotation)	853,562,880
RESULTS	
NASS Census Dry Weight (lbs/6-year rotation)	6,428,160,000
CDL Dry Weight (lbs/6-year rotation)	5,092,034,653

JUNEAU COUNTY

CDL Dairy Acres	35,951
% Daily Haul Acres	0.50
% Storage Acres	0.50
% 6-Year Rotation Receiving Manure	0.33
% Dry (Liquid)	0.06
% Dry (Solid)	0.24
Pounds manure per gallon liquid	8.34
Storage Application Rate - Corn Years (ga/acre/yr)	10,000
Storage Application Rate - 1st Year Alfalfa (ga/acre/yr)	3,000
DH Application Rate - Corn Years (tons/acre/yr)	25
DH Application Rate - 1st Year Alfalfa (tons/acre/yr)	8
Cattle Census 2010 (head cattle)	28,000
Avg. manure output per year (tons/cow)	16
Census Dry Weight Output (lbs/6-year rotation)	1,290,240,000
FROM DAIRY CDL PIXELS	
CDL Rotation Dry Weight Total from DH (lbs/6-year rotation)	503,307,220
CDL Rotation Dry Weight Total from Storage (lbs/6-year rotation)	206,880,838
CDL Rotation Dry Weight Total from DH & Storage (lbs/6-year rotation)	710,188,058
FROM CONTINUOUS CORN CDL PIXELS	
Total Continuous Corn (Acres)	1,977
% Cont. Corn Assumed to be Dairy (Acres)	0.50
Dairy from Cont. Corn pixels (Acres)	989
CDL Rotation Dry Weight Total from DH (lbs/6-year rotation)	13,840,388
CDL Rotation Dry Weight Total from Storage (lbs/6-year rotation)	7,915,120
CDL Rotation Dry Weight Total from DH & Storage (lbs/6-year rotation)	21,755,508
GRAZED LANDS ESTIMATE	
Land Area (Acres)	7,500
Dry Weight Output - Assuming 1.5 cows per acre (lbs/6-year rotation)	518,400,000
RESULTS	
NASS Census Dry Weight (lbs/6-year rotation)	1,290,240,000
CDL Dry Weight (lbs/6-year rotation)	1,250,343,566

LINCOLN COUNTY

CDL Dairy Acres	26,551
% Daily Haul Acres	0.33
% Storage Acres	0.67
% 6-Year Rotation Receiving Manure	0.33
% Dry (Liquid)	0.06
% Dry (Solid)	0.24
Pounds manure per gallon liquid	8.34
Storage Application Rate - Corn Years (ga/acre/yr)	10,000
Storage Application Rate - 1st Year Alfalfa (ga/acre/yr)	3,000
DH Application Rate - Corn Years (tons/acre/yr)	25
DH Application Rate - 1st Year Alfalfa (tons/acre/yr)	8
Cattle Census 2010 (head cattle)	12,500
Avg. manure output per year (tons/cow)	16
Census Dry Weight Output (lbs/6-year rotation)	576,000,000
FROM DAIRY CDL PIXELS	
CDL Rotation Dry Weight Total from DH (lbs/6-year rotation)	247,813,598
CDL Rotation Dry Weight Total from Storage (lbs/6-year rotation)	203,724,019
CDL Rotation Dry Weight Total from DH & Storage (lbs/6-year rotation)	451,537,617
FROM CONTINUOUS CORN CDL PIXELS	
Total Continuous Corn (Acres)	889
% Cont. Corn Assumed to be Dairy (Acres)	0.50
Dairy from Cont. Corn pixels (Acres)	444
CDL Rotation Dry Weight Total from DH (lbs/6-year rotation)	4,147,213
CDL Rotation Dry Weight Total from Storage (lbs/6-year rotation)	4,743,463
CDL Rotation Dry Weight Total from DH & Storage (lbs/6-year rotation)	8,890,676
GRAZED LANDS ESTIMATE	
Land Area (Acres)	1,000
Dry Weight Output - Assuming 1.5 cows per acre (lbs/6-year rotation)	69,120,000
RESULTS	
NASS Census Dry Weight (lbs/6-year rotation)	576,000,000
CDL Dry Weight (lbs/6-year rotation)	529,548,293

SAUK COUNTY

CDL Dairy Acres	84,694
% Daily Haul Acres	0.85
% Storage Acres	0.15
% 6-Year Rotation Receiving Manure	0.33
% Dry (Liquid)	0.06
% Dry (Solid)	0.24
Pounds manure per gallon liquid	8.34
Storage Application Rate - Corn Years (ga/acre/yr)	10,000
Storage Application Rate - 1st Year Alfalfa (ga/acre/yr)	3,000
DH Application Rate - Corn Years (tons/acre/yr)	25
DH Application Rate - 1st Year Alfalfa (tons/acre/yr)	8
Cattle Census 2010 (head cattle)	82,000
Avg. manure output per year (tons/cow)	16
Census Dry Weight Output (lbs/6-year rotation)	3,778,560,000
FROM DAIRY CDL PIXELS	
CDL Rotation Dry Weight Total from DH (lbs/6-year rotation)	2,015,718,453
CDL Rotation Dry Weight Total from Storage (lbs/6-year rotation)	146,214,119
CDL Rotation Dry Weight Total from DH & Storage (lbs/6-year rotation)	2,161,932,572
FROM CONTINUOUS CORN CDL PIXELS	
Total Continuous Corn (Acres)	16,223
% Cont. Corn Assumed to be Dairy (Acres)	0.50
Dairy from Cont. Corn pixels (Acres)	8,111
CDL Rotation Dry Weight Total from DH (lbs/6-year rotation)	193,052,662
CDL Rotation Dry Weight Total from Storage (lbs/6-year rotation)	19,483,069
CDL Rotation Dry Weight Total from DH & Storage (lbs/6-year rotation)	212,535,731
GRAZED LANDS ESTIMATE	
Land Area (Acres)	5,000
Dry Weight Output - Assuming 1.5 cows per acre (lbs/6-year rotation)	345,600,000
RESULTS	
NASS Census Dry Weight (lbs/6-year rotation)	3,778,560,000
CDL Dry Weight (lbs/6-year rotation)	2,720,068,303

ADAMS COUNTY

CDL Dairy Acres	23,507
% Daily Haul Acres	0.40
% Storage Acres	0.60
% 6-Year Rotation Receiving Manure	0.33
% Dry (Liquid)	0.06
% Dry (Solid)	0.24
Pounds manure per gallon liquid	8.34
Storage Application Rate - Corn Years (ga/acre/yr)	10,000
Storage Application Rate - 1st Year Alfalfa (ga/acre/yr)	3,000
DH Application Rate - Corn Years (tons/acre/yr)	25
DH Application Rate - 1st Year Alfalfa (tons/acre/yr)	8
Cattle Census 2010 (head cattle)	11,000
Avg. manure output per year (tons/cow)	16
Census Dry Weight Output (lbs/6-year rotation)	506,880,000
FROM DAIRY CDL PIXELS	
CDL Rotation Dry Weight Total from DH (lbs/6-year rotation)	263,274,523
CDL Rotation Dry Weight Total from Storage (lbs/6-year rotation)	162,325,668
CDL Rotation Dry Weight Total from DH & Storage (lbs/6-year rotation)	425,600,192
FROM CONTINUOUS CORN CDL PIXELS	
Total Continuous Corn (Acres)	3,369
% Cont. Corn Assumed to be Dairy (Acres)	0.50
Dairy from Cont. Corn pixels (Acres)	1,685
CDL Rotation Dry Weight Total from DH (lbs/6-year rotation)	18,869,195
CDL Rotation Dry Weight Total from Storage (lbs/6-year rotation)	16,186,534
CDL Rotation Dry Weight Total from DH & Storage (lbs/6-year rotation)	35,055,729
GRAZED LANDS ESTIMATE	
Land Area (Acres)	500
Dry Weight Output - Assuming 1.5 cows per acre (lbs/6-year rotation)	34,560,000
RESULTS	
NASS Census Dry Weight (lbs/6-year rotation)	506,880,000
CDL Dry Weight (lbs/6-year rotation)	495,215,921

WOOD COUNTY

CDL Dairy Acres	72,992
% Daily Haul Acres	0.40
% Storage Acres	0.60
% 6-Year Rotation Receiving Manure	0.33
% Dry (Liquid)	0.06
% Dry (Solid)	0.24
Pounds manure per gallon liquid	8.34
Storage Application Rate - Corn Years (ga/acre/yr)	10,000
Storage Application Rate - 1st Year Alfalfa (ga/acre/yr)	3,000
DH Application Rate - Corn Years (tons/acre/yr)	25
DH Application Rate - 1st Year Alfalfa (tons/acre/yr)	8
Cattle Census 2010 (head cattle)	45,500
Avg. manure output per year (tons/cow)	16
 Census Dry Weight Output (lbs/6-year rotation)	 2,096,640,000
 FROM DAIRY CDL PIXELS	
CDL Rotation Dry Weight Total from DH (lbs/6-year rotation)	817,513,998
CDL Rotation Dry Weight Total from Storage (lbs/6-year rotation)	504,049,934
CDL Rotation Dry Weight Total from DH & Storage (lbs/6-year rotation)	1,321,563,932
 FROM CONTINUOUS CORN CDL PIXELS	
Total Continuous Corn (Acres)	3,275
% Cont. Corn Assumed to be Dairy (Acres)	0.50
Dairy from Cont. Corn pixels (Acres)	1,637
CDL Rotation Dry Weight Total from DH (lbs/6-year rotation)	18,337,405
CDL Rotation Dry Weight Total from Storage (lbs/6-year rotation)	15,730,350
CDL Rotation Dry Weight Total from DH & Storage (lbs/6-year rotation)	34,067,755
 FROM MANAGED GRAZED LANDS	
GRAZED LANDS ESTIMATE (Acres)	3,000
Dry Weight Output - Assuming 1.5 cows per acre (lbs/6-year rotation)	207,360,000
 RESULTS	
NASS Census Dry Weight (lbs/6-year rotation)	2,096,640,000
CDL Dry Weight (lbs/6-year rotation)	1,562,991,687

Appendix D.5

Monthly TSS and TP loads were estimated using an empirical model within Fluxmaster software (Schwarz et al., 2006). The Fluxmaster modeling process for the WRB is described in Section 5.2.3. To interpret the performance of the load estimation models, we have included information about each site and measures of accuracy in Table 8 and Table 9. This appendix includes more detailed information about each model for each site, specifically the values of each fitted coefficient, and the p-values associated with the fit of each coefficient. Models were fit according to a 5 or 7-parameter model structure template. The 5 and 7-parameter models are structured as follows:

$$\tilde{c}_t = \gamma_0 + \gamma_q \tilde{q}_t + \gamma_T T_t + \gamma_S \sin(2\pi T_t) + \gamma_C \cos(2\pi T_t) + e_t$$

$$\tilde{c}_t = \gamma_0 + \gamma_q \tilde{q}_t + \gamma_{q^2} \tilde{q}_t^2 + \gamma_T T_t + \gamma_{T^2} T_t^2 + \gamma_S \sin(2\pi T_t) + \gamma_C \cos(2\pi T_t) + e_t,$$

where at time t , \tilde{c}_t is the concentration of a chemical constituent, \tilde{q}_t is the log daily streamflow, T_t is the decimal time with whole numbers representing the year, and the decimal numbers representing the fraction of the year. The coefficients, γ_0 , γ_q , γ_{q^2} , γ_T , γ_{T^2} , γ_S , and γ_C are estimated and e_t represents the residual error. The coefficient values and their associated p-values are listed here.

D.5.1 TSS

Station Name	Intercept		Flow		Flow Squared		Sine		Cosine		Trend		Trend Squared	
	γ_0	p	γ_q	p	γ_{q^2}	p	γ_s	p	γ_c	p	γ_T	p	γ_{T^2}	p
Baraboo River at Main Street, Reedsburg, WI	-0.002	0.999	0.577	0.001	–	–	-0.012	0.918	-0.773	0.000	–	–	–	–
Baraboo River near Baraboo, WI	-0.380	0.375	0.580	0.000	–	–	0.041	0.526	-1.188	0.000	-0.027	0.015	–	–
Big Eau Pleine River at Big Eau Pleine Dam	2.293	0.000	-0.075	0.126	–	–	-0.335	0.000	-0.817	0.000	–	–	–	–
Big Eau Pleine River at Stratford, WI	2.365	0.000	-0.579	0.000	0.091	0.018	-0.387	0.000	-1.282	0.000	–	–	–	–
Big Rib River at Rib Falls, WI	-1.327	0.076	0.416	0.000	–	–	-0.198	0.108	-0.882	0.000	0.014	0.856	–	–
Big Roche a Cri Creek at Hwy 21	0.384	0.639	0.118	0.501	–	–	-0.059	0.534	-0.629	0.000	-0.037	0.613	–	–
Eau Claire River at Kelly, WI	-1.382	0.003	0.502	0.000	–	–	-0.054	0.589	-0.693	0.000	–	–	–	–
Fenwood Creek at Bradley, WI	1.164	0.000	-0.008	0.890	0.036	0.007	-0.050	0.704	-0.940	0.000	-0.127	0.108	-0.193	0.009
Freeman Creek at Halder, WI	1.188	0.000	0.152	0.105	–	–	0.001	0.998	-0.600	0.001	-0.079	0.403	–	–
Lemonweir at New Lisbon	2.456	0.000	-0.104	0.032	–	–	0.044	0.519	-0.178	0.006	–	–	–	–
Little Eau Pleine River near Rozellville, WI	2.184	0.000	-0.070	0.265	–	–	-0.179	0.177	-0.829	0.000	-0.307	0.001	–	–
Mill Creek at County Hwy PP	0.599	0.019	0.097	0.129	–	–	-0.006	0.966	-0.809	0.000	-0.099	0.273	–	–
Mill Creek near Hewitt, WI	1.370	0.014	0.583	0.002	–	–	0.234	0.356	-0.343	0.299	–	–	–	–
Mill Creek near Junction City, WI	2.631	0.001	-0.138	0.368	–	–	-0.196	0.372	-1.100	0.000	–	–	–	–
Pine River at Center Avenue near Merrill, WI	-1.245	0.001	0.459	0.000	–	–	-0.012	0.929	-0.417	0.007	-0.199	0.025	–	–
Plover River at Hwy 10/66	-10.483	0.078	4.561	0.044	-0.442	0.039	0.309	0.000	-0.753	0.000	0.031	0.601	-0.023	0.711
Prairie River near Merrill, WI	-7.895	0.053	3.016	0.041	-0.235	0.073	0.188	0.136	-0.455	0.001	–	–	–	–
Ten Mile Creek near Nekoosa	-0.706	0.254	0.535	0.001	–	–	0.524	0.000	-0.351	0.002	–	–	–	–
West Branch of Baraboo River at Hillsboro, WI	1.762	0.000	0.378	0.018	–	–	-0.177	0.122	-0.798	0.000	–	–	–	–
Wisconsin River at Merrill, WI	1.267	0.052	0.020	0.815	–	–	-0.172	0.002	-0.671	0.000	-0.024	0.038	–	–
Wisconsin River at Rhinelander	2.553	0.002	-0.264	0.034	–	–	-0.221	0.000	-0.286	0.000	–	–	–	–
Wisconsin River at Wisconsin Dells	1.235	0.138	0.080	0.416	–	–	-0.344	0.000	-0.839	0.000	-0.020	0.130	–	–
Wisconsin River at Wisconsin Rapids	-0.761	0.261	0.337	0.000	–	–	-0.579	0.000	-0.997	0.000	–	–	–	–
Yellow River at Babcock	1.647	0.000	0.174	0.001	–	–	-0.246	0.017	-0.806	0.000	–	–	–	–
Yellow River at Hwy 21	2.944	0.000	-0.071	0.227	–	–	-0.221	0.029	-0.780	0.000	-0.110	0.108	–	–

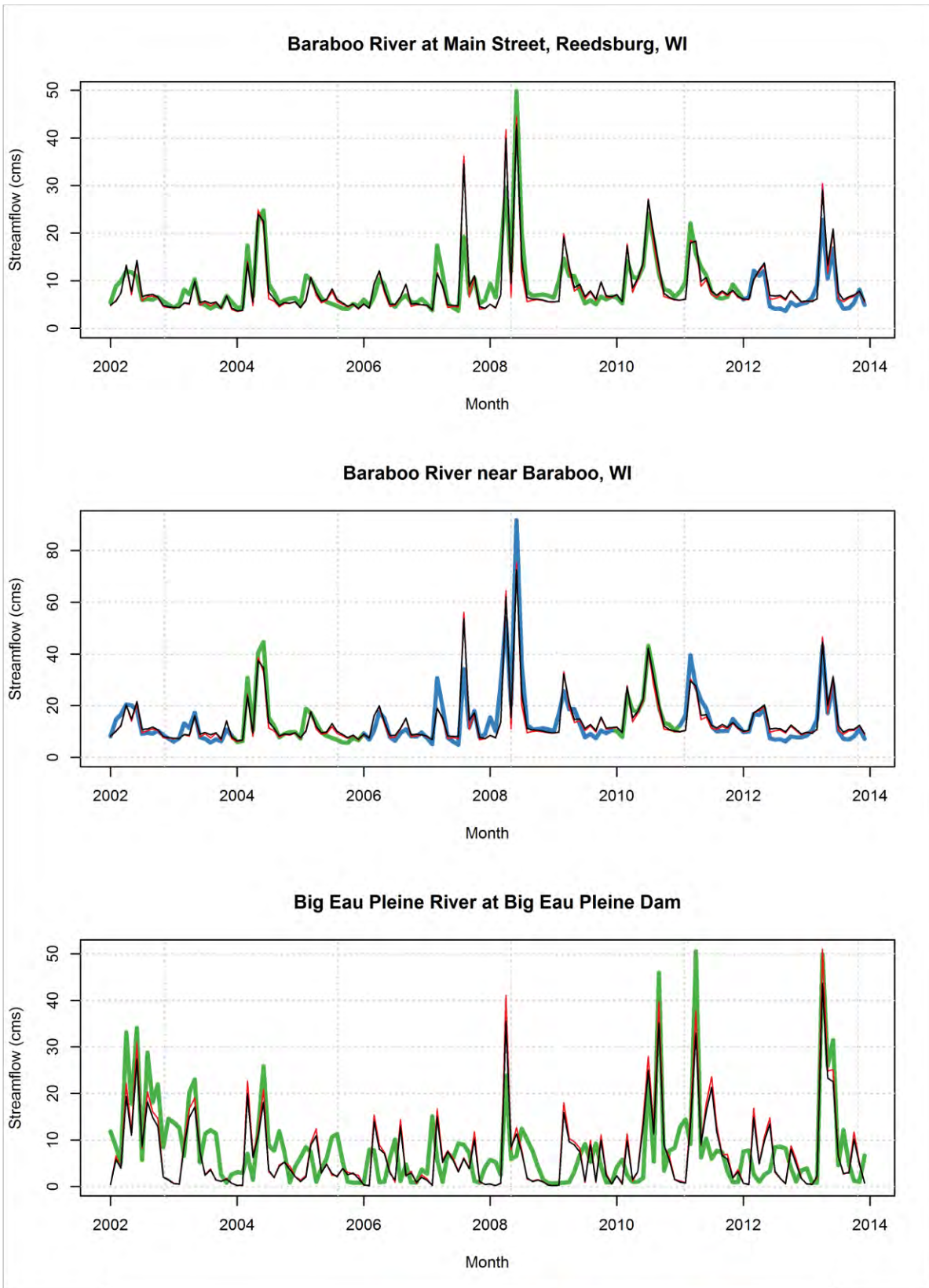
D.5.2 TP

Station Name	Intercept		Flow		Flow Squared		Sine		Cosine		Trend		Trend Squared	
	γ_0	p	γ_q	p	γ_{q^2}	p	γ_s	p_{b_sin}	γ_0	p	γ_q	p	γ_{q^2}	p
Baraboo River at Main Street, Reedsburg, WI	-4.606	0.000	0.480	0.000	-	-	-0.157	0.009	-0.348	0.000	-	-	-	-
Baraboo River near Baraboo, WI	-4.129	0.000	0.382	0.000	-	-	-0.101	0.004	-0.460	0.000	-0.025	0.000	-	-
Big Eau Pleine River at Big Eau Pleine Dam	-2.609	0.000	0.043	0.169	-	-	-0.040	0.482	-0.331	0.000	-	-	-	-
Big Eau Pleine River at Stratford, WI	-2.075	0.000	0.185	0.000	-	-	-0.218	0.000	-0.538	0.000	-0.053	0.000	-	-
Big Rib River at Rib Falls, WI	-0.684	0.773	0.374	0.112	-0.009	0.667	-0.130	0.031	-0.324	0.000	-0.965	0.124	0.062	0.159
Big Roche a Cri Creek at Hwy 21	-6.103	0.090	0.930	0.535	-0.080	0.608	-0.052	0.384	-0.131	0.025	-0.033	0.453	0.020	0.643
Eau Claire River at Kelly, WI	-4.787	0.000	0.377	0.000	-	-	0.045	0.486	-0.170	0.010	-0.007	0.707	-	-
Fenwood Creek at Bradley, WI	-2.554	0.000	-0.038	0.294	0.036	0.000	-0.165	0.016	-0.532	0.000	-0.065	0.075	-0.043	0.205
Freeman Creek at Halder, WI	-2.744	0.000	-0.172	0.262	0.059	0.044	-0.132	0.122	-0.363	0.000	0.030	0.751	-0.046	0.315
Lemonweir at New Lisbon	-2.718	0.000	0.090	0.024	-	-	-0.039	0.464	-0.220	0.000	-	-	-	-
Little Eau Pleine River near Rozellville, WI	-1.980	0.000	0.203	0.005	-0.020	0.024	-0.173	0.001	-0.338	0.000	-0.041	0.254	0.041	0.282
Mill Creek at County Hwy PP	-2.455	0.000	0.148	0.000	-	-	-0.160	0.008	-0.350	0.000	-0.040	0.311	-	-
Mill Creek near Hewitt, WI	-0.766	0.008	-0.007	0.935	-	-	0.023	0.855	-0.080	0.642	-	-	-	-
Mill Creek near Junction City, WI	-1.597	0.001	0.023	0.807	-	-	-0.008	0.948	-0.505	0.002	-	-	-	-
Pine River at Center Avenue near Merrill, WI	-5.127	0.000	0.615	0.005	-0.035	0.132	-0.016	0.763	-0.110	0.047	-0.129	0.001	0.048	0.239
Plover River at Hwy 10/66	-5.566	0.000	0.379	0.000	-	-	0.079	0.127	-0.406	0.000	0.016	0.641	-	-
Prairie River near Merrill, WI	-8.735	0.000	1.864	0.004	-0.140	0.016	0.095	0.061	-0.127	0.015	-	-	-	-
Spirit River at Spirit Falls	-3.215	0.000	0.115	0.039	-	-	0.080	0.485	-0.205	0.071	-	-	-	-
Spirit River at Spirit River Dam	-2.896	0.000	0.018	0.522	-	-	-0.235	0.000	-0.041	0.349	-	-	-	-
Ten Mile Creek near Nekoosa	-4.012	0.000	0.237	0.000	-	-	0.140	0.001	-0.211	0.000	-	-	-	-
West Branch of Baraboo River at Hillsboro, WI	-2.952	0.000	0.274	0.075	-	-	0.080	0.471	-0.310	0.006	-	-	-	-
Wisconsin River at Castle Rock Dam	-4.695	0.000	0.223	0.000	-	-	-0.208	0.000	-0.189	0.000	-	-	-	-
Wisconsin River at Chuck's Landing	-3.918	0.000	0.153	0.000	-	-	-0.097	0.007	-0.223	0.000	-	-	-	-
Wisconsin River at Herb Mitchell Landing	-2.313	0.000	-0.074	0.053	-	-	-0.053	0.020	-0.142	0.000	-	-	-	-
Wisconsin River at Lake DuBay Dam	-3.385	0.000	0.120	0.002	-	-	-0.113	0.005	-0.221	0.000	-0.027	0.081	-	-
Wisconsin River at Merrill, WI	-3.902	0.000	0.132	0.000	-	-	-0.050	0.044	-0.144	0.000	0.008	0.098	-	-
Wisconsin River at Nekoosa Dam	-3.389	0.000	0.116	0.002	-	-	-0.075	0.054	-0.259	0.000	-	-	-	-
Wisconsin River at Petenwell Dam	-2.630	0.000	0.028	0.559	-	-	-0.213	0.000	-0.248	0.000	-0.056	0.004	-	-
Wisconsin River at Rainbow Lake	-0.762	0.453	-0.440	0.011	-	-	-0.205	0.005	-0.048	0.481	-	-	-	-
Wisconsin River at Rhinelander	-3.652	0.000	0.030	0.680	-	-	-0.058	0.077	-0.096	0.006	-	-	-	-
Wisconsin River at Rothschild, WI	-4.620	0.000	0.235	0.000	-	-	-0.132	0.000	-0.168	0.000	-	-	-	-
Wisconsin River at Stevens Point Dam	-3.823	0.000	0.148	0.000	-	-	-0.119	0.000	-0.281	0.000	-	-	-	-
Wisconsin River at Wausau Dam	-4.585	0.000	0.230	0.000	-	-	-0.087	0.025	-0.117	0.003	-	-	-	-
Wisconsin River at Wisconsin Dells	-3.914	0.000	0.150	0.000	-	-	-0.084	0.003	-0.270	0.000	-0.017	0.001	-	-
Wisconsin River at Wisconsin Rapids	-3.297	0.000	0.101	0.000	-	-	-0.061	0.028	-0.266	0.000	-0.017	0.002	-	-
Wisconsin River below Prairie du Sac Dam	-4.163	0.000	0.165	0.020	-	-	-0.204	0.002	-0.304	0.000	-0.013	0.754	-	-
Yellow River at Babcock	-1.420	0.000	-0.163	0.252	0.025	0.098	-0.183	0.030	-0.285	0.000	-	-	-	-
Yellow River at Hwy 21	-3.744	0.054	0.303	0.032	-0.016	0.196	-0.108	0.029	-0.271	0.000	0.119	0.815	-0.011	0.759

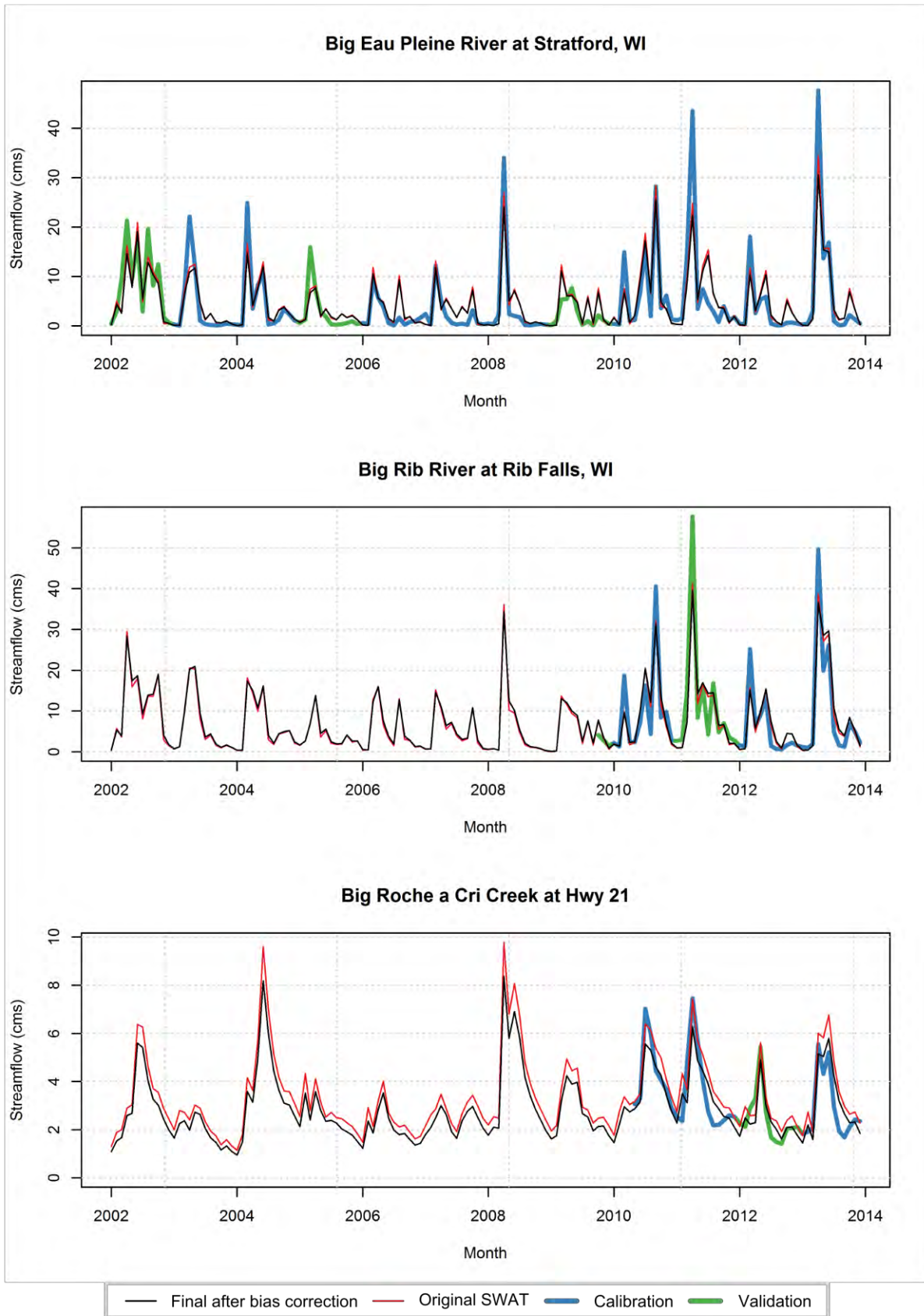
Appendix D.6

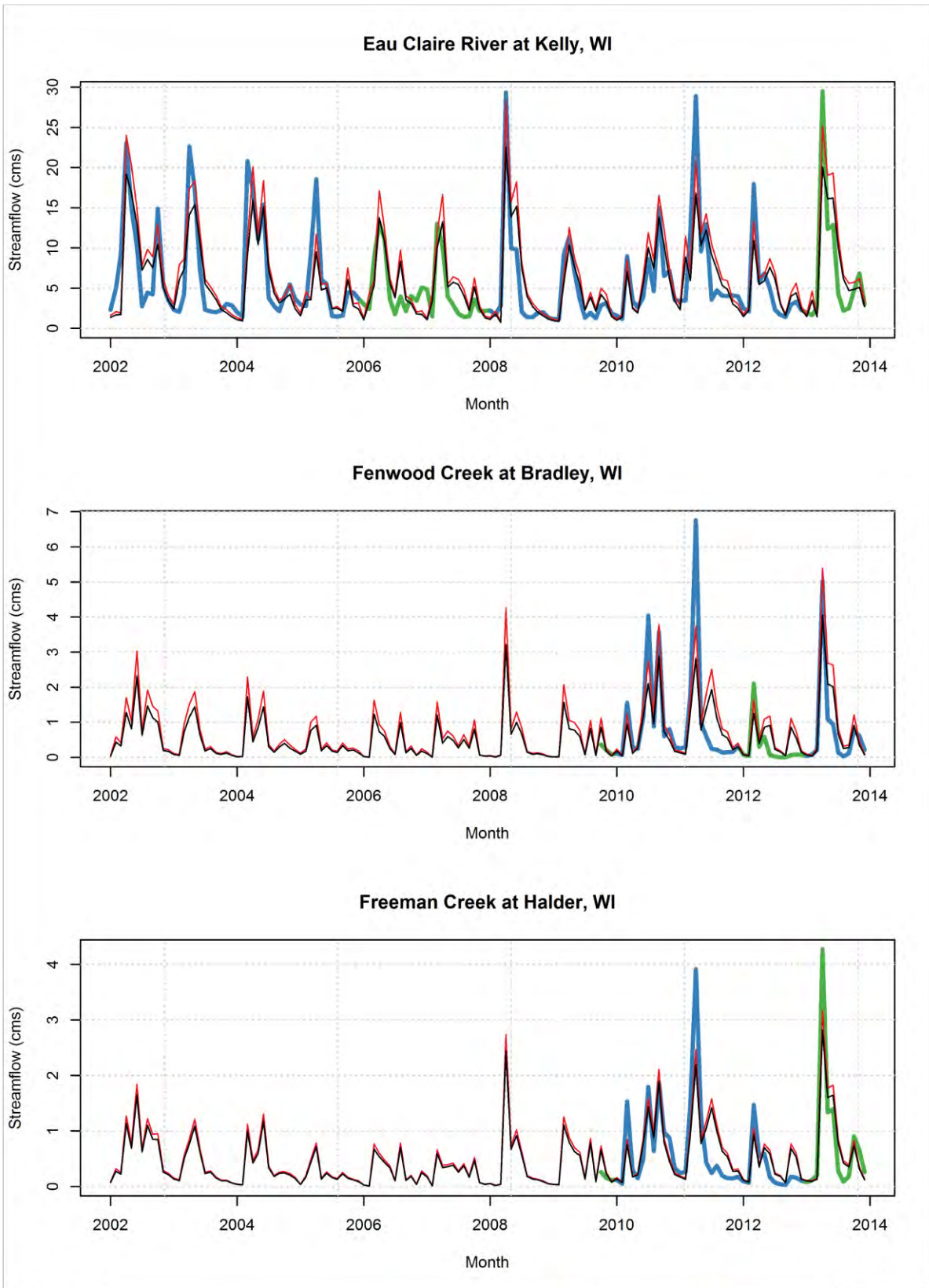
Figures showing simulated and observed streamflow, TSS, and TP loads over time can be useful for assessing accuracy as well as diagnosing specific temporal issues with a model. For each gage site listed in Table 13, we have include these temporal plots, each with two sets of observed streamflow or load and two sets of simulated streamflow or load. The observation set is split into calibration sets (blue) and those that were set aside for either quantitative validation or other qualitative assessment of accuracy (green). The simulation set is split into the original SWAT calibration results (red) and the final model results adjusted for routing and bias correction (black).

D.6.1 Streamflow

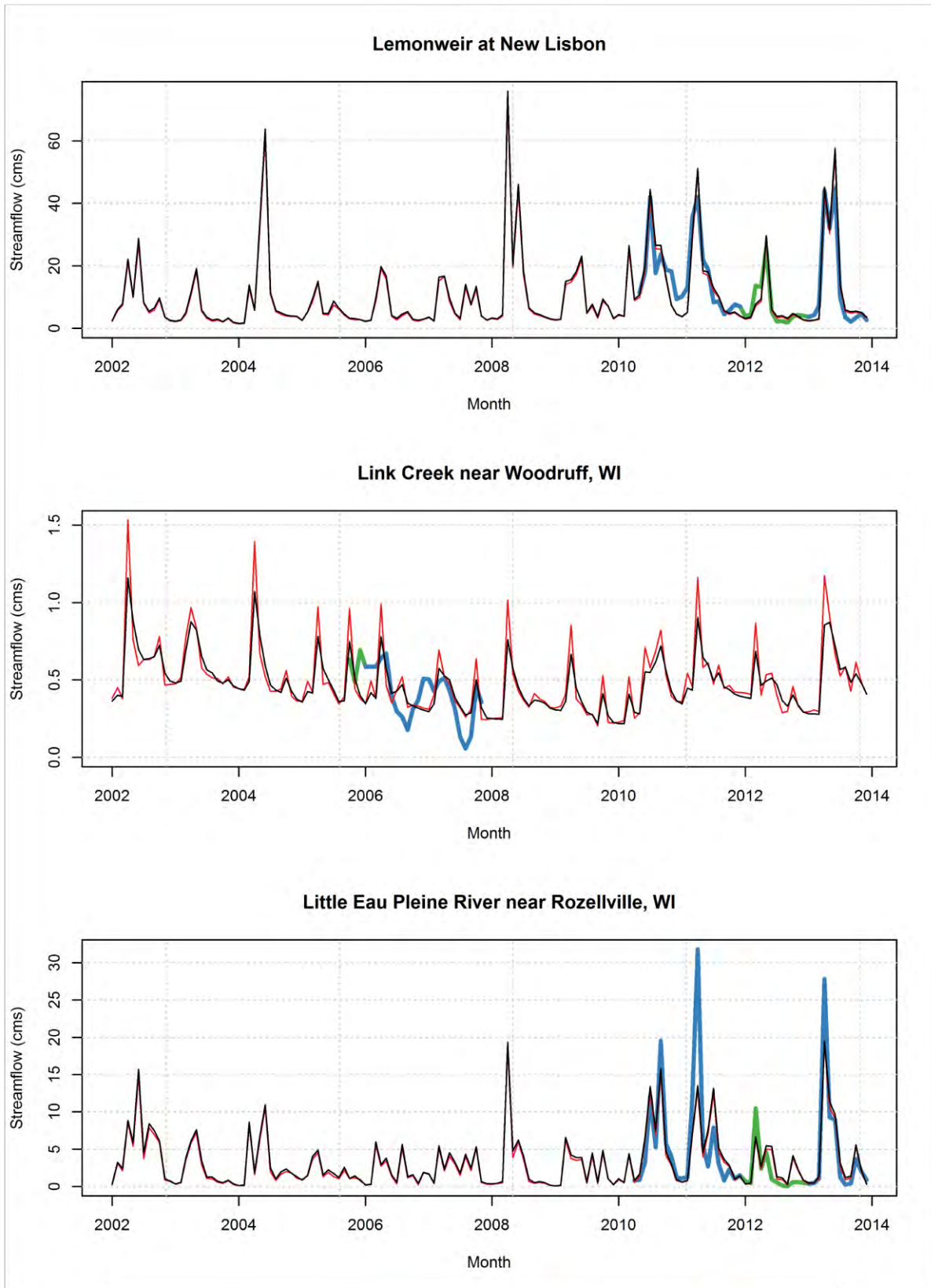


— Final after bias correction — Original SWAT — Calibration — Validation

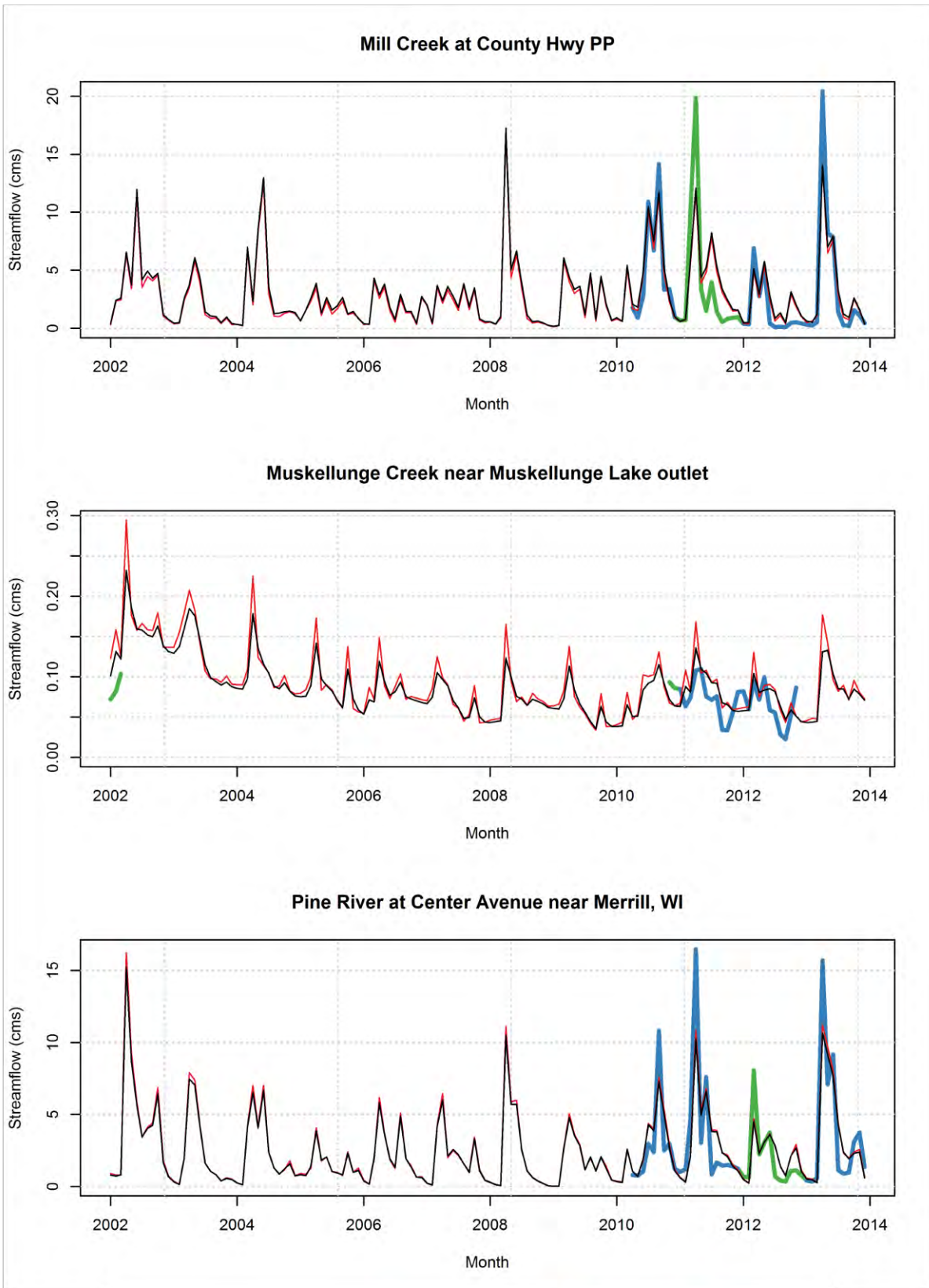




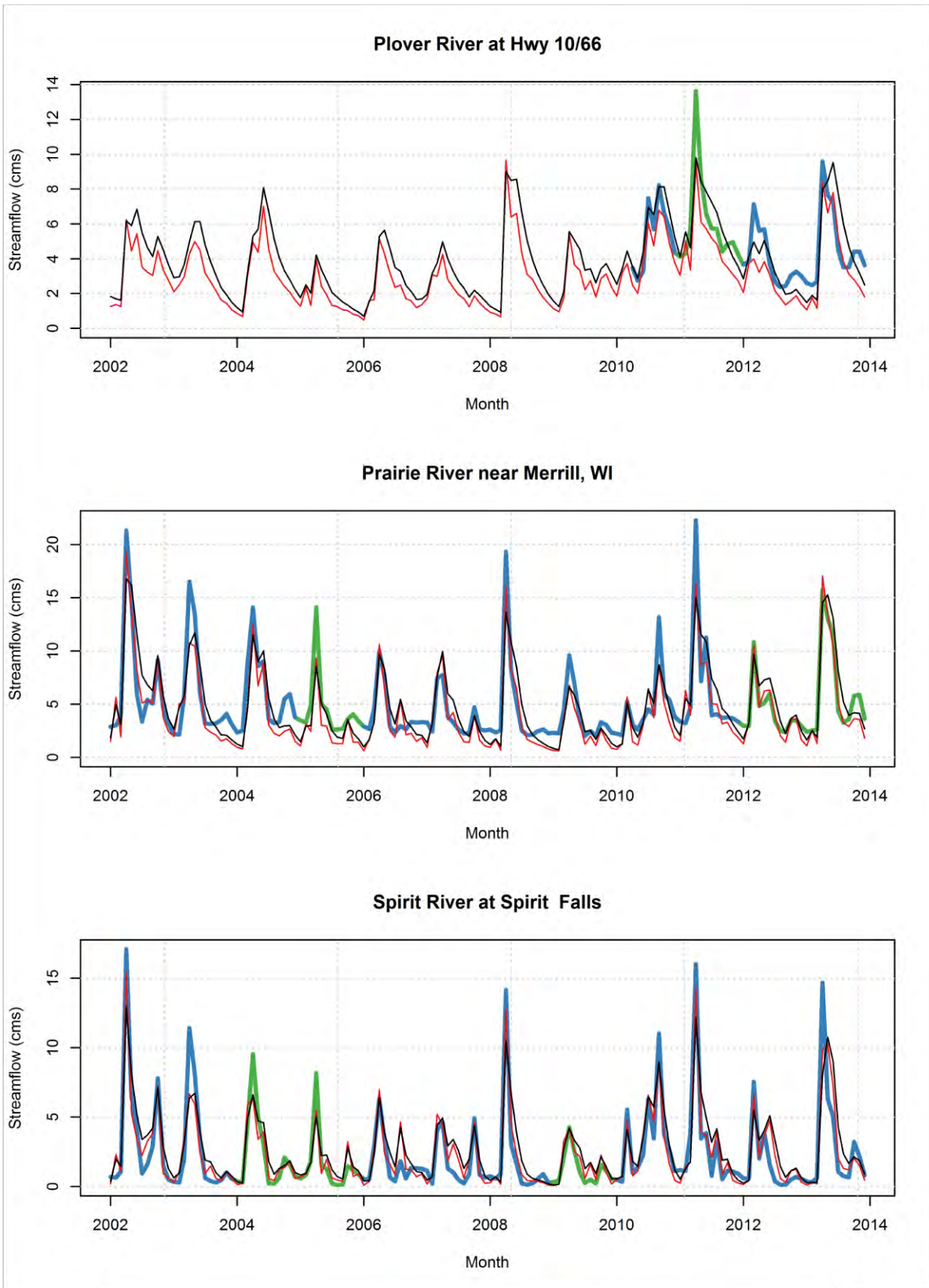
— Final after bias correction — Original SWAT — Calibration — Validation



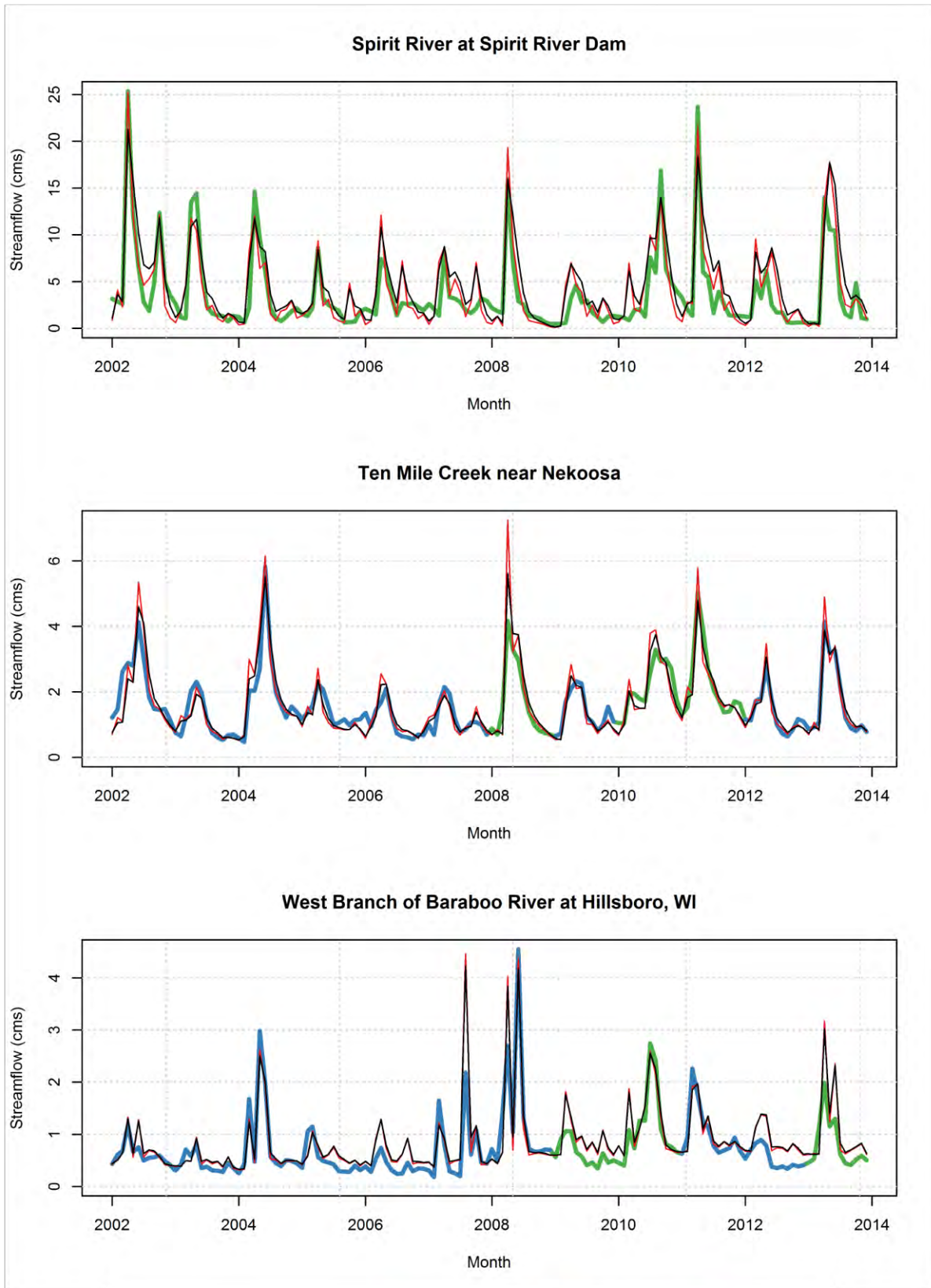
— Final after bias correction — Original SWAT — Calibration — Validation



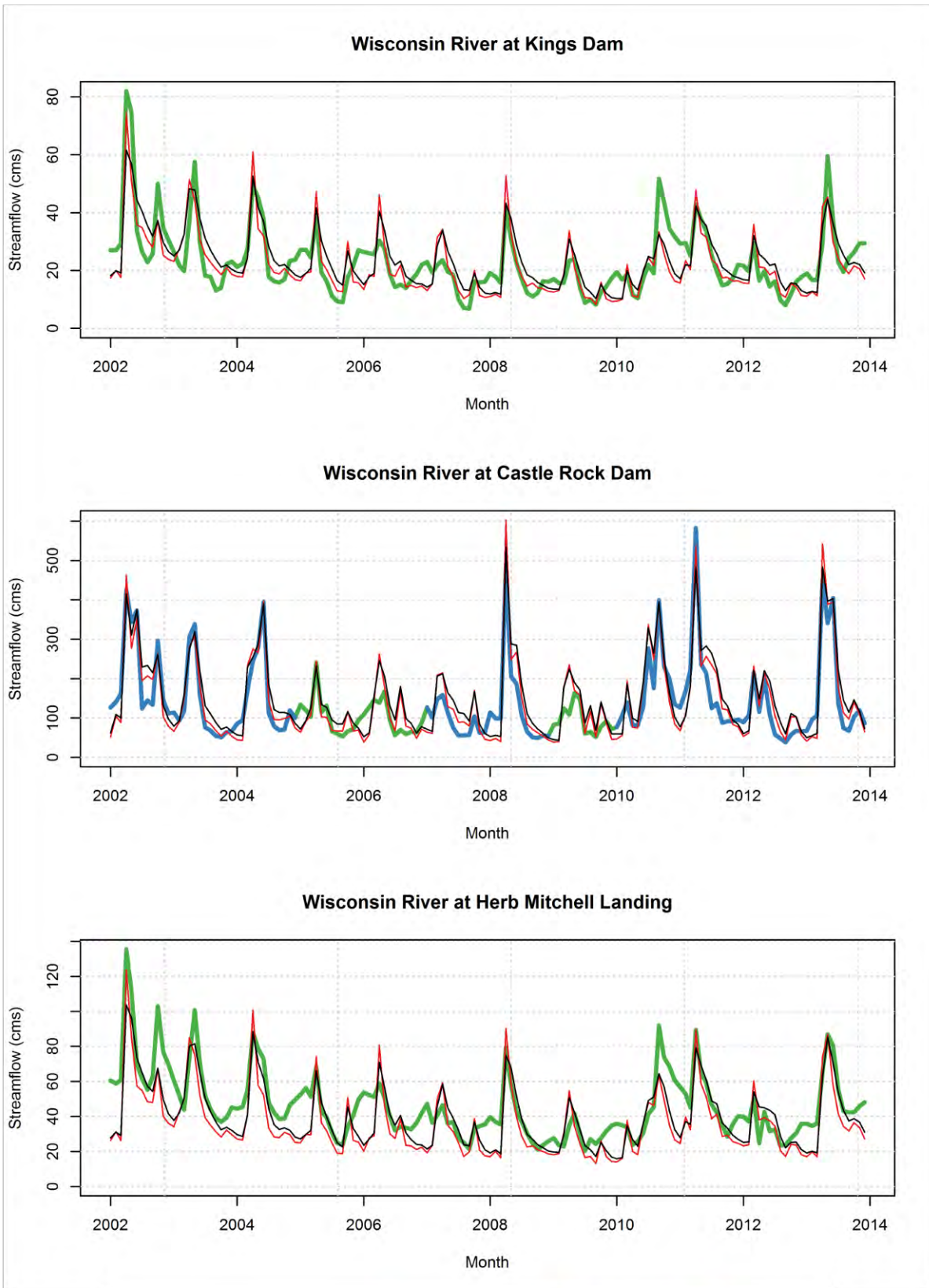
— Final after bias correction — Original SWAT — Calibration — Validation



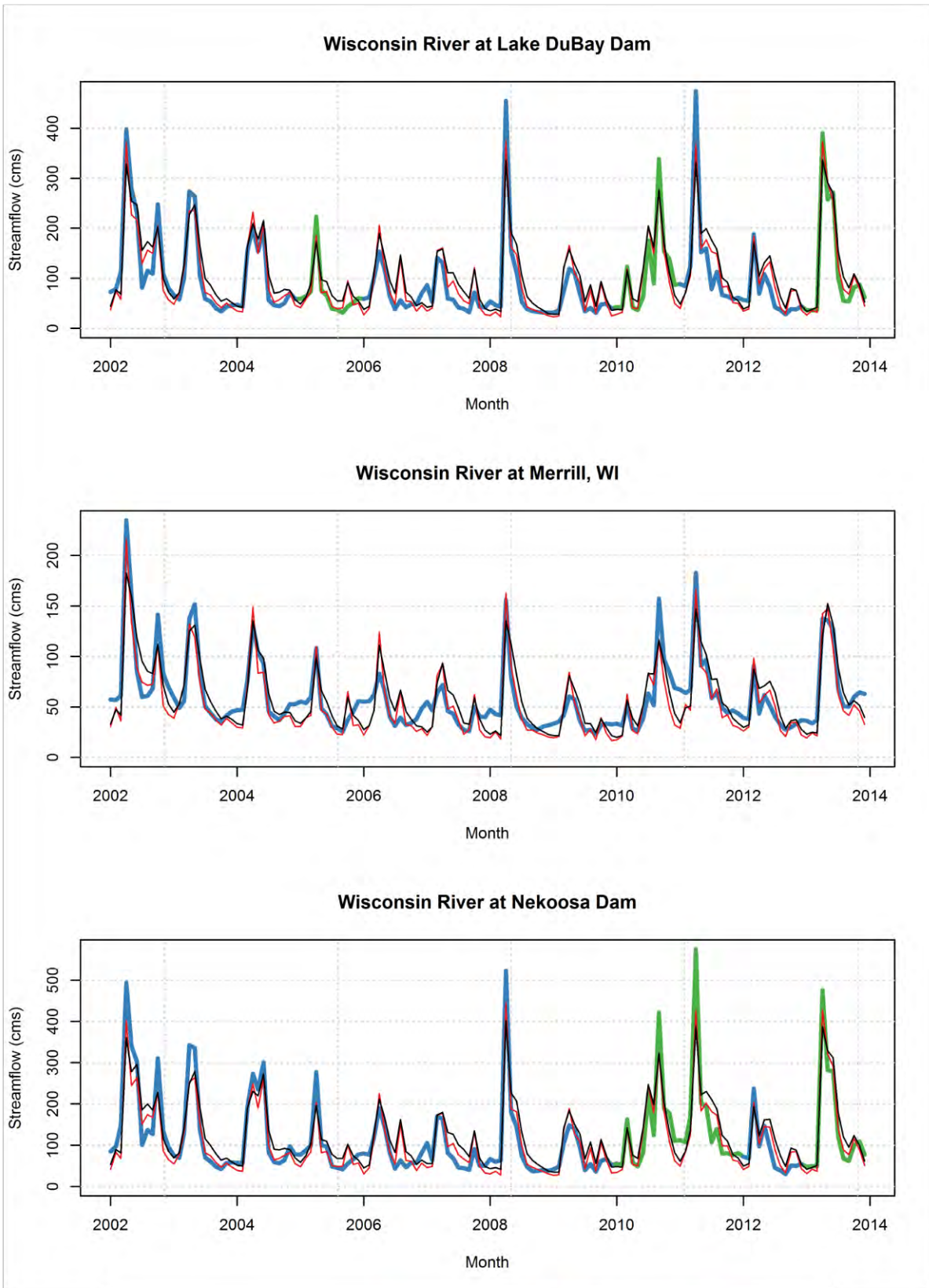
— Final after bias correction — Original SWAT — Calibration — Validation



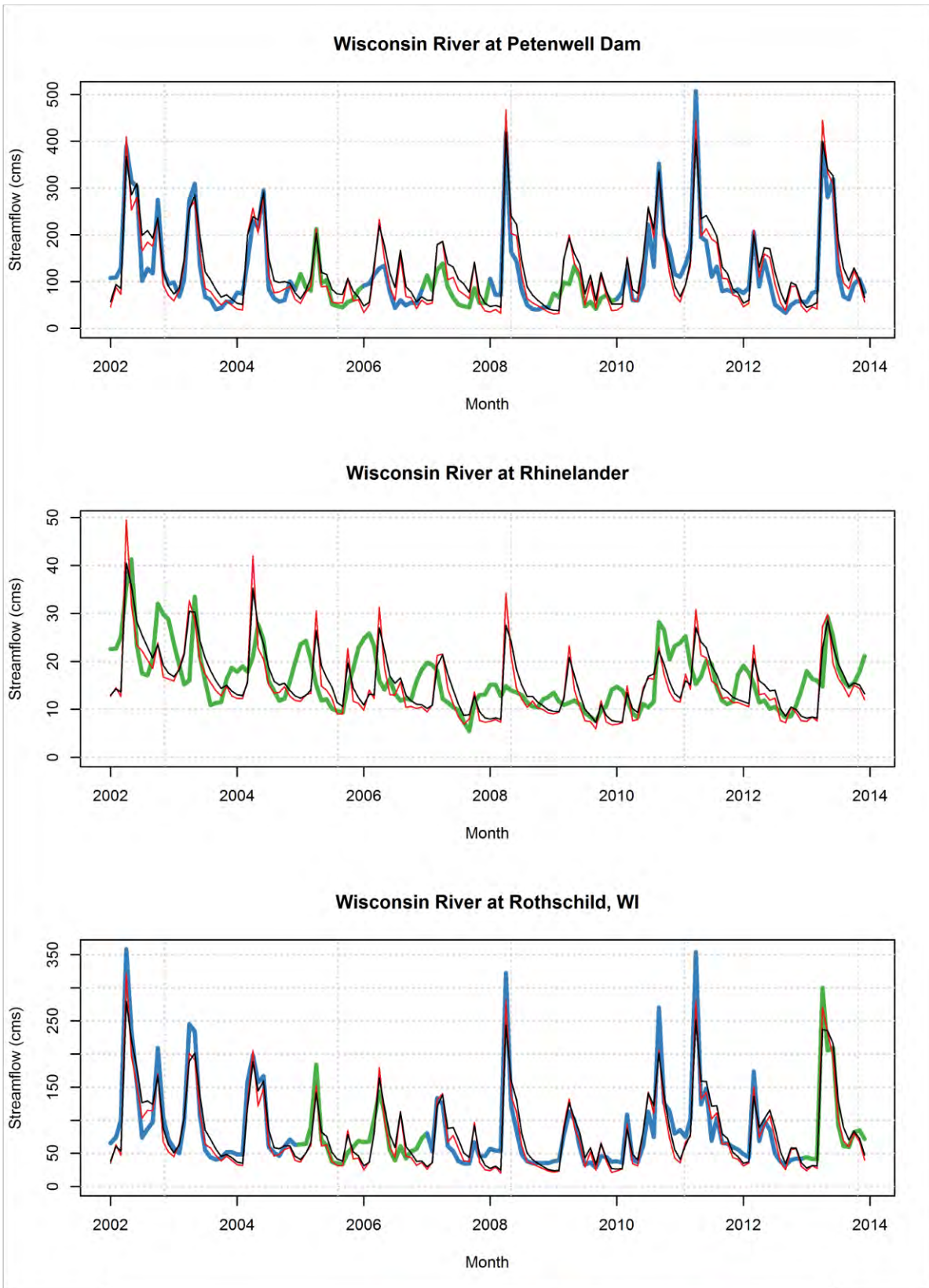
— Final after bias correction — Original SWAT — Calibration — Validation



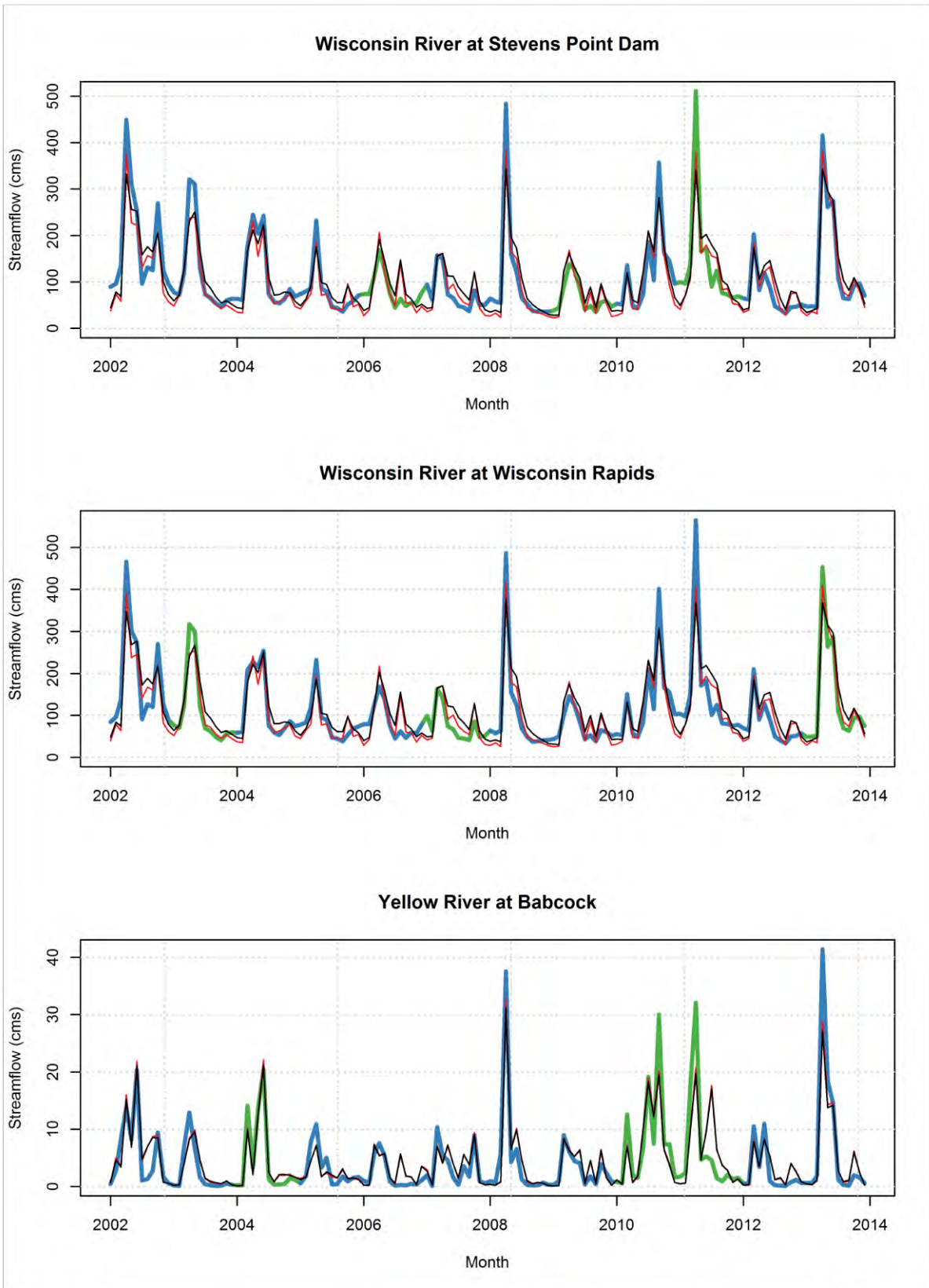
— Final after bias correction — Original SWAT — Calibration — Validation

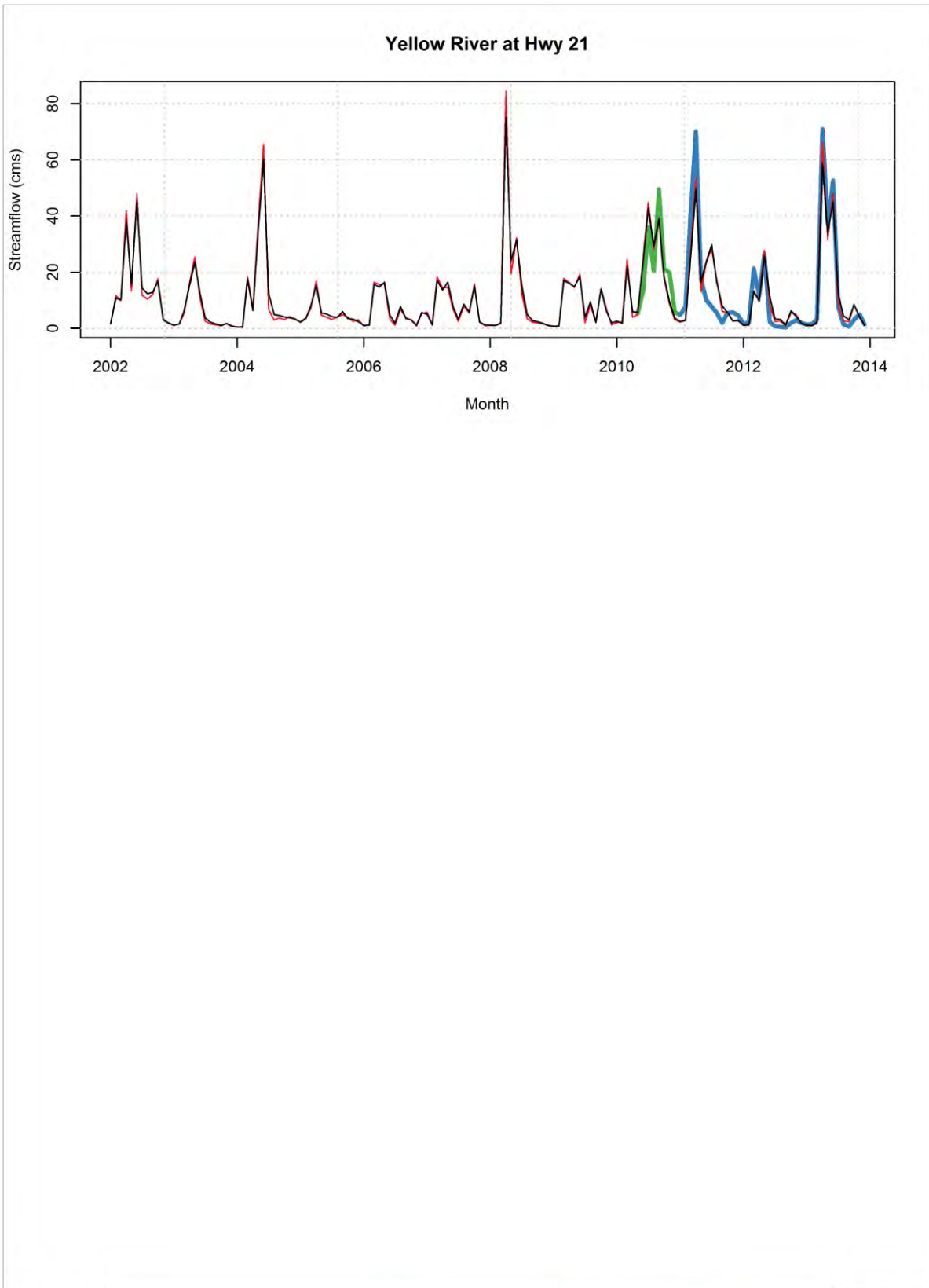


— Final after bias correction — Original SWAT — Calibration — Validation

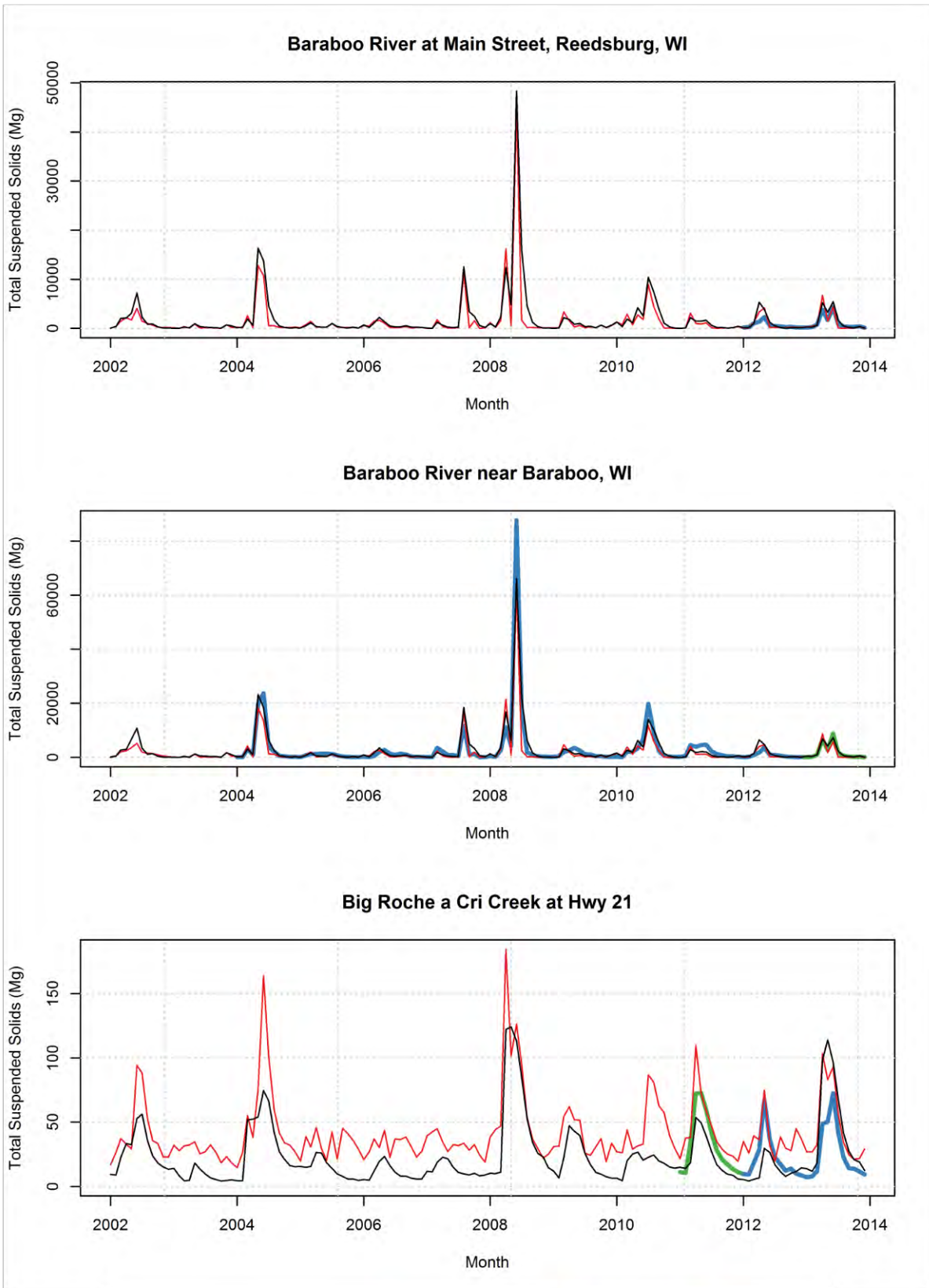


— Final after bias correction — Original SWAT — Calibration — Validation

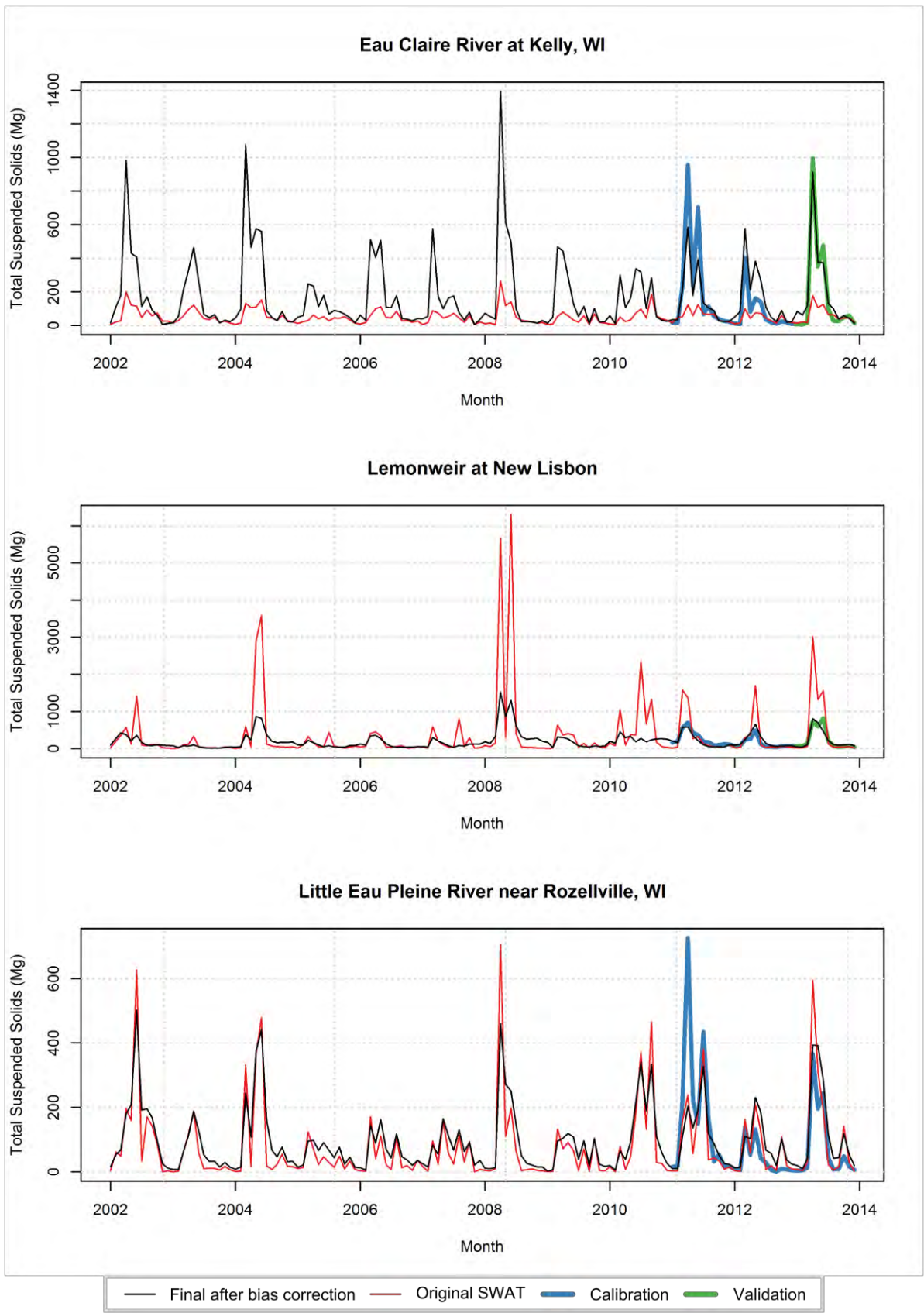


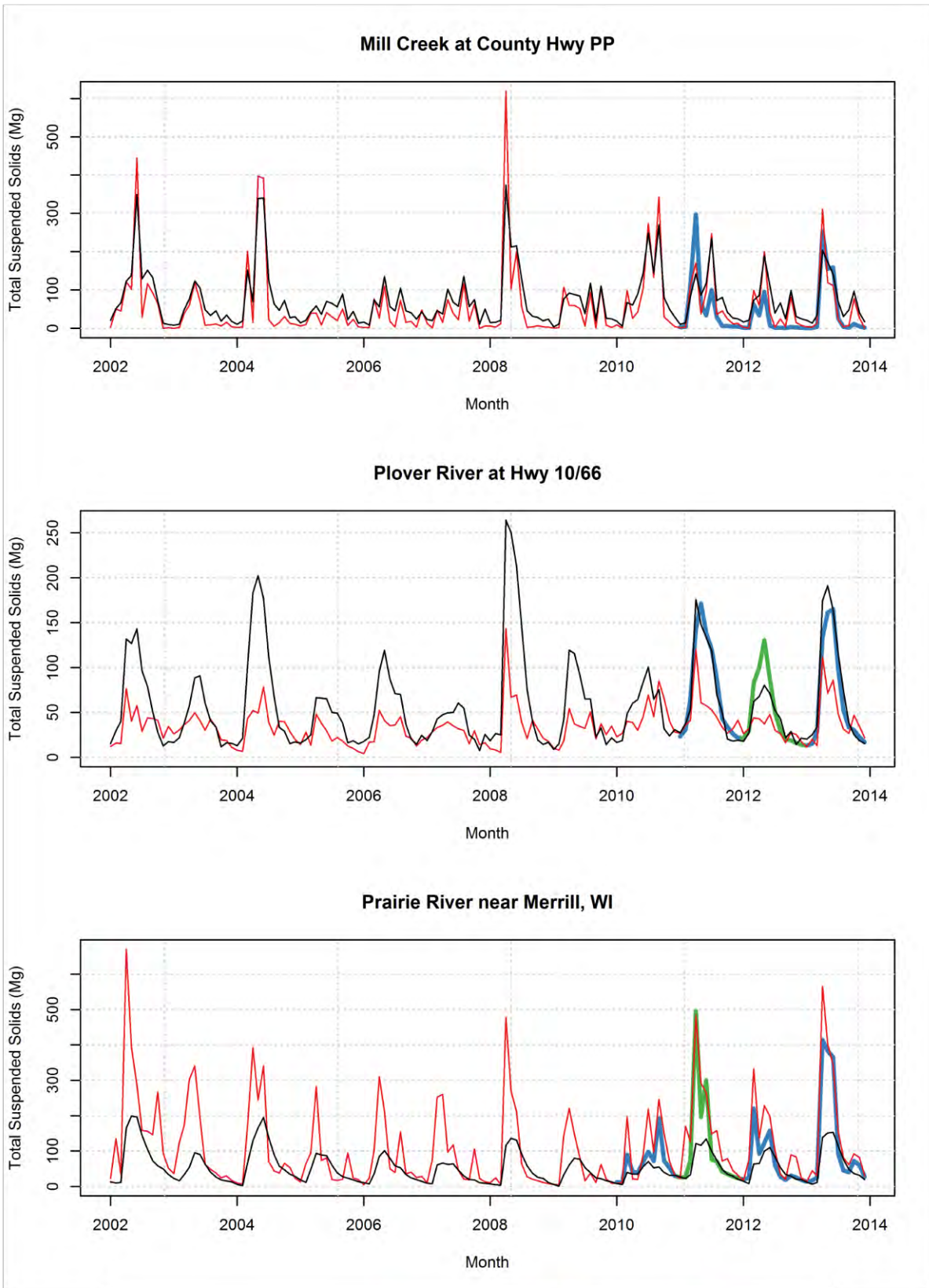


D.6.2 Total Suspended Solids

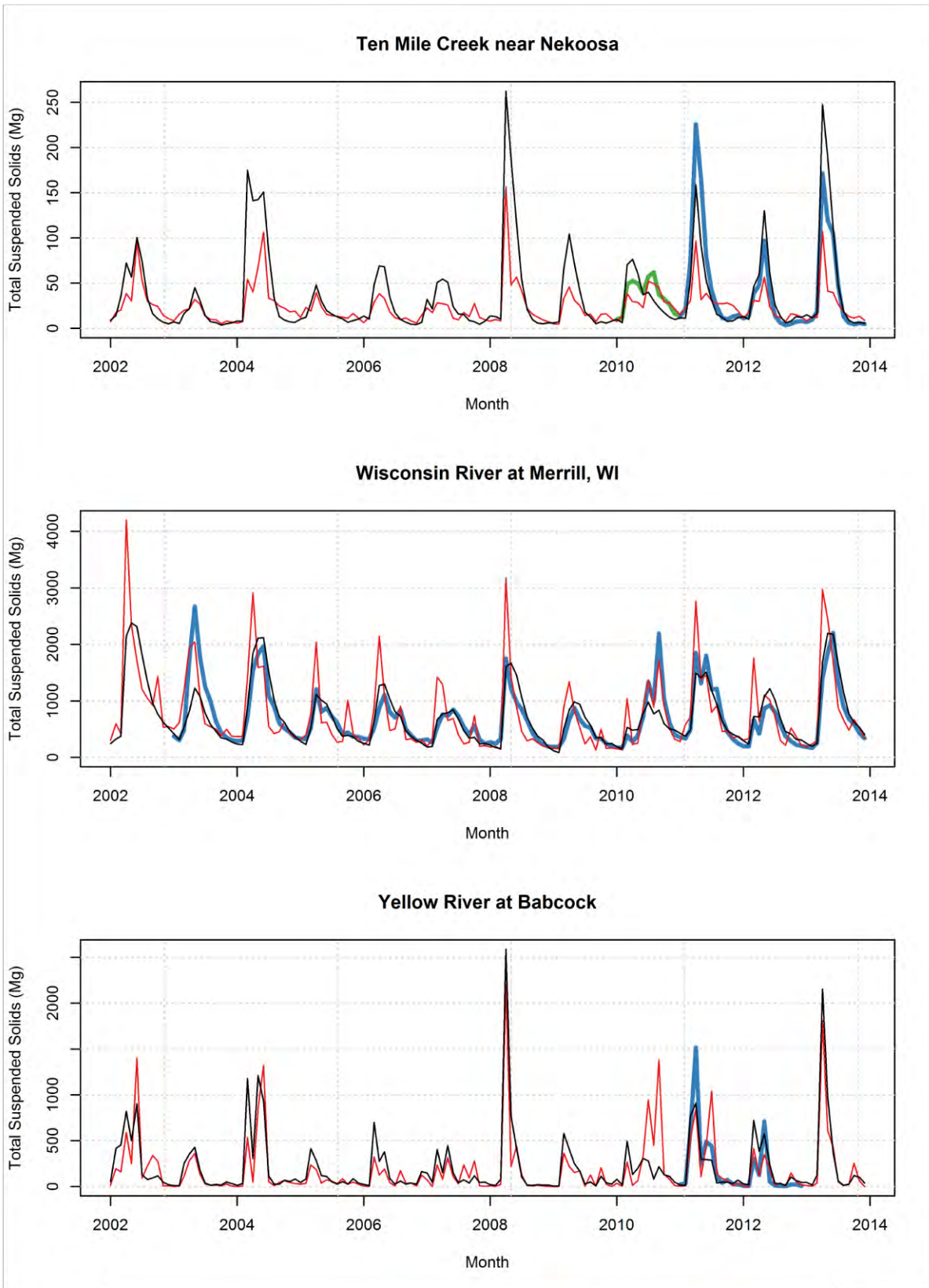


— Final after bias correction — Original SWAT — Calibration — Validation

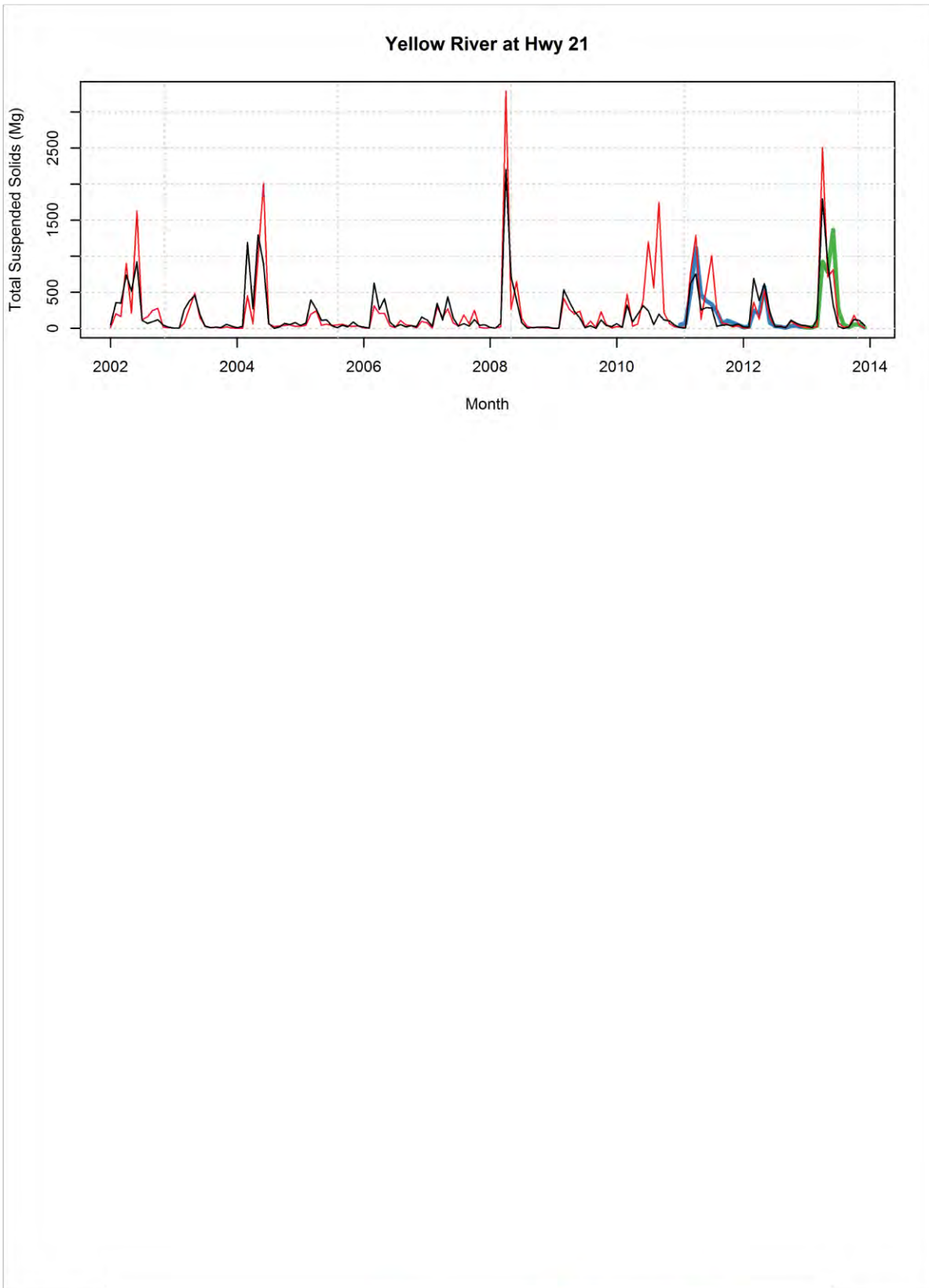




— Final after bias correction — Original SWAT — Calibration — Validation

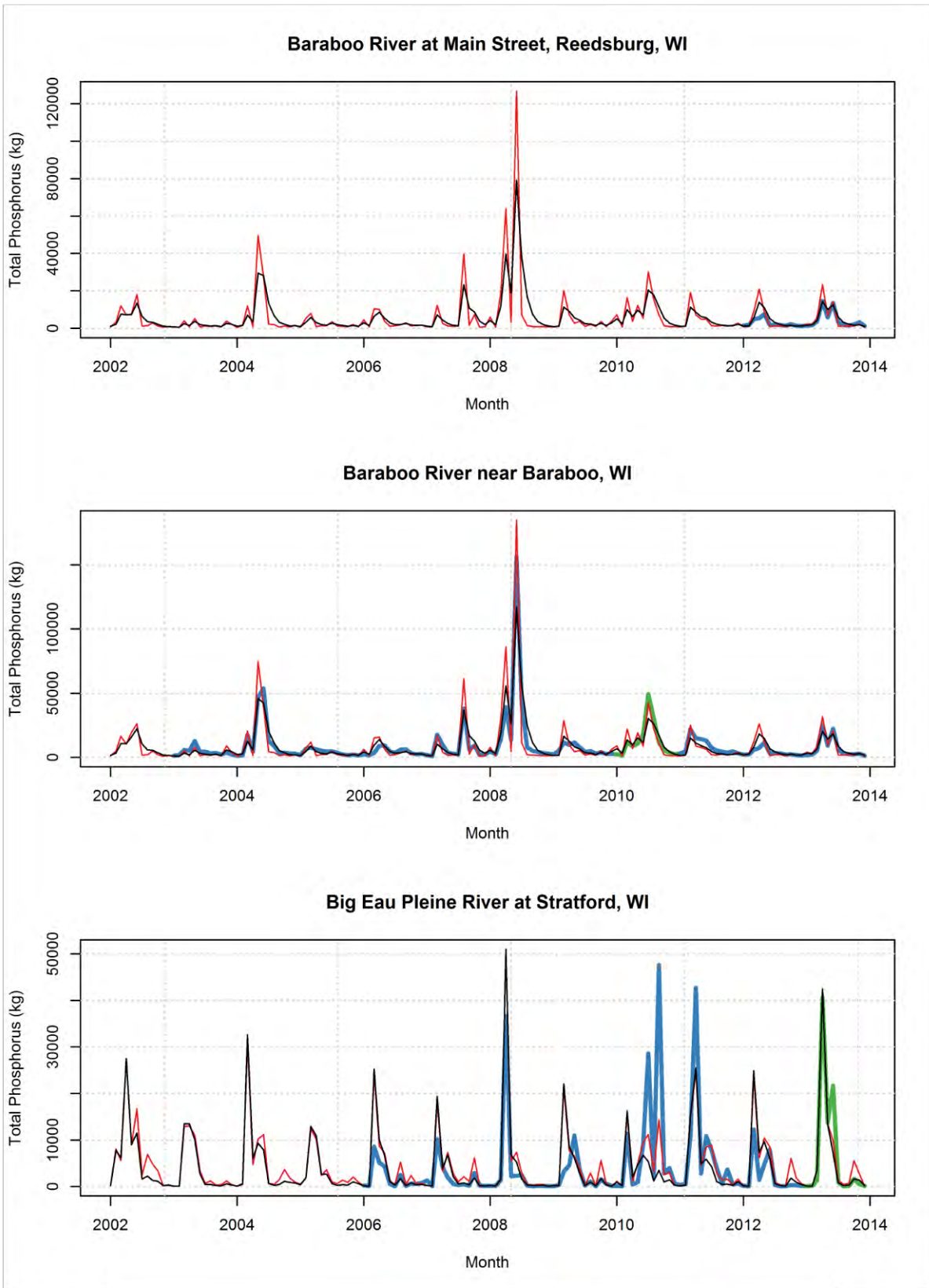


— Final after bias correction — Original SWAT — Calibration — Validation

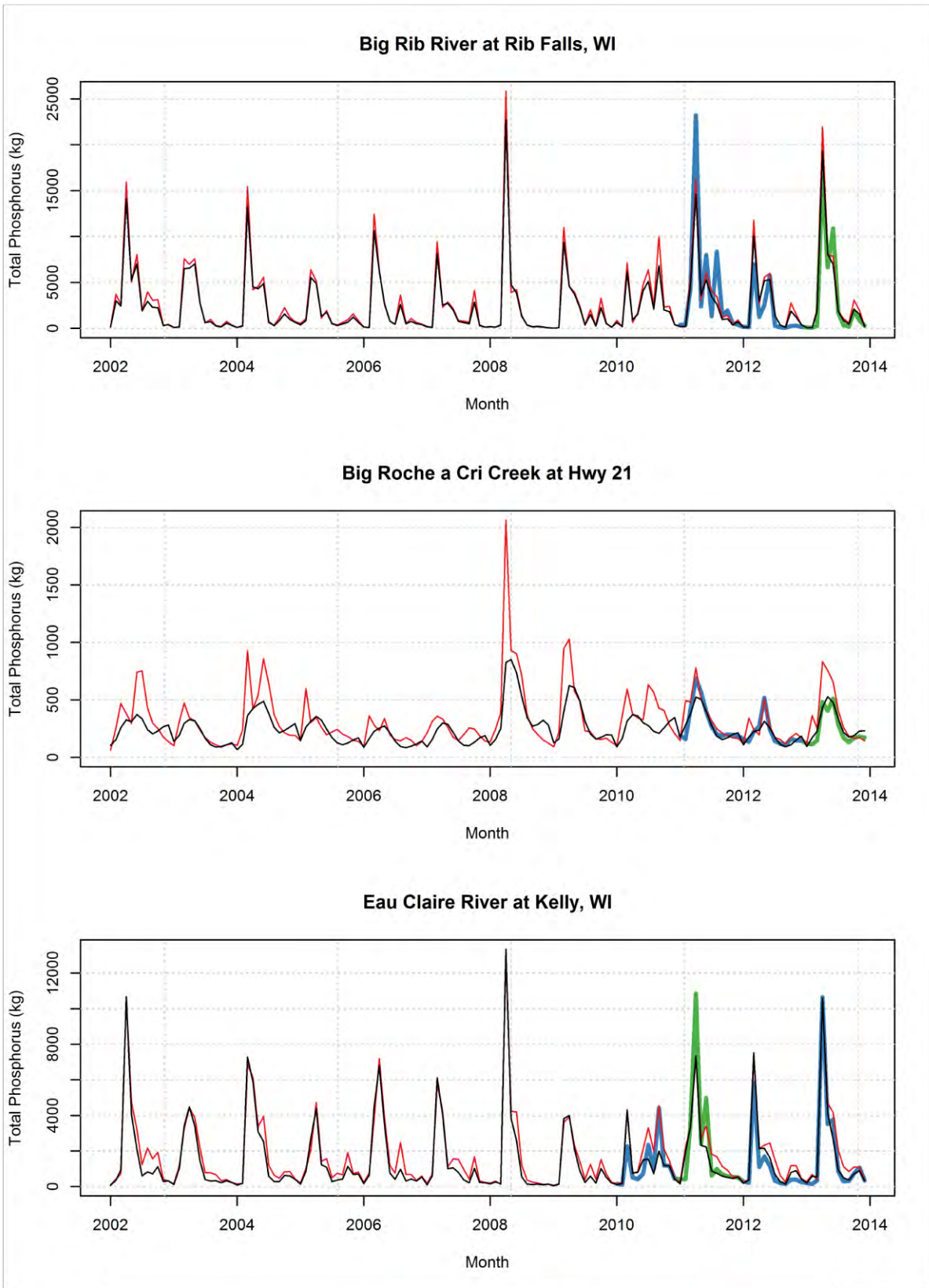


— Final after bias correction — Original SWAT — Calibration — Validation

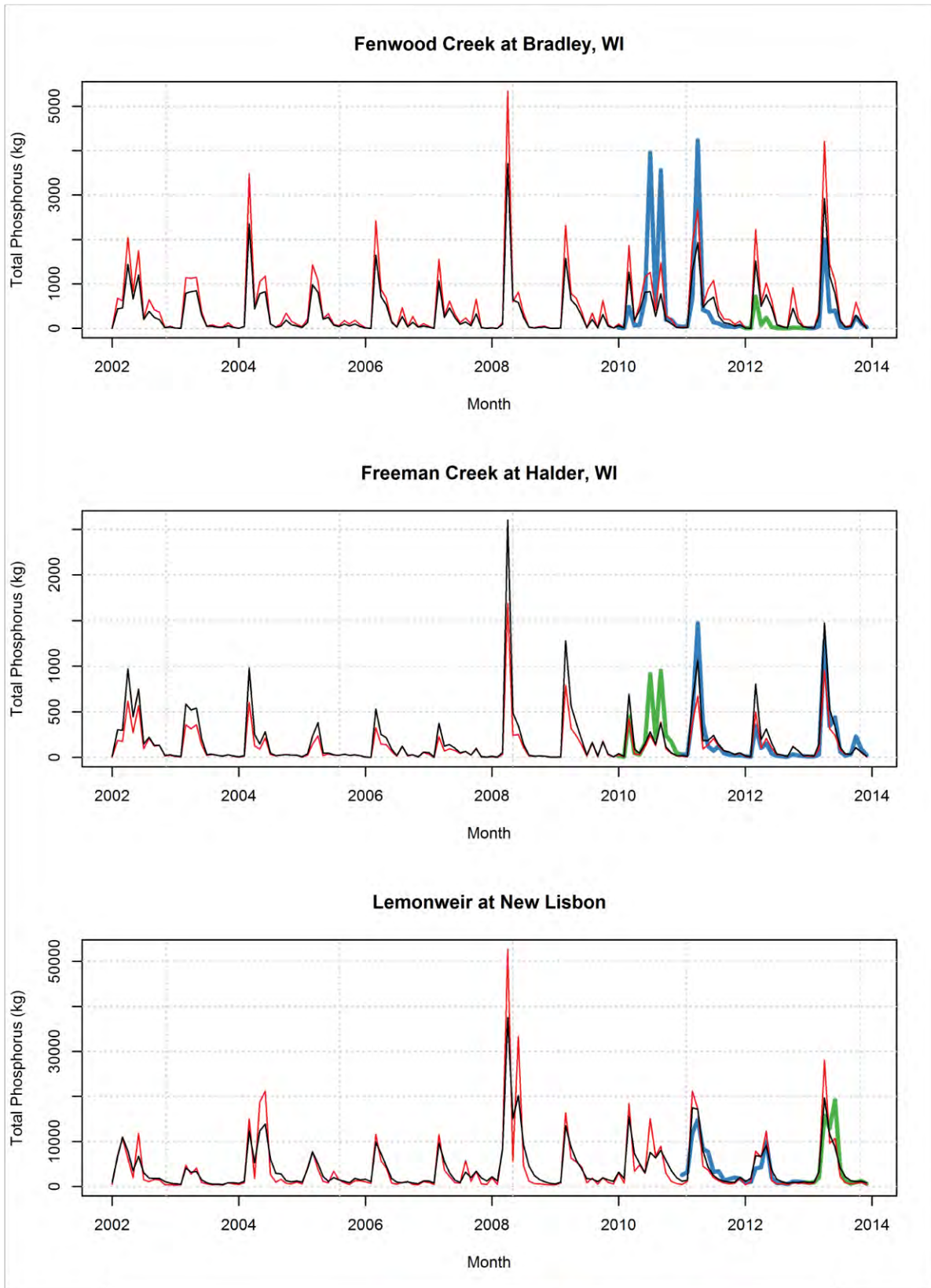
D.6.3 Total Phosphorus



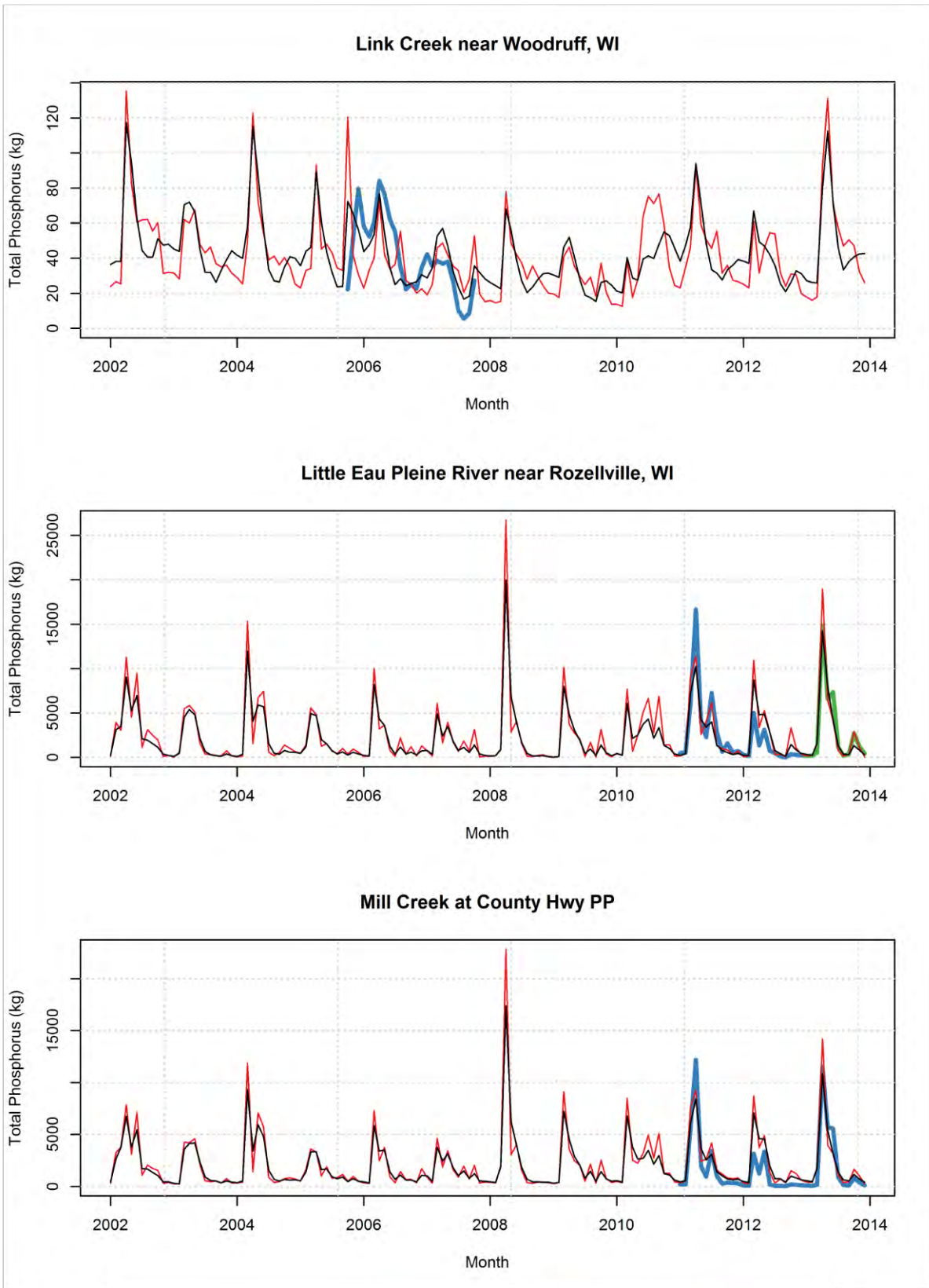
— Final after bias correction — Original SWAT — Calibration — Validation



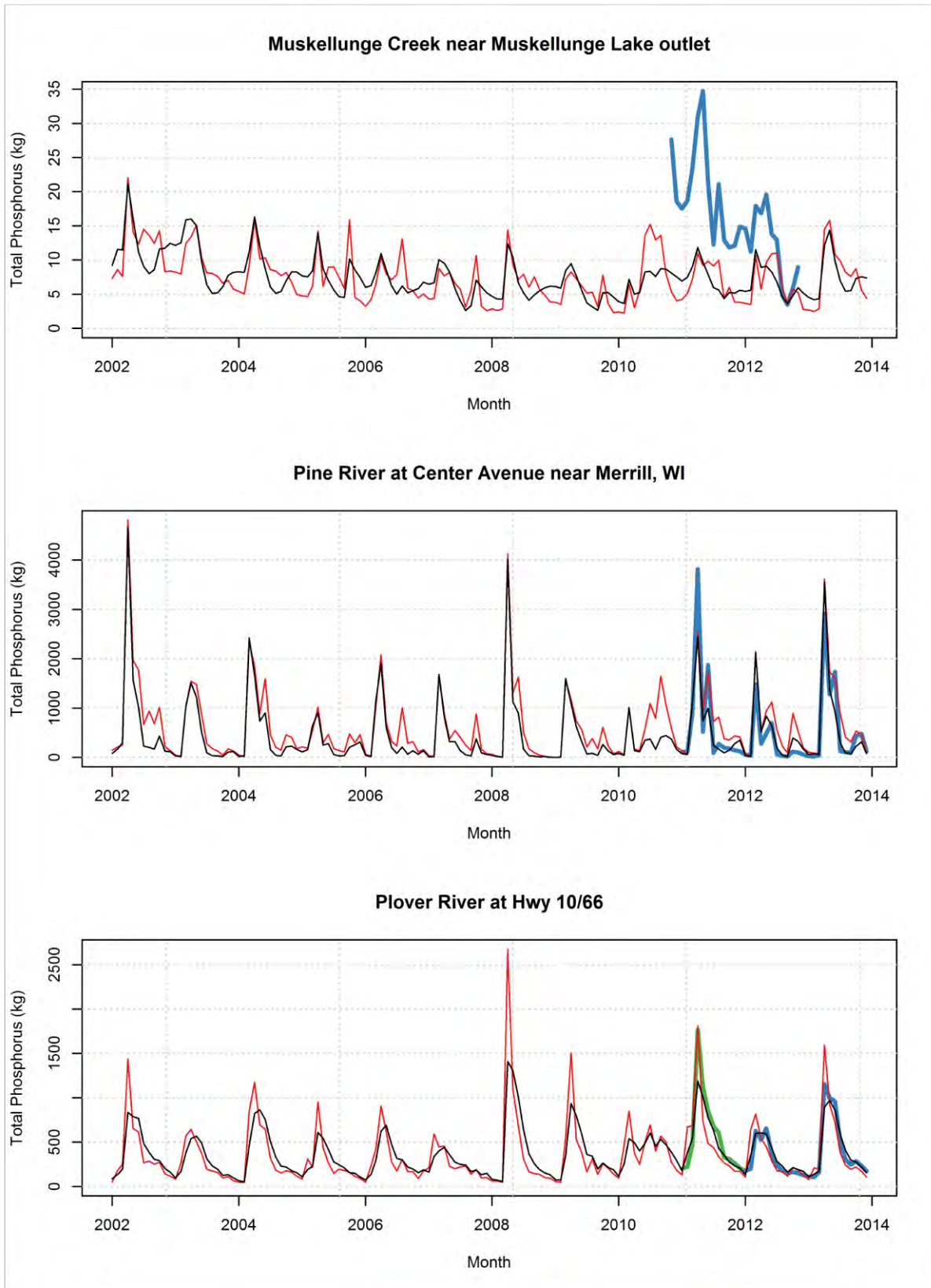
— Final after bias correction — Original SWAT — Calibration — Validation

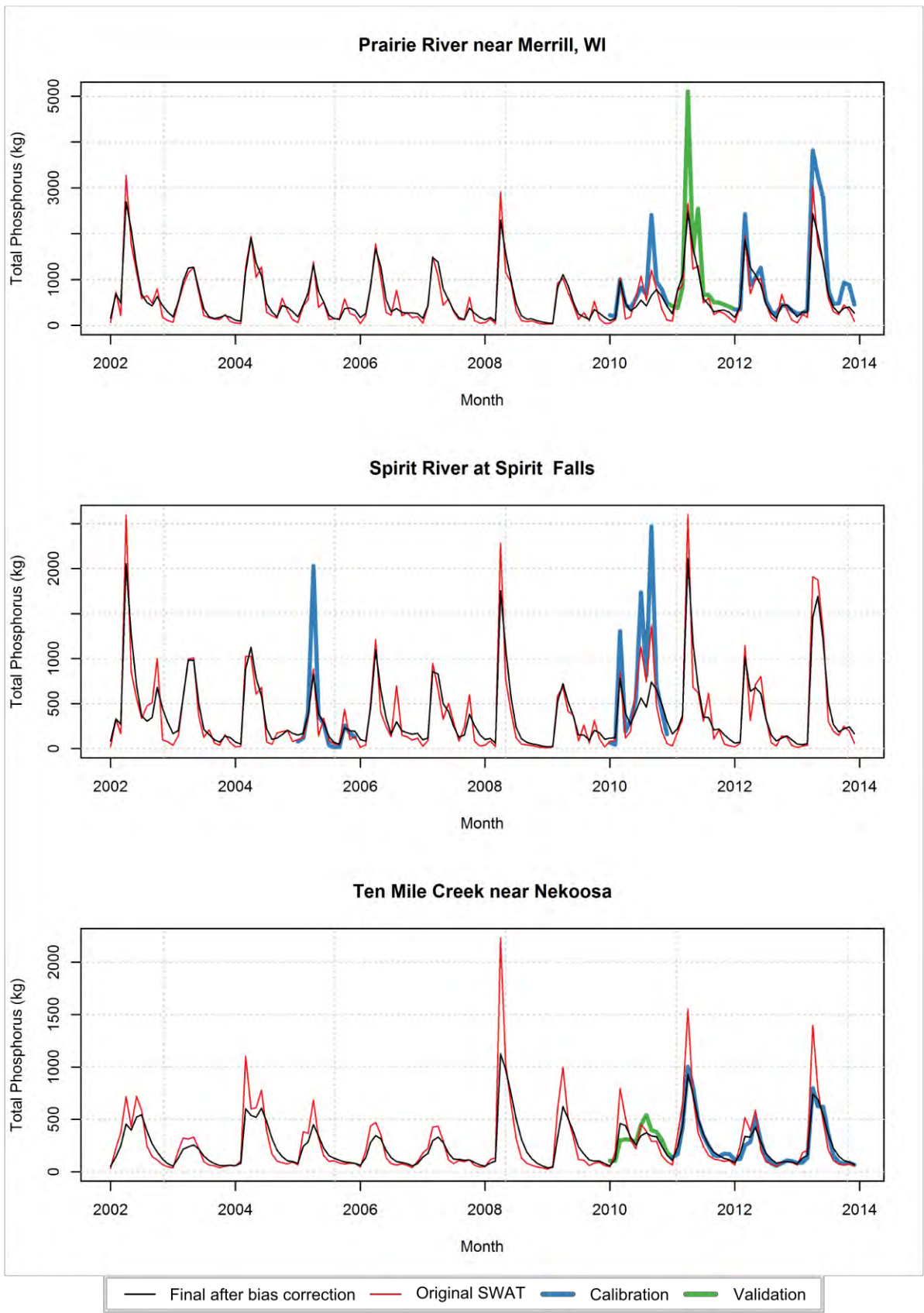


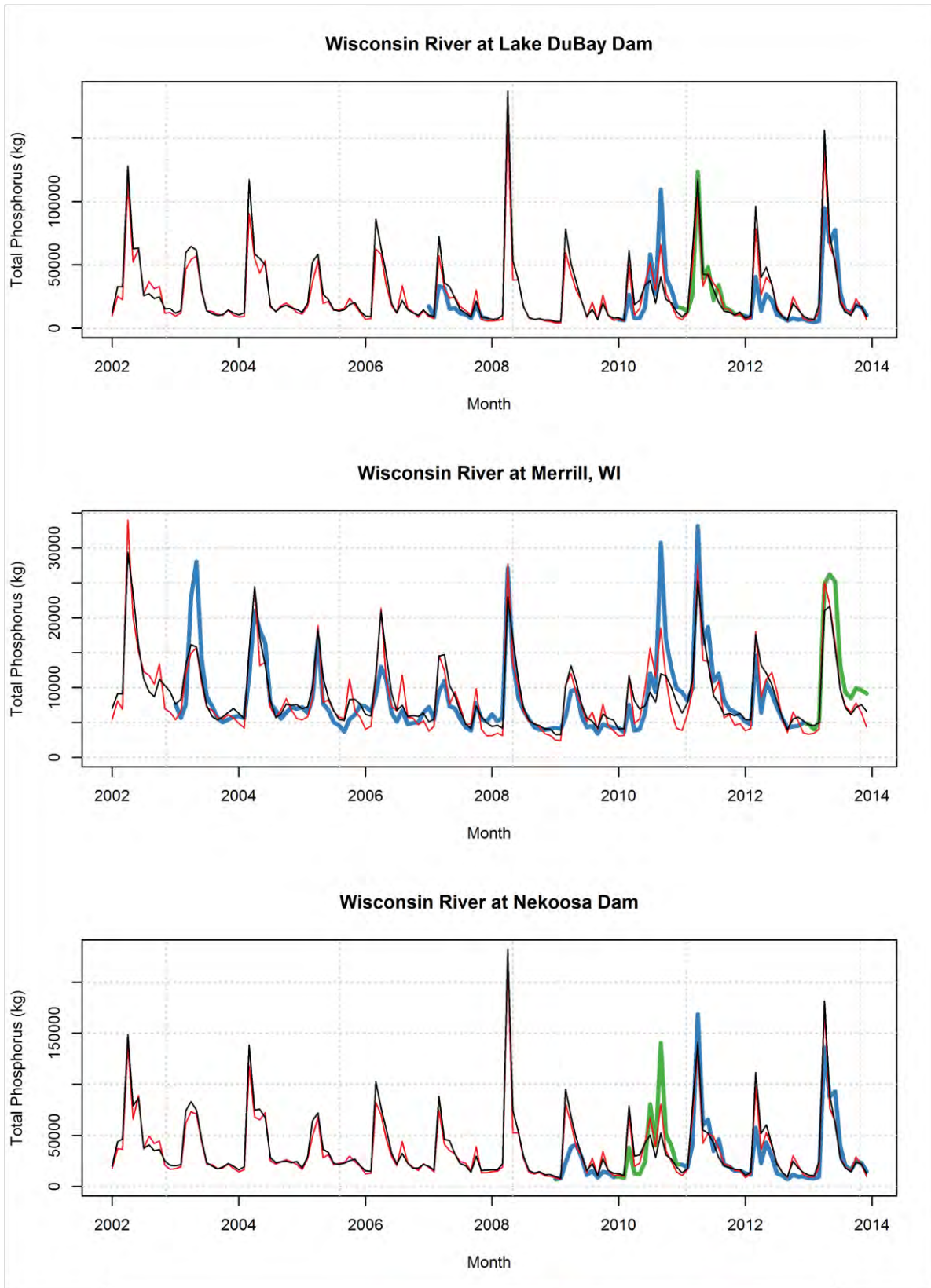
— Final after bias correction — Original SWAT — Calibration — Validation



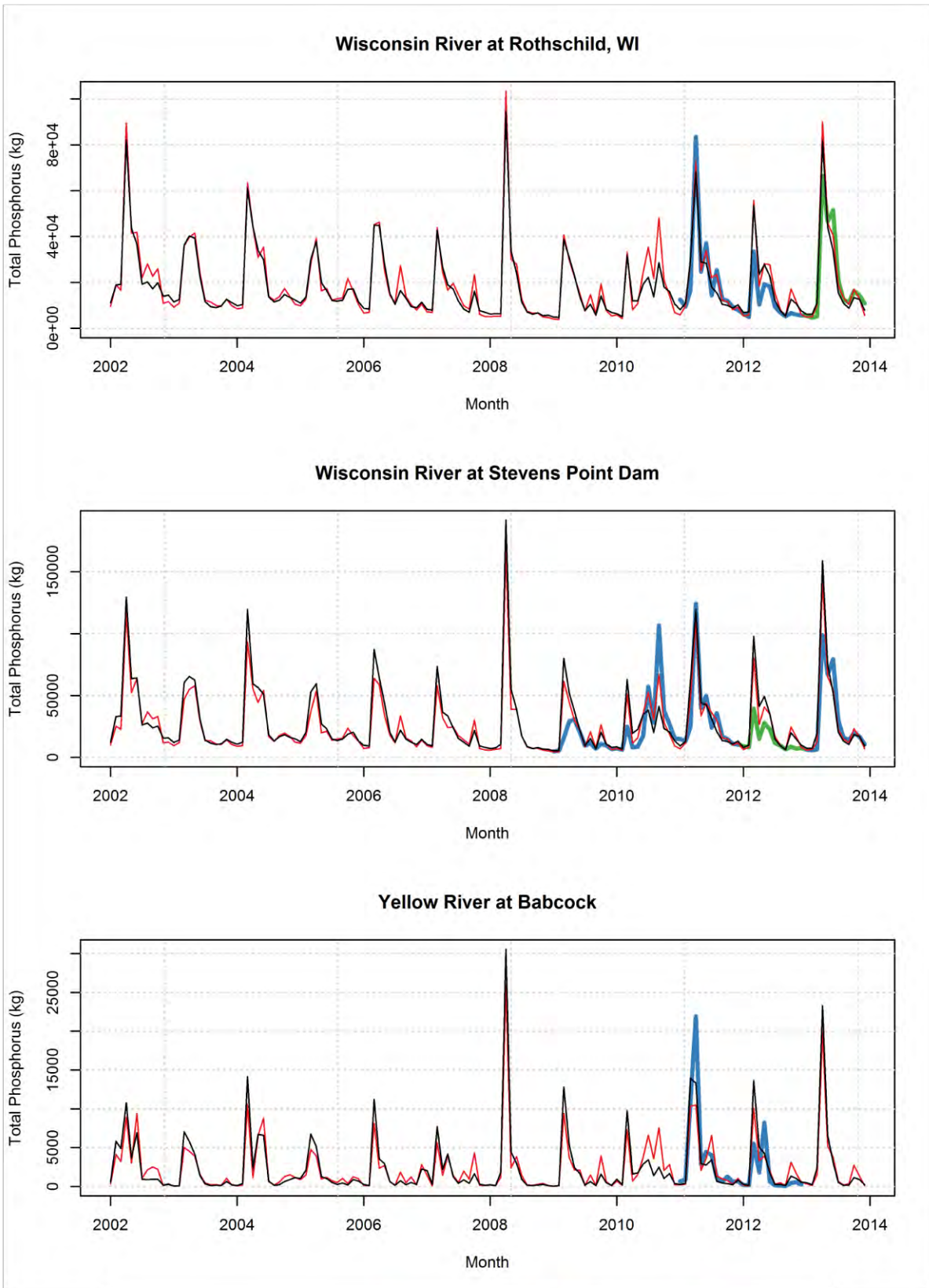
— Final after bias correction — Original SWAT — Calibration — Validation







— Final after bias correction — Original SWAT — Calibration — Validation



— Final after bias correction — Original SWAT — Calibration — Validation

